T.R.
ONDOKUZ MAYIS UNIVERSITY
INSTITUTE OF GRADUATE STUDIES
DEPARTMENT OF HISTOLOGY AND EMBRYOLOGY

POSSIBLE EFFECTS OF *Adansonia digitata* AND *Nigella sativa* ON RAT HIPPOCAMPUS AFTER EXPOSURE TO 900 MHZ ELECTROMAGNETIC FIELD

Doctoral Thesis

Hamza Mohamed Sharif Alamin MOHAMED

Supervisor
Prof. Dr. Süleyman KAPLAN

SAMSUN
2020

T.R.

ONDOKUZ MAYIS UNIVERSITY

INSTITUTE OF GRADUATE EDUCATION

The thesis prepared by Hamza Mohamed Sharif Alamin Mohamed entitled "Possible effects of *Adansonia digitata* and *Nigella sativa* on rat hippocampus after exposure to 900 MHz electromagnetic field" has been supervised by Prof. Suleyman Kaplan and accepted by the committee members as PhD thesis of the Department of Histology and Embryology, following the examination on the date ----/---- /2020.

Chairman: Prof. Süleyman Kaplan, Ondokuz Mayis University

Member: Prof. Dr. Mustafa Ayyıldız ,Ondokuz Mayis University

Member: Prof. Dr. Abdurrahman Aksoy, Ondokuz Mayis University

Member: Prof. Dr. Aydin Him, Bolu Abant İzet Baysal Üniversitesi

Member: Prof. .Dr. Berrin Zuhal Altunkaynak, Okan Üniversitesi

CONFIRMATION

This thesis has been approved by the committee members that already stated above and determined by the Institute Executive Board.

…. / …. /.....

Prof. Ali BOLAT

Head of Institute of Graduate Education

ÖZET

900 MHZ ELEKTROMANYETİK ALANA MARUZ KALMIŞ SIÇAN HİPOKAMPUSU ÜZERİNE BAOBAB VE ÇÖREK OTU'NUN MUHTEMEL ETKİLERİNİN ARAŞTIRILMASI

Hamza Mohamed Sharif Alamin MOHAMED

Ondokuz Mayıs Üniversitesi

Lisansüstü Eğitim Enstitüsü

Histoloji ve Embriyoloji Ana Bilim Dalı,

Doktora, Temmuz/2020

Danışman: Prof. Dr. Süleyman KAPLAN

Bu çalışma, cep telefonları tarafından yayılan elektromanyetik alanın (EMA) hipokampusun piramidal nöronları üzerindeki olası etkilerine odaklanmak ve bu olumsuz etkilerin azaltılmasında baobab (BA) ve çörek otunun (ÇO) rolünü değerlendirmek üzere tasarlanmıştır. Çalışmamızda 12 haftalık 56 adet *Wistar albino* cinsi erkek sıçan kullanıldı. Sıçanlar rastgele olarak her grup yedi sıçandan oluşmak üzere sekiz gruba ayrıldı. Kontrol (Kont), BA ve ÇO grupları EMA'ya maruz bırakılmadı. Sham grubu EMA'ya maruz bırakılmadan EMA sisteminde tutuldu. EMA + BA, EMA + ÇO, EMA + BA + ÇO ve EMA grupları, 28 gün boyunca her gün, günde 60 dakika 900 MHz EMA'ya maruz bırakıldı. Sıçan hipokampusunun cornu ammonis (CA)'daki piramidal nöronların sayısı, optik parçalama tekniği kullanılarak hesaplandı. Histopatolojik değişiklikler ışık ve elektron mikroskobu ile değerlendirildi. Ayrıca, katalaz ve süperoksit dismutaz enzimlerin aktivitesi kan serum örneklerinde değerlendirildi.

Stereolojik veri analizi, EMA grubunun CA'sındaki piramidal nöronların toplam sayısında, kontrol ve sham gruplarına göre anlamlı bir fark olmadığını ortaya koymuştur. BA ve ÇO birlikte kullanıldığında; EMA+BA+ÇO grubunun EMA grubuna göre anlamlı derecede ($p<0.01$) koruma gösterdiği gözlendi. Kont grubu ile BA grubu ($p<0.01$) ve ÇO grubu ($p<0.05$) karşılaştırıldığında aralarında anlamlı derecede bir fark olduğu görüldü. 900 MHz EMA hipokampustaki piramidal nöronlarda olumsuz değişikliklere neden olmaktadır. BA ve ÇO'nun bitkisel içeriğinin kombinasyonu, EMA`nın yan etkilerine karşı koruyucu bir etkiye sahip olduğu gözlendi.

Anahtar Sözcükler: şifalı bitkiler, elektromanyetik alan, hipokampus, çörek otu, stereoloji.

ABSTRACT

POSSIBLE EFFECTS OF *Adansonia digitata* AND *Nigella sativa* ON RAT HIPPOCAMPUS AFTER EXPOSURE TO 900 MHZ ELECTROMAGNETIC FIELD

Hamza Mohamed Sharif Alamin MOHAMED

Ondokuz Mayıs University

Institute of Graduate Studies

Department of Histology and Embryology

Ph.D., July/2020

Supervisor: Prof. Dr. Süleyman KAPLAN

The present study was designed to focus on the possible effects of the electromagnetic field (EMF) emitted by the mobile phones on the pyramidal neurons of hippocampus and to evaluate the role of *Adansonia digitata* (AD) and *Nigella sativa* (NS) in the decrease of these adverse effects. Fifty-six, 12-weeks-old *Wistar albino male* rats were used for the present study. The rats were randomly divided into eight groups; each group consisted of seven rats. The Control (Cont), AD and NS groups were not exposed to EMF. Sham group was kept in the EMF exposure system without being exposed to the EMF. EMF+AD, EMF+NS, EMF+AD+NS and EMF groups were exposed to 900 MHz EMF for 28 days, 60 minutes (min) per day. The number of the pyramidal neurons in the cornu ammonis (CA) of the hippocampus was estimated by using the optical fractionator technique. Histopathological changes were evaluated by light and electron microscopes. Moreover, the activities of the catalase and superoxide dismutase enzymes were also estimated in the blood serum samples.

Analysis of stereological data has revealed that the total number of the pyramidal neurons in the CA of the EMF group was not significantly different with the Cont and the Sham groups. A significant protection of AD and NS was observed when used combined in the EMF+AD+NS group in comparison to EMF group ($p<0.01$). A significant difference was observed between the Cont when compared with the AD group ($p<0.01$) and NS group ($p<0.05$). 900 MHz EMF causes adverse changes in the structures of neurons and neuroglia as well as the number of pyramidal neurons in hippocampus. The combination of herbal substances of AD and NS has a protective effect against EMF side effects.

Keywords: herbals, electromagnetic field, hippocampus, *Nigella sativa*, stereology.

ACKNOWLEDGEMENTS

First of all, I thank to Allah so much for success me for the performance of this work throughout the PhD journey. I would say that it was a wonderful opportunity for me working at the Ondokuz Mayis University for PhD studies.

I would like to express, my sincere gratitude and appreciation to my supervisor Professor Dr. Süleyman Kaplan who encouraged me throughout my PhD journey with his continuous support and advice. I have learned from him a lot and the newest in stereological techniques and electromagnetic field at the Department of Histology and Embryology, Faculty of Medicine, Ondokuz Mayis University.

I would like to express my sincere thanks and gratitude to Prof. Dr. Ayman Ahmed Warille for his boundless support, which has always prompted me to work more.

I express my most honest gratitude and thanks to Prof. Dr. Berrin Zuhal Altunkaynak for her generous help and collaboration. I could not find words to express my honest and deeply thanks and appreciation to my colleague Dr. Ömür Gülsüm Deniz who assisted me from the beginning to the end of my thesis works; also, I would never forget that she gave me excellent advices and guidance. My deeply gratitude and thank to my colleague Res. Assist. Gamze Altun for her kindly help and distinguishing support throughout my works. I am very grateful and thankful to my colleagues, especially, Dr. Kıymet Kübra Yurt, Dr. Elfide Gizem Kıvrak and Res. Assist. Adem Kocaman for their cooperation and supports. I want to thank to everybody in the Department of Histology and Embryology for their help and supports.

On the personal level, I would like to thank my mother Sittana Abdullah, who has always cared and encouraged me to complete my work. My brothers and sisters (Fatima and Omnia) were indeed great, the success of this work wouldn't have been easy without all of you carrying me several paces forward.

Finally, my profound gratitude and thankful to my small family my wife Azza Abdelrahim and my sons (Mohamed and Omer) without for their help, encouragement and patience, my thesis was not possible. I dedicate this thesis to the soul of my father Mohamed Sharif and my mother Sittana Abdallah and my family and my country Sudan.

CONTENTS

ABBREVIATIONS

AD	**:** *Adansonia digitata*
asf	**:** Area Sampling Fraction
BBB	**:** Blood Brain Barrier
BS	**:** Black Seed
CA	**:** Cornu Ammonis
CAT	**:** Catalase
CE	**:** Coefficient of Error
CNS	**:** Central Nervous System
Cont	**:** Control
CV	**:** Coefficient of Variation
Da	**:** Dalton
DG	**:** Dentate Gyrus
DNA	**:** Deoxyribonucleic acid
DPPH	**:** 2,2-diphenyl-1-picrylhydrazyl
ELF	**:** Extremely Low Frequency
EMF	**:** Electromagnetic Field
EMR	**:** Electromagnetic Radiation
FRAP	**:** Ferric Iron Reduction Antioxidant Power
GSH-Px	**:** Glutathione Peroxidase
GSM	**:** Global System for Mobile Communications
H_2O_2	**:** Hydrogen Peroxide
IF	**:** Intermediate Frequency Fields
Kg	**:** Kilogram
MHz	**:** Megahertz
NS	**:** *Nigella sativa*
RFR	**:** Radiofrequency Radiation
RF	**:** Radiofrequency
RNS	**:** Reactive Nitrogen Species
ROS	**:** Reactive Oxygen Species

Rpm **:** Revolutions per minute

SD **:** Standard Deviation

SOD **:** Superoxide Dismutase

SRS **:** Systematic Random Sampling

ssf **:** Section Sampling Fraction

T **:** Tesla

TPX : Thioredoxin

TQ **:** Thymoquinone

tsf **:** Thickness Sampling Fraction

VLF **:** Very Low Frequency

W **:** Watts

WHO **:** World Health Organization

µm **:** Micrometer

°C **:** Centigrade

1. INTRODUCTION

Mobile phone use has flourished during the past few decades to this day with an estimated 7.9 billion users worldwide. It has become an integral part of daily life (Ebrahim et al., 2016). The effects of mobile phone radiation on human health have become an area of interest to researchers globally, as a result of the enormous increase in this mobile technology worldwide and relative health hazard. Also, ear related symptoms have been on the increase with the consistent use of mobile communication devices (Parasuraman et al., 2017; Wall et al., 2019).

The World Health Organization (WHO) has created an electromagnetic field (EMF) survey project to assess scientific evidence on negative of healthiness impacts and the results of the International Agency for Research on Cancer (IARC) of WHO confirmed that radiofrequency (RF) radiation from the devices that emit non-ionizing RF signals as a probable human carcinogen group (Jadia et al., 2019; Migault et al., 2019). Therefore, many scientific studies contain reports certain the risk of mobile phone use on the health of society (Lahkola et al., 2007; Russell, 2018). It has been observed rats exposed to low-frequency EMF increase the peroxidation of fat in the brain and as a consequence, adverse effects in the frontal lobe cortex occur (Lee et al., 2017; Mishra and Chowdhary, 2018). Also, it has been documented that, the long-term exposure to EMF during the postnatal period damages the neurons in the cerebellum of female rats model (Chen et al., 2017).

Previous studies indicated that long-term exposure to EMF radiation from a mobile phone may result in benefits and harms, which the most prominent of these harms are health effects such as increased blood pressure, headache, memory loss, tumors, weak immune system, Parkinson's disease and brain cancer (D'Angelo et al., 2015; Perez et al., 2019; Wyszkowska et al., 2019).

On the other hand, there are some positive health effects due to exposure to EMF radiation such as helping bone recovery and reducing the toxic influence of chemotherapy (Saikhedkar et al., 2014). There is a study that revealed that the radiation of EMF from cell phone may be responsible for many diseases such as headache and various types of heart diseases and memory loss in the short term (Pall, 2016; Miah and Kamat, 2017).

In addition, the effects of EMF exposure occur on the cellular level in development and genetic structure cycles. Some of the previous studies have drawn attention to changes in chromosome and chromatin, in which EMF exposure has been shown to create DNA damage and peroxidation by causing oxidative stress in rats (Yokus et al., 2005; Duan et al., 2015). There are many studies investigating the possible non-carcinogenic effects of cells' exposure to EMF, which focus on the physiological changes, musculoskeletal problems, reproductive activity and cognitive functions (Hintzsche and Stopper, 2010; Yildirim et al., 2015; Gustafsson et al., 2017).

The central nervous system (CNS) is feasible to be affected after exposure to the emitted EMFs when using mobile phones near the brain. Also these effects have been detected in the cerebellum, neurotransmitter release, memory and learning function (Narayanan et al., 2010; Deniz et al., 2017). The impacts of EMF exposure to on human being are still not completely understood because of ethical issues and the complexity of the organism, while experimental studies on animals show important results in this regard.

Some of previous studies investigated the negative influences of EMF on organs and systems, especially focused on the nervous system (Sonmez et al., 2010; Poprac et al., 2017). It is noted that modern studies indicate that some parts of the CNS has produced neurons during the life, the links between the newly generated neurons in the brain (i.e. hippocampus), may reach up around 2 years maximum (Kheifets et al., 2005).

The hippocampus is an essential part of the limbic system that is enhanced in learning and storing memories. In this context, the Cornu Ammonis (CA) region (i.e. CA3 region) (Eichenbaum et al., 2016).

The newly generated neurons, which originate from the subgranular zone (SGZ) then, finally differentiate to dentate granule cells (Marín-Burgin et al., 2012; Kempermann et al., 2015). It has critical functions closely related to the hippocampus such as memory and memory-related functions like olfaction (Gould, 2007).

The process of neurogenesis during pregnancy continues in the brain and ends before birth. Dentate gyrus (DG) is one of the brain regions where formation of new neurons continues throughout the life of which granular neurons are present while pyramidal neurons are found in CA (Baptista and Andrade, 2018). These two groups of

neurons form the main types of neurons in the hippocampus (Gage, 2000). Neurogenesis occurs in some brain regions throughout life, the hippocampus is one of these sites of postnatal neurogenesis (Ernst and Frisén, 2015).

Usually the brain is the main target organ of the electromagnetic fields emitted during long-term use of cell phones, so the possibility of an increased risk of brain tumours is a concern (Brzozek et al., 2018). Numerous studies have presented that neuron loss may be triggered by oxidative stress (Bolla, 2015; Bagheri Hosseinabadi et al., 2019).

Researches have shown that it is difficult to directly assess the potential adverse effects of exposure to EMFs, and therefore these effects accumulate over a long period to appear clearly. Based on this idea, the scientists concentrated on the harmful effects on human health in the range between (900 MHz - 1800 MHz) EMF radiation (Panagopoulos et al., 2007).

In this context, we utilized 900 MHz EMF exposures to *Wistar albino* rats to see possible effects of EMF radiation on the hippocampus, based on the fact that Global System for Mobile Communications (GSM) operators operate at a frequency of 900 MHz, consequently a lot of research has been done to find out the effects of this frequency on humans (Aly and Crum, 2016).

Studies conducted as mentioned above have revealed the effect of cell phones on the CNS. In this context, EMF produced by cell phones attracts the attention of researchers due to its side effects on organisms. It is believed that experimental studies supported by future epidemiological studies would clarify the point as to whether or not exposure to EMF exposure is a cause of cell damage (Koehl and Abrous, 2011).

The body of the organism is distinguished by the presence of various mechanisms to counteract oxidative stress by producing antioxidants, which are naturally produced an endogenous antioxidants such as superoxide dismutase (SOD), glutathione peroxidase (GSH-Px), catalase (CAT), thiouroxine (TPX) or supplied externally by eating foods rich in antioxidants that boost your body’s immunity (Pizzino et al., 2017; Surai et al., 2019).

Accumulation of reactive oxygen species (ROS) occurs due to disequilibrium between their productions and removing by antioxidants, this build up of ROS leads to oxidative stress (Hybertson et al., 2011; Dasuri et al., 2013). Oxidative stress may affect

cell organelles, leading to impairment of cell membrane by altering the morphological and effectiveness of proteins and fatty peroxidation (Stefi et al., 2019).

Also, oxidative stress increases risk influences of many diseases and may cause structural damage to the DNA molecule (Valko et al., 2007; Liguori et al., 2018). Many studies have shown that brain is susceptible to oxidative stress owing to its high metabolic rate and high degree of oxygen needing, thus oxidative stress has a role in the neurodegenerative diseases (Wang and Michaelis, 2010; Liu et al., 2017).

Many researchers highlighted that exposure to EMFs may increase the production of ROS, which leads to oxidative stress. Therefore, ROS is considered one of the main risk factors causing the appearance of degenerative nervous diseases, such as multiple sclerosis and Alzheimer's disease. It has also been observed that oxidative stress may contribute to the development of Parkinson's disease and cause some mental disorders (Bortkiewicz, 2019; Gallastegi et al., 2019).

Although it has been confirmed that neurodegenerative diseases share common mechanisms such as mitochondrial dysfunction, protein accumulation and oxidative stress. However, all of these phenomena have been studied separately so far, and oxidative stress has been shown to be the main cause of neuronal impairment (Terzi et al., 2016).

The *Adansonia digitata* (AD) fruit is commonly used in African country is rich in flavonoids, minerals, vitamins as ascorbic acid (vitamin C) and essential amino acids, which makes it effective antioxidant, with other properties such as anti-inflammatory, analgesic and antipyretic properties, it is also known as antimicrobial and antiviral, as well as antidiarrheal agent, it plays role in protecting the liver (Kaboré et al., 2011).

Nigella sativa (NS) is a medicinal plant utilized worldwide and is distinctive and considered as a system of herbal remedies locally (Demir et al., 2020). The important healing properties of this plant are due to the presence of thymoquinone (TQ), which is rich in antioxidants (Khan, 2019). The main active compounds that derived from *Nigella sativa* are TQ, p-cymene and carvacrol (Gulsen et al., 2016).

These facts lead us to say that NS is effective as diuretic, anti-cancer treatments and has anti-inflammatory, anti-microbial, Immunity activities, anti-anxiety, anti-oxidant, and anti-inflammatory (Kooti et al., 2016; Fanoudi et al., 2019).

The purpose of the present study is to recognize the potential effect of *Adansonia digitata* and *Nigella sativa* on hippocampus after rat exposed to radiation 900 MHz field and to assess the effect of pressure on the hippocampus. Additional to that the prevalence level of the structural alterations can be determined due to EMF in the hippocampus and identify the duration taken by EMF radiation to induce these structural changes. However, to our knowledge there are a limited number of studies concerning EMF radiation and the roles of AD and NS in the pyramidal cells and granule cells of the hippocampus after EMF exposure. Besides, we noted that there are no stereological studies regarding the neuroprotective effects of AD and NS on the hippocampus after EMF exposure. However, their possible effects neuroprotective on the adult hippocampal neurogenesis after EMF exposure are still unknown. This issue would be clarified by this study.

2. GENERAL INFORMATION

2.1. Electromagnetic Field Components and General Features

The EMF consists of a group of waves that move through space in tremendous speed. They contain fields of electric and magnetic energy (Bürgi et al., 2008; Organization, 2010).

EMFs categorized according to their frequencies into Extremely low frequency (ELF) at range (1–300 Hz), Low frequency (LF) range up to100 kHz and High frequency (HF) up to 300 GHz (**Figure 1**). In recent times, worldwide exposure to radio frequency bands that have types such as radar, TV, mobile phones, radio, and microwave have created concern about potential risks from its emission (Röösli et al., 2010). Particularly, Controversial are the biophysical mechanisms by frequency domains associated with exposure to the magnetic field may affect human health (Brix et al., 2001; Gobba et al., 2011).

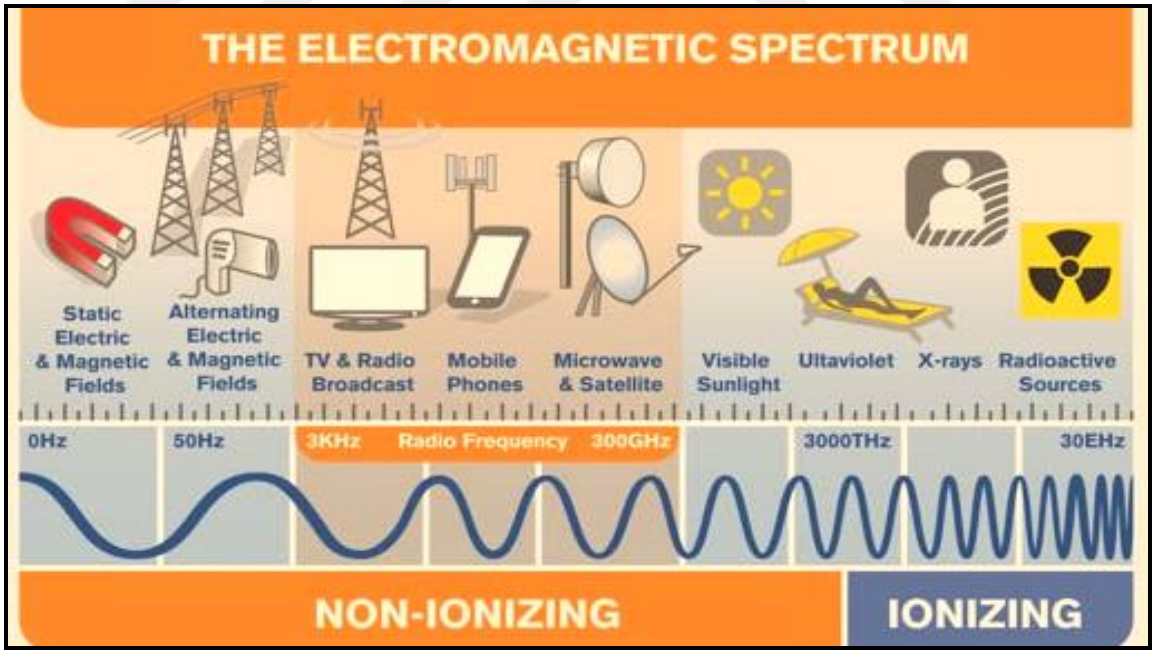

Figure 1. Electromagnetic spectrum showing the distribution of radiation sources in different frequencies (Union, 2013).

2.1.1. Electrical Field

Electric fields arise from the voltage used to pass the current in the wire. The forces of the electric field act on stationary electrically charged objects. They include major resources of cables, hidden electrical wires and electrical appliances, which associated with important biological influences. Electric fields have positive and negative charges (Engiz, 2018).

There is much research that highlighted on the effect of non-ionizing electromagnetic fields on sleep, cancerogenic influences and neurodegenerative diseases (Wessapan and Rattanadecho, 2018; Fernandez et al., 2019).

2.1.2. Magnetic Field

The field which act on moving electrically charged objects is called a magnetic field; it is measured by unit called Tesla (T). Among the main sources of the magnetic field are electric cables, electrical wires, electrical appliances and most electrical devices. Unlike electric fields, magnetic fields exist when operating an electrical device or device or when the power line is activated (Funk et al., 2009). Magnetic fields have beneficial and harmful biological effects; researches are still continuous in this field. Research studies that magnetic fields (i.e. EMF) that may associated with harmful health effects as leukaemia in childhood and cardiovascular effects (Miguel-Bilbao et al., 2017).

2.1.3. Specific Absorption Rate

To measure the integration of mobile phones with safety standards, a measure is used to determine the amount of RF energy absorbed by the tissue. This measure, as known as the specific absorption rate (SAR) is represented in Watts per kilogram of body weight (W/kg) (Iyama et al., 2008; Hossain et al., 2015; Hardell, 2017). There is an inverse relationship between Sar and the distance, the longer the distance between the body and the mobile phone the lower the value of SAR (Lee et al., 2017).

Unlike ionizing radiation, the RF energy has no effect on chemical bonds (i.e. DNA), it has non-ionizing radiation with relatively low frequency, Further, its biological effect can be sorted into thermal effect and non-thermal effect. The thermal effect is a

known consequence of RF exposure (Faruque et al., 2011). This effect takes place at the outer surface of the brain while the phone is on use, its magnitude and duration are considered brief and tolerable by the brain, but if the duration lasted more it can lead to a rise in body temperature, the non-thermal effect is upon the biological events within the cell via electromagnetic effect. The quantity of the electric and magnetic fields may affect and stimulate SAR value to increase. That is means the power density is increasing influenced by SAR value (Chen et al., 2017).

2.1.4. Electromagnetic Field and its Effects on Health

The chemical and electrical nature of the brain is complex. Thus, neurodegeneration can occur following exposure to EMFs, this exposure can lead to chemical, electrical, morphological and behavioural alterations among cells and tissues (Belyaev et al., 2015).

It is strongly associated with some disorders as hyperactivity, learning disabilities and behavioural problems at school for children exposed to electromagnetic fields during foetal and infant life (Sage and Burgio, 2018).

Previous studies indicated that EMF production can cause severe harm to human health especially for different tissues and organs, which disrupts their active functions (Lahkola et al., 2007; Sauter et al., 2011).

Health systems concerns prompted the researchers more suggestions to reduce exposure to non-ionizing radiation; Therefore, it was found that exposure to the EMF reduces and harms brain cells, in particular pyramidal and purkinje cells due to oxidative stress after exposure to 900 MHz and increases BBB permeability (Nittby et al., 2008; Grellier et al., 2014).

2.2. Oxidative Stress Effects and Antioxidant Defence

Oxidative stress can result from excessive accumulation of free radicals ROS and reactive nitrogen species (RNS), its occur following normal cellular metabolism, their harmful effect can be demonstrated as the destruction of DNA leading to many consequences including neurodegenerative diseases (**Figure 2**) (Lawson et al., 2017).

More experimental and clinical researches have presented that oxidative damage plays an important role in neurons injury and leads to partly loss memory as in Alzheimer's disease (Pham-Huy et al., 2008; Pena-Bautista et al., 2019). Also, oxidative stress may weaken the enzymatic activity of the protein and increase the secretion of fatty oxidation in various cells of the body (Kim et al., 2015). Therefore, the indisputable issue is that oxidative stress causes many diseases that hinder health and life such as of ageing, infertility, kidney diseases, many cardiovascular diseases and oxidizing the nucleic acids (Salim, 2017).

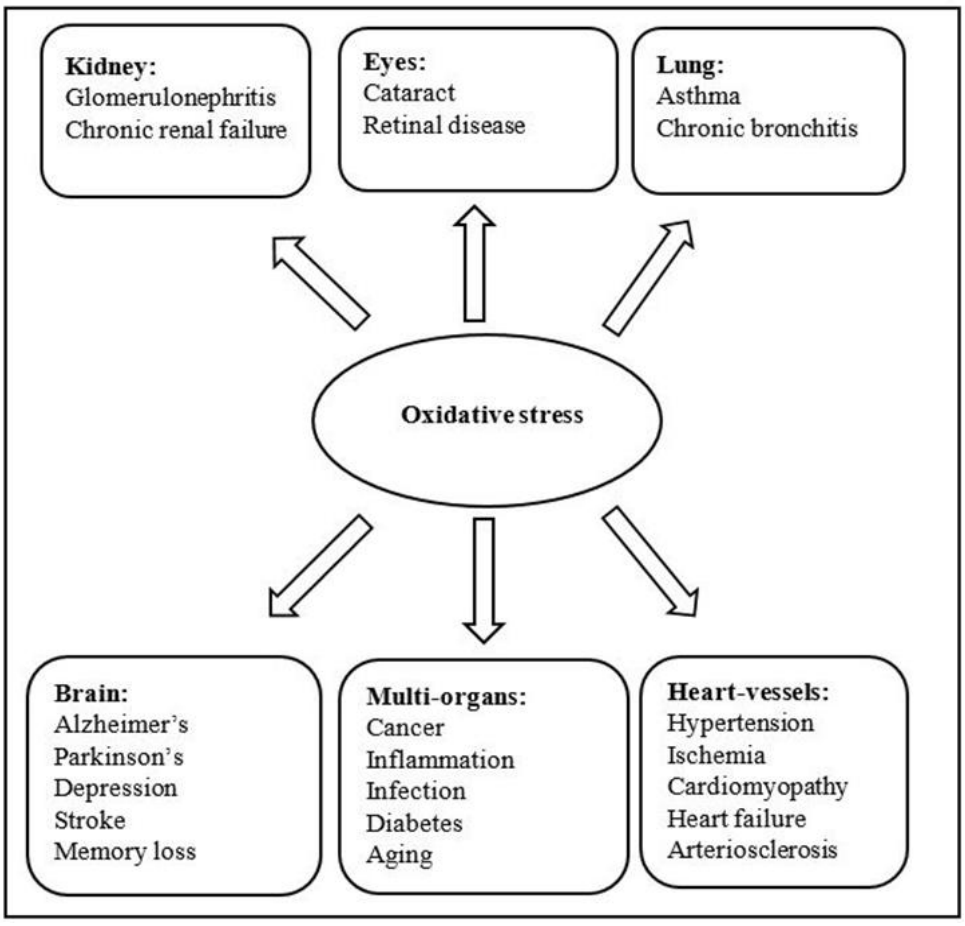

Figure 2. Oxidative stress-induced diseases in humans (Redrawn from Pham-Huy et al., 2008).

2.3. Hippocampus

2.3.1. Development of the Hippocampus

The development of the brain begins during 3rd week from the neuroectoderm, the appearance of the neural plate and tube. The neural plate develops by stimulation of the opposite part of the ectodermal layer through The notochord.

At the end of the 3rd week, the two sides of the nerve plate rise to form the neural folds. Therefore, between the two folds, the neural groove appears. The neural folds are combined in the median plane to form the neural tube. It contains two remaining holes, cephalic and caudal neuropores that connected to the amniotic cavity. The cephalic neuropore was closed on the 25th day while the closure of the caudal neuropore at the 27^{th} day of embryonic development.

When the neurulation is fully completed, the cranial end swells to form the vesicle of the brain, which gives different parts of the brain. The caudal end of the neural tube develops as a spinal cord. After the closure of cranial neuropore, two primary contractions occur to form prosencephalon, mesencephalon, and rhombencephalon, in craniocaudally respectively.

During the fifth week, two additional secondary contractions appear in the prosencephalon and rhombencephalon regions. Therefore, prosencephalon forms telencephalon and diencephalon. The hindbrain gives rise to the metencephalon and myelencephalon. While midbrain remains as midbrain during this period development. The brain contains five secondary cerebral vesicles.

The telencephalon is located at the cephalic end of the brain vesicle, which has two lateral swellings and the central part called lamina terminalis. The lateral wall of the prosencephalon on both sides fades to form the cerebral hemispheres at the beginning of the fifth week. The basal portion of the cerebral hemispheres begins to develop and extends to the floor of the lateral ventricle and around the interventricular and Monro foramina during the sixth week.

The area between the medial wall of the cerebral hemisphere and the roof of the brainstem is thin and without neuroblasts. It consists of choroid plexus, a single layer of the ependymal tissue and vascular system. Due to the uneven development of different parts of

the cerebral hemisphere, this region grows in the lateral ventricular cavity through the choroid fissure. The wall of the hemisphere above the choroid fissure becomes thickened to form the hippocampus (Sadler, 2015).

It was difficult to describe the development of the entire foetal hippocampal formation due to the rapid change in its shape. During the ninth week, the hippocampus forms between the left and right hippocampus. During the second trimester intrauterine life, the development of the hippocampus shows rotations and folding (**Figure 3**) (Insausti, 2010).

The hippocampus begins to rotate thought the reflection process, which can be completed at the twenty-first week of pregnancy in foetal development to have a seahorse shape (Duvernoy et al., 2013). The fold of DG and CA develop progressively in the temporal lobe, then with the gradually closed hippocampal fissure. At week 24, the embryonic hippocampus can be recognizing very clear the adult hippocampus (Seress et al., 2001).

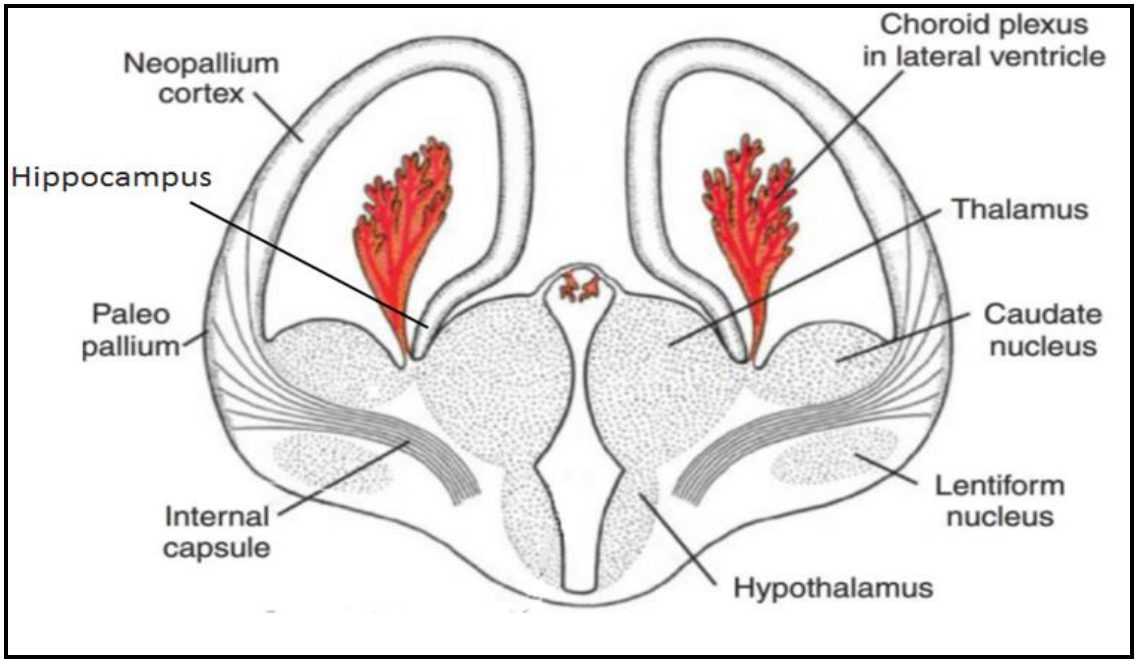

Figure 3. shows the stage of hippocampus development through the cerebral hemispheres in a 10-week fetus (Modified from Sadler, 2015)

2.3.2. Histology of the Hippocampus

The hippocampus is one of the archicortex portions. The CA region has six stratuae, arranged as moleculare, lacunosum, radiatum, pyramidale, oriens and the alveus from outer to inner direction (**Figure 4**) (Cutsuridis et al., 2010).

The alveus is a part of the hippocampus, which bulges into the temporal portion of the lateral ventricle. The bolus of the alveus has and efferent and afferent nerve fibers. The efferent fibers exiting from the hippocampus and the subiculum, and connects with septal area. While afferent fibres entering the medial wall of the hippocampus as fimbria continuation of the alveus (Boccara et al., 2015).

The stratum layer consists of basket cells, which are numerous and scattered to separate pyramidal axons on their way to reach their destination in the alveus. The stratum layer contains also the basal dendrites and interneurons of pyramidal cells. There are no clear boundaries of the stratum oriens in man because of its incomplete delineation of below stratum pyramidale (Hussein, 2009).

The stratum pyramidale contains pyramidal neurons, which are the most common type of neurons in the CA. The cell body of the pyramidal neurons has a triangular shape. The base is directed toward the alveus, while the apical part of the soma is directed toward the remnant of the hippocampal sulcus. The efferent nerve fibers arise from pyramidal neurons that cross the stratum oriens to relay in the alveus. The main connection of the pyramidal neurons between the septal nuclei and to the opposite hippocampus. Apical dendrites of each pyramidal neuron have sufficient lengths to pass the area of the CA region and terminated in the stratum molecular. The basal dendrites of the cell body, ending in the stratum oriens. Pyramidal neurons of the hippocampus have a distinct pattern of dendritic duplication, so they are called “double pyramidal” (Slomianka et al., 2011).

The pyramidal neurons of this layer lie in a bundle of nerve fibers originating from the basket cells of the stratum oriens. The stratum pyramidale also includes stellate neurons and basket cell interneurons like other parts of CA (Duvernoy, 2005). The stratum radiatum has striations lines, due to the parallel arrangement of nerve fibers. The apical dendrites, from the pyramidal neurons of the stratum pyramidale, form the main component of this layer (Hammond, 2015).

The perforating fibers and their collateral are predominant in the Stratum lacunosum layer. They have a parallel path with the CA surface. The stratum molecular consists of apical dendrites of the pyramidal neurons and few numbers of interneurons. As the sulcus of the hippocampus gradually decreases as the hippocampus develops, it becomes difficult to distinguish between the DG and the stratum molecular in CA, as it merges (Burwell and Agster, 2008).

.

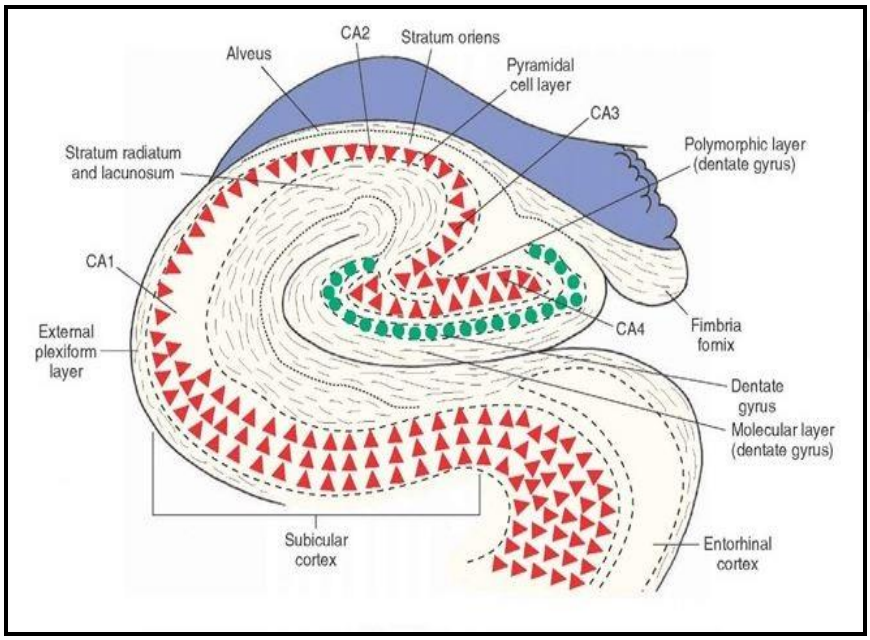

Figure 4. Shows Cornu Ammonis regions in different layers (Modified from Pang et al., 2019)

2.3.3. Functional Anatomy of the Hippocampus

The hippocampus is located within the temporal lobe, which is considered a distinguished region in the brain and participates as a main part of limbic system. The shape of the hippocampus appears like (the sea horse in Greek word) in coronal plane view. The CA, DG and the subiculum are main parts of hippocampus. Structural hippocampus organizes and contains of three parts: head, body, and tail (Ranganath et al., 2005). Hippocampus extends about 5 cm anteroposterior direction. The head of hippocampus is connected to the amygdala, which is located in anteroposterior side of the head (**Figure 5**).

The posterior part of the uncus has relationship with medial part of hippocampus. The DG terminate just caudal to the calcarine sulcus of the occipital lobe (Kesner, 2013).

The hippocampus consists of two layers of cells in the form of a pyramid. The outer layer consists of large pyramidal cells, while the inner layer consists of medium-sized pyramidal cells (Cappaert et al., 2015).

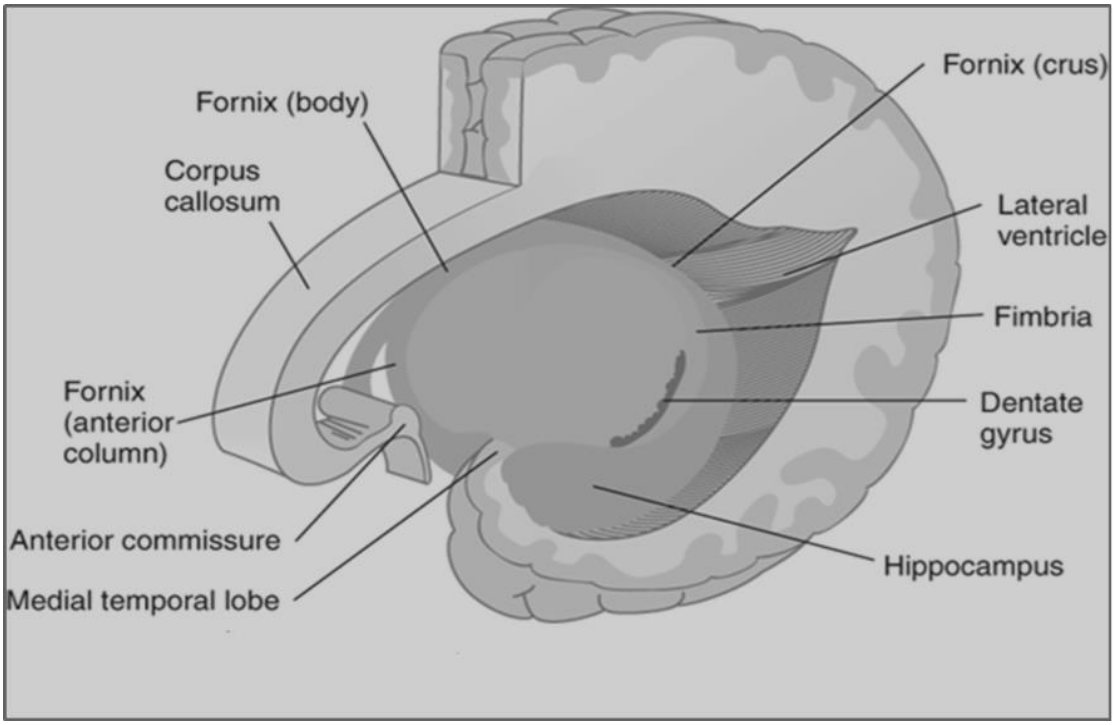

Figure 5. Hippocampus and structure related (Redrawn from Waxman, 2010)

The pyramidal cells in the hippocampus are grouped into four parts according to their size and density; these are CA1, 2, 3 and 4. The cells in CA1 are small in comparison to CA3 cells, while the latter is loosely close to each other in comparison to those of CA1.

The hippocampal sulcus separates the DG from the hippocampal gyrus while the fimbrio dentate sulcus separates the dentate gyrus from the fimbria of the hippocampus, the dentate gyrus appears partly at the surface of the brain. The alveus comprises a layer of cells at the inner border of the ventricle, efferent fibers are collected and run forming the fimbriae. The subiculum forms a transitional zone that is located between the bordering entorhinal cortex and the Ammon's horn (O'Neill et al., 2017).

2.3.3.1. The Papez Circuit

The circuit of papez includes several brain regions, which was described in 1937 by neuroanatomist called James Papez. This circuit joins the connections between the hippocampus, medial diencephalon and cingulate gyrus. The connections of the information start from hippocampus through the cingulate gyrus, cingulum and parahippocampal gyrus, then reaching to mammillary body through fornix, then circuit end and feedback to the cortex is accomplished through mammillothalamic fibers, relaying information from the hypothalamus to the anterior nucleus of the thalamus. The anterior nucleus of the thalamus projects fibers to the cingulate gyrus, cingulum and parahippocampal gyrus retain to the first step from hippocampus. The circle, presented by McLean in 1952, is a model that explains the limbic system (**Figure 6**) (Waxman, 2010).

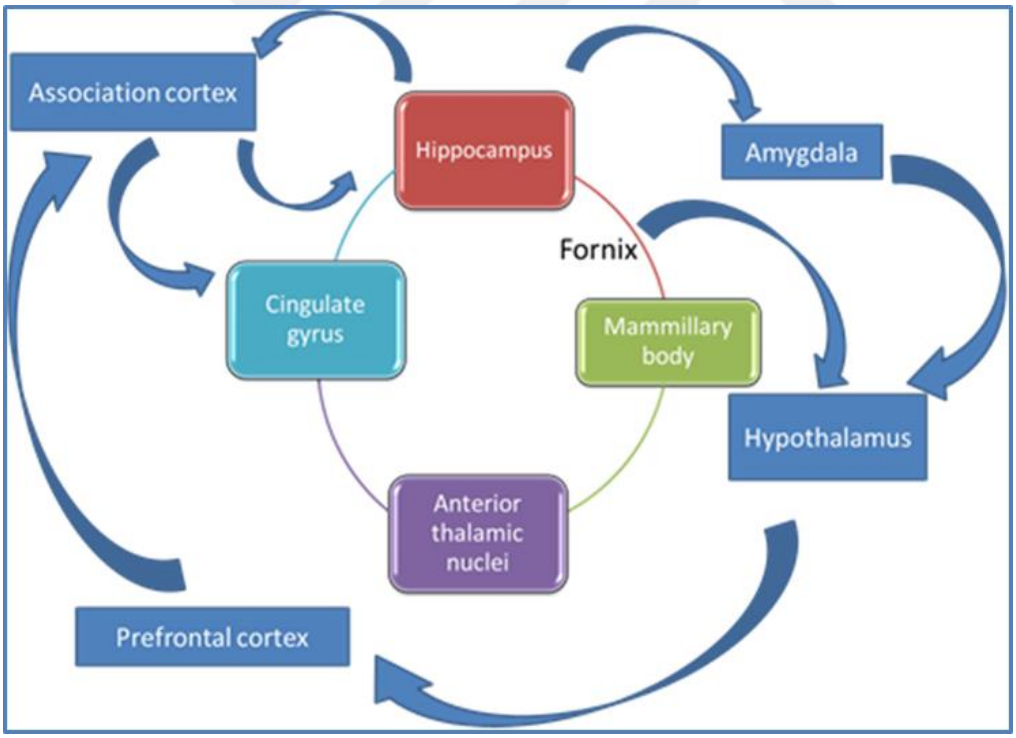

Figure 6. Papez circuit (Redrawn from Cardinali, 2018)

2.3.4. Regions of Cornu Ammonis in the Hippocampus

There are four regions of Cornu Ammonis named as (CA1, CA2, CA3 and CA4) (Duvernoy et al., 2013). CA1 region is a continuation of the sub-curriculum, and this region is characterized by the presence of a few rows of medium-sized of pyramidal neurons. Their cell body has a triangular shape. (Ogawa et al., 2018).

The CA2 region consists of large, highly oval and dense neurons unlike CA1 and located near or at the top of the CA. The CA3 region represents the region where the CA bends to curve within the DG curvature. The body of the pyramidal neurons in this region is similar to those in the CA2 region but neurons in the CA3 region have low density than those in CA2. The CA3 region is marked by the unmyelinated fibers presence, which arising from the DG (Wible, 2013).

CA4 is conveniently located within the DG curvature. Therefore, it is easy to defecate between CA4 and the CA3 region. The cell body of the neuron in the CA4 region is spherical, giant, less numerous and sparse (Su et al., 2018).

2.3.5. Hippocampus Functions

The hippocampus plays key roles in spatial navigation, learning and memory owing to its dense connections with other brain regions (Stella et al., 2012). In addition, the connections between the hippocampus and the cerebral cortex have a role in the information process. Multi/mono Synaptic path (direct path) is an important path for learning and memory (Morgado-Bernal, 2011). The amygdala is the primary regulator of emotional behaviour; the hippocampus has mutual ties with the amygdala that facilitate mutual influences in regulating emotional behavior. This influence on emotional behaviour is dominated by the amygdala more than the hippocampus (Toyoda et al., 2011).

The hippocampus also plays a role in motor functions because it is an important part of the ventral striatum ring (Molnar, 2011). The functions of the hippocampus are greatly affected by the generation of new neurons within the DG, and thus the flexibility of the hippocampus will increase because the DG receives most of the nerve signals that enter the hippocampus (Gonçalves et al., 2016).

The neurogenesis process continues throughout life in two major regions of the brain DG hippocampus and olfactory bulb (Ming and Song, 2005).

About 700 new granular cells in a human DG are produced daily, implying that the formation of neurons in adulthood can add significant structural and functional plasticity in the triple synaptic circles of the hippocampus (Spalding et al., 2013). The subgranular region of the DG produces new granular neurons that are incorporated into the hippocampus circuit to influence important hippocampal functions such as learning and spatial memory formation by performing a pattern separation on the signals transmitted from the cerebral cortex. Cumulative evidence suggests that the formation of hippocampal neurons plays primary hippocampal roles (Jin, 2016). In this regard, the neurogenesis in the DG generates neurons that are linked to the circuits of the hippocampus to influence an important function such as memory and learning (Adler et al., 2018).

2.4. *Adansonia digitata*

Adansonia digitata (AD) is a unique tree because it is a multi-benefit that belongs to the Malvaceae family (Talari et al., 2017). AD fruit tree grows naturally in dry African regions, mostly in tropical Africa. It is distinguished by its enormous size with a very large trunk, reaching to a height of 23 m or more with a lifespan of several hundred years (**Figure 7**) (Hussain et al., 2019).

It has common names in Sudan, such as Gongulaze and Tebaldi (**Figure 8**), it has other indigenous names are common around the world such as Baobab (in English), dead-rat tree, monkey bread, and upside down tree (Satti, 2018).

It is observed that in many African countries, all parts of it are used where the trees are located. AD fruit has been classified as a food ingredient in Europe and the United States, and therefore it has nutritional values (Sokeng et al., 2019). Antioxidant activities are exhibited by some phytochemicals in fruits (Genovese et al., 2008). It has been prove that diseases caused by oxidative stress can be effectively treated with the phenolic compounds present in AD (Haminiuk et al., 2012).

AD is distinguished as a dietary supplement and a powerful anti-oxidant and anti-inflammatory, aided by the presence of polysaccharides that inhibit the Cyclooxygenase

(COX) -1 and COX-2 and more efficient in COX-2 inhibition than COX-1 (Makawi et al., 2019).

Vitamin C is found in high content in the pulp of the fruit, its concentration is ranged from 1723 to 4991 mg/kg; it is 10 times more than that of the oranges. The pulp also is rich in pectin and contains sugar; however, there is no starch (Imge et al., 2010).

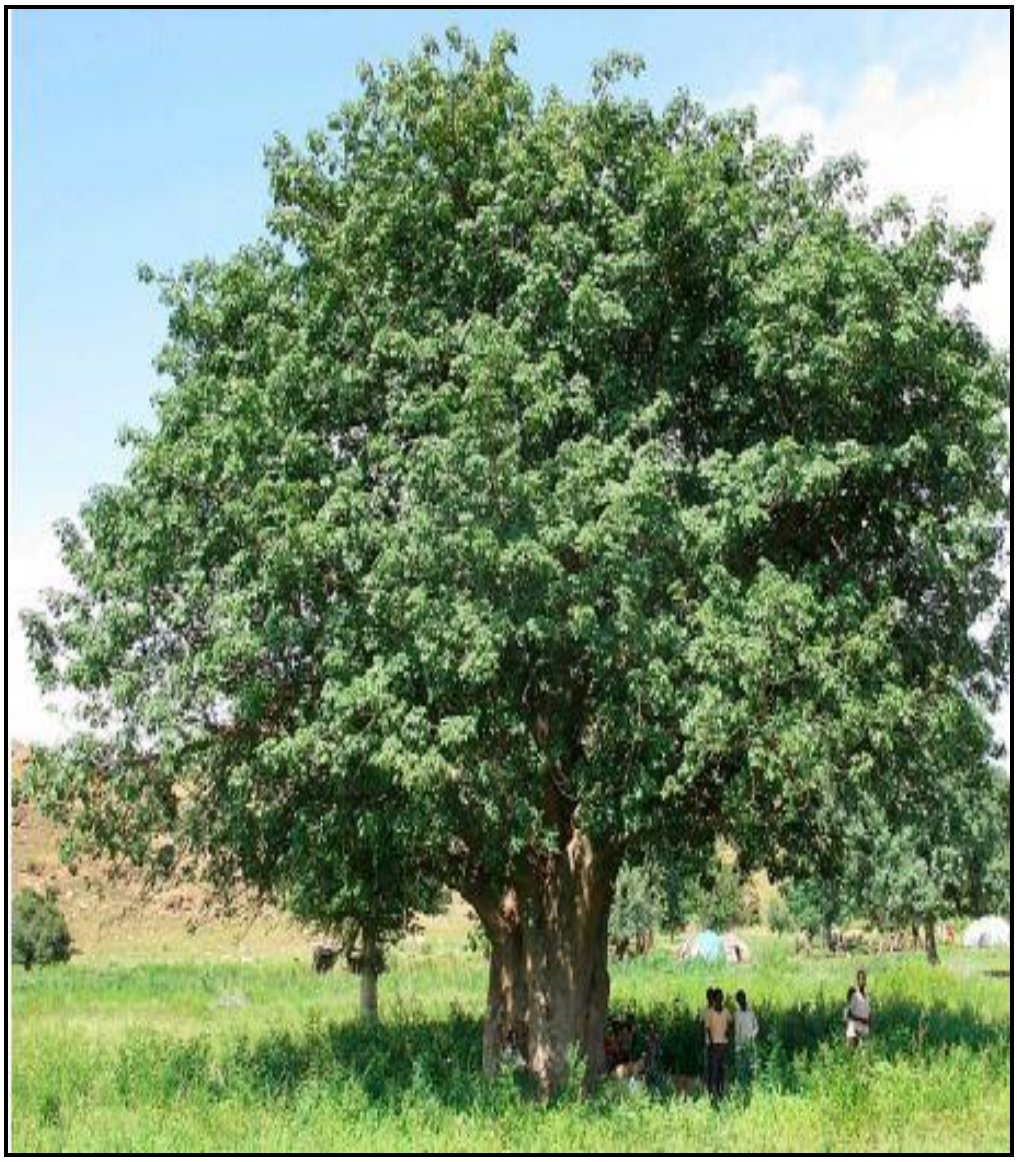

Figure 7. *Adansonia digitata* tree (Wiehle et al., 2014)

The tree of the AD is useful as a source of feed and medicine in African tradition in several regions, its seed is rich in oil and protein as well as energy, it contains vitamin C and is considered as an antioxidant, it is sometimes referred to as the “chemist tree” or the “small pharmacy” (Vertuani et al., 2002).

Figure 8. *Adansonia digitata* fruit

2.4.1. Traditional Use of *Adansonia digitata* Fruit

AD fruit is used as a food source, as well as in complementary medicine. This plant has received great attention from researchers as it found leaves, seeds and bark used to treat diarrhea, anemia, malaria and tuberculosis, as well as fever, and fruit is used to treat microbial infections (Vermaak et al., 2011).

AD fruit was chosen for study along with several indigenous fruits because of their crucial importance for rural communities (Buchmann et al., 2010).

The effects of anti-inflammatory and analgesic of the aqueous extract of AD fruit pulp has been proven in rat models, which serve the basis for its use in human for its earlier mentioned attributes (Elsaid, 2013).

Numerous diseases such as diarrhea, malaria and microbial infections are treated using AD plant parts. Its vitamin C content is estimated to be 7 to 10 times more than oranges; therefore, rich content of vitamin C makes it an efficient antioxidant (Althwab et al., 2019).

AD has various benefits; it is known as an antimicrobial, antiviral, anti-inflammatory as well as antioxidant (Rahul et al., 2015). The analysis of phytochemical of AD revealed its contents of phytosterols, amino acids, flavonoids, fatty acids, minerals, and vitamins. It also contains thiamine, iron, lysine, and calcium, in its seeds; its properties make it a valuable product for the local societies (Kamatou et al., 2011).

2.4.2. Bioactive Compounds and Nutritional Attributes of *Adansonia digitata*

The contents of AD pulp shows high levels of minerals (magnesium, iron, calcium, and sodium) as well as sugars, vitamin C, essential amino acids, organic acids, sterols, saponins, triterpenes, cellulose, tannins, flavonoids and fibers, leaves hold proteins of good quality while seeds comprise essential oils with provitamin A carotenoids as well as fatty acids with linoleic and in high concentration. It shows anti-inflammatory, antioxidant, antipyretic, analgesic, hepatoprotective, antidiarrhea, as well as antimicrobial properties (De Caluwé et al., 2010; Tembo et al., 2017).

It is worth noting that the baobab fruit pulp has a well-documented anti-oxidant capacity. This is evidence of the presence of antioxidant properties, flavonoids, and vitamins in most local fruits, which can play a role in extending the shelf life of drinks and food derivatives in factories and companies. This prevents the oxidation of fats in food (Assogbadjo et al., 2012).

It has become noticeable that interest in fruits provides health benefits, as a recent study indicated that and attracted attention to phenolic compounds in AD fruit, as they act as potential agents for the prevention and treatment of many diseases linked with oxidative stress (Kabine et al., 2015).

2.5. *Nigella sativa*

Nigella sativa (NS) is an annual herbaceous plant, which belongs to the botanical family of Ranunculaceae. The height of the plant is about 20-60 cm (**Figure 9**). The Black seeds (BS) in the Middle East and Arab countries are known as *'Habbet el Baraka', 'Habbah Sauda' and 'Kamun aswad'* and they are shaped like angular (**Figure 10**) (Nasreen et al., 2018). The beneficial properties of NS oil are coming from TQ, which is one of the most active constituents of the NS (Vaz et al., 2018).

Figure 9. *Nigella sativa* plant (Sharma et al., 2009)

2.5.1. Traditional Use of *Nigella sativa*

NS plants have been used conventionally since a long time ago in Northern Africa, Middle East, Asia and used in herbal medicine all over the world for the treatment of many diseases like asthma, diarrhoea, and dyslipidemia (Erbogaa, 2015).

It has been observed that the treatment effects of NS oils and TQ enhance protection against nephrotoxic and hepatotoxicity caused by diseases. Therefore, NS has been used to treat various diseases since ancient times (Al-Rouby and Gawish, 2013).

Figure 10. *Nigella sativa* seeds

In Middle and Far East this herb was used for complains and for the treatment of asthma and respiratory inflammation, headaches, severe back pain and high blood pressure, obesity and dysentery, the effect of this herb has Islamic interpretation (Ali and Blunden, 2003).

NS has anti-diabetic, immunological enhancement, anti-ulcerogenic, antibacterial, anti-carcinogenic and it has amazing efficacy mainly due to TQ content and rich in antioxidants (Sahak et al., 2016; Perveen, 2019). Thus we can say that it has a traditional therapeutic effect for diseases such as burns, skin infections, asthma, coughs, diabetes and joint pain and this makes it the focus of attention of researchers (Butt and Sultan, 2010).

Numerous studies conducted in-vivo and in-vitro indicate that NS has an antioxidant effect that enhances neuroprotective against neurodegenerative disorders (Sedaghat et al., 2014; Islam et al., 2015).

NS has a protective role versus renal toxicity (Yaman and Balikci, 2010). NS oil can be an effective treatment that greatly reduces testicular damage by inhibiting the risk of the impacts of oxidative stress (Mohamed et al., 2015). It is used as a medicinal plant to treat various diseases (Ali and Blunden, 2003; Asiaei et al., 2017).

Nevertheless, the possibility of an effective neuroprotective treatment is based upon the fact that NS oil has protective effects on fat peroxidation in hippocampus in rat model brain ischemia injery (Hosseinzadeh et al., 2007).

It has been studied that the radical scavenging activity of NS are very important because of the harmful role of free radicals in our biological systems, so it is considered useful in treating many diseases that occur as a result of free radicals or oxidative stress (Burits and Bucar, 2000). Furthermore, the study showed that the use of NS helps to prevent and improve the treatment of nervous system disorders such as neurotoxicity and memory in seizure (Tavakkoli et al., 2017; Demirel et al., 2018).

In this context, It has become necessary to conduct more qualitative studies on antioxidants and the toxic effects of this substance in order to understand metabolic mechanisms due to the wide use of NS in alternative medicine.

2.5.2. Bioactive Compounds and Nutritional Attributes of *Nigella sativa*

The chemical composition of NS contains protein, carbohydrates, saponins, fibers and oil. Also includes 36–38% fixed oils, which are arachidic, palmitic, oleic, linoleic, stearic, myristic, linoleic acids (Cascella et al., 2018). The main phenolic compounds of NS are thymol, carvacrol, p-cymene, TQ ($C_{10}H_{12}O_2$), as well as thymohydroquinone are the most important active compounds in NS (Jaswal and Shukla, 2015).

3. MATERIAL AND METHODS

3.1. Preparation of Aqueous Extract of Herbals

3.1.1. Preparation of Aqueous Extract of *Adansonia digitata*

The dried powdered fruits of AD belong to Malvaceae Family. The powdered fruits were purchased from the Khartoum market in Sudan. The powdered pulp sample, 50 g was weighed then was immersed in distilled water for one hour, filtered through filter paper and stored at -20°C until used. The extract was freshly prepared every week.

3.1.2. Preparation of Aqueous Extract of *Nigella sativa*

The NS was purchased from the Khartoum market in Sudan. The seeds were crushed and 65 g was weighed. The crushed NS was immersed in distilled water. The aqueous extraction was immersed in distilled water for one hour and filtered through filter paper. The extract prepared every week freshly and kept at -20°C until used (**Figure 11**).

Figure 11. Aqueous extracts of *Adansonia digitata* and *Nigella sativa*

3.2. Experimental Animals

This study was conducted at the Animal Research Center of Ondokuz Mayis University with the approval of the ethics committee on 30.03.2018 and numbered 2018/17.

Fifty-six male *Wistar albino* rats, 12 weeks old and weighing 300±50 g were obtained from the Experimental Animal Research Center of Ondokuz Mayis University. The animals were kept in polypropylene cages with clean wood shaving bedding at 25 ± 1° C, 50% relative humidity and 12 h light/12 h dark cycle. Animals had free access to food and water (**Figure 12**).

Figure 12. Male *Wistar albino* rats of the present study

3.3. Experimental Study Design

In this study, 56 male *Wistar albino* rats were randomly divided into 8 groups, each containing 7 rats as follows:

1. **Group (A):** Control group (n: 7)

This group will not be exposed to any special protocol for 28 days.

2. **Group (B):** Sham group (n: 7)

This group was exposed to the stress condition in a special chamber for one hour between 08:00 -09:00 am, for a period of 28 days at the same as EMF groups. However, this group was not exposed to EMF radiation. Throughout the experiment, rats were fed with standard pellet diet and tap water was available ad libitum.

3. **Group (C):** EMF group (n: 7)

This group was exposed to EMF of 900 MHz for 60 min/day between 09:00 -10:00 a.m. for a period of 28 days (**Figure 13**).

4. **Group (D):** EMF+ AD group (n: 7)

This group were received aqueous extract of AD (300 mg/kg/day) by oral gavage and exposed to EMF between 09:00 -10:00 a.m. for a period of 28 days.

Figure 13. The device was used to expose 900 MHz EMF radiation for rats in the round plastic cage

5. **Group (E):** EMF+ NS group (n: 7)

This group were received aqueous extract of NS (400 mg/kg/day) by oral gavage and exposed to EMF between 10:00 -11:00 a.m. for a period of 28 days.

6. **Group (F):** EMF + AD + NS group (n: 7)

This group were received aqueous extract of AD (300 mg/kg/day) + aqueous extract of NS (400 mg/kg/day) by oral gavage and exposed to EMF between 10:00 -11:00 a.m. for a period of 28 days.

7. **Group (G):** AD (n: 7)

This group was received aqueous extract of AD (300 mg/kg/day) by oral gavage for a period of 28 days (**Figure 14**).

Figure 14. Oral gavage was used for rats to receive aqueous extract of *Adansonia digitata*

8. **Group (H):** NS group (n: 7)

This group was received aqueous extract of NS (400 mg/kg/day) by oral gavage for a period of 28 days (**Figure 15**).

Figure 15. Oral gavage was used for rats to receive aqueous extract of *Nigella sativa*

In EMF given groups, we used 900 to 1800 MHz; 2-Watts output signal generator can operate the frequency (Microwave Test Transmitter, Set Electronic Ltd., Turkey). Round plastic cage with 16 separate parts, electromagnetic waves that can transmit monopole special EMF exposure apparatus comprising an EMF meter used to measure the antenna and electric field intensity (Holaday Industry Co., Adapazari, Turkey) (Bilgici et al., 2013) were used.

In order to achieve EMF exposure in the relevant groups, the monopole antenna is placed perpendicular to the plastic cage to provide equal EMF distribution.

Air holes of one cm in diameter were made on the cage to reduce the stress of the rats in the polycarbonate cage. For exposure, the respective rats were positioned at an equal distance from each other, with the head portions facing the monopole antenna. Rats belonging to the EMF group were subjected to EMF exposure for a period of 28 days.

3.4. Preparation of Samples

3.4.1. Perfusion

The rats were anesthetized intraperitoneally at 50 mg/kg ketamine (Ketalar®, Pfizer, Istanbul, Turkey) and 5 mg/kg xylazine (Xylazinbio®, Intermed pharmacy store, Ankara, Turkey) (Yurt et al., 2018).

Figure 16. Anaesthetic solutions were used before perfusion procedure

The rats were placed on the mesh; the chest cavity was opened to make the heart clearly visible. A plastic cannula was inserted into the heart through the top of the left ventricle and was supplied with 0.9% of the saline solution. Before the giving the saline solution, an incision was made in the right atrium. When the blood was completely removed, the tissue was fixed with 10% formalin. Tetanic contractions in rats had shown to be a sign of successful detection for a good perfusion level. The rats were decapitated after body hardening. Furthermore, the brain tissues were removed from the skulls and placed in small plastic containers. Post-fixation was performed with 10% formalin for 2 weeks. The solutions were changed every 3 days. The right and left hemispheres of the brains were separated from each other.

The right hemispheres were used for light microscopy and stereological analysis. One left hemisphere from each group was used for electron microscopic examination.

3.4.2. Follow-up of Tissue Processing

After the post-fixation period of 2 weeks, the right hemispheres were placed in the tissue tracking cassettes and placed under the tap water overnight with appropriate labelling and 10% formalin was removed from the tissue. Then, the tissues were dehydrated by passing through alcohol series (70%, 80%, 96%, and 100%). Afterward, the tissues were treated with xylene to remove the alcohol and render tissues transparent and facilitate paraffin infiltration (**Table 1**). Tissue follow-ups were performed using the tissue-monitoring device (Thermon Shandon Citadel, Germany) (**Figure 17A**). The tissues taken from hot paraffin were embedded in paraffin-filled L-bars, which were squarely shaped on a smooth surface. Then all the groups were labelled in a double-blind manner by inserting the rectangular small cardboards and codes inside the blocks (**Figure 17B**).

3.4.3. Sectioning procedure

The sections were taken using a rotary microtome (Leica RM 2245, Leica Instruments, Nussloch, Germany) with disposable metal microtome blades (Type N35, Feather Company, Osaka, Japan) to obtain 4 μm and 20 μm sections from the paraffin blocks for light microscopic and stereological investigations.

According to the result of the pilot study and systematic random sampling strategy, we took 1/6 section in 20 μm thick sections for stereological analysis and 4 μm thin sections for light microscope (**Figure 17C**). Sections were placed at a water temperature of 45ºC in the water bath (Leica HI1210) containing powdered gelatine to allow the tissue to adhere strongly on the glass. Sections taken from the water bath were taken to the slides for staining. The slides were allowed to stand overnight at 58°C to remove the paraffin from the tissues and stained with cresyl violet for light microscopy and stereological analysis.

Table 1. Routine tissue processing stages for brain tissue

Chemicals	Duration
70% alcohol (Ethyl Alcohol-Tekkim Chemicals -Turkey)	1 hour
80% alcohol	Overnight
96% alcohol	1 hour
100% alcohol	2 hours
100% alcohol	2 hours
100% alcohol	2 hours
Xylene (Sigma-Aldrich)	1 hour
Xylene	1 hour
Xylene	1 hour
Paraplast (Tekkim Chemicals -Turkey)	1 hour 30 minutes
Paraplast	1 hour 30 minutes

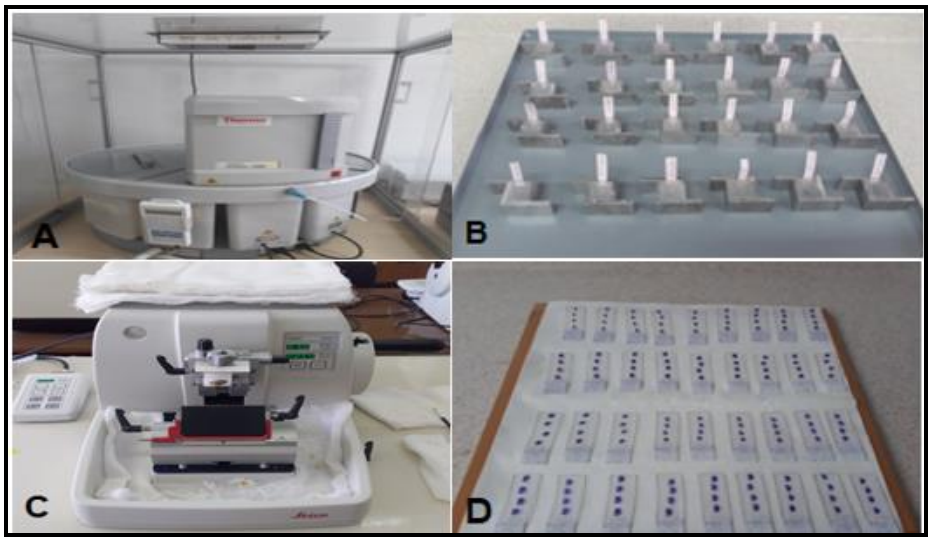

Figure17. (A) Fixed brain tissue was put it in the tissue processing device, (B) followed by embedding with L-shaped iron moulds, (C) thick and thin sections were taken by using a Leica microtome, (D) sections were deparaffinised and then stained with cresyl violet

3.4.4. Cresyl Violet Staining Process

Brain tissue sections were stained by the cresyl violet staining procedure obtained by dissolving 0.1 g of cresyl violet in 100 ml of distilled water (**Table 2**).

Table 2. Cresyl violet staining procedure

Chemicals	Duration
Xylene (Sigma-Aldrich)(x4)	30 minutes
100% Alcohol (x2)	10 minutes
96% Alcohol	10 minutes
80% Alcohol (Ethyl Alcohol-Tekkim Chemicals -Turkey)	10 minutes
70% Alcohol	10 minutes
Distilled water	5 minutes
Cresyl violet (Sigma C5042-10G)	4 minutes
Distilled water	5 minutes
70% Alcohol	5 minutes
80% Alcohol	5 minutes
96% Alcohol	5 minutes
Cresyl violet solution	Shaking
96% Alcohol	5 minutes
100% Alcohol	5 minutes
Xylene (x2)	40 minutes
Entellan (Merck)	For covering

A single section has been conducted as a pilot study to determine the penetration time of the tissue dye before incorporating sections of all groups in the staining. The cover glass was mounted in slides by using drops of entellan and allowed to dry for several days (**Figure 17D**).

3.4.5. Tissue Preparation for Electron Microscopy

One left hemisphere of brain from each group was fixed in glutaraldehyde. After fixation in glutaraldehyde, the brains were dissected into small pieces using a binocular dissecting microscope to obtain the hippocampus. Then the sampled tissues were processed according to the protocol in (**Table 3**) and embedded in resin.

Table 3. Chemicals and duration in tissue processing for electron microscopic examination

Chemicals	Duration
4% Glutaraldehyde	1 hour
0.1 M Phosphate buffer for washing	4 x15 minutes
1% Osmium tetroxide	1.5 hour (dark)
0.1 M Phosphate buffer for washing	4 x15 minutes
50% Acetone	15 minutes
70% Acetone	15 minutes
95% Acetone	15 minutes
100% Acetone	15 minutes
100% Acetone	15 minutes
Propylene oxide	20 minutes
Propylene oxide	20 minutes
50% Propylene oxide + 50% Araldite mixture	1 hour
100% Araldite	1 hour

The resin-embedded tissue blocks were sectioned by an ultra microtome (Leica Ultracut UCT, Leica Microsystems GmbH, Germany) using a glass knife. Semi-thin sections in 0.5 μm thickness ware taken on glass slides and stained with 1% toluidine blue prepared with sodium borate. Thin sections of 70 nm thickness have been taken for histopathological examination by scanning transmission electron microscope (STEM) (JEOL, JSM-7001F, Tokyo, Japan).

3.5. Stereological Analysis

3.5.1. Stereology

The basis of stereological methods is to provide quantitative and unbiased estimates, which obtain three-dimensional data from two-dimensional sections. By means of the principle of these techniques is data that does not deviate systematically from the real value are obtained. And also, the achievement of the real value with a small error in a short time would be possible (Altunkaynak et al., 2012).

Unbiased and reliable stereological methods have been used in many studies (Schmitz et al., 2014; Geuna and Herrera-Rincon, 2015).The systematic random sampling (SRS) is the basis for the implementation of the rules of stereological methods. Analysis of tissue samples which were taken from the tissue to be held at equal intervals in order to give equal opportunity to each point sampling (Schmitz and Hof, 2005; Brown, 2017).

3.5.2. Optical Fractionator Method and its Application

The total numbers of pyramidal neurons in the hippocampus of rats were estimated by using optical fractionator technique, which is one of the objective and reliable stereological methods. For this purpose, we used a stereology workstation that consists of a computer-assisted software with supporting of stereological analysis (Stereo Investigator 9.0, Microbrightfield, Colchester, USA) found in the Histology and Embryology Department, Faculty of Medicine, Ondokuz Mayis University and Histology and Embryology Department, Faculty of Medicine, Recep Tayyip Erdogan University (**Figure 18**).

Figure 18. Stereology analysis system

The optical fractionator technique makes it possible to calculate the total number of cells or particles in thick sections. In the implementation of this method, a stereological probe, optic disector and SRS, is applied together (Gundersen and Jensen, 1987). The optical fractionator method is not influenced by the size and orientation of the particles and also from shrinking or expanding of the structure during histological tissue procedures. This is one of the most effective particles counting method used in stereology (West et al., 1991). In this study, 20 μm coronal sections were taken from the right cerebral hemisphere at 1/12 sampling interval according to the SRS. This process was carried out by taking randomly one section from the whole, after this, other sampled sections would be selected according to the first one, 1/12, first selection provides randomness, other selection provides systematic. This approach is called the SRS (West et al., 1991). The first section selection has been applied to each animal. Then, every sequential 12^{th} section was taken from the series. Sectioning was continued until the brain tissue was completed in the block and about 20-30 sections of each rat brain were taken. Thus, the section-sampling rate is

(1/12), which is one of the parameters essential to estimate the total number of cells according to the optical fractionator technique.

The pyramidal neurons are counted by the optical fractionator technique, which based on the pilot study the border of CA1, CA2, and CA3 regions were determined by using stereotaxic atlas (Paxinos and Watson, 2007). In the pilot study, the size of the counting frame was determined as 3600 μm^2, the step interval was 14400 μm^2, and the area sampling fraction (asf) was 3600 μm^2 / 14400 μm^2.

The total number of neurons obtained after the stereological analysis of the sections was estimated by using the formula given below (West et al., 1991). At this point, the total number of pyramidal cells in the hippocampus (N) was determined by the following formula:

$$N = \sum Q^{-} \cdot \frac{1}{ssf} \cdot \frac{1}{asf} \cdot \frac{1}{tsf}$$

Where ΣQ^{-} represents the total number of counted disector pyramidal cells, which were counted cells in all sampled section from the whole hippocampus for each animal. *ssf* is a section-sampling fraction, which represents the ratio of the microscopic sections that were taken for the stereological analysis from the whole right hemisphere (*1/12*). *asf* represents the ratio of the sectional area that was used in the sampled sections (*3600 μm^2 / 14400 μm^2*). *tsf* is thickness sampling fraction, represents the part of the investigated section in the z axis (*h/mean thickness*).

3.5.3. Unbiased Counting Frame

The unbiased counting frame is a simple rectangle with four borders made up of two types of lines, a thick continuous line (exclusion line) with extensions and a thin dashed line (inclusion line) (**Figure 19**). To obtain highly accurate data during stereological analysis, every single particle should be sampled once during the counting. The unbiased counting frame counting rules are different from other counting frames. The particles which are hitting the inclusion line or completely inside of the unbiased counting frame will be

counted, the particles hitting the exclusion line, or it is extensions will not be counted, in addition to that the particles completely outside the unbiased counting frame will not be counted. The unbiased counting frame is the most efficient and reliable counting frame for particle counting (Gundersen, 1977).

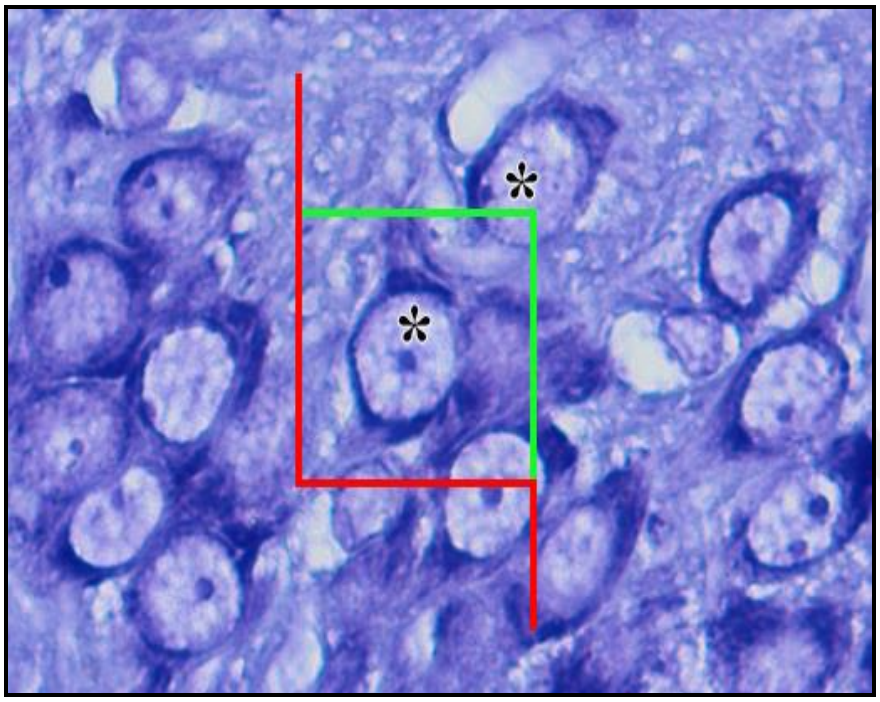

Figure 19. Unbiased counting frame. Countable neurons were indicated by star

3.6. Biochemical Analysis

3.6.1. Blood Sample Collection

Before the perfusion procedure 3 ml of intracardiac blood was collected from the heart of rats into blood collection tubes, then the blood centrifuged at 4°C (Hermle Labor Technik GmbH - Z 300 K Universal Centrifuge with a cooling system, Germany) for 15 min at 2000 rpm. The serum samples were obtained and stored at -80°C until biochemical analysis was done. The CAT and SOD enzyme activities in the serum samples were analysed by measuring absorbance values (**Figure 20**).

3.6.2. Analysis of Catalase Enzyme Activity

CAT is antioxidant enzyme involved in the detoxification of hydrogen peroxide (H_2O_2), which is a toxic product of normal aerobic metabolism. The H_2O_2 at a low level stimulates the expression of stress-associated proteins and antioxidant enzymes, thus providing a response against oxidants.

Figure 20. Centrifuge device

The conversion of the H_2O_2 molecule into oxygen and water occurs by the CAT enzyme. CAT demonstrates peroxidatic activity, in which low molecular weight alcohols can serve as electron donors (Das and Saha, 2009). To determine the oxidative effect, Cayman's Catalase Assay Kit (Cayman Chemical Company, USA) utilized for determination of enzyme activity in the serum. The basic principle in the method is based on the CAT enzyme reaction with methanol in the presence of H_2O_2. In this reaction, formaldehyde acts as a chromogen, causing a pink colour in the reaction. After the relevant reactions, the absorbance of the samples was measured at 540 nm. CAT samples were read by a BioTek Synergy 4 microplate-reader (**Figure 21**).

3.6.3. Analysis of Superoxide Dismutase Enzyme Activity

Extremely reactive radicals generated by enzymes, such as mitochondrial electron chain and xanthine oxidase, appear in different pathologies with accumulation of superoxide anions (O2-) in cells and tissues (Storz, 2006; Hassan et al., 2017). The role of SODs in modifying pathophysiology of various disease processes has been revealed in genetically modified mice (Santo et al., 2016).

Figure 21. BioTek Synergy 4 Microplate-Reader Device

Accumulation of these molecules and other oxidant radicals should be avoided in order to resist the toxic effects of oxygen in aerobic organisms. When oxygen toxicity occurs in living tissues, an enzymatic defence mechanism initiated by SOD catalyzes the dismutation of oxygen and metalloenzymes (Assady et al., 2011). In the present study for assessing oxidative stress, SOD enzyme activity was measured using the SOD assay kit (Cayman Chemical Company, USA). The main principle of the SOD assay kit used is based on the principle that xanthine-xanthine oxidase reaction results in the reaction with tetrazolium compound and purple reaction by removing superoxide radicals.

The SOD in the sample removes the superoxide radicals from the medium and inhibits the reaction of the tetrazolium compound with oxygen. The absorbance values of the purple-coloured solutions obtained after the experiment were measured by using Tecan Sunrise Microplate Reader (**Figure 22**) at a wavelength of 450 nm.

Figure 22. Sunrise Microplate Reader Device

3.7. Determination of Total Phenolic Content and Antioxidant Power

3.7.1. Preparation of Sample Extract

The samples extraction of AD and NS were made by ultrasound-assisted extraction with 80% methyl alcohol. For this, 2.5 g of the sample was added to 50 ml of 80% methyl alcohol at 20 °C for 30 minutes in an ultrasonic water bath, then at room temperature for 2 hours. Centrifuge for 15 minutes at 3000 rpm to remove turbidity. The pre-analysis samples were filtered through a 0.45µm filter.

3.7.2. Method to Assess the Total Phenolic Content

Singleton and Rossi's (1965) method of determining the total phenolic content was modified. 2.5 ml of Folin-Ciocalteu reagent was added to a 0.5 ml of sample diluted with

the appropriate amount of methyl alcoholand then after 5 minutes add 7.5% sodium carbonate solution to mixture and kept in dark room for 2 hours. At the end of the period, the total phenolic content was calculated by the standard calibration curve, which was read at 760 nm wavelength and expressedas gallic acid equivalents.

3.7.3. Methods to Assess the Antioxidant Power

3.7.3.1. Ferric Iron Reduction Antioxidant Power (FRAP)

Samples extracted with methyl alcohol are diluted in an appropriate proportion; 10: 1: 1 (v: v: v) 300 mM acetate buffer: mixed with 10 mM 2,4,6-tripyridyl-s-triazine (TPTZ) solution (dissolved in 40 mM HCl): 20 mM FeCl3, the absorbance at 593 nm was determined on the spectrophotometer (Gao et al., 2000).

3.7.3.2. Determination of DPPH Free-Radical Scavenging Effect

The method described by Tural and Koca (2008) was used to determine the reduction effect of 2,2-diphenyl-1- picrylhydrazyl (DPPH radical) 50 ml of methyl alcohol containing extract were mixed with 1 ml of 100 μM DPPH solution and kept at room temperature in the dark until the reaction was completed and the absorbance at 517 nm was determined.

3.8. Statistical Analysis

Numerical data of the groups obtained in this study were evaluated statistically using the SPSS program (SPSS version 21.0; SPSS Inc., Chicago, IL, USA). The data used were expressed as Mean ± Standard Deviation (SD). Normality and homogeneity tests were performed and all groups showed normal distribution. Differences between the groups were assessed by One-Way ANOVA, Tukey tests. $P < 0.05$ was considered statistically significant.

4. RESULTS

The present study was conducted to investigate the effects of AD and NS on the rat hippocampus that was exposed to 900 EMF MHz by the optical fractionator technique. Tissue sections were also analysed histopathologically by means of the light and electron microscopes. Besides, BioTek Synergy 4 microplate-reader and Tecan Sunrise Microplate Reader were used for biochemical analysis.

4.1. Stereological Findings

The total number of the pyramidal neurons was calculated in the whole hippocampal regions (CA1, CA2, and CA3) using the optical fractionator technique. Estimation of the pyramidal neuron numbers in the CA regions of the hippocampus was done for the Cont group that was not exposed to 900 EMF MHz, Sham group that was put in EMF exposure system while the system was turned off, EMF group that was exposed to 900 EMF MHz, EMF+AD group that was given AD and exposed to 900 EMF MHz, EMF+NS group that was given NS and exposed to 900 EMF MHz, EMF+AD + NS group that was given AD and NS then exposed to 900 EMF MHz, AD group that was given AD, NS group that was given NS.

4.1.1. Findings in the CA1 + CA2 Regions

The mean total number of the pyramidal neurons in the CA1 + CA2 regions of the hippocampus, the coefficient of error (CE) and the coefficient of variation (CV) are shown in the following table and figure (**Table 4; Figure 23**).

As a result of the statistical analysis that was applied to the stereological data collected from the CA1 + CA2 regions of the hippocampus, the following results were obtained. It was found that the mean number of neurons in the EMF groups significantly decreased compared to the mean number of the neurons in the EMF+AD+NS and AD groups ($p<0.05$). The mean neuron number of the Cont group was not significantly different from the mean cell number in Sham, EMF, EMF+NS, EMF+AD groups ($p>0.05$). On the other hand, the mean number of neurons in the Cont group was significantly

different from the NS and AD, EMF+AD +NS groups ($p<0.01$). That means herbals (AD and NS) may stimulate neurogenesis.

Moreover, a significant protection in the mean number of the pyramidal neuron was observed between the EMF+AD+NS and the EMF group ($p<0.05$). Similarly, a significant difference was found between the AD group and the EMF group in the mean number of the pyramidal neuron ($p<0.05$).

Table 4. The mean number of the pyramidal neurons in the CA1 + CA2 regions (Mean± SD), CE and CV values

Groups	**Number of neurons**	**CE**	**CV**
Cont	265919± 9279	0.04	0.03
Sham	265173 ± 17893	0.04	0.06
EMF	270132± 15691	0.05	0.05
EMF+AD	262978± 23252	0.02	0.08
EMF+NS	260912 ± 12868	0.02	0.04
EMF+AD+NS	301155 ± 10802	0.03	0.03
AD	301589 ± 12607	0.03	0.03
NS	291379 ± 6282	0.03	0.01

On the other hand, no significant differences were found in terms of the mean number of the pyramidal neurons when comparing the EMF group with the EMF+AD, EMF+NS, NS groups. Otherwise, no significant differences were found between Cont and Sham groups ($p>0.05$) (**Table 5**).

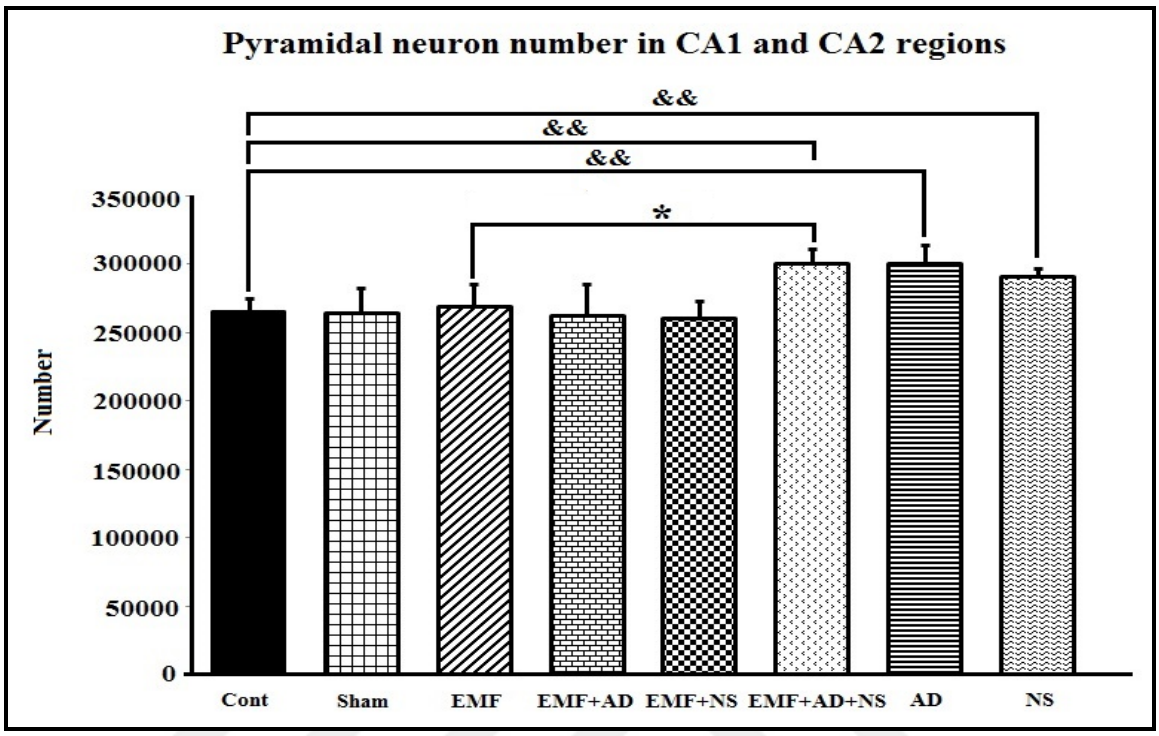

Figure 23. The graph shows the differences in the number of pyramidal neurons in the CA1 + CA2 regions of the hippocampus after exposure to EMF for 60 min. Significant differences at $p<0.05$ level were indicated by (*) while significant differences at $p<0.01$ level were indicated by (&&)

Table 5. The degree of significance between groups in the CA1 + CA2 regions

Comparison between groups	**Significance**
EMF with Cont group	1.000
EMF with Sham group	1.000
Cont with Sham group	1.000
EMF+AD with EMF group	1.000
EMF+NS with EMF group	1.000
EMF+AD+NS with EMF group	.037
Cont with AD group	.002
Cont with NS group	.003
Cont with EMF+AD group	1.000
Cont with EMF+NS group	1.000
Cont with EMF+AD+NS group	.001

4.1.2. Findings in the CA3 Region

The mean number of the pyramidal neurons in the CA3 region of the hippocampus, the CE and the CV are shown in the following table and figure (**Table 6**; **Figure 24**).

As a result of the statistical evaluation of the stereological analysis of the pyramidal neurons in the CA3 region of the hippocampus, a significant reduction was observed in the number of the pyramidal neurons when the EMF group compared to the EMF +AD +NS and AD groups ($p<0.05$). The mean total number of neurons in the CA3 of the Cont group was significantly lower than the EMF+AD+NS, NS and AD groups ($p<0.05$). On the other hand, there was no significant difference between Cont compared with EMF, EMF+NS, EMF+AD groups ($p>0.05$). Moreover, a significant increase was seen in the mean number of the pyramidal neuron in the EMF+AD+NS compared to the EMF group ($p<0.05$). Similarly, highly significant increase was found in the mean number of the pyramidal neuron in the AD compared to the EMF group ($p<0.01$). On the other hand, no significant difference was observed in terms of mean number of the pyramidal neurons when the EMF group compared with the Sham, EMF+NS and EMF+AD group or when the Cont group compared with the Sham group ($p>0.05$) (**Table 7**).

Table 6. The mean number of the pyramidal neurons in the CA3 region (Mean± SD), CE and CV values

Groups	Number of neurons	CE	CV
Cont	219332 ±7105	0.02	0.03
Sham	228238±19155	0.02	0.08
EMF	222156±8713	0.05	0.04
EMF+AD	220644 ±16783	0.02	0.07
EMF+ NS	215050 ± 13207	0.03	0.06
EMF+AD+ NS	241469 ± 5639	0.02	0.02
AD	245032 ± 5476	0.025	0.02
NS	239096 ± 3917	0.02	0.02

Table 7. The degree of significance between groups in CA3 region

Comparison between groups	Significance
EMF with Cont group	1.000
EMF with Sham group	.974
Cont with Sham group	.830
EMF+AD with EMF group	1.000
EMF+ NS with EMF group	.940
EMF+AD+NS with EMF group	.039
Cont with AD group	.002
Cont with NS group	.032
Cont with EMF+AD group	1.000
Cont with EMF+NS group	.997
Cont with EMF+AD+NS group	.011

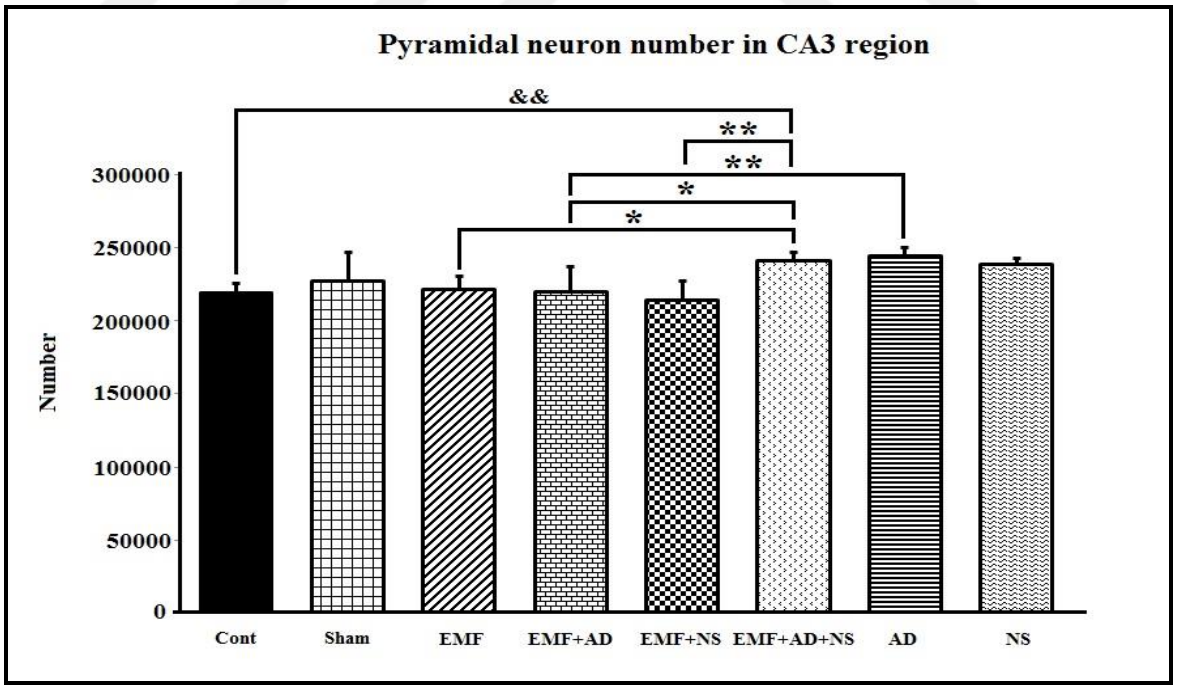

Figure 24. It shows the differences in the total number of pyramidal neurons in the CA3 region of the hippocampus after EMF exposure for one hour. Significant differences at $p<0.05$ level were indicated by (&&) and (*) while significant differences at $p<0.01$ level were indicated by (**)

4.1.3. Findings in the Whole CA Regions

Estimation of the mean number of the pyramidal neurons in all regions (CA1, CA2, and CA3) of the hippocampus resulted with sum of the mean number of pyramidal neurons in the whole hippocampus. The values of the CE and CV are presented in the following tables and figures **(Table 8; Figure 25)**.

As a result of the statistical evaluation of the stereological analysis of the total neurons in the CA region of the hippocampus, the mean number of the total pyramidal neurons in the EMF groups was highly significantly decreased when compared to the EMF+AD+NS and AD groups ($p<0.01$). Mean number of the total pyramidal neurons in the EMF group was not seen significantly different when compared with the Cont and Sham groups ($p>0.05$). There was highly significant difference in terms of total pyramidal neurons in the CA of the Cont group compared to the AD, NS and EMF+AD+NS groups ($p<0.01$).

Table 8. Total number of the hippocampal pyramidal neurons in the CA (Mean± SD), CE and CV values

Groups	Total number of neurons	CE	CV
Cont	485251±13791	0.02	0.03
Sham	493411±36387	0.02	0.07
EMF	492288±24250	0.02	0.06
EMF+AD	483622±39573	0.02	0.08
EMF+ NS	475962±25091	0.02	0.05
EMF+AD+NS	542624 ±10295	0.03	0.02
AD	546621±15828	0.03	0.03
NS	530476±8481	0.03	0.01

On the other side, there was a significant difference in terms of total pyramidal neurons in the CA of the Sham group when compared to the AD and EMF+AD+NS groups ($p<0.05$). Furthermore, highly significant protection was found when the mean number of total pyramidal neurons in the EMF+AD+NS compared with the EMF group ($p<0.01$). Similarly, highly significant neuroprotection/neurogenesis was found when the mean number of total pyramidal neurons in the AD group compared with the EMF group

($p<0.01$). While there were no significant differences between the EMF group with EMF+AD, EMF+NS and NS groups in terms of the mean number of the total pyramidal neurons ($p>0.05$) or between the Cont and Sham groups ($p>0.05$) (**Table 9**).

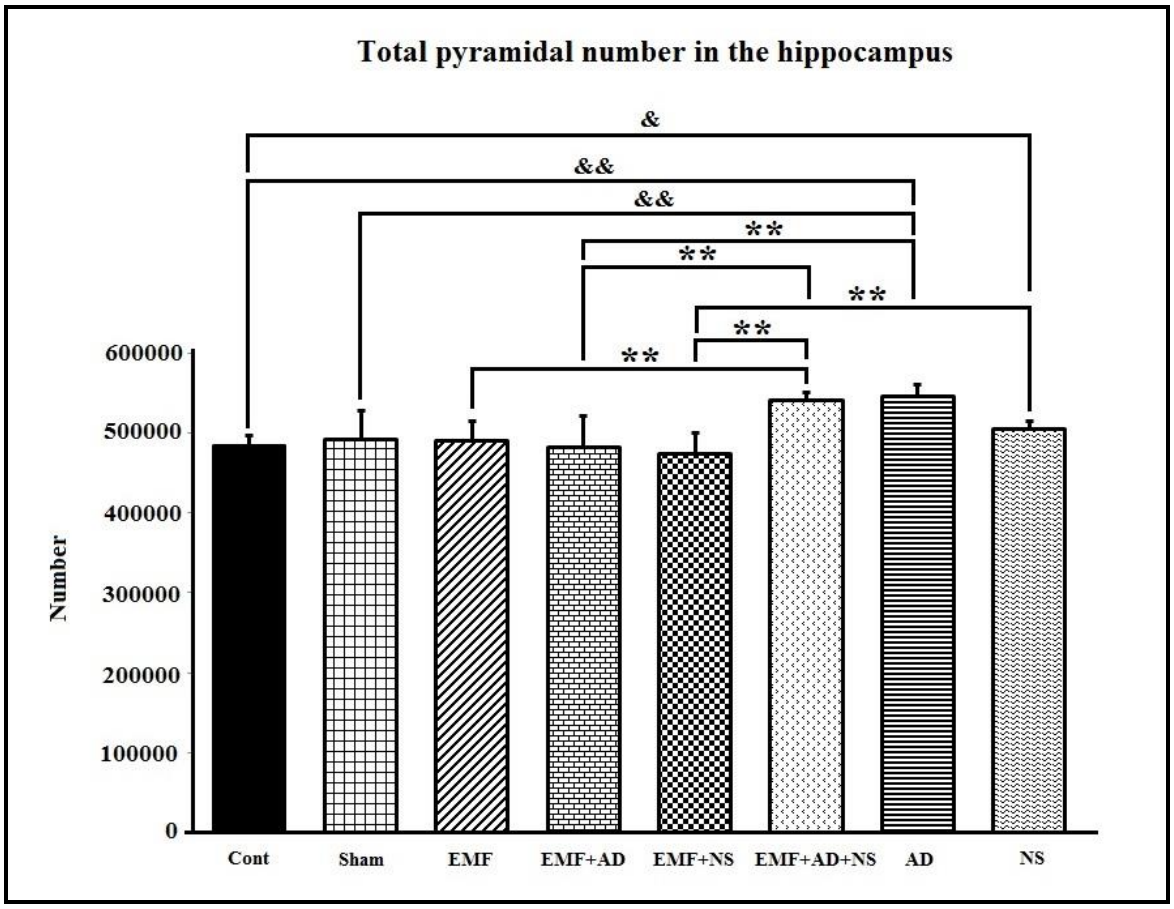

Figure 25. It shows differences in the number of total pyramidal neurons in the whole hippocampus after exposure to one hour EMF. Significant differences at $p<0.05$ level, were indicated by (&) while significant differences at $p<0.01$ level were indicated by (&&) and (**)

Table 9. The degree of significance between groups in CA region

Comparison between groups	Significance
EMF with Cont group	.999
EMF with Sham group	1.000
Cont with Sham group	.999
EMF+AD with EMF group	.997
EMF+ NS with EMF group	.920
EMF+AD+NS with EMF group	.006
Cont with AD group	.000
Cont with NS group	.020
Cont with EMF+AD group	1.000
Cont with EMF+NS group	.997
Cont with EMF+AD+NS group	.001

4.2. Light Microscopic Findings

4.2.1. Light Microscopic Findings by Cresyl violet stain

Cresyl violet staining was applied to the sections of the hippocampus. These sections were taken from all experimental groups; the CA regions in the sections were examined by light microscopy. The findings are given below.

4.2.1.1. Light Microscopic Findings in CA1 + CA2 Regions

Light microscopic images in the CA1 + CA2 regions showed substantial number of normal pyramidal neurons that have clear boundaries and the nuclei were seen in the Cont and the Sham groups as well as in the AD and NS groups.

The morphological evaluation of the EMF+ AD and EMF+ NS groups showed that the neuron boundaries and the nuclei of the cells related to these groups were clear, the structure of neurons is commonly well preserved. The numerical density of the protected neurons in these groups is higher than in the EMF group. Furthermore, it was observed that the degenerated neurons (darkly stained) in the EMF group was more abundant than in the

EMF+ AD and EMF+ NS groups. On the other hand, a large number of dark stained nuclei and a great number of neurons that have indistinct boundaries were observed in the EMF group. A high number of degenerated neurons in the CA1 + CA2 regions of hippocampus were observed in the EMF groups compared to the Cont group. However, the numerical density of the normal pyramidal neurons in the EMF+ AD+NS group was higher than EMF group (**Figure 26, 27, 28, 29, 30, 31, 32, and 33**).

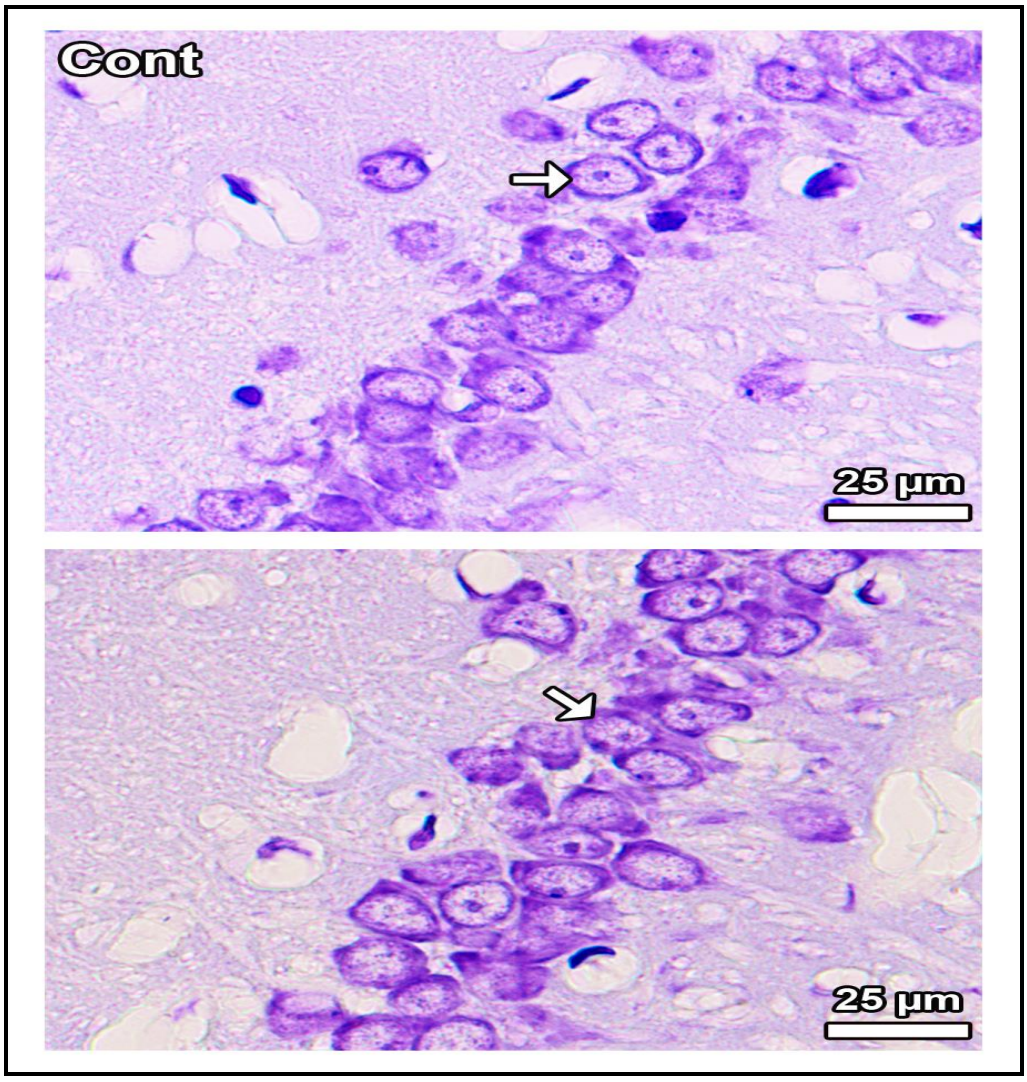

Figure 26. Microscopic views of the pyramidal neurons in the CA1 + CA2 regions of hippocampus stained with cresyl violet are seen. The arrows indicate the healthy pyramidal neurons. Cresyl violet staining, 5 µm thickness of paraffin section

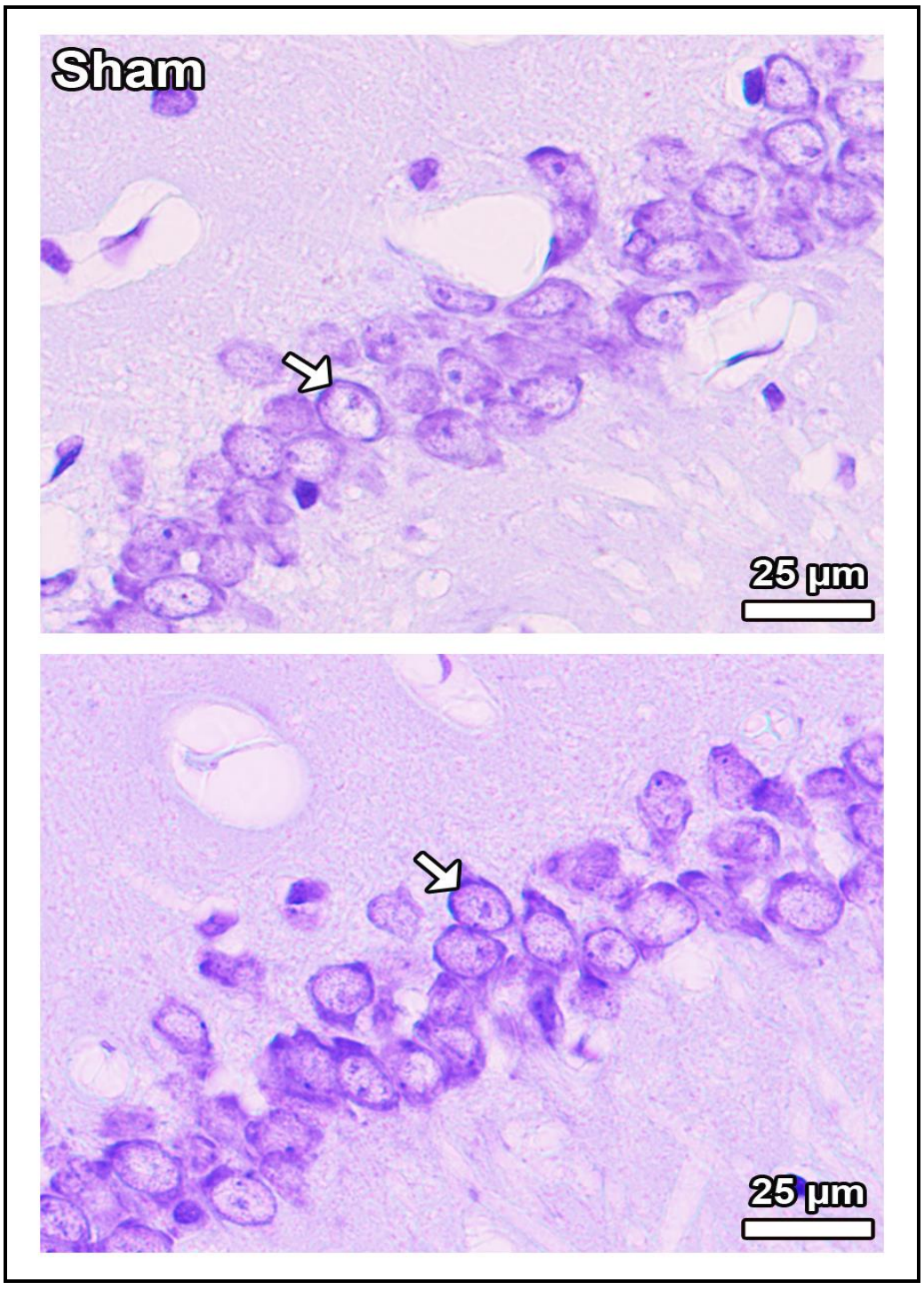

Figure 27. Microscopic views of the pyramidal neurons in the CA1 + CA2 regions of hippocampus stained with cresyl violet are seen. The arrows indicate the healthy pyramidal neurons. Cresyl violet staining, 5 µm thickness of paraffin section

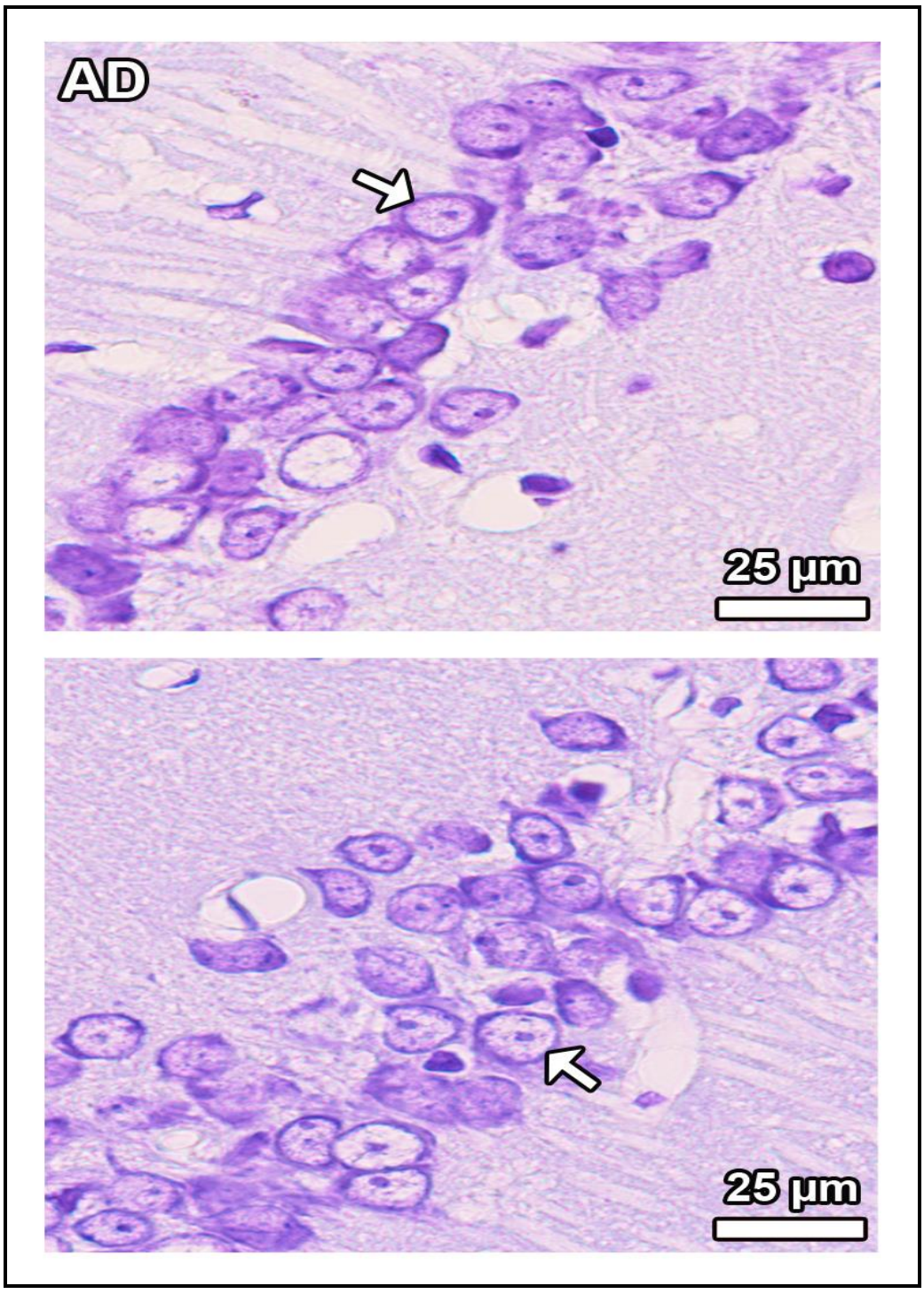

Figure 28. Microscopic views of the pyramidal neurons in the CA1 + CA2 regions of hippocampus stained with cresyl violet are seen. The arrows indicate the healthy pyramidal neurons. Cresyl violet staining, 5 µm thickness of paraffin section

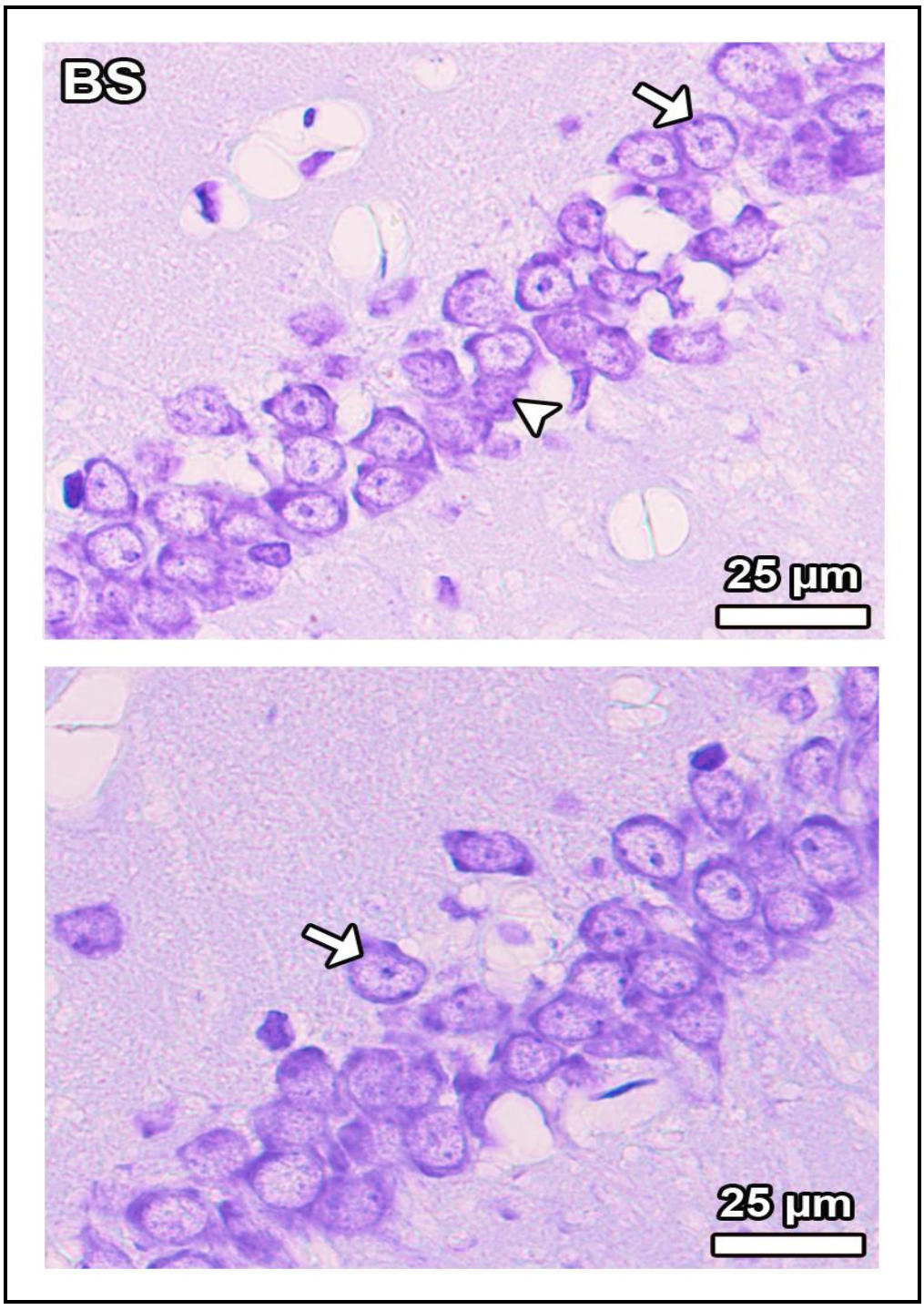

Figure 29. Microscopic views of the pyramidal neurons in the CA1 + CA2 regions of hippocampus stained with cresyl violet are seen. The arrows indicate the healthy pyramidal neurons. The arrows indicate the healthy pyramidal neurons, while arrowhead shows a degenerated pyramidal neuron. Cresyl violet staining, 5 µm thickness of paraffin section

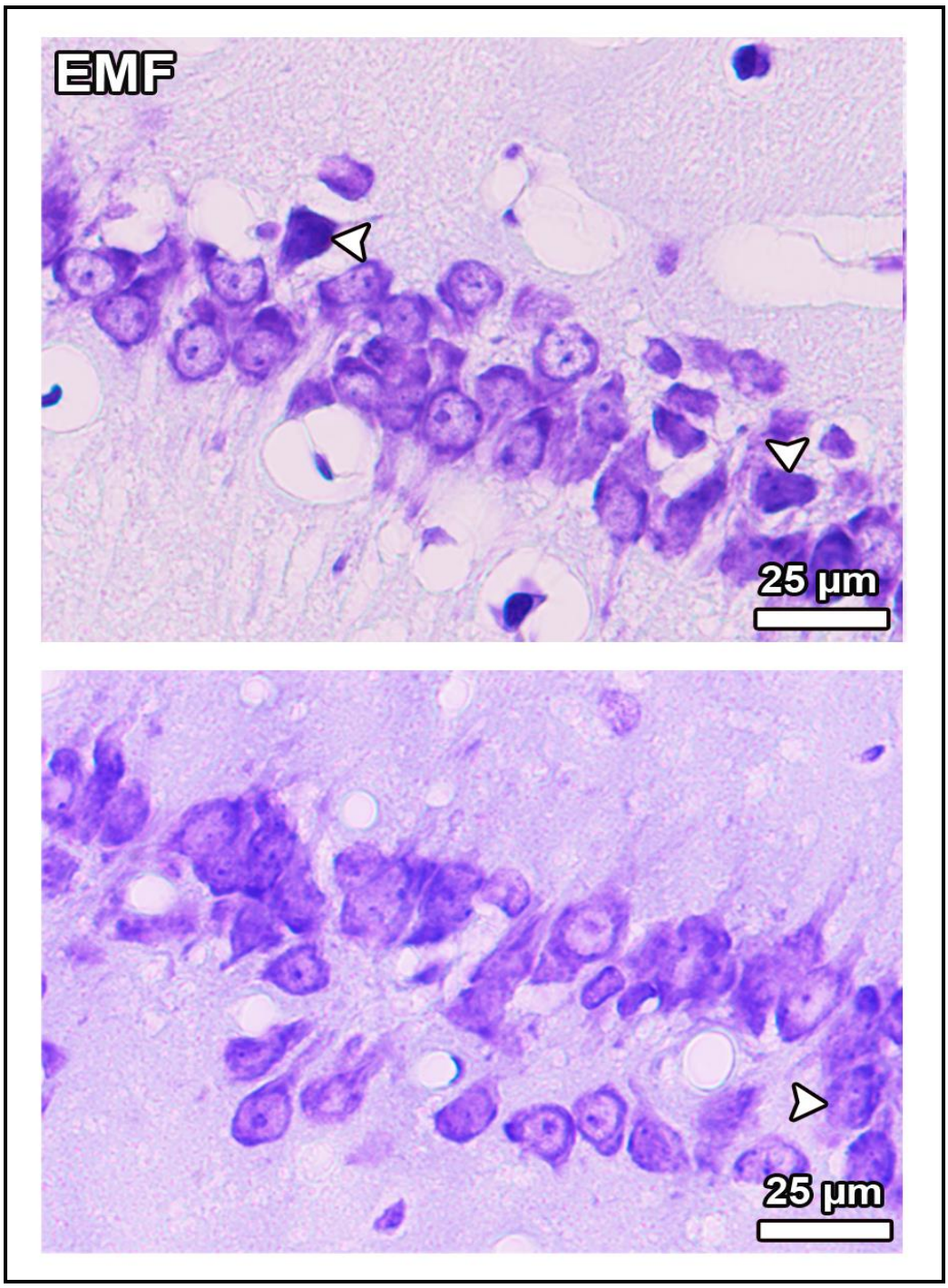

Figure 30. Microscopic views of the pyramidal neurons in the CA1 + CA2 regions of hippocampus stained with cresyl violet are seen. The arrowheads show degenerated pyramidal neurons. Cresyl violet staining, 5 µm thickness of paraffin section

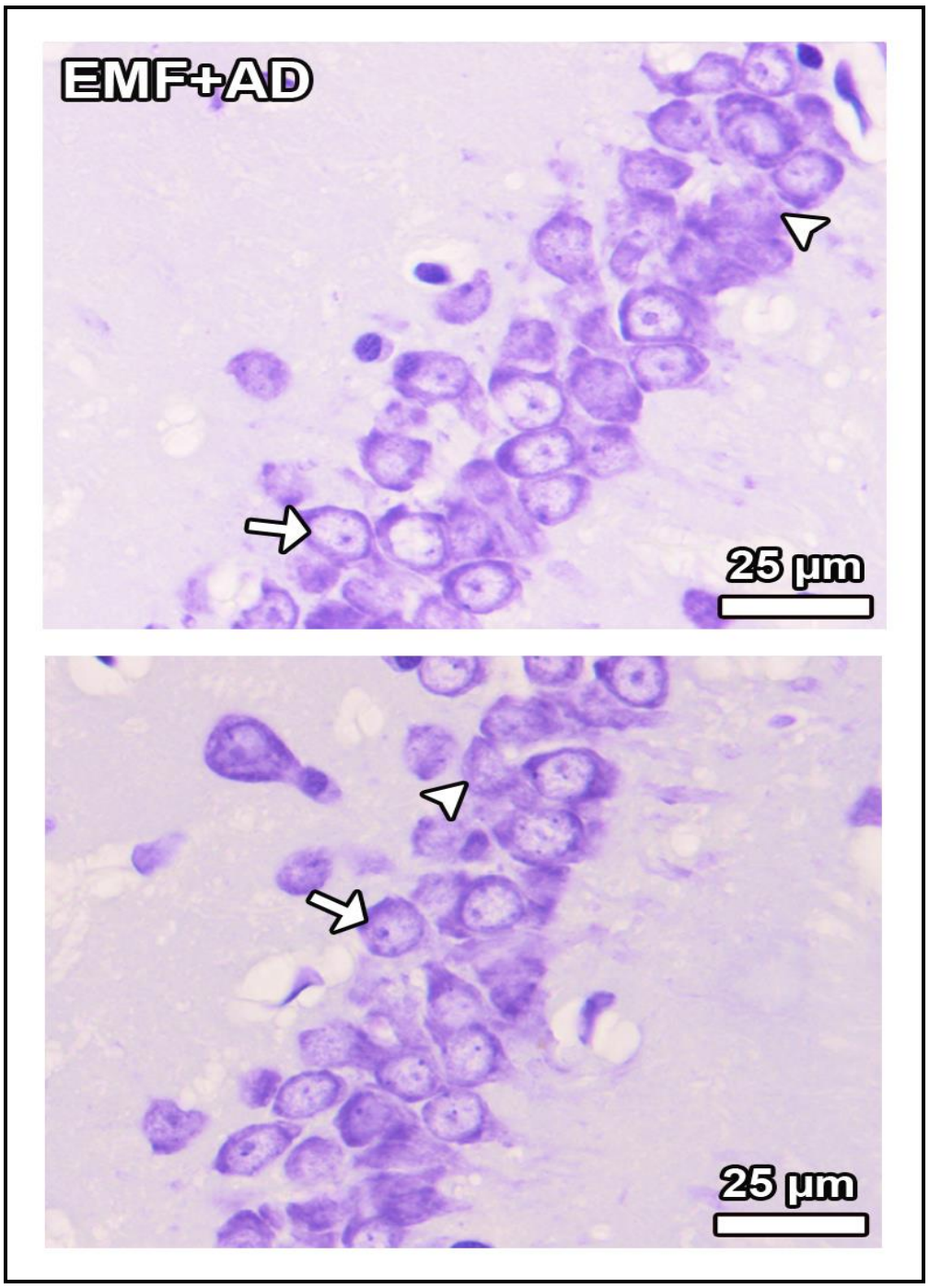

Figure 31. Microscopic views of the pyramidal neurons in the CA1 + CA2 regions of hippocampus stained with cresyl violet are seen. The arrows indicate the healthy pyramidal neurons. The arrows indicate to healthy pyramidal neurons, while arrowheads show degenerated pyramidal neurons. Cresyl violet staining, 5 µm thickness of paraffin section

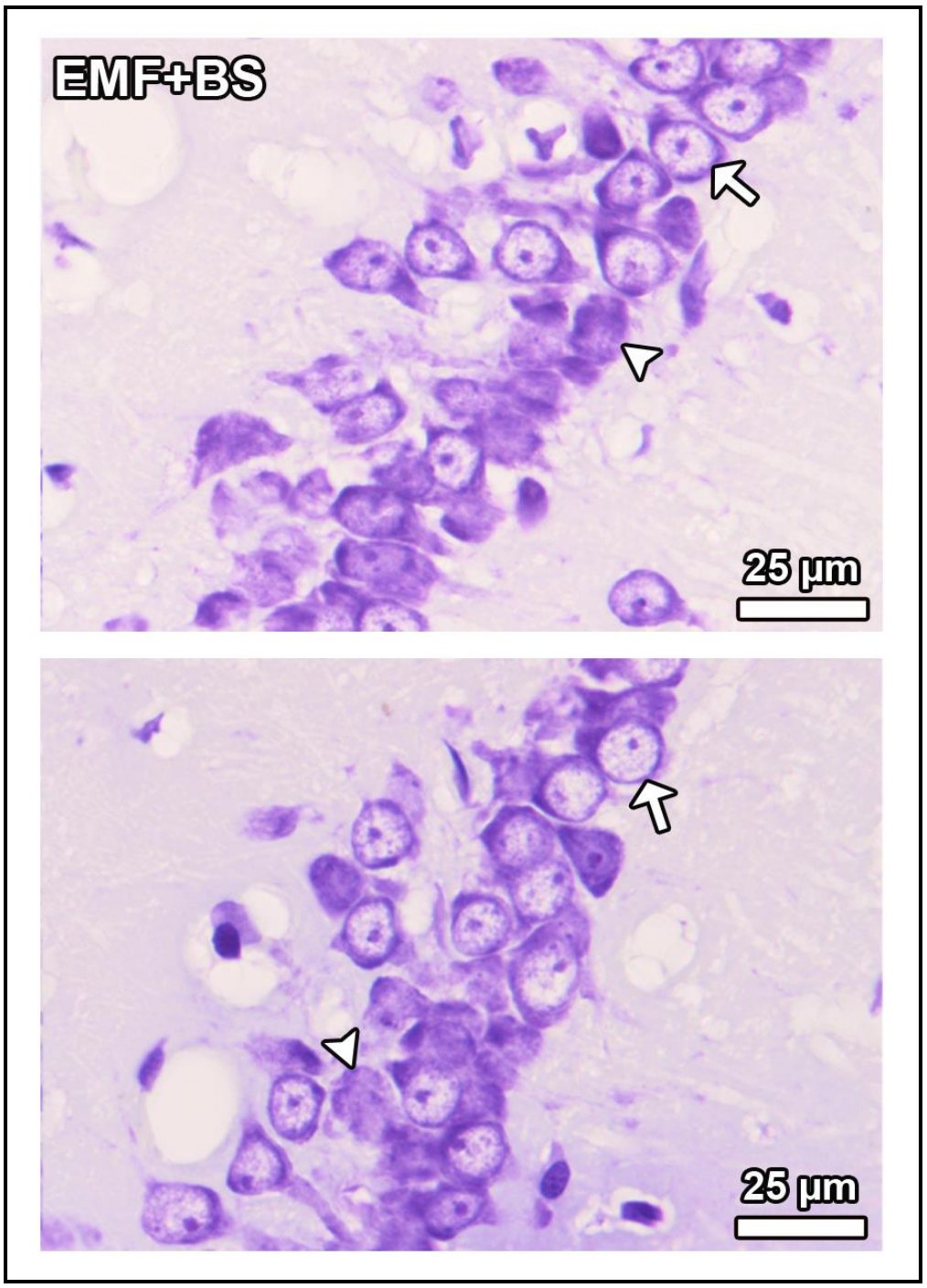

Figure 32. Microscopic views of the pyramidal neurons in the CA1 + CA2 regions of hippocampus stained with cresyl violet are seen. The arrows indicate the healthy pyramidal neurons. The arrows indicate the healthy pyramidal neurons, while arrowheads show degenerated pyramidal neurons. Cresyl violet staining, 5 µm thickness of paraffin section

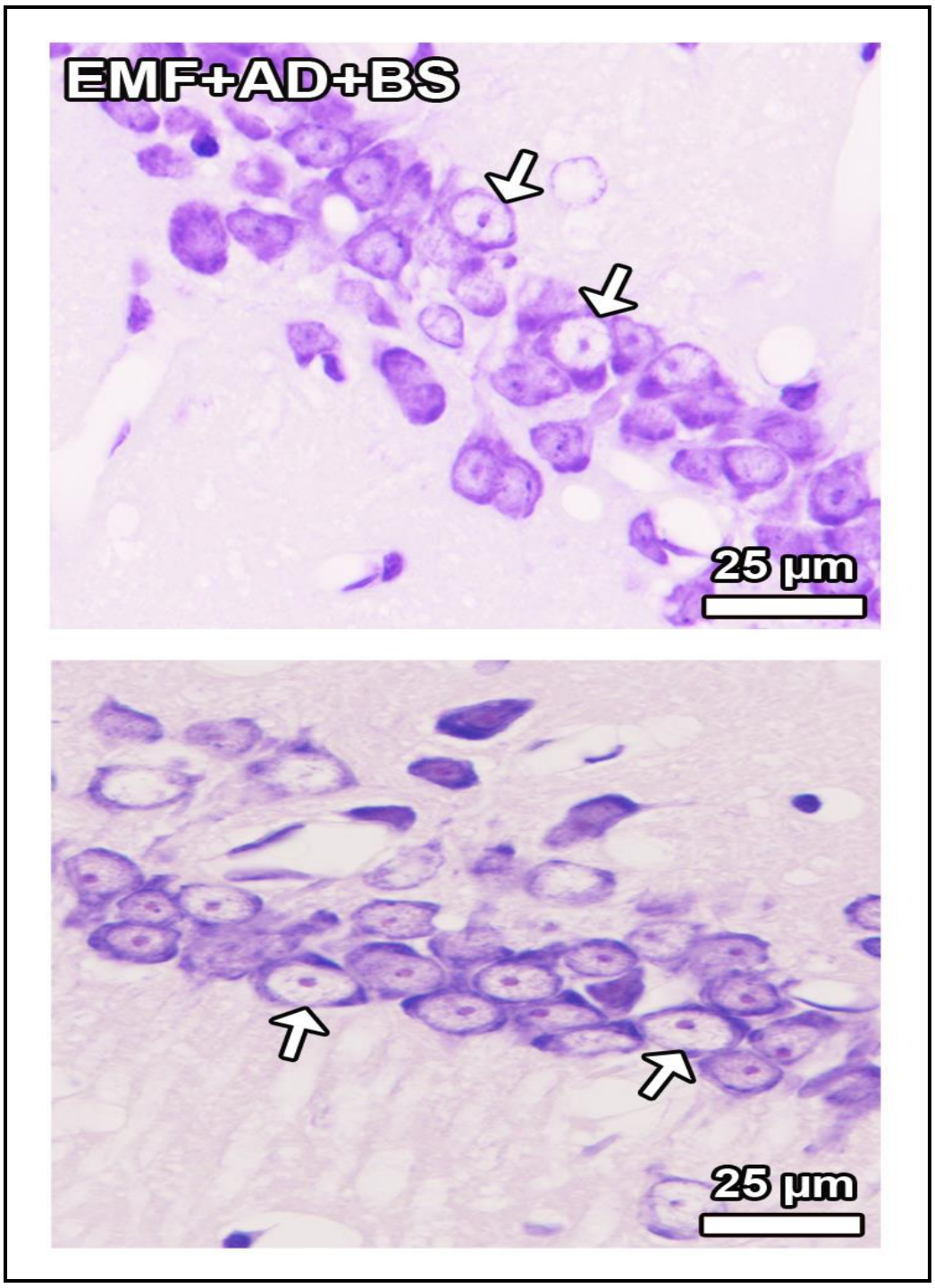

Figure 33. Microscopic views of the pyramidal neurons in the CA1 + CA2 regions of hippocampus stained with cresyl violet are seen. The arrows indicate the healthy pyramidal neurons. The arrows indicate the healthy pyramidal neurons. Cresyl violet staining, 5 µm thickness of paraffin section

4.2.1.2. Light Microscopic Findings in CA3 Region

The general structure of the CA3 region in the hippocampus and the morphology of the normal neurons were observed in the Cont, Sham, AD and NS groups. It was seen that the structures of neurons and the boundaries of them in those groups were clear than the neurons of EMF group. On the other hand, most of neurons in EMF+AD+ NS group were healthy but a few of them darkly stained. The neurons and nuclei boundaries in this group were quite clear in the comparison of the EMF group. Regarding the number of degenerated neurons that were stained darkly in the EMF group was higher than the sham group.

Darkly stained nuclei and cytoplasm in the EMF group were also prominent compared to the Cont group. The degeneration and cell depletion in the EMF group was greater than in the EMF+AD and EMF+NS group. The cell boundaries in the EMF exposed groups were not clearly identified, and neurons with darkly stained cytoplasm were observed more frequently in the EMF group compared with the other groups.

It was qualitatively distinguished that exposure to EMF caused the neuron loss and decreasing its size (shrunken) (**Figure 34, 35, 36, 37, 38, 39, 40 and 41**). Furthermore, in the sections of EMF group, nuclei of neurons that heterochromatic stained were found more frequently in the CA1 and CA2 regions compared to the CA3 region.

Present study's histopathological findings of light microscope showed that degenerated neurons were frequently seen in EMF group in comparison of the EMF+NS and EMF+AD groups.

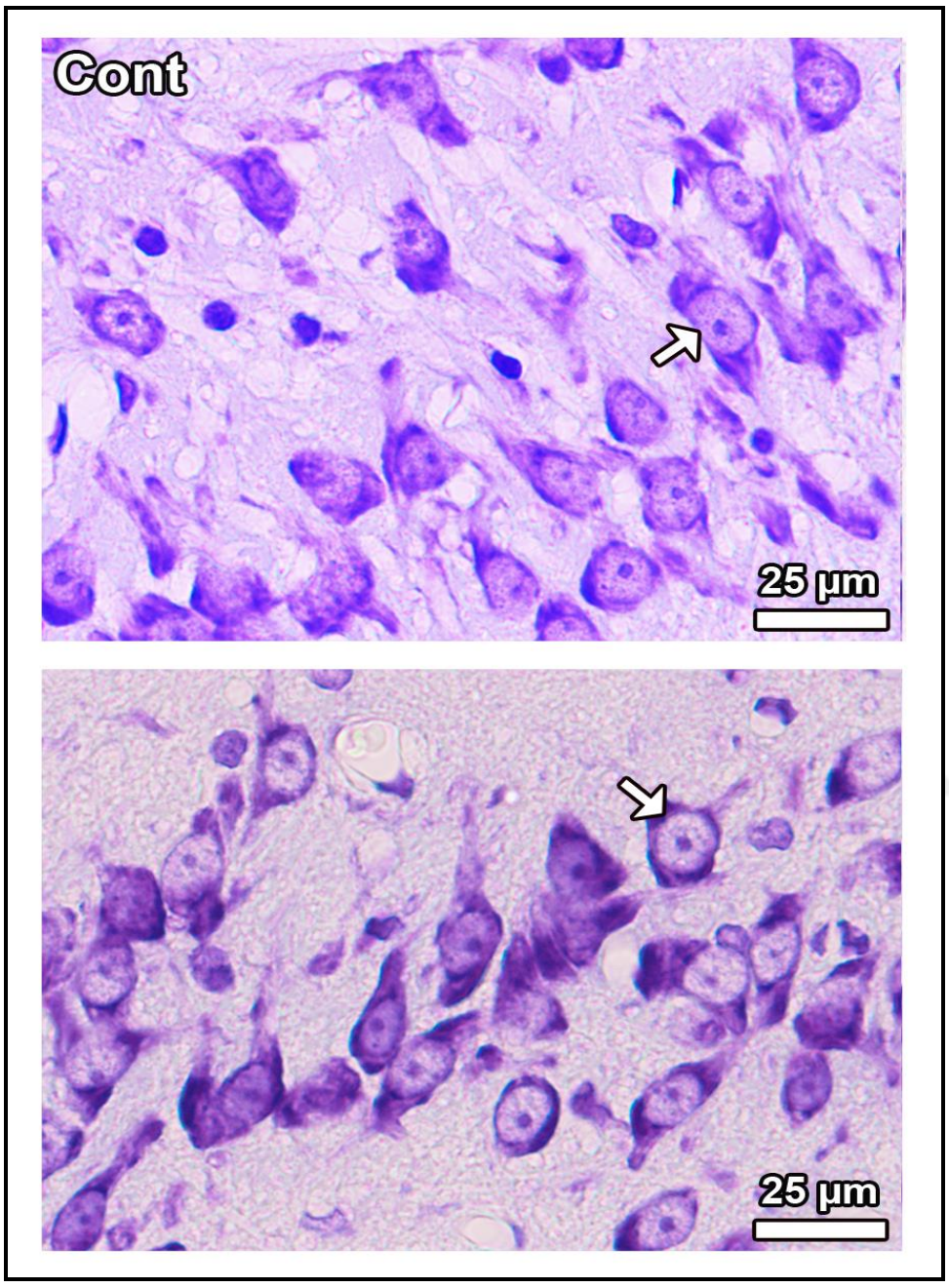

Figure 34. Microscopic views of the pyramidal neurons in the CA3 region of hippocampus stained with cresyl violet are seen. The arrows indicate the healthy pyramidal neurons. Cresyl violet staining, 5 µm thickness of paraffin section

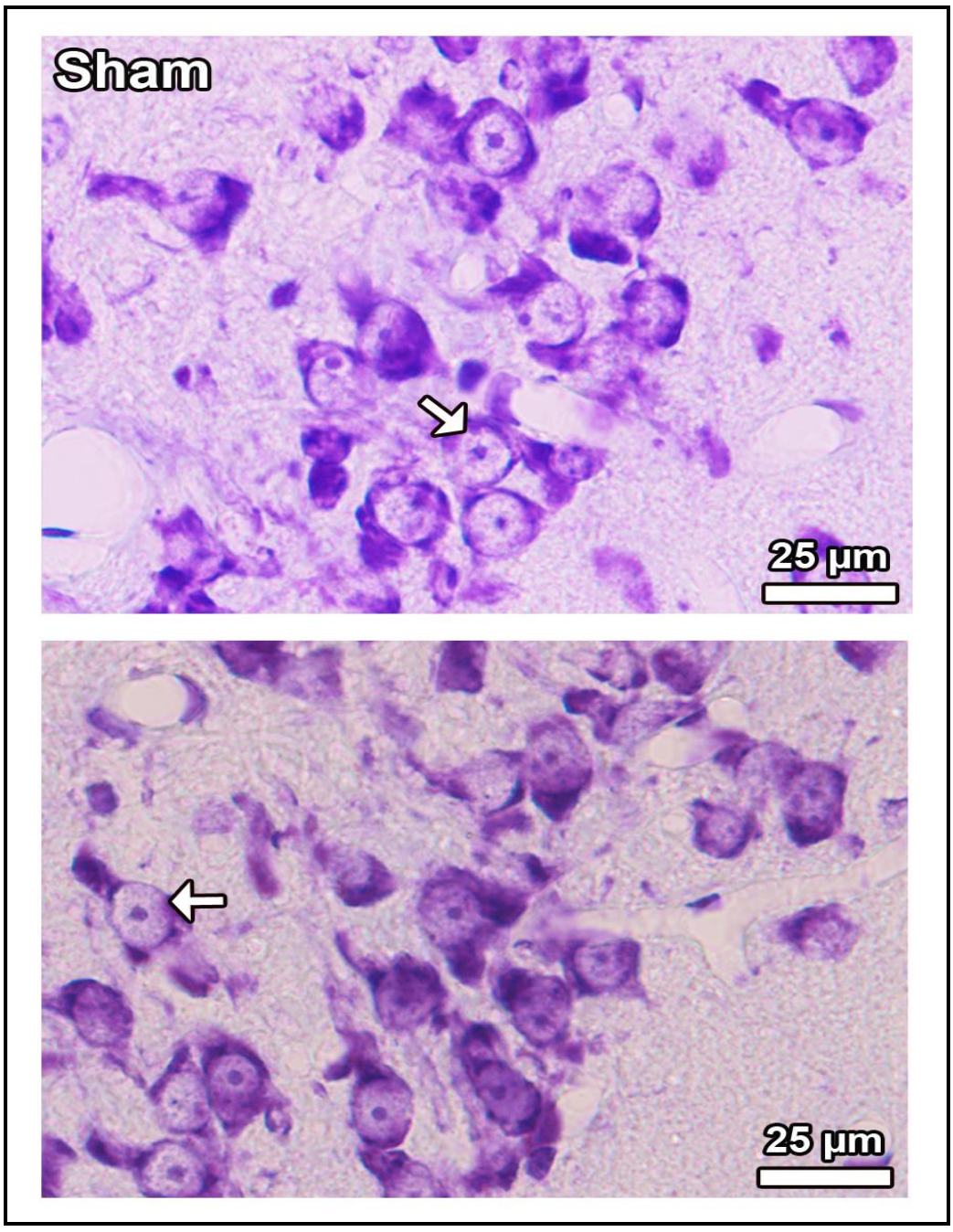

Figure 35. Microscopic views of the pyramidal neurons in the CA3 region of hippocampus stained with cresyl violet are seen. The arrows indicate the healthy pyramidal neurons. Cresyl violet staining, 5 µm thickness of paraffin section

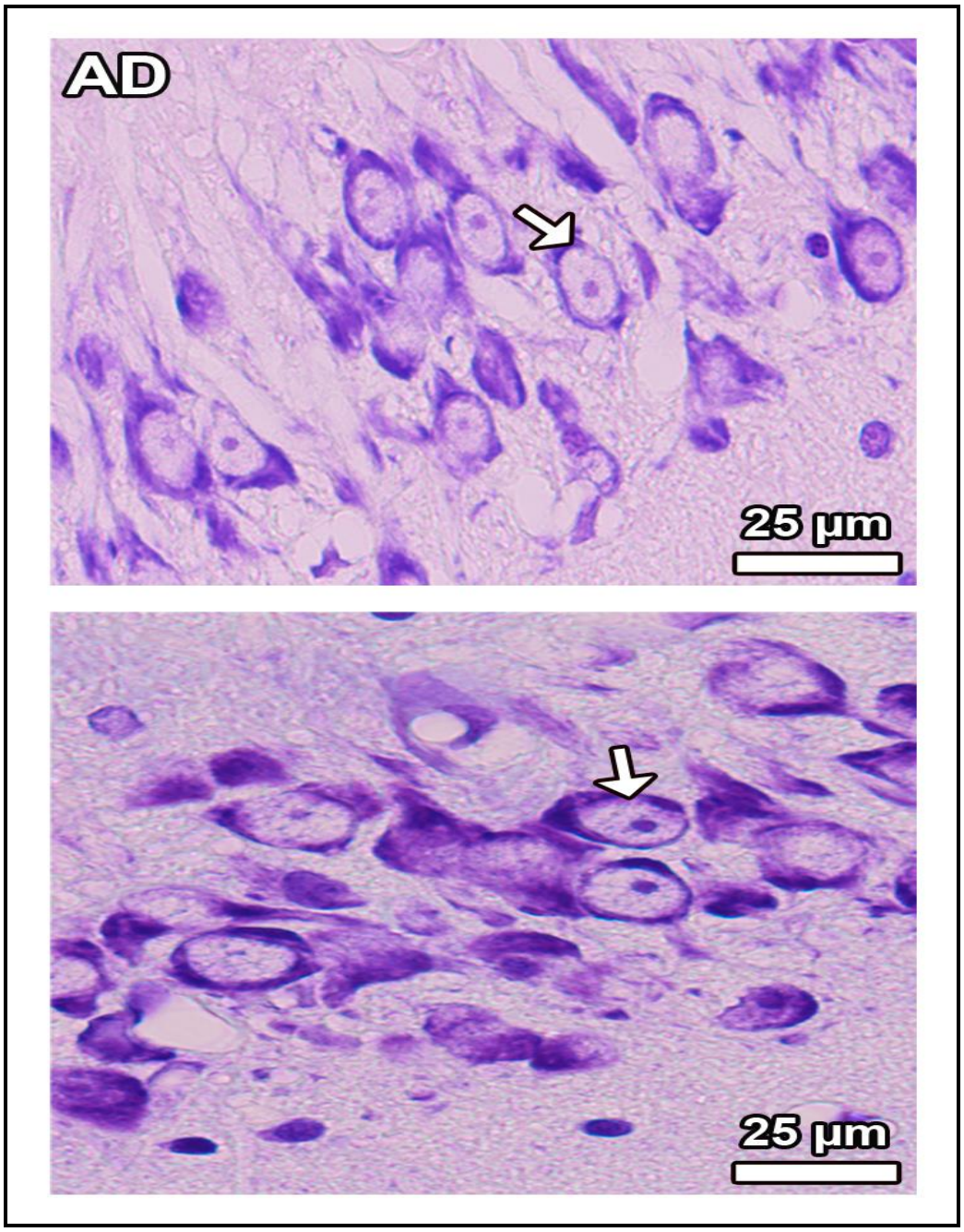

Figure 36. Microscopic views of the pyramidal neurons in the CA3 region of hippocampus stained with cresyl violet are seen. The arrows indicate the healthy pyramidal neurons. Cresyl violet staining, 5 µm thickness of paraffin section

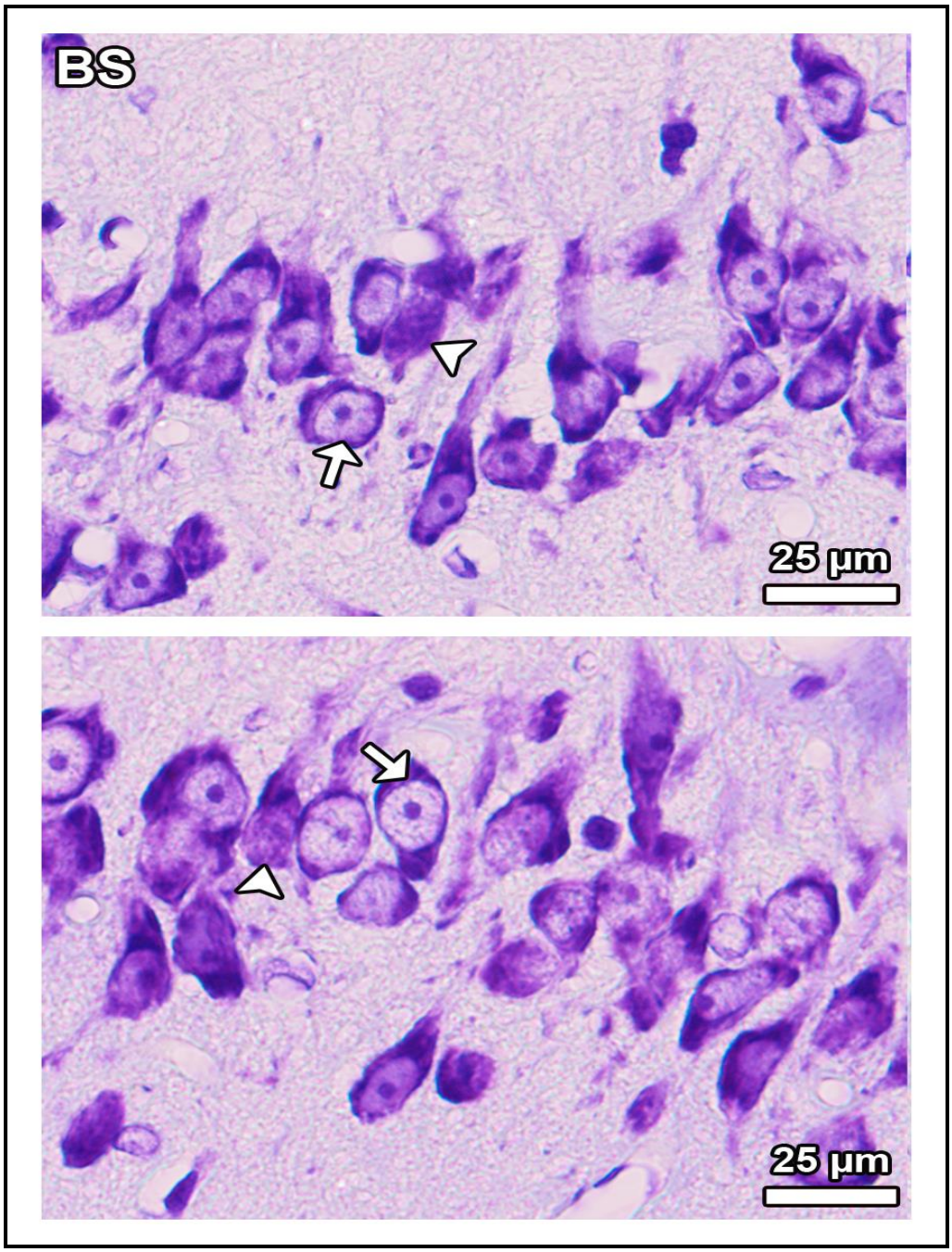

Figure 37. Microscopic views of the pyramidal neurons in the CA3 region of hippocampus stained with cresyl violet are seen. The arrows indicate the healthy pyramidal neurons, while arrowheads show degenerated pyramidal neurons. Cresyl violet staining, 5 µm thickness of paraffin section

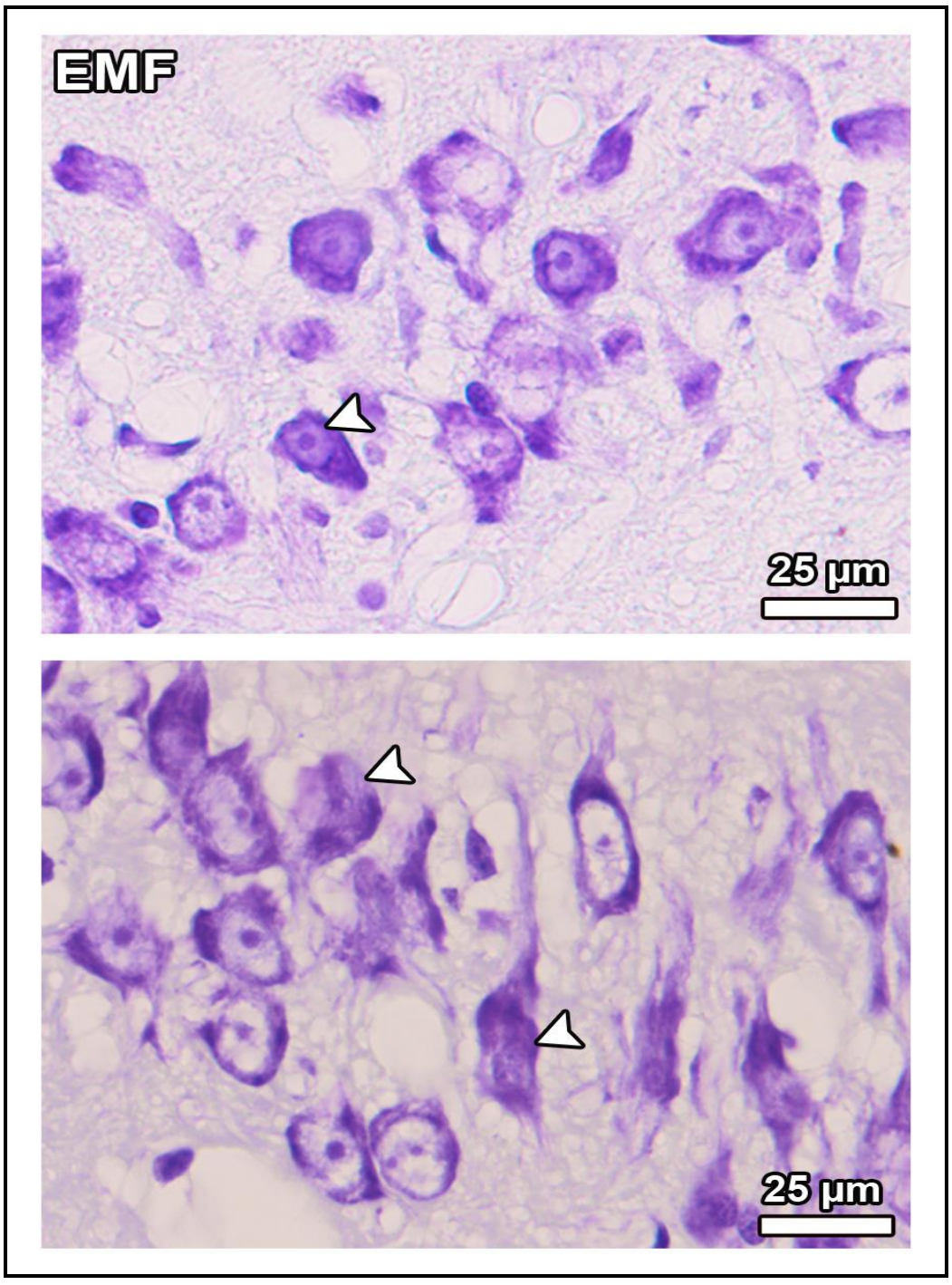

Figure 38. Microscopic views of the pyramidal neurons in the CA3 region of hippocampus stained with cresyl violet are seen.The arrowheads show degenerated pyramidal neurons. Cresyl violet staining, 5 µm thickness of paraffin section

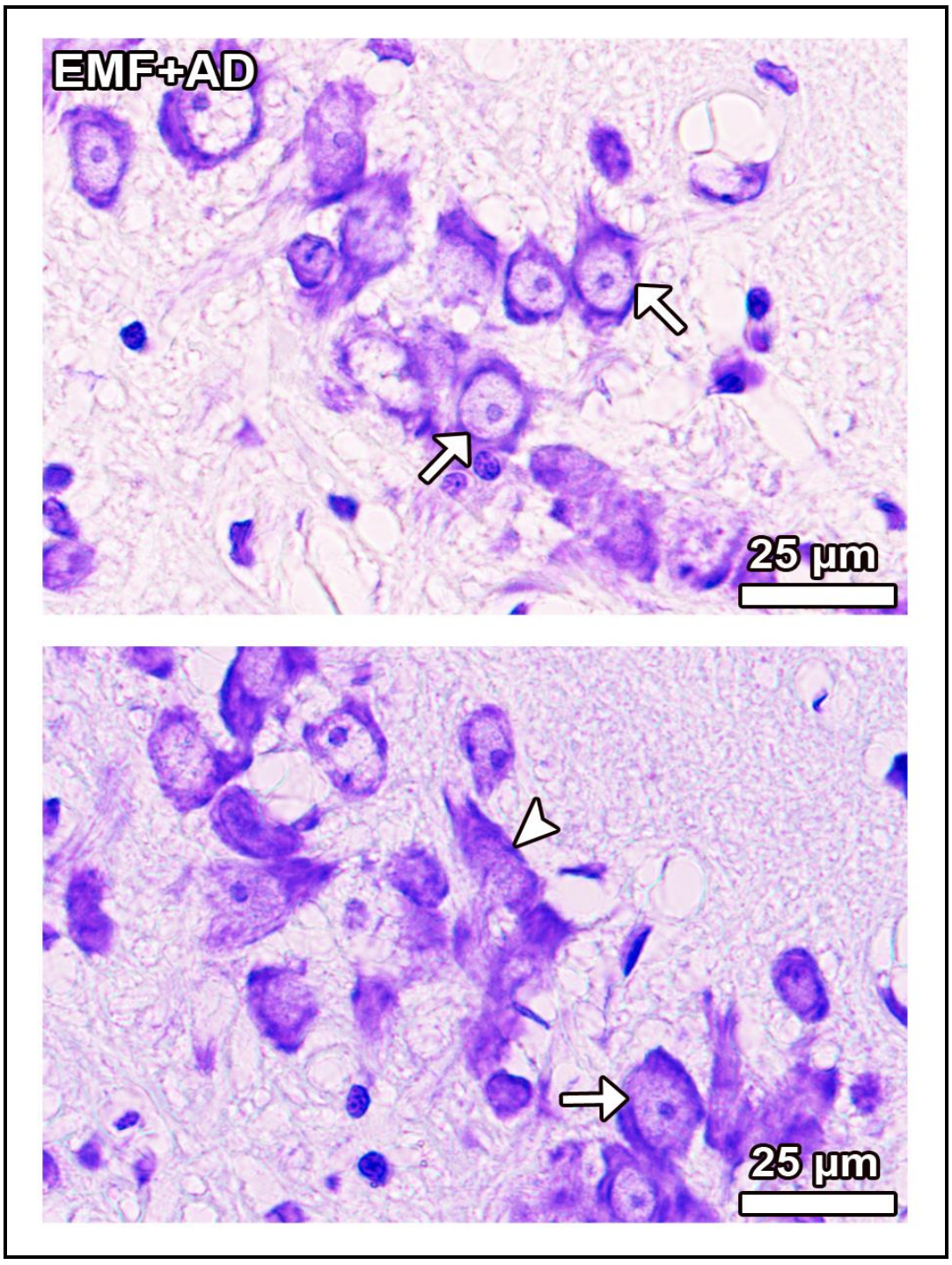

Figure 39. Microscopic views of the pyramidal neurons in the CA3 region of hippocampus stained with cresyl violet are seen. The arrowhead shows degenerated pyramidal neuron, while arrows show healthy pyramidal neurons. Cresyl violet staining, 5 µm thickness of paraffin section

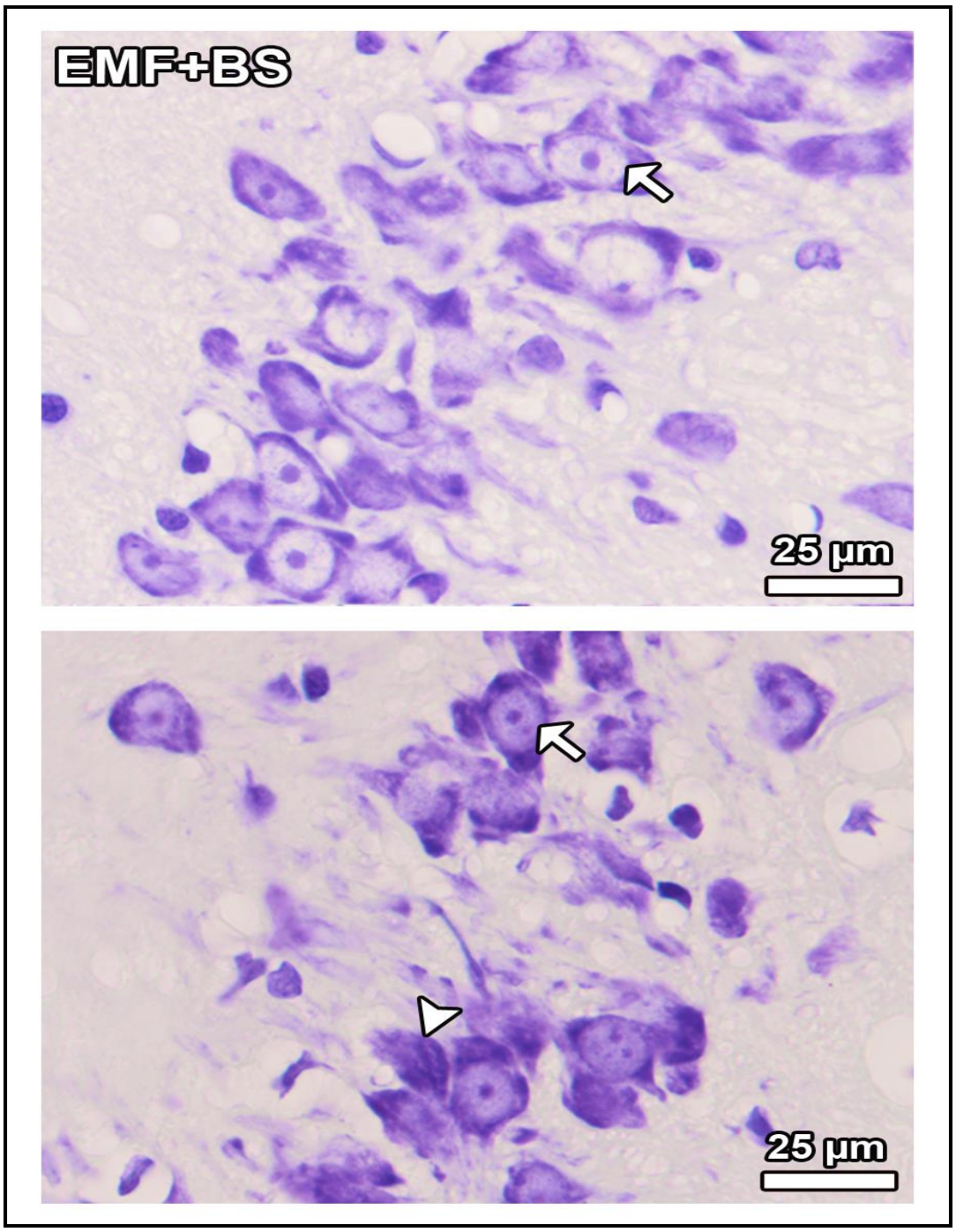

Figure 40. Microscopic views of the pyramidal neurons in the CA3 region of hippocampus stained with cresyl violet are seen. The arrowheads show degenerated pyramidal neurons, while arrows show healthy pyramidal neurons. Cresyl violet staining, 5 µm thickness of paraffin section

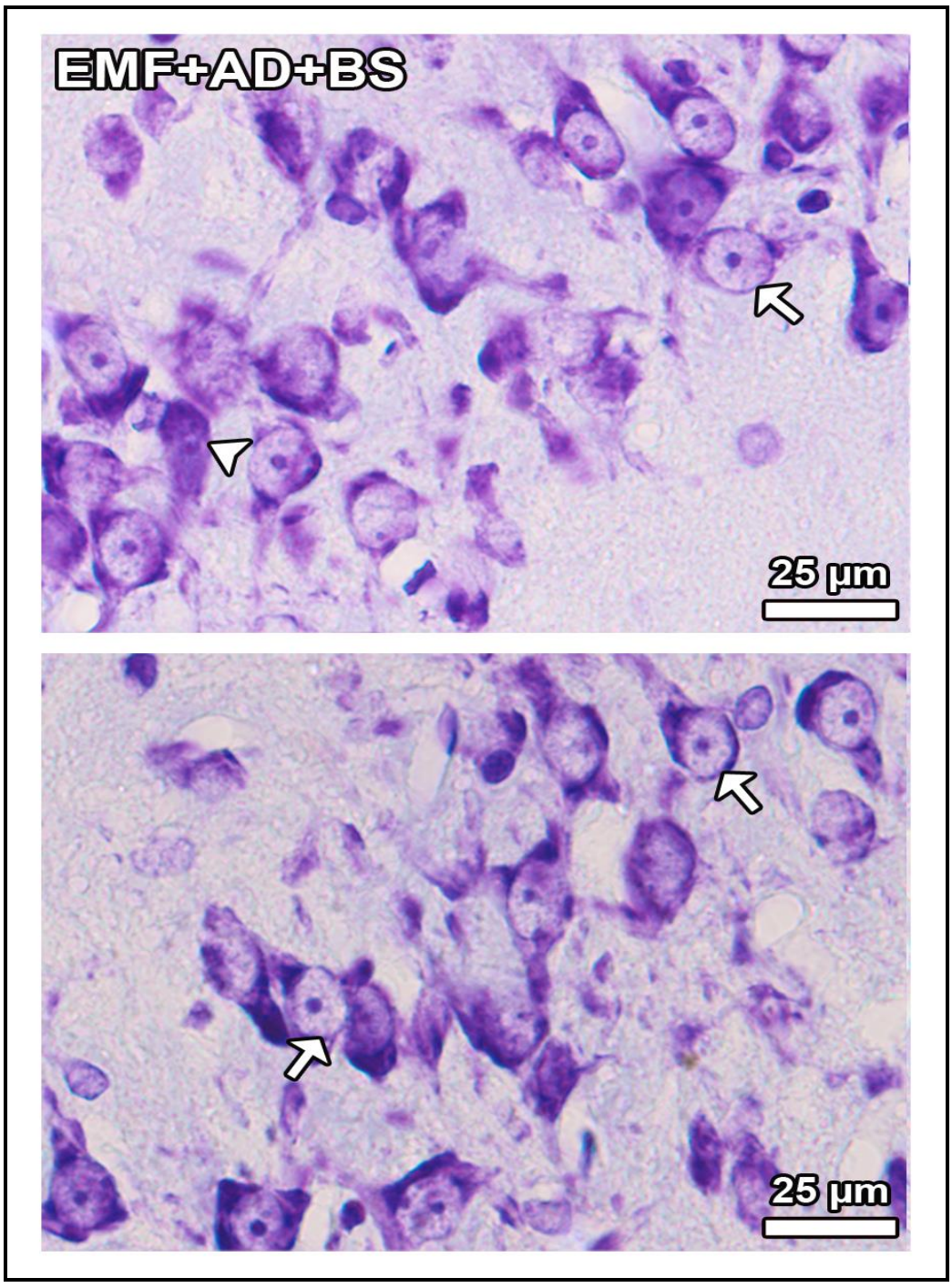

Figure 41. Microscopic views of the pyramidal neurons in the CA3 region of hippocampus stained with cresyl violet are seen. The arrowheads show degenerated pyramidal neurons, while arrows show healthy pyramidal neurons. Cresyl violet staining, 5 µm thickness of paraffin section

4.2.2. Light Microscopic Findings in Resin Sections

Toluidine blue staining was applied to the resin sections of the hippocampus. These sections were taken from all groups; the CA regions in the sections were examined by light microscopy.

Light microscopic images taken from the hippocampal region in the Cont group showed that pyramidal cells and granular cells are in the normal morphology, their nuclei are clearly observed (**Figure 42, 43, 44, 45, 46, 47, 48, 49, 50 and 51**). A few numbers of the dark cells and axons are found.

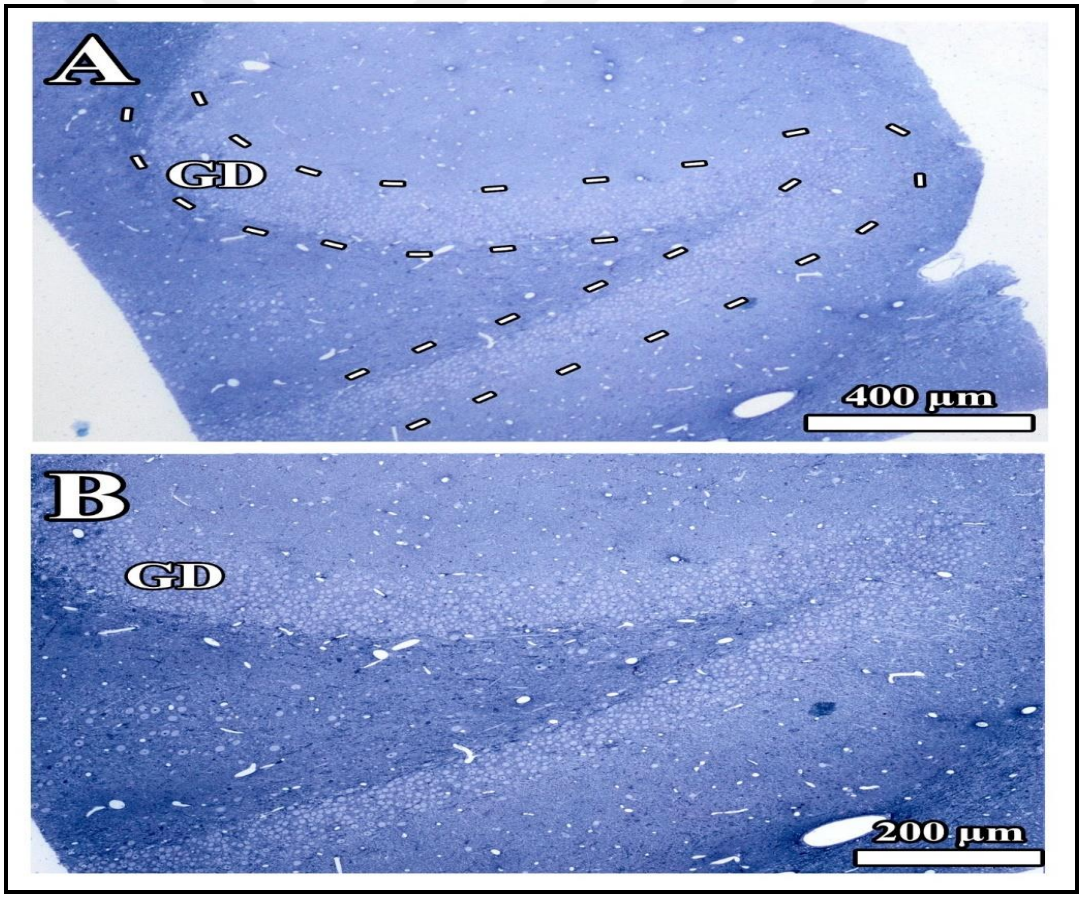

Figure 42. (A, B) Images taken from the hippocampal region of the Cont group are seen. The border of dentate gyrus (GD) is clearly observed. Some part of CA region is also seen. Both types of regions in the hippocampus show normal appearance. Vessels in this region are intact and there is no gap between them and the surrounding tissue. Toluidine blue stained semi-thin (0.5 µm) resin section

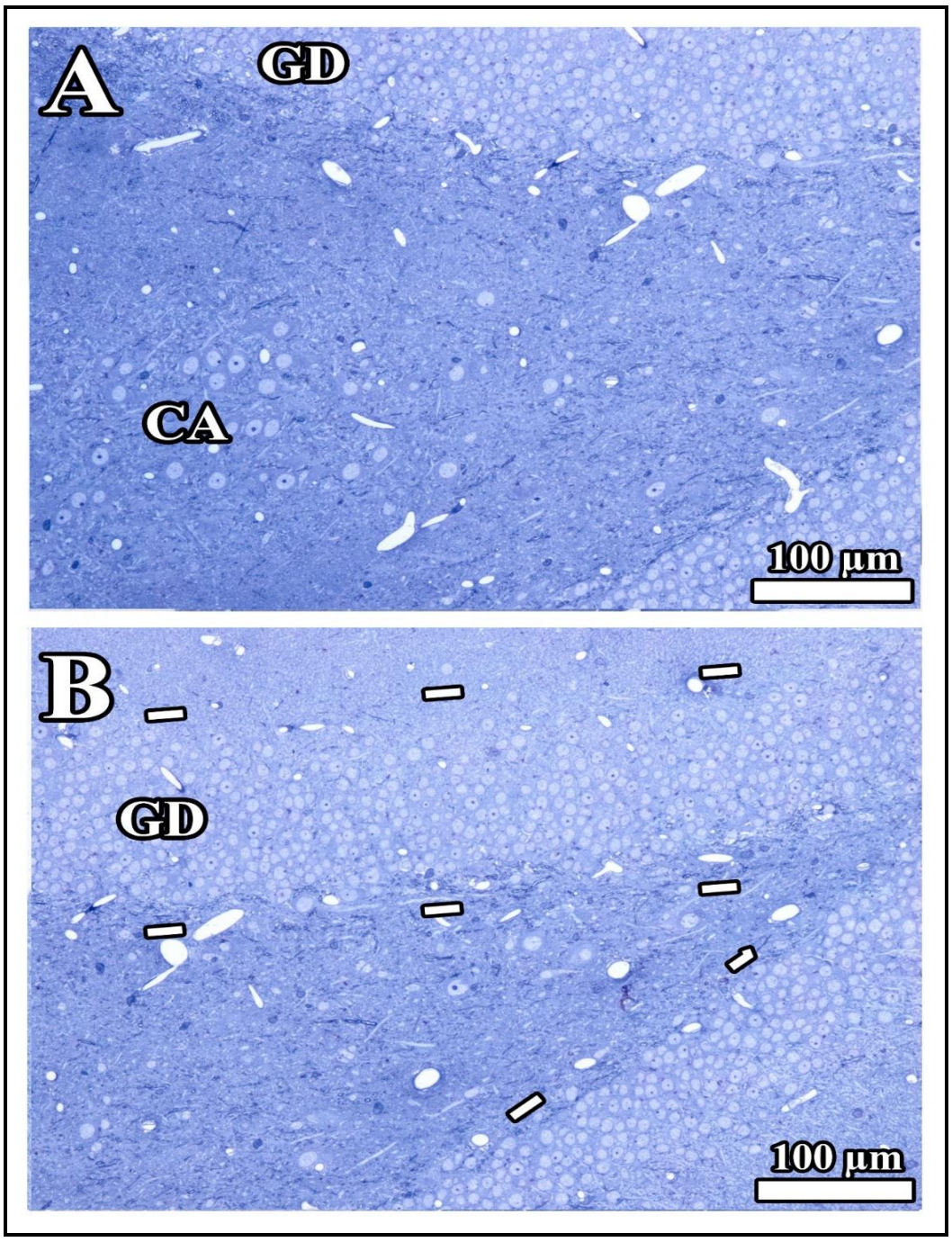

Figure 43. (A, B) Hippocampal regions in the Cont group are seen. The border of dentate gyrus (GD) is clearly observed. Some part of CA region is also seen. Both types of regions in the hippocampus show normal appearance. Granular cells and their nuclei are spherical in shape. The distance between them looks normal. Vessels in this region are intact. Toluidine blue stained semi-thin (0.5 µm) resin section

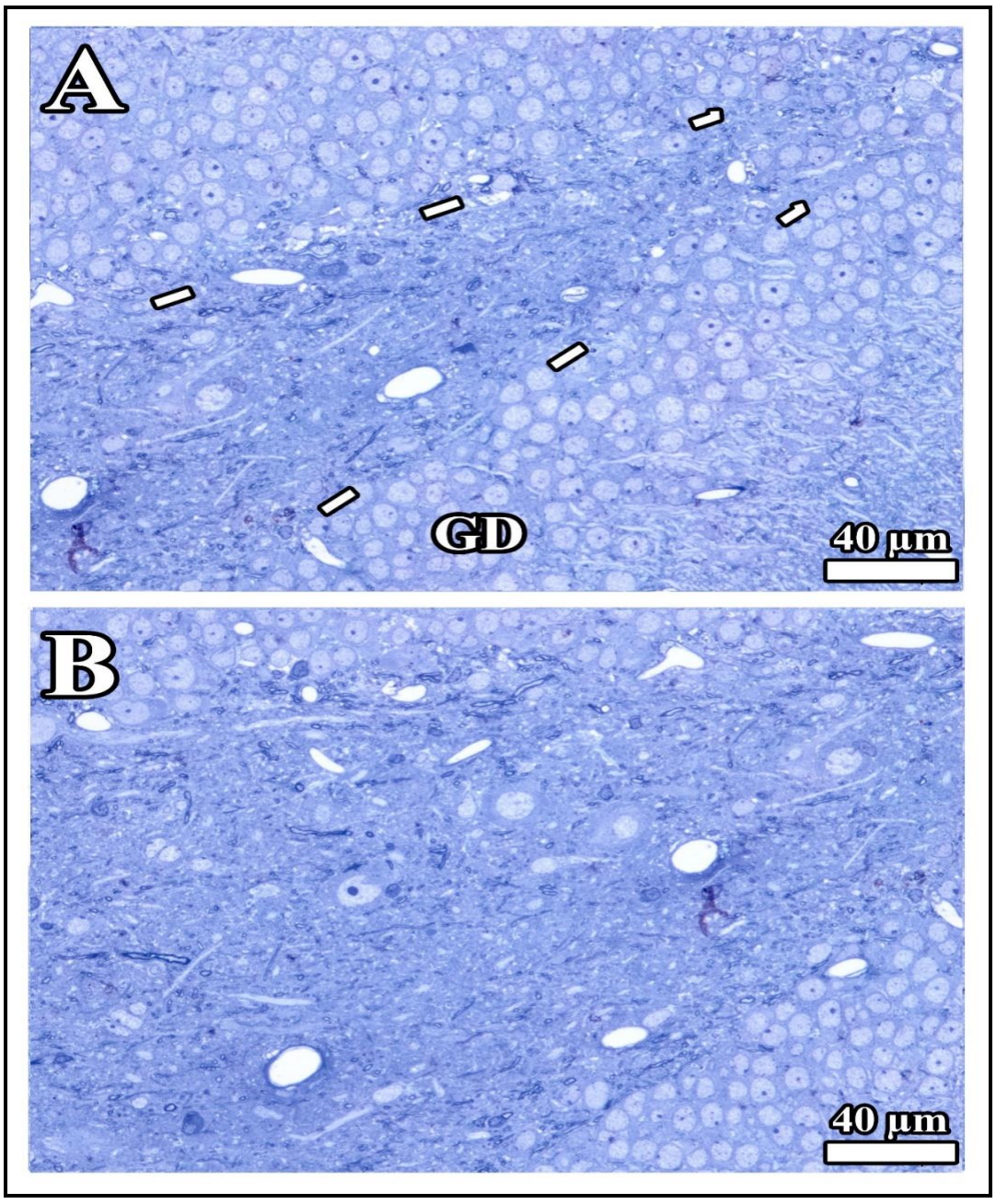

Figure 44. (A, B) High magnifications of images from hippocampal regions in the Cont group are seen. The border of dentate gyrus (GD) is clearly observed. Between the arms of DG and some of neurons belong to CA region are also seen. A few numbers of the dark cells and healthy axons are found. Both types of regions in the hippocampus show in normal appearance. Granular cells and their nuclei are spherical in shape. The distance between them looks normal. Vessels in this region are intact. Toluidine blue stained semi-thin (0.5 µm) resin section

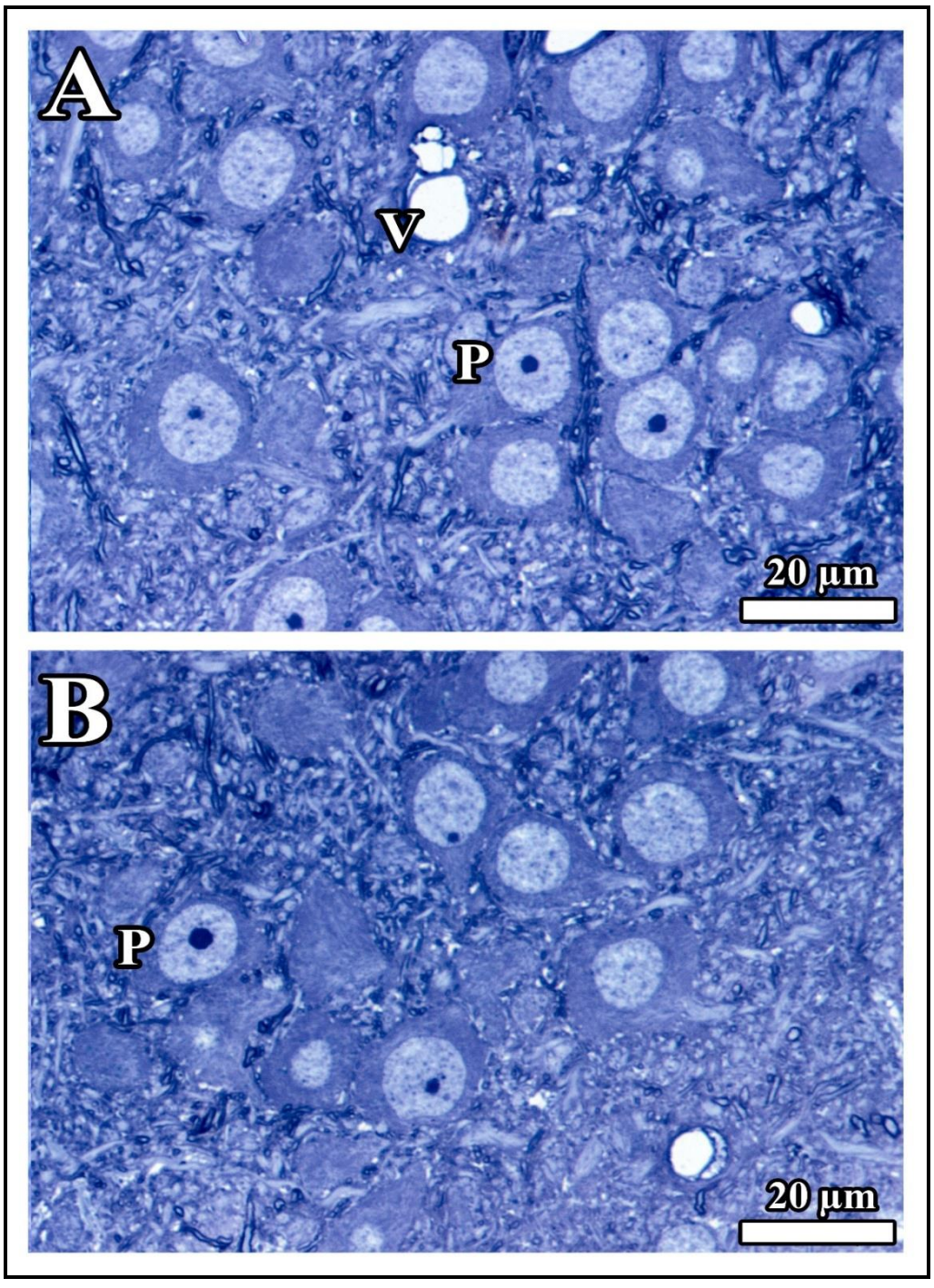

Figure 45. Images taken from the hippocampal region of the Cont group are seen. The border of pyramidal neurons and their nuclei in the CA region are clearly observed. Each pyramidal cell has an oval shaped nucleus. Vessels (V) in this region are intact and there is no gap between them and the surrounding tissue. Toluidine blue stained semi-thin (0.5 µm) resin section

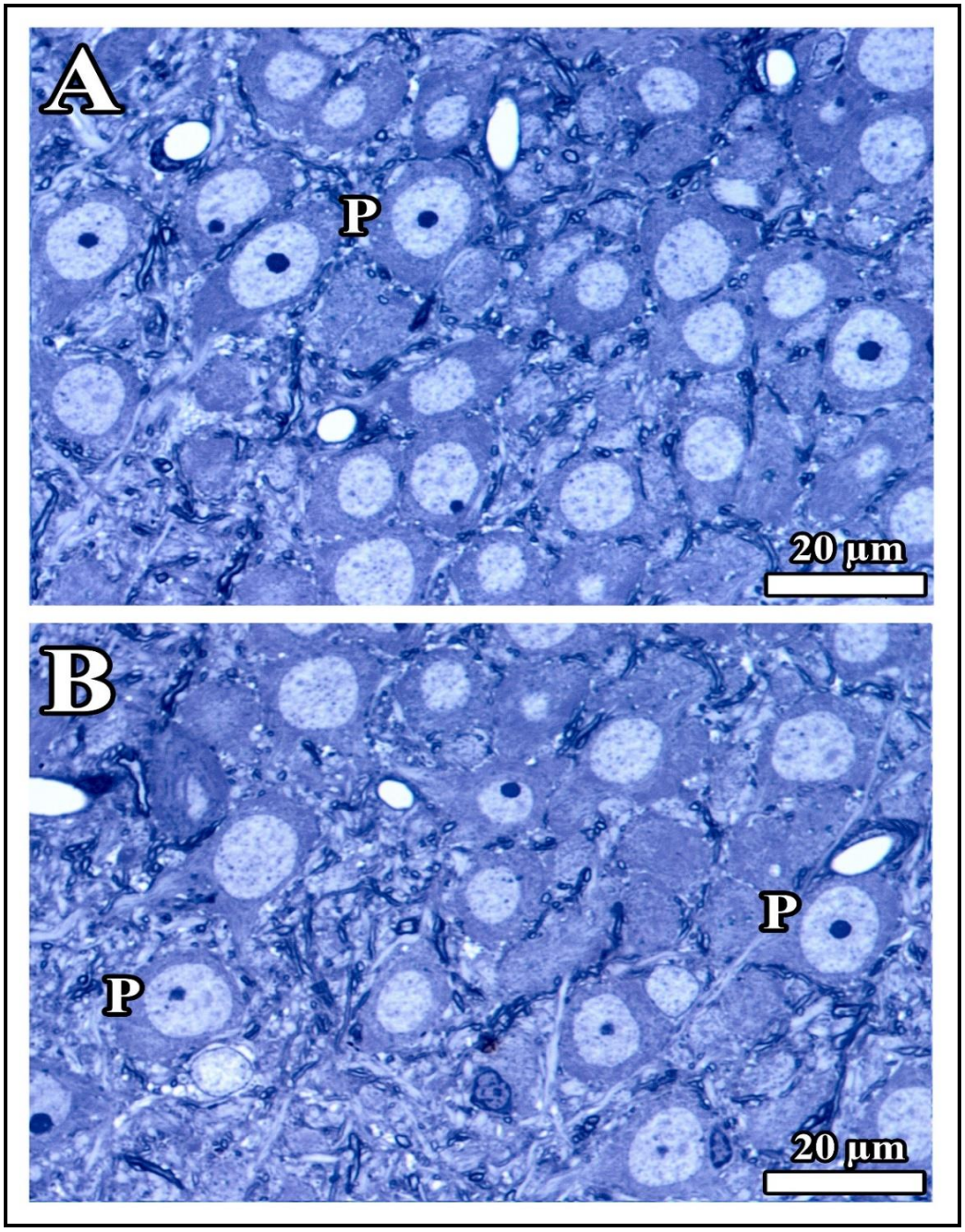

Figure 46. Images taken from the hippocampal region of the Cont group are seen. Accumulations of the pyramidal neurons (P) are found, the border of these neurons and their nuclei in the CA region are clearly observed. Each pyramidal cell has an oval shaped nucleus. Some of axons belong to neurons are also seen. Vessels in this region are intact and there is no gap between them and the surrounding tissue. Toluidine blue stained semi-thin (0.5 µm) resin section

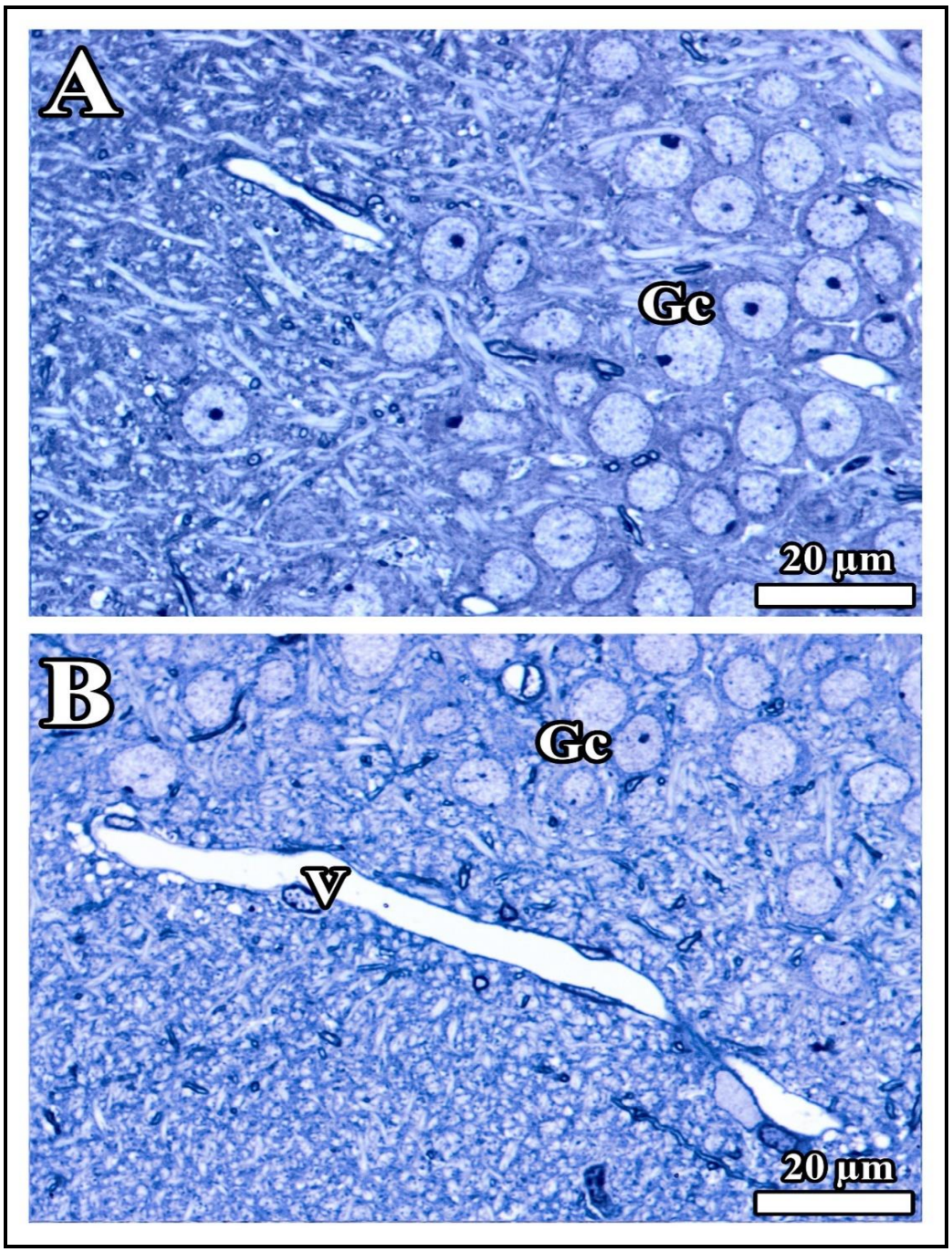

Figure 47. (A, B) High magnification of images from the hippocampal region belong to dentate gyrus in the Cont group are seen. Spherical shaped granular cells (Gc) in the dentate gyrus look in normal structure. Axons belong to granular cells that sectioned in longitudinal and in transverse are seen intact. Vessels (V) around this region are intact since there is no shrinkage and space between surrounding tissue. Toluidine blue stained semi-thin (0.5 µm) resin section

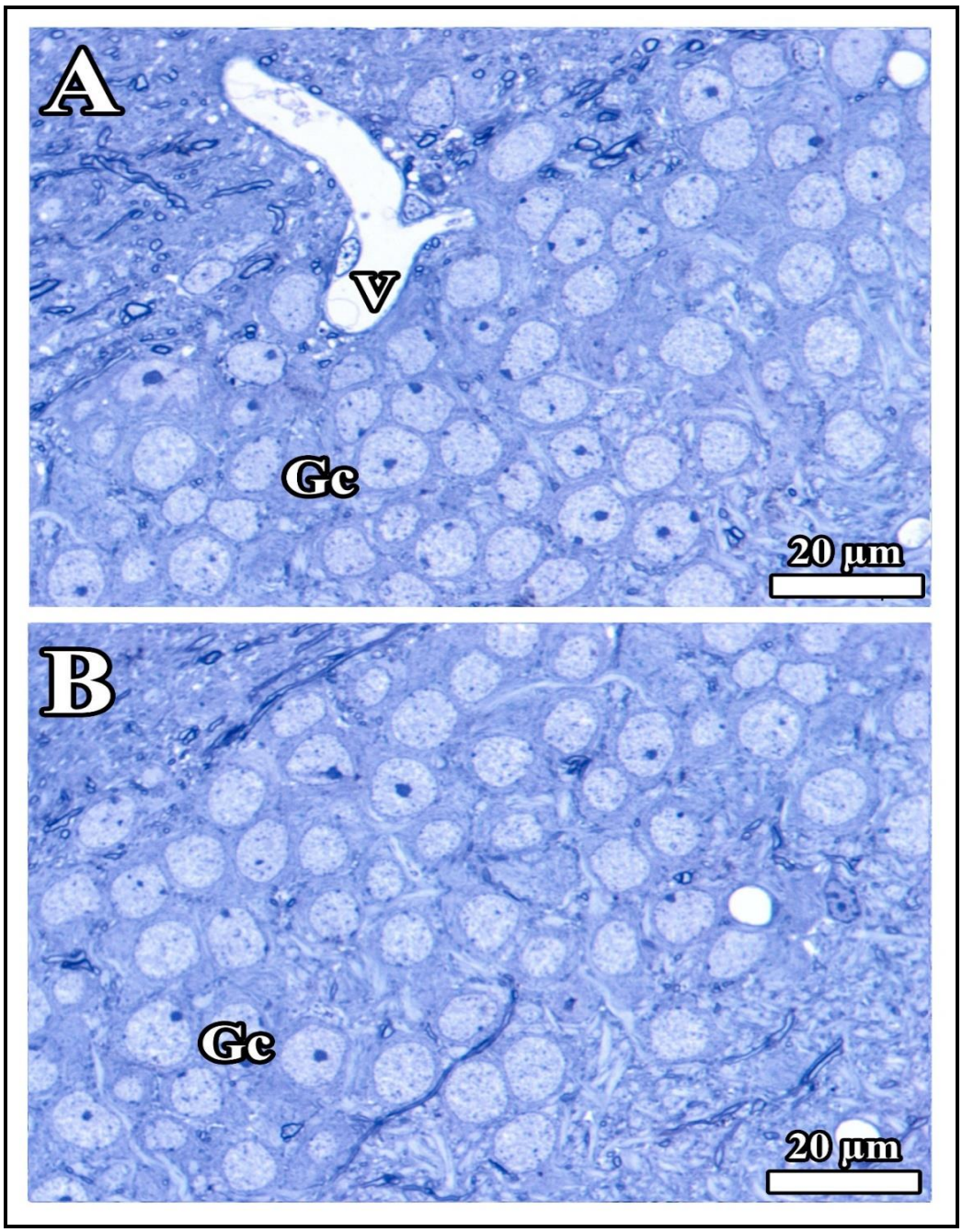

Figure 48. (A, B) High magnifications images of hippocampal region belong to dentate gyrus (GD) in the Cont group are seen. Spherical shaped granular cells (Gc) in the dentate gyrus not only looks in normal structure but also the distance between them is fine. A huge number of axons belong to granular cells that sectioned in longitudinal and in transverse are seen. Vessels (V) around this region are also intact since there is no shrinkage and gap between surrounding tissue. Toluidine blue stained semi-thin (0.5 µm) resin section

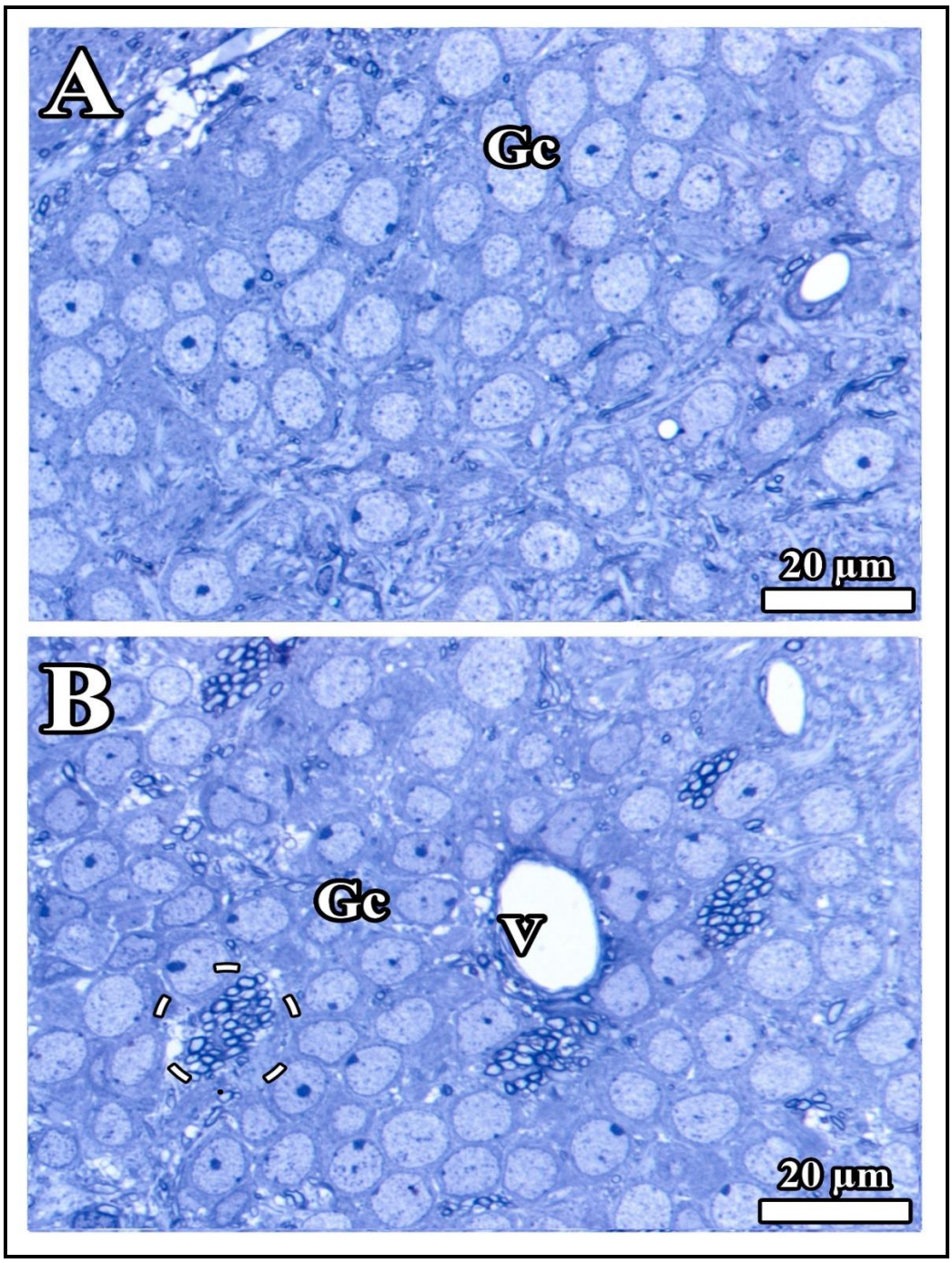

Figure 49. (A, B) A magnified images from the hippocampal region belong to dentate gyrus in the Cont group are seen. There are many cross-sectioned axons bundles seen between spherical shaped granular cells (Gc) in the dentate gyrus look in normal structure. Intact vessels (V) that lined by well-preserved endothelial cells are seen. Toluidine blue stained semi-thin (0.5 µm) resin section

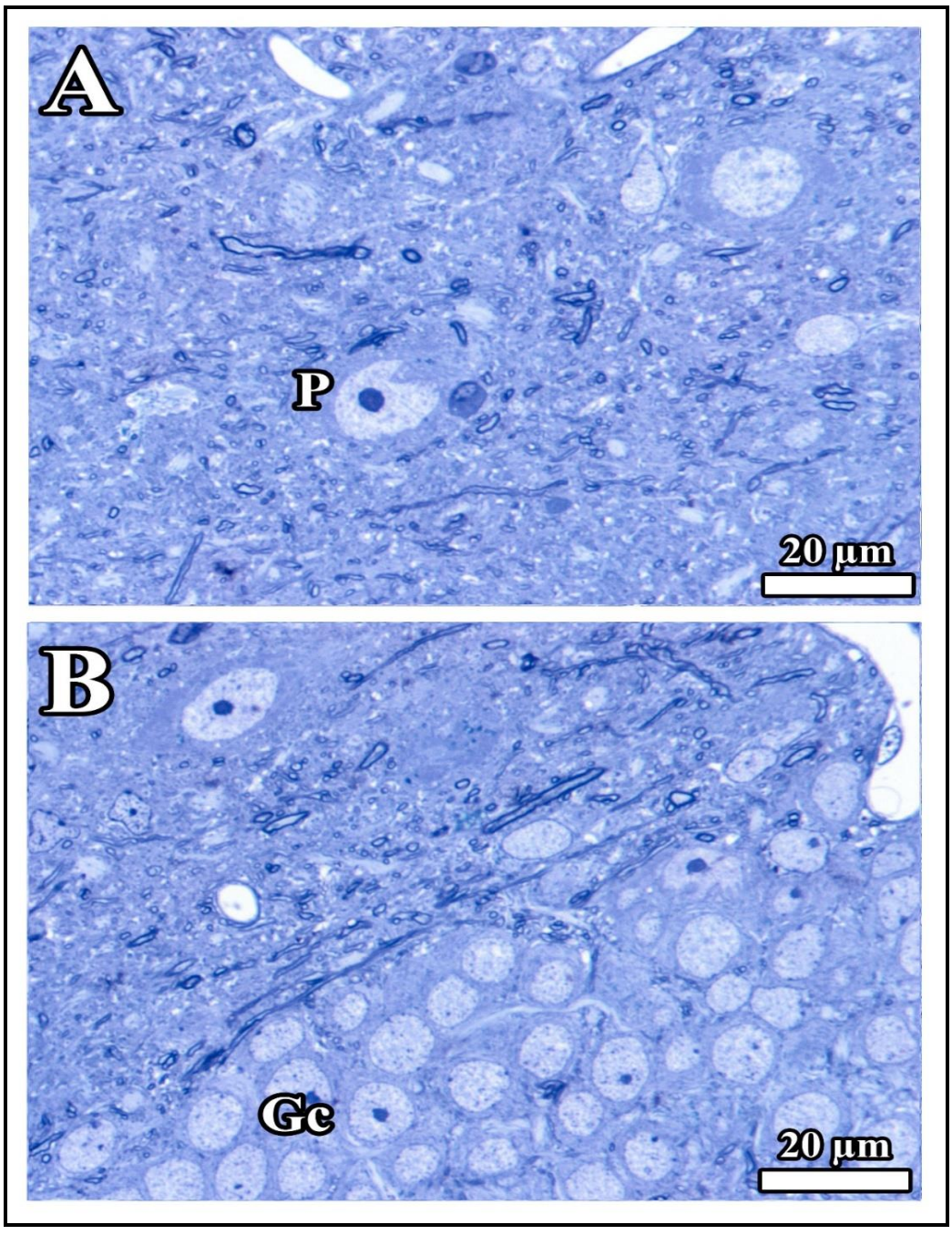

Figure 50. (A) A magnified image of CA region from the hippocampus belong to the Cont group is seen. Some of well-preserved and large neurons (P) in this region are found. Around these neurons many longitudinally or transversely sectioned myelinated axon can be seen. (B) An image that was taken from CA and dentate gyrus is observed. Spherical (Gc) and oval shaped (P) neurons are seen in normal structure. Between and around them many of nerve fibers can be found. Toluidine blue stained semi-thin (0.5 µm) resin section

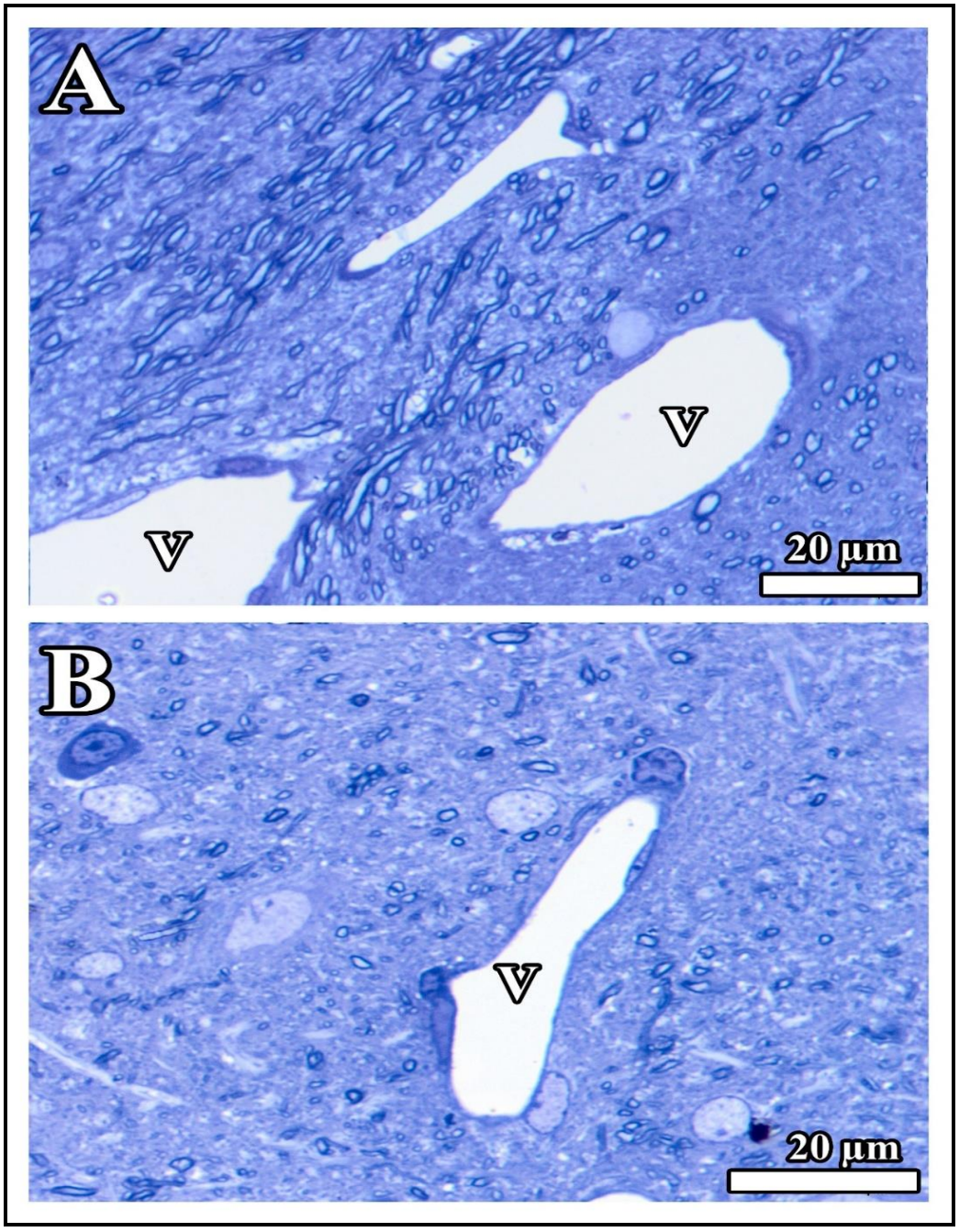

Figure 51. (A, B) Images taken from the Cont group are seen. Large and small size capillaries (V) are observed. These structures have a normal wall and there is no gap between the wall and surrounding tissues. Some of axons were cut in longitudinally and other transversely. Even these vessels have very thin wall but its lumen are intact, nuclei of endothelial and pericyte are seen in normal structure. Toluidine blue stained semi-thin (0.5 µm) resin section

Regarding the Sham group, the images taken from hippocampal region showed that, pyramidal cells and granular cells are in the normal morphology. The perikaryon of cells can be seen clearly (**Figure 52, 53, 54, 55, 56, 57, 58, 59 and 60**). Dark cells have an angular shape. Also some as dark cells found if compared with the Cont group.

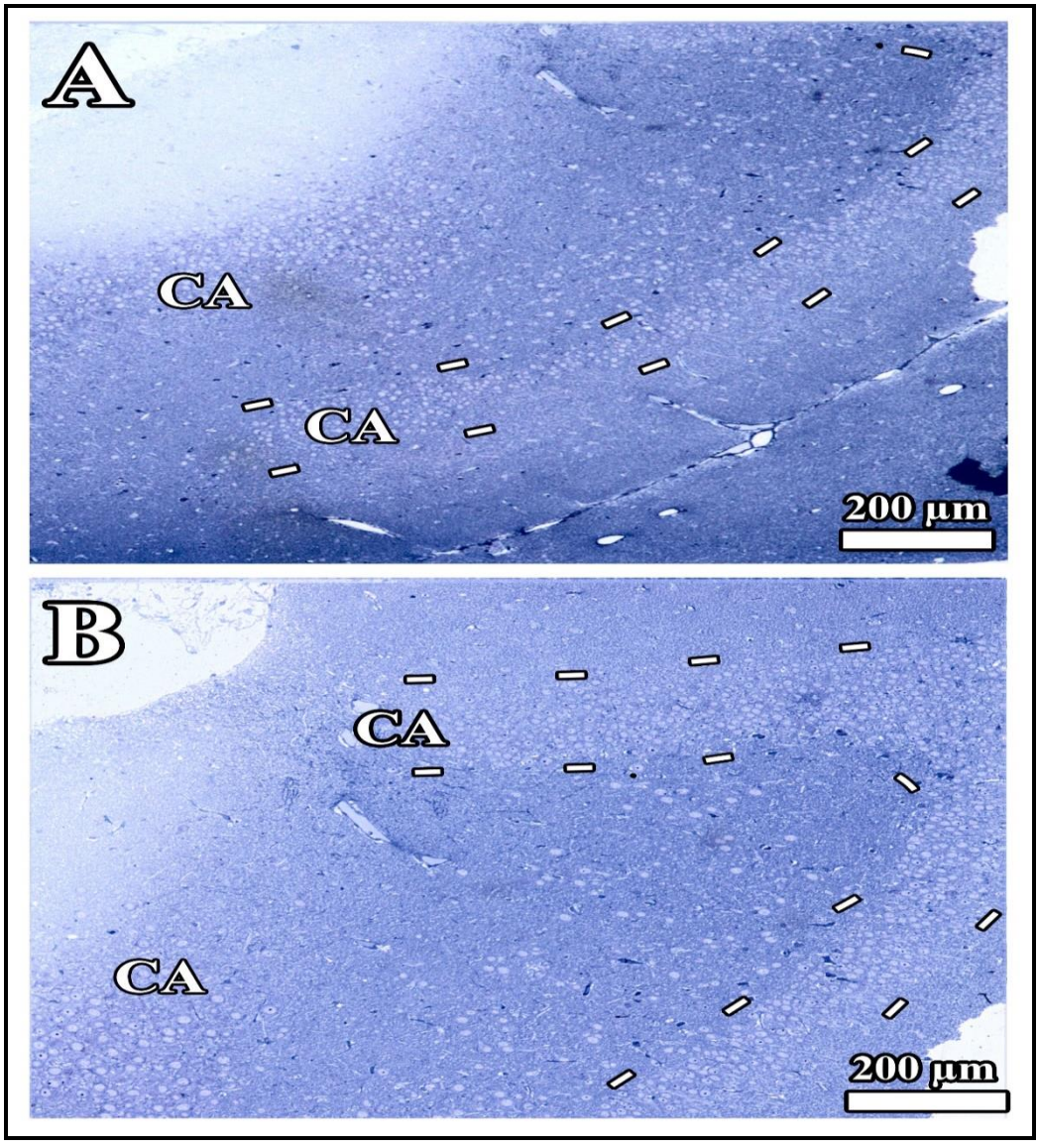

Figure 52. (A, B) Images taken from the hippocampus belong to the Sham group are seen. General structure of CA looks in normal morphology. Toluidine blue stained semi-thin (0.5 µm) resin section

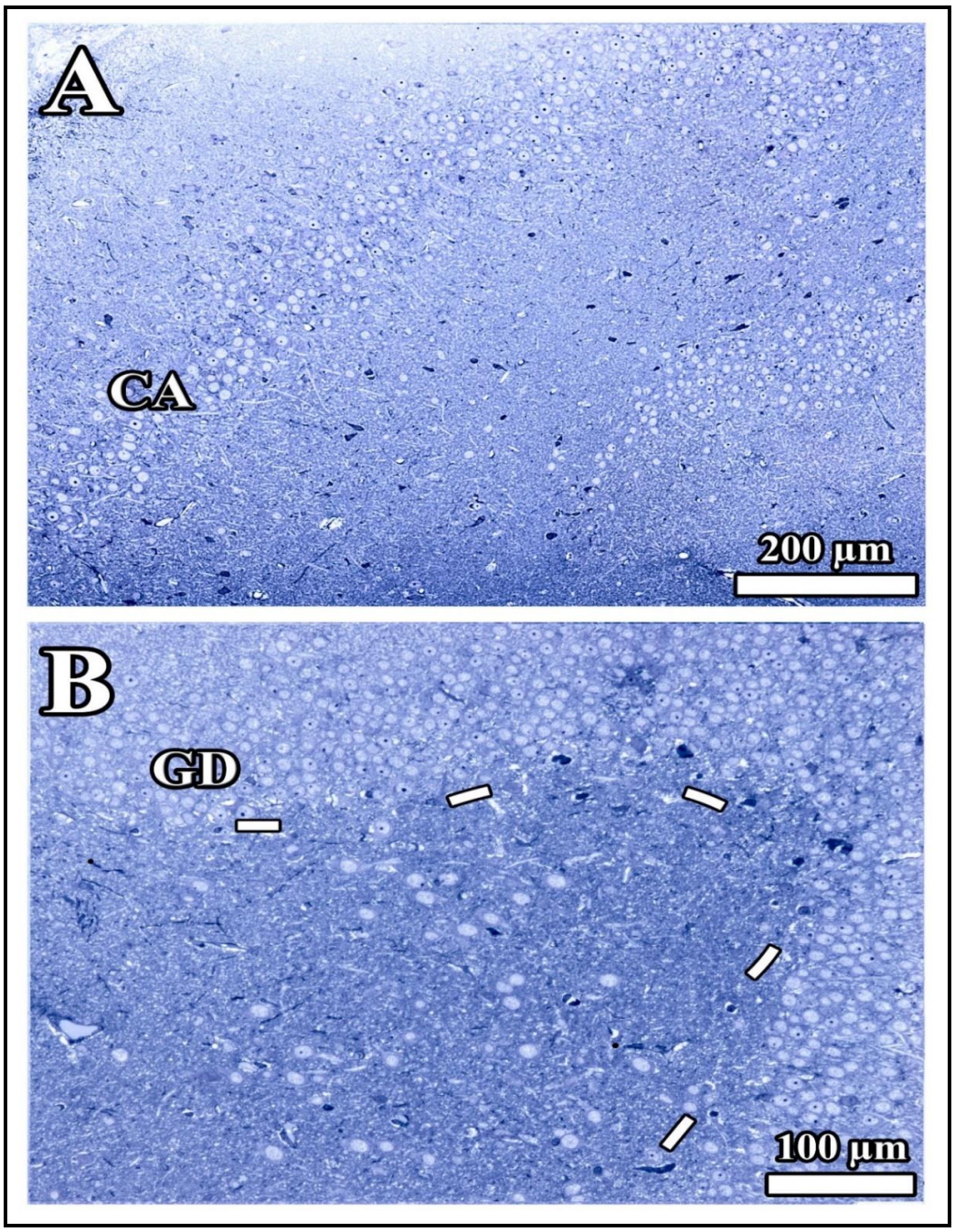

Figure 53. (A, B) Images taken from the hippocampus belong to the Sham group are seen. General structure of CA and GD shows normal appearance. Pyramidal cells in the CA region and granular cells in the GD are showed normal appearance. Some of dark cells are seen in the both regions, CA and GD. Toluidine blue stained semi-thin (0.5 µm) resin section

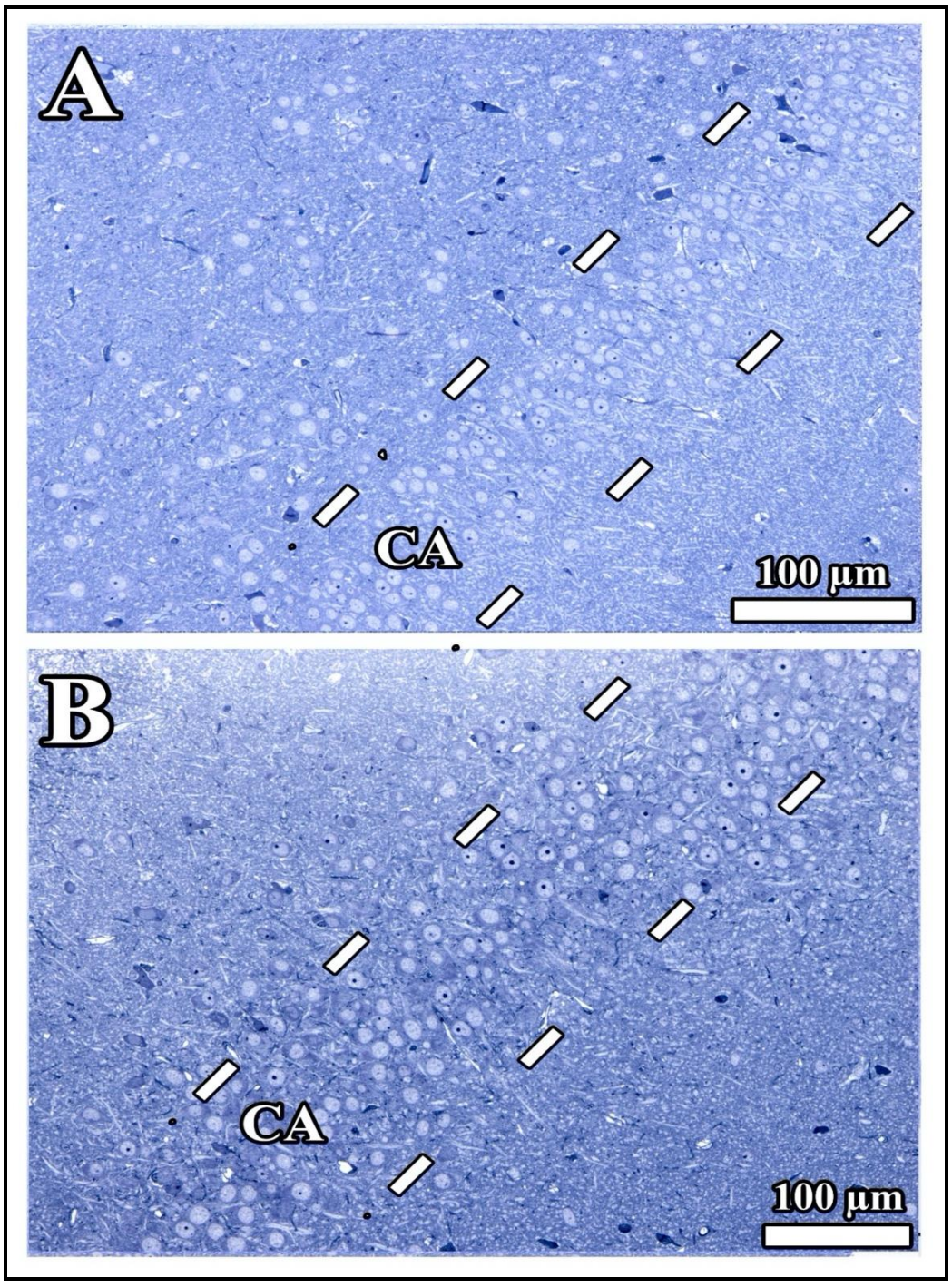

Figure 54. (A, B) Images taken from the CA region of hippocampus belong to the Sham group are seen. General structure of CA shows normal appearance. Pyramidal cells in the CA region are showed also normal structure. Some of dark cells are seen around in the CA region. The distance between pyramidal cells is normal. Toluidine blue stained semi-thin (0.5 µm) resin section

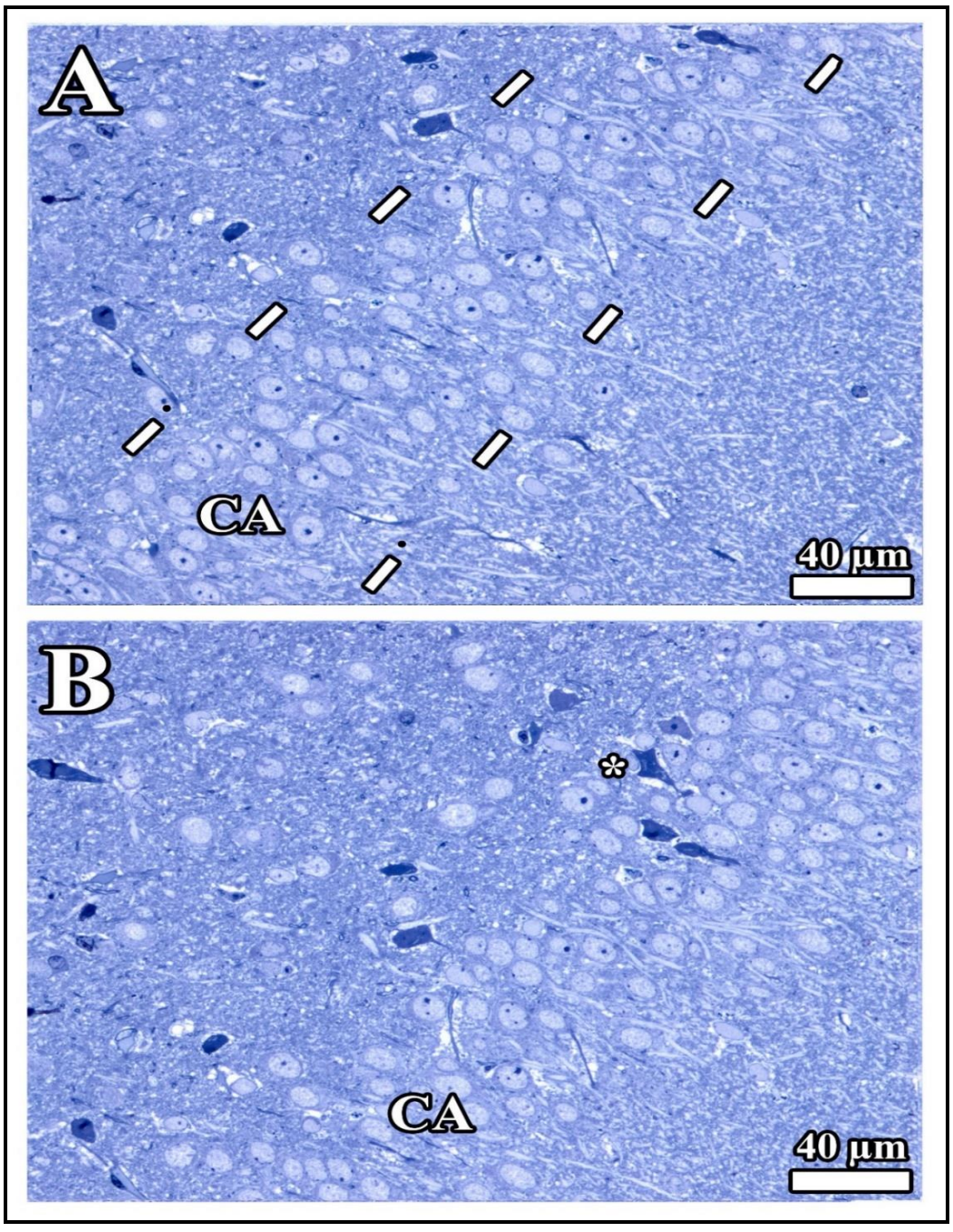

Figure 55. (A, B) Images taken from the CA region of hippocampus belong to the Sham group are seen. General structure of CA looks normal and pyramidal cells in this region are also seen in normal. The nuclei of pyramidal cells have oval shape. Some of dark cells (*) are found around and inside of the CA region, many of axons belong to the pyramidal cells can be observed. The distance between pyramidal cells is normal. Toluidine blue stained semi-thin (0.5 µm) resin section

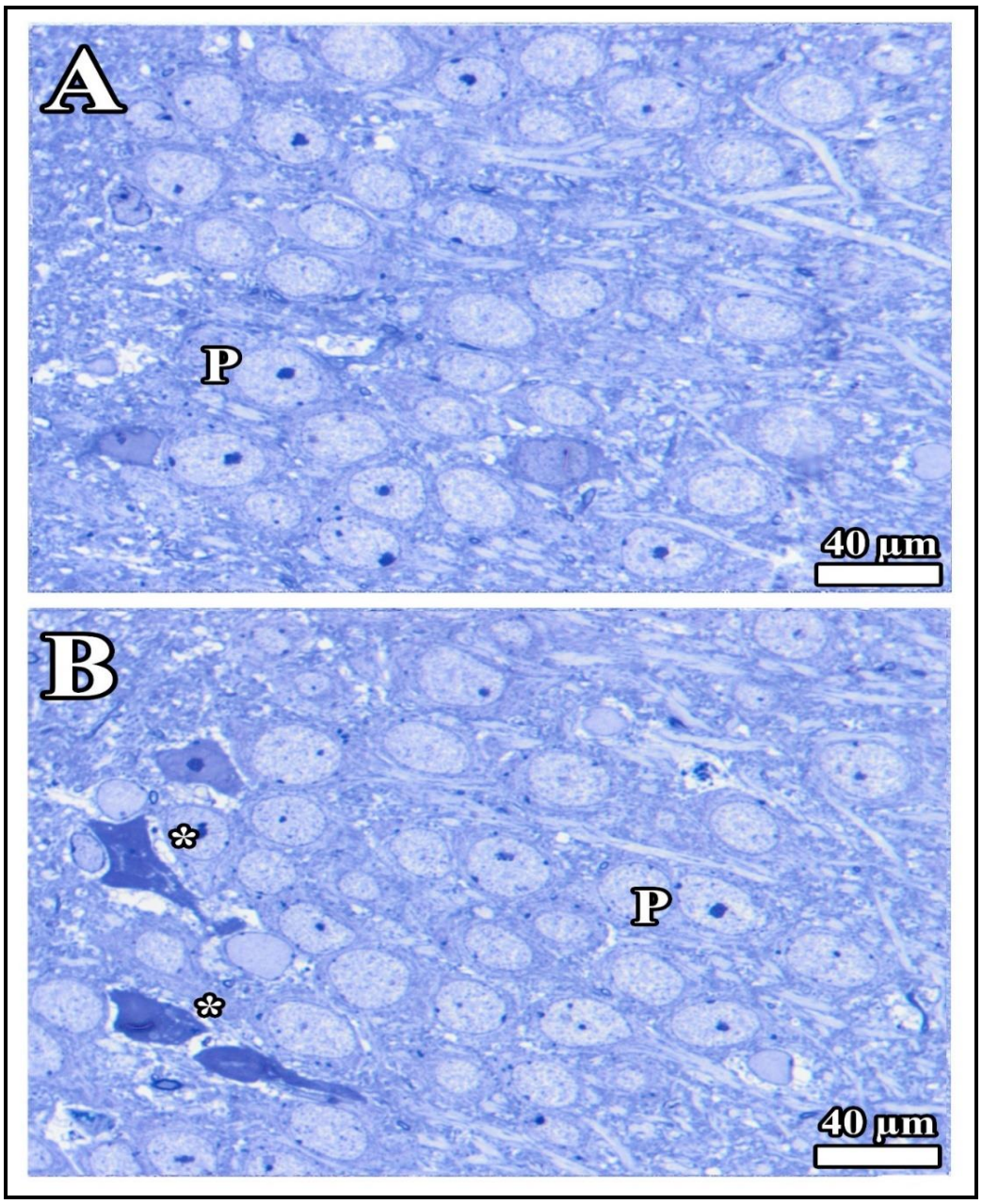

Figure 56. (A, B) Images taken from the CA region of hippocampus belong to the Sham group are seen. General structure of CA looks normal and pyramidal cells (P) in this region are also showed normal appearance. The nuclei of pyramidal cells have oval shape. Some of dark cells (*) are seen around and inside of the CA region, many of axons that sectioned longitudinally belong to the pyramidal cells can be seen. The distance between pyramidal cells is normal and the border of nuclei can be seen clearly. Dark cells have an angular shape; these cells may be going to death. Toluidine blue stained semi-thin (0.5 µm) resin section

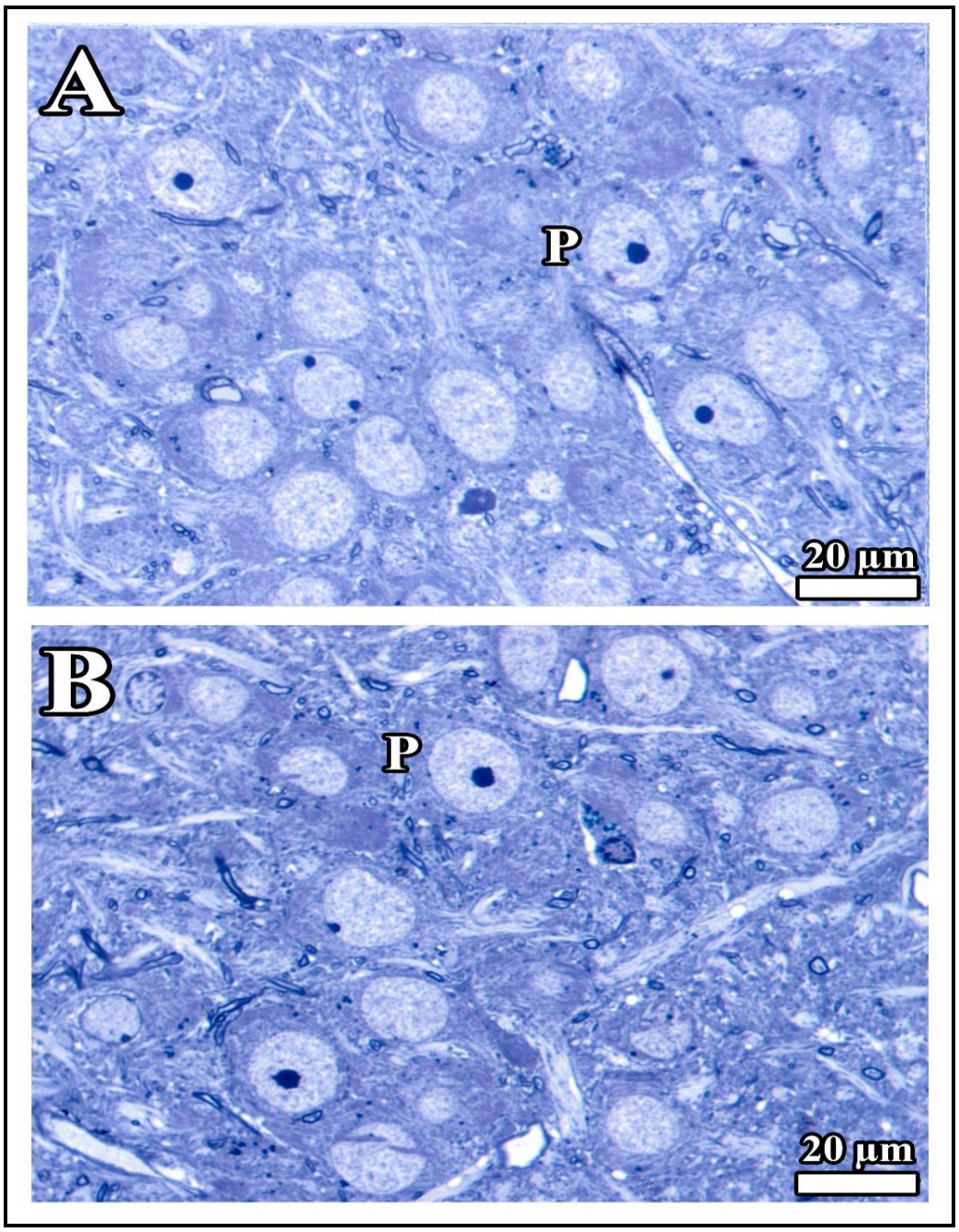

Figure 57. (A, B) Images taken from the CA region of hippocampus belong to the Sham group are seen. General structures of pyramidal cells in this region are showed normal appearance. The nuclei of pyramidal cells have oval shape and clear border. The distance between pyramidal cells (P) is normal and the border of nuclei as well as perikaryon of cells can be seen clearly. Cross-and the longitudinal sections of axons are seen circular and longitudinal as darkly stained structure. Toluidine blue stained semi-thin (0.5 µm) resin section

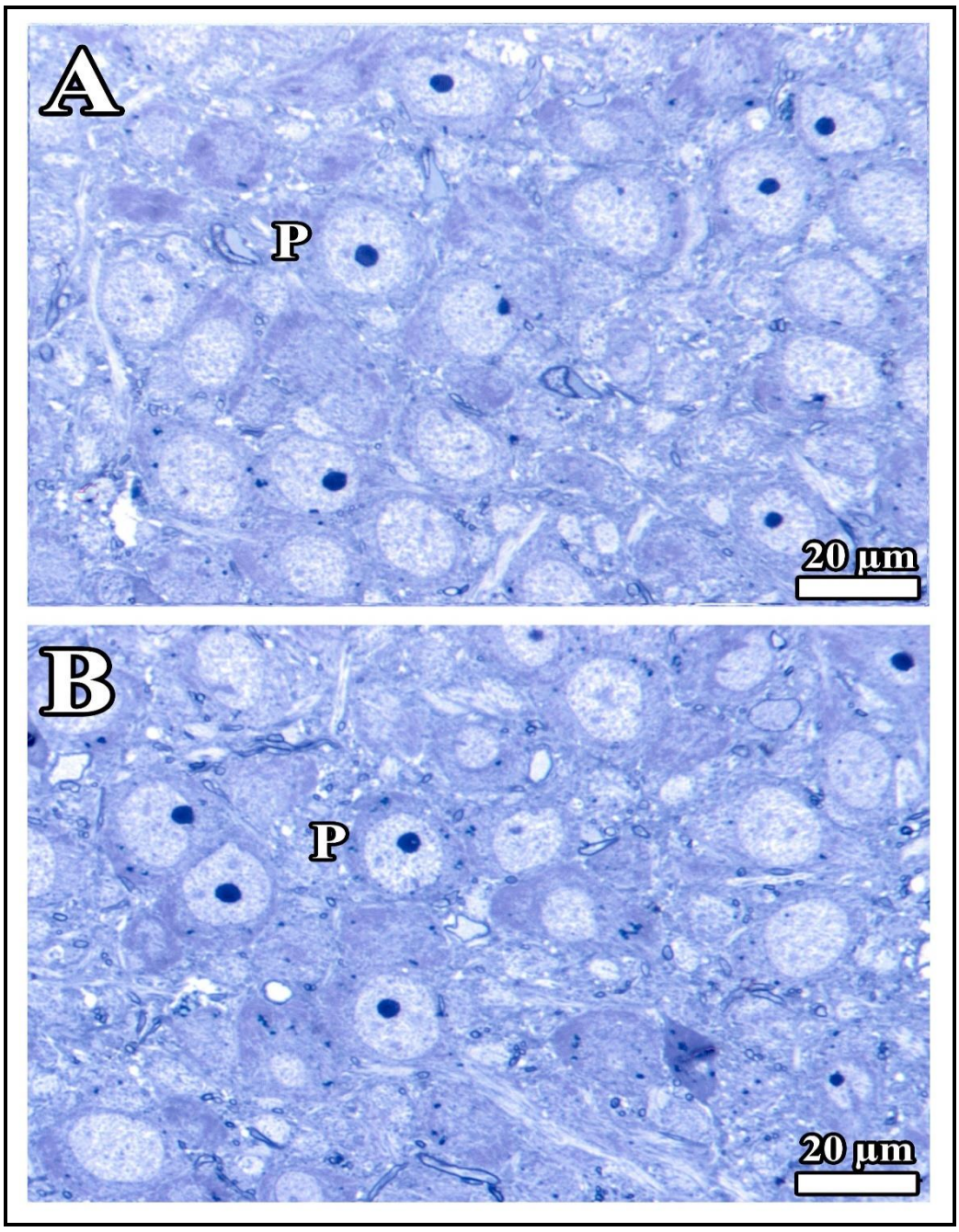

Figure 58. (A, B) Images taken from the CA region of hippocampus belong to the Sham group are seen. General structures of pyramidal cells (P) in this region are showed normal appearance. The nuclei of pyramidal cells have oval shape and the clear border. The distance between pyramidal cells is normal and the border of nuclei as well as darkly stained perikaryon of some cells can be seen. Toluidine blue stained semi-thin (0.5 µm) resin section

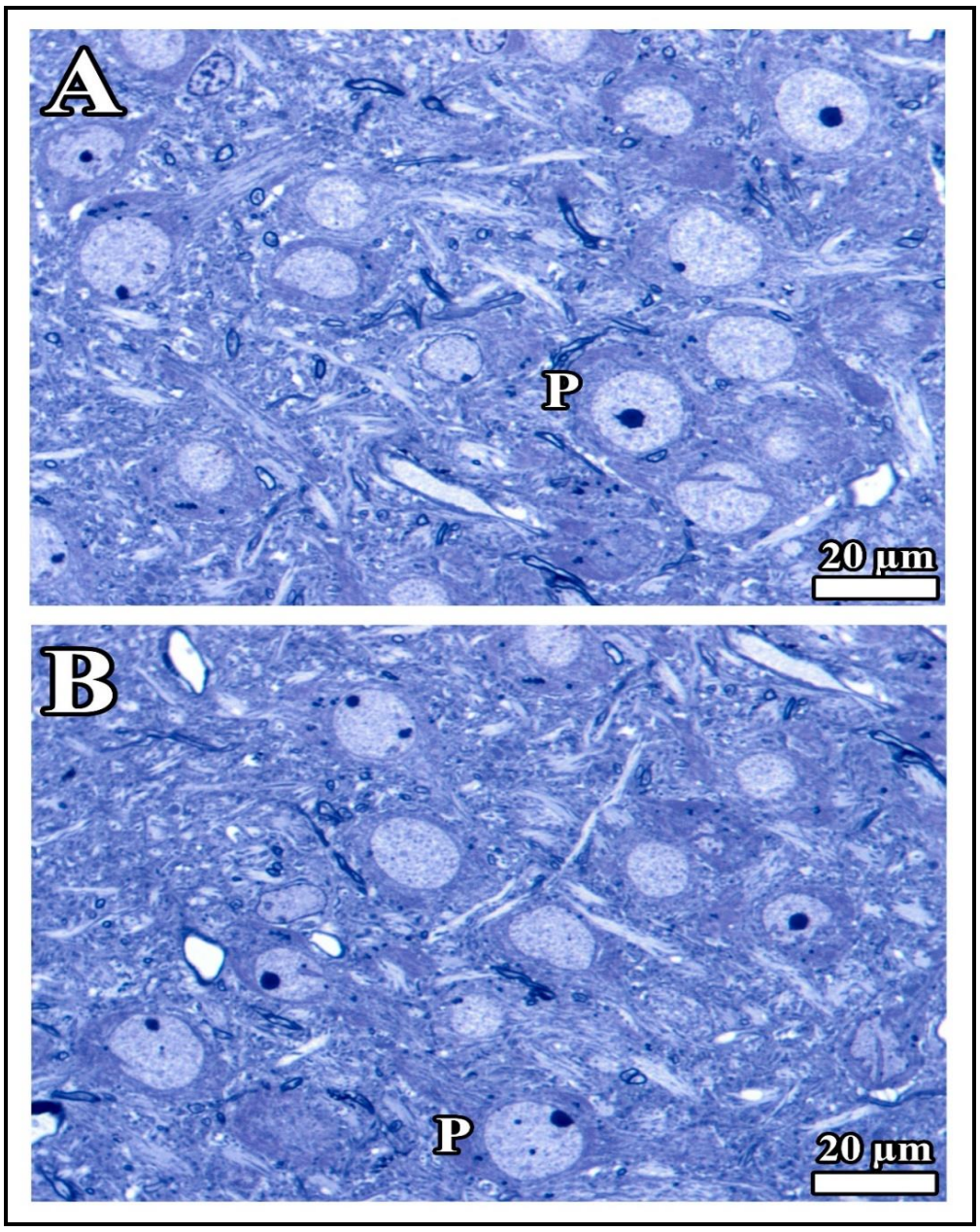

Figure 59. (A, B) Images taken from the CA region of hippocampus belong to the Sham group are seen. General structures of pyramidal cells (P) in this region are showed normal appearance. The nuclei of pyramidal cells have oval shape and the clear border. Most of cells have very dark and large nucleolus. The distance between pyramidal cells is normal and the border of nuclei as well as darkly stained perikaryon of cells can be seen clearly. Cross-and the longitudinal section of axons are seen circular and longitudinal as dark structure. Toluidine blue stained semi-thin (0.5 µm) resin section

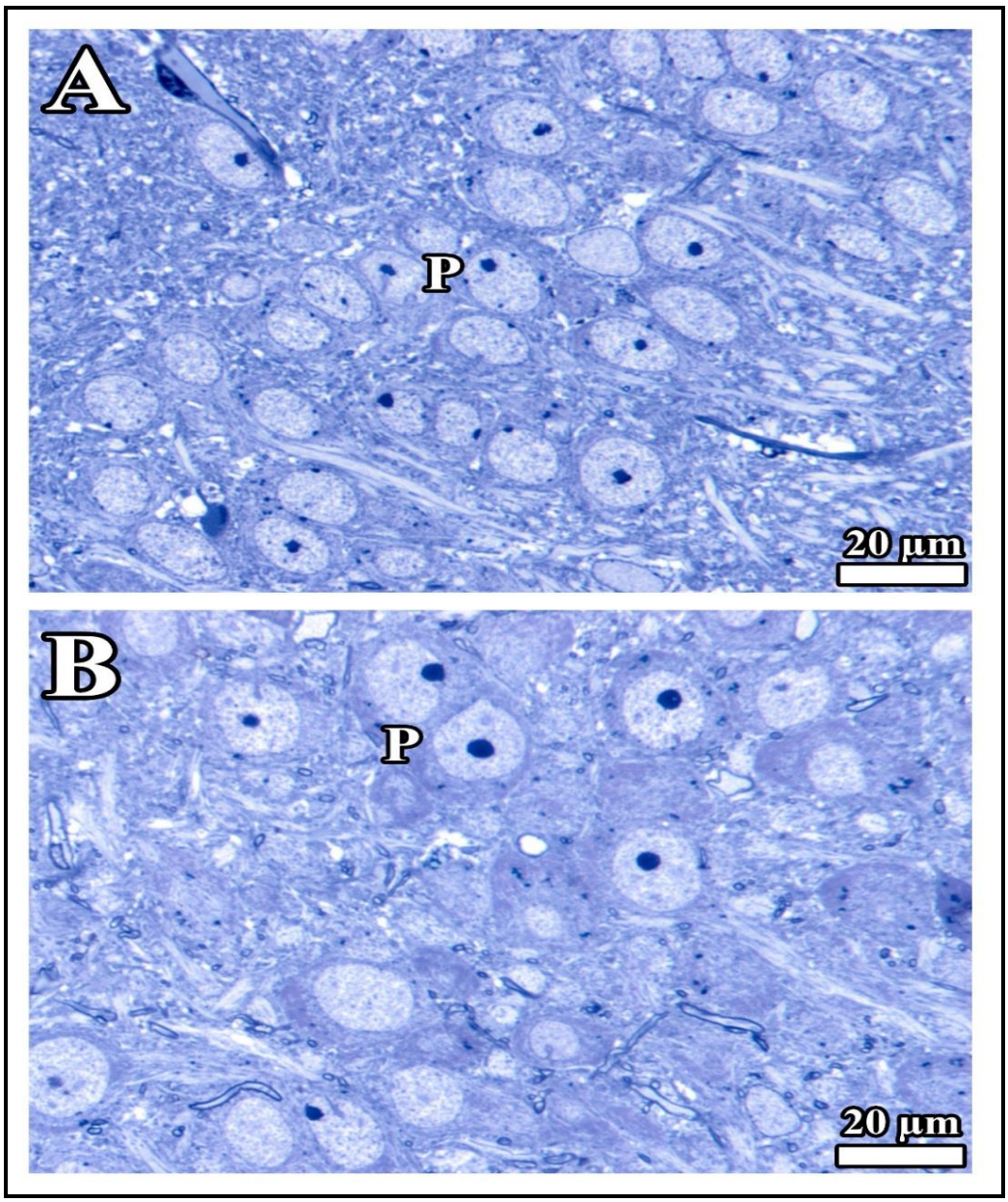

Figure 60. (A, B) Images taken from the CA region of hippocampus belong to the Sham group are seen. General structures of pyramidal cells (P) in this region are showed normal appearance. The nuclei of pyramidal cells have oval shape and clear border. Most of the cells have very dark and large nucleolus. The distance between pyramidal cells is normal and the border of nuclei as well as darkly stained perikaryon of cells can be observed clearly. Cross- and longitudinal sections of axons are seen circular and longitudinal as dark structures. As it can be seen, axons of pyramidal cells accumulated around pyramidal cell layer. Toluidine blue stained semi-thin (0.5 µm) resin section

Regarding the AD group, the images taken from hippocampal region have showed that general structure of CA region looks in normal (**Figure 61, 62, 63, 64, 65 and 66**). The pyramidal neurons look healthy and their perikaryon can be seen clearly. A well-preserved choroid plexus in third ventricle and ependymal cells are observed.

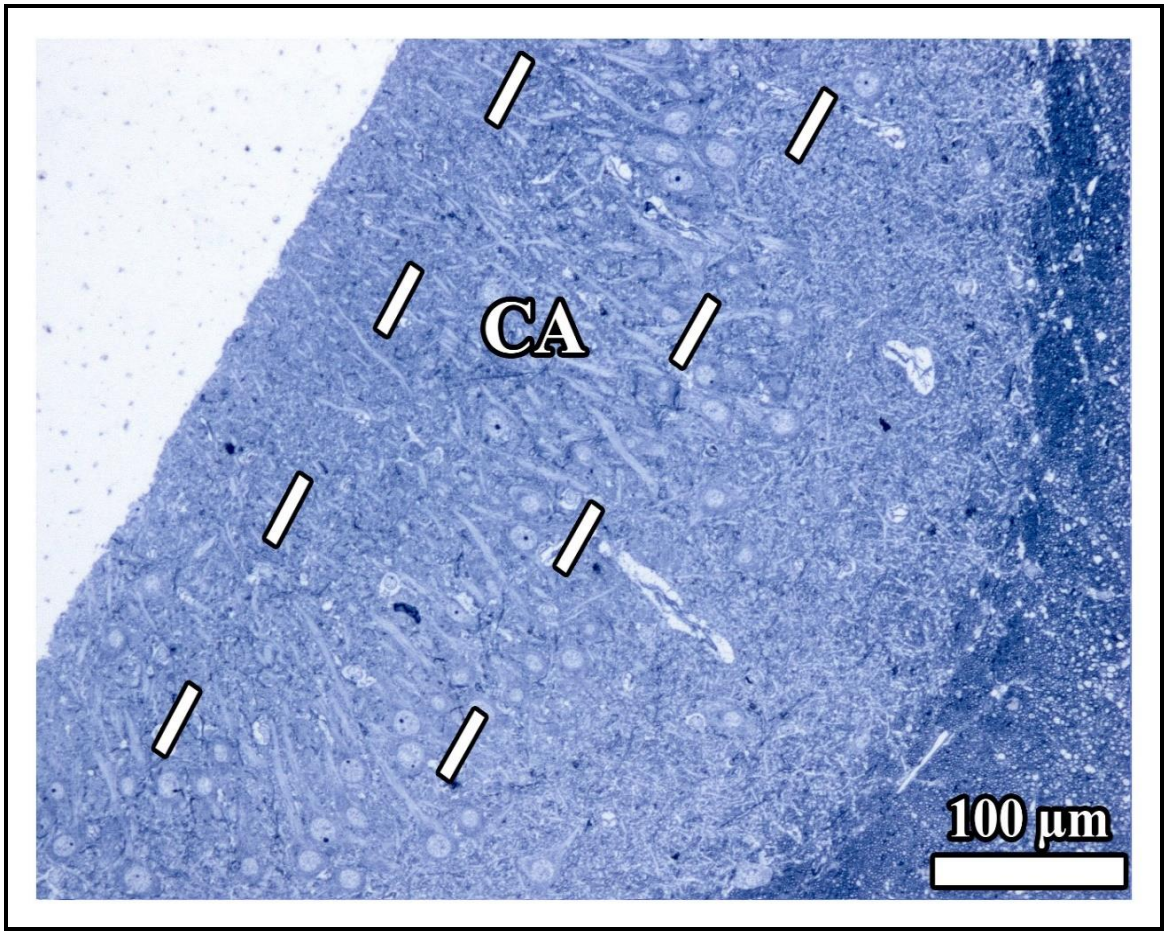

Figure 61. (A, B) The image taken from the CA region of hippocampus belong to the AD group are seen. General structure of CA region looks in normal. Their axons and nucleus are clearly observed. Some of the vessels are collapsed possibly as a result of low-quality fixation. Toluidine blue stained semi-thin (0.5 µm) resin section

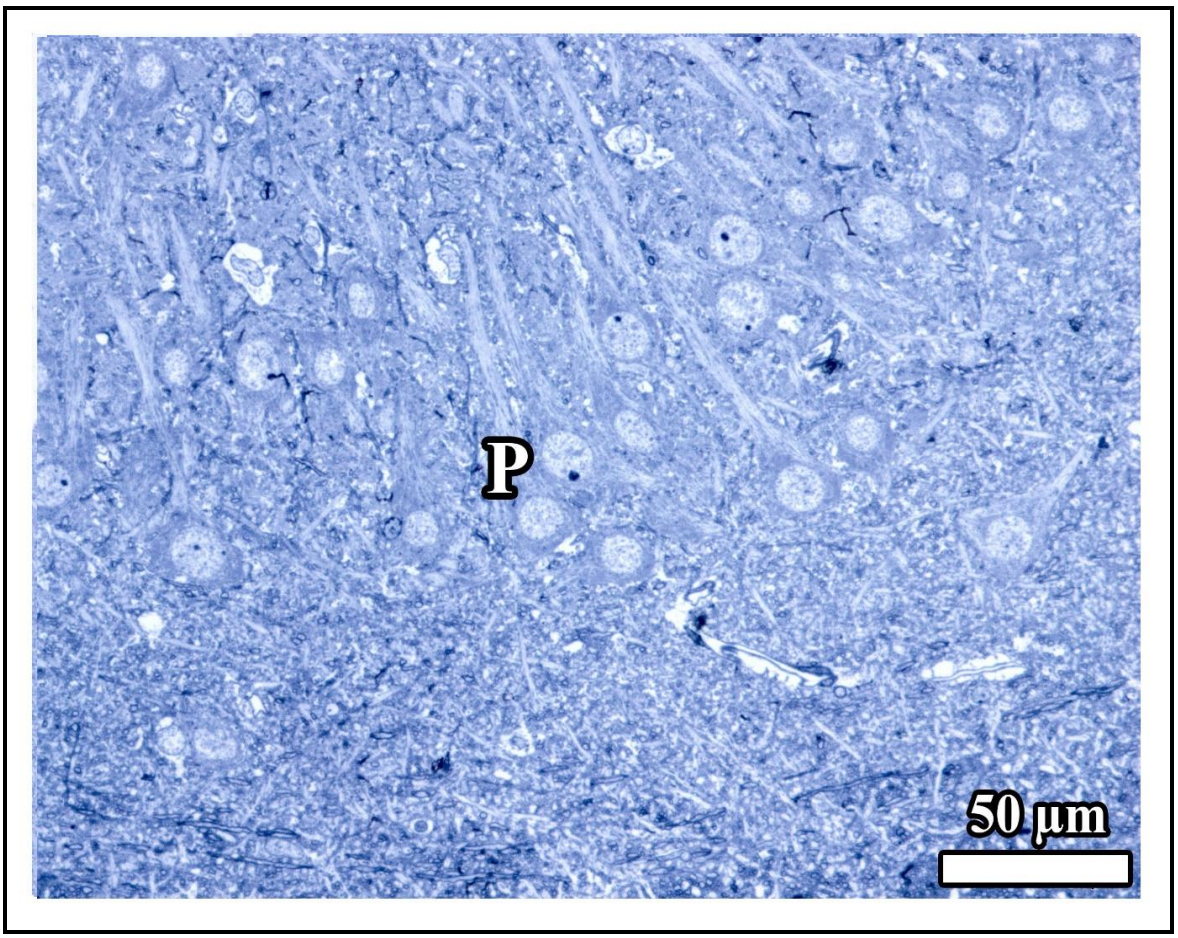

Figure 62. The image taken from the CA region of hippocampus belong to the AD group are seen. General structure of CA region looks in normal. Their axons and nucleus are clearly observed and pyramidal neurons (P) in this region have long axons. The border of nucleus and perikaryon can be seen clearly. Some of the vessels are collapsed possibly as a result of low-quality fixation. Toluidine blue stained semi-thin (0.5 µm) resin section

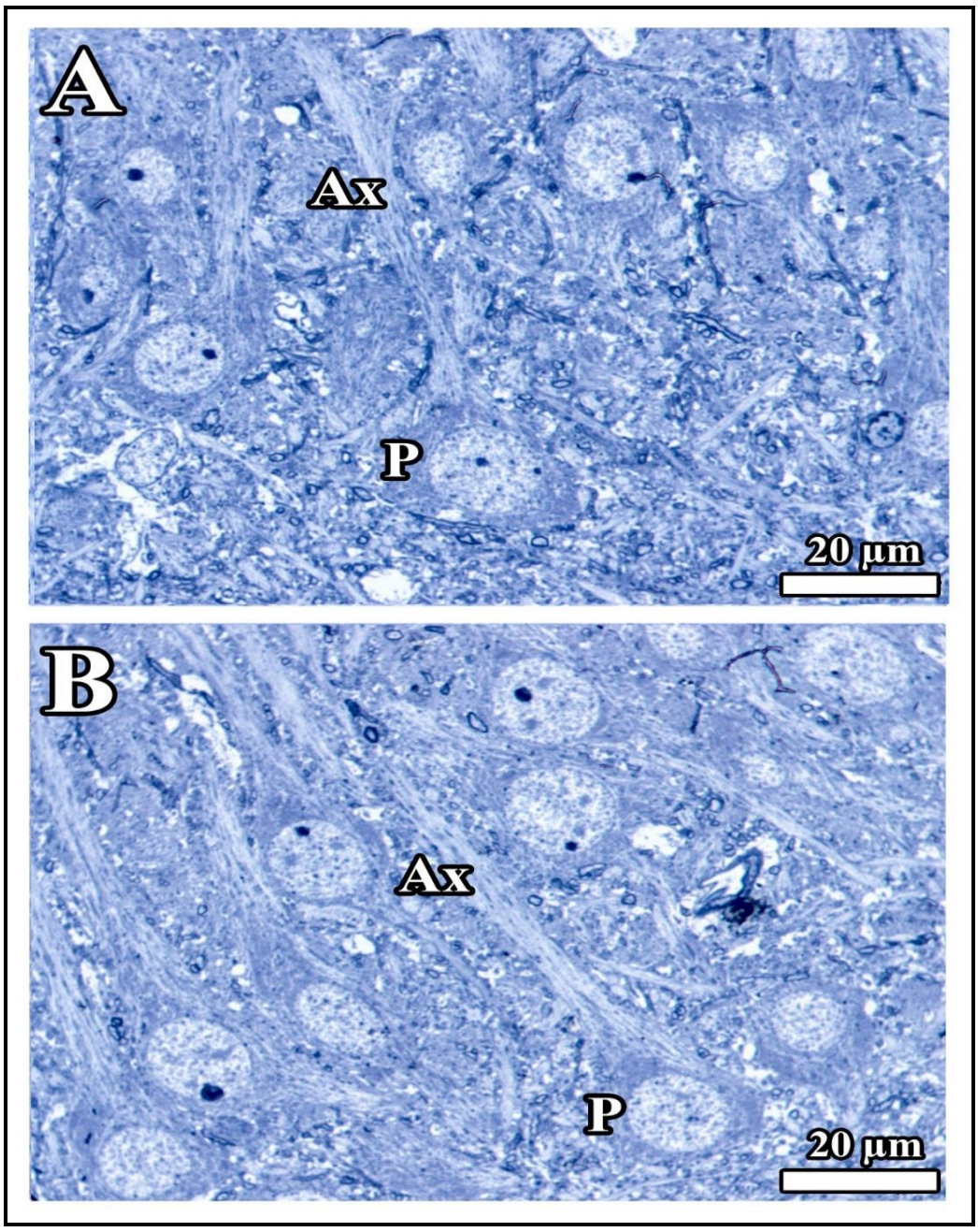

Figure 63. (A, B) Images taken from the CA region of hippocampus belong to the AD group are seen. General structure of CA region looks in normal appearance. Their axons (Ax) and nucleus are clearly observed and pyramidal neurons (P) in this region have very long axons. The border of nucleus and perikaryon can be seen clearly, since each perikaryon delineated by cross sections of axons. Pyramidal shape perikaryon has a spherical nucleus; this is a typical shape of pyramidal cells in the CA region of hippocampus. Toluidine blue stained semi-thin (0.5 µm) resin section

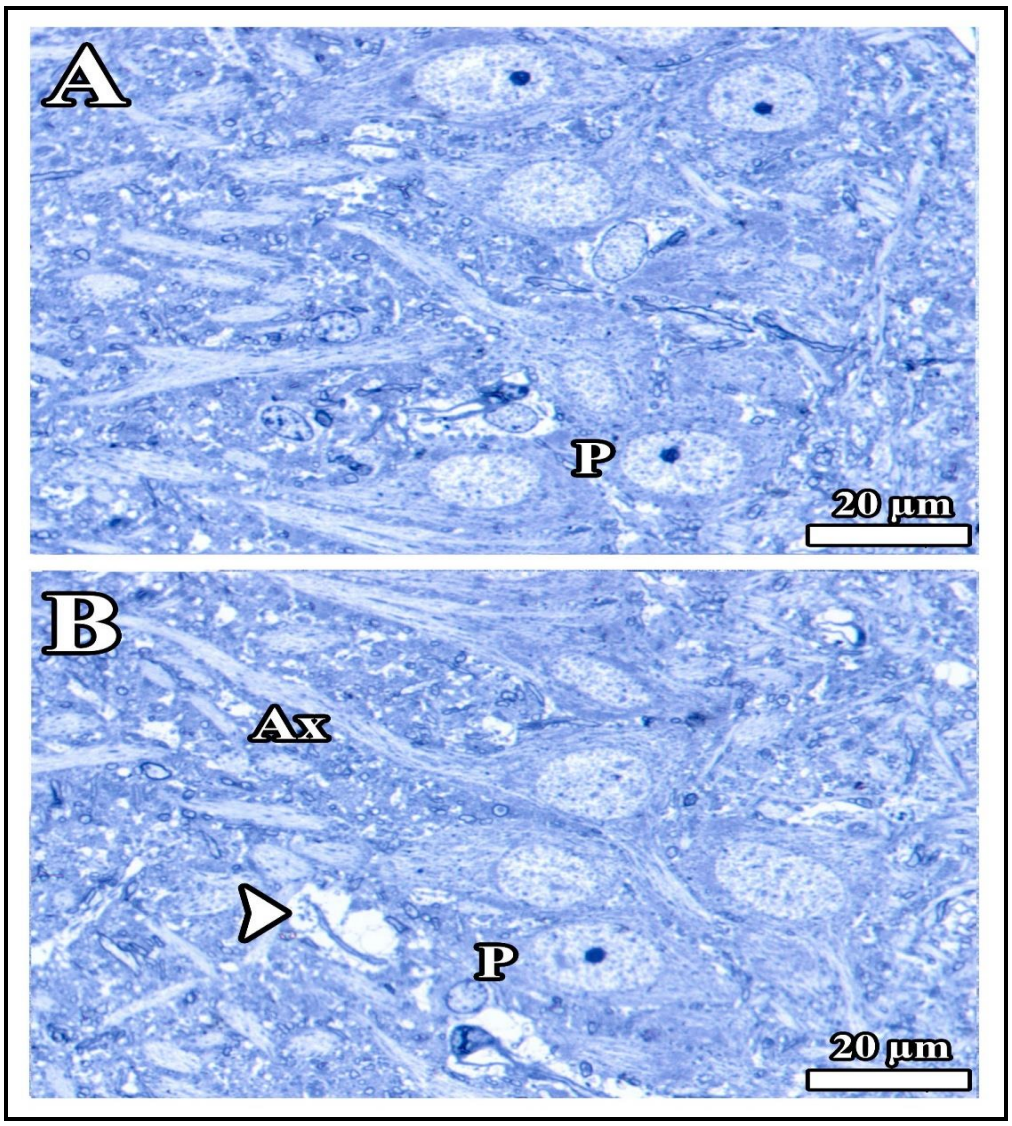

Figure 64. (A, B) Images taken from the CA region of hippocampus belong to the AD group are seen. General structure of CA region looks in normal appearance. Their axons (Ax) and nucleus are clearly observed and pyramidal neurons (P) in this region have very long axons. The border of nucleus and perikaryon can be seen clearly, since each perikaryon delineated by cross sections of axons. Pyramidal shape perikaryon has a spherical nucleus; this is a typical shape of pyramidal cells in the CA region of hippocampus. Some of the vessels (arrowhead) are collapsed possibly as a result of low-quality fixation. Toluidine blue stained semi-thin (0.5 µm) resin section

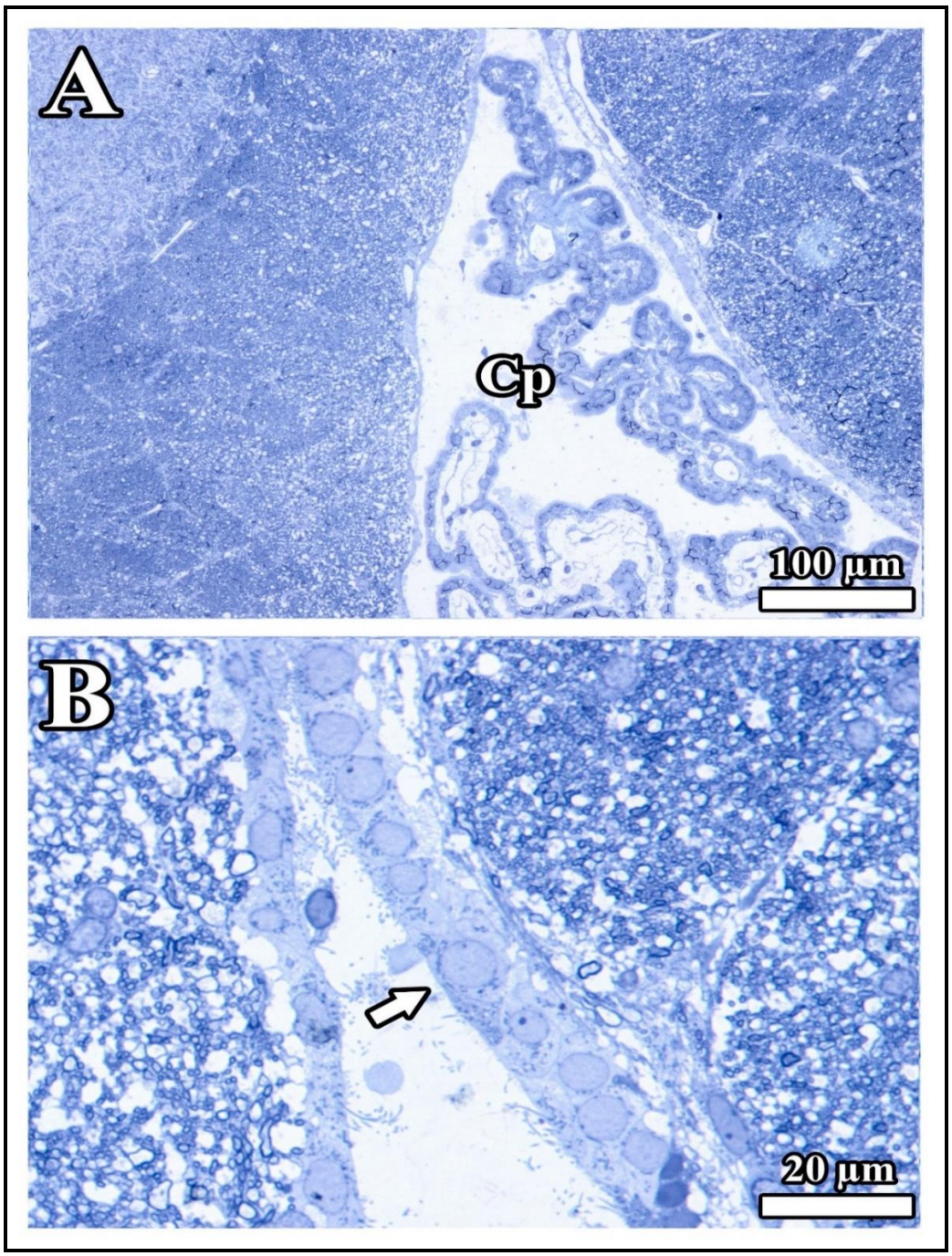

Figure 65. (A, B) Images taken from the third ventricle of brain that belong to the AD group are seen. A well-preserved choroid plexus (Cp) and ependymal cells (arrow) are observed. Cross sections of axons are found in the white matter of brain. All of these structures look normal; some of ependymal cells have cilia at apical pole of its. Toluidine blue stained semi-thin (0.5 µm) resin section

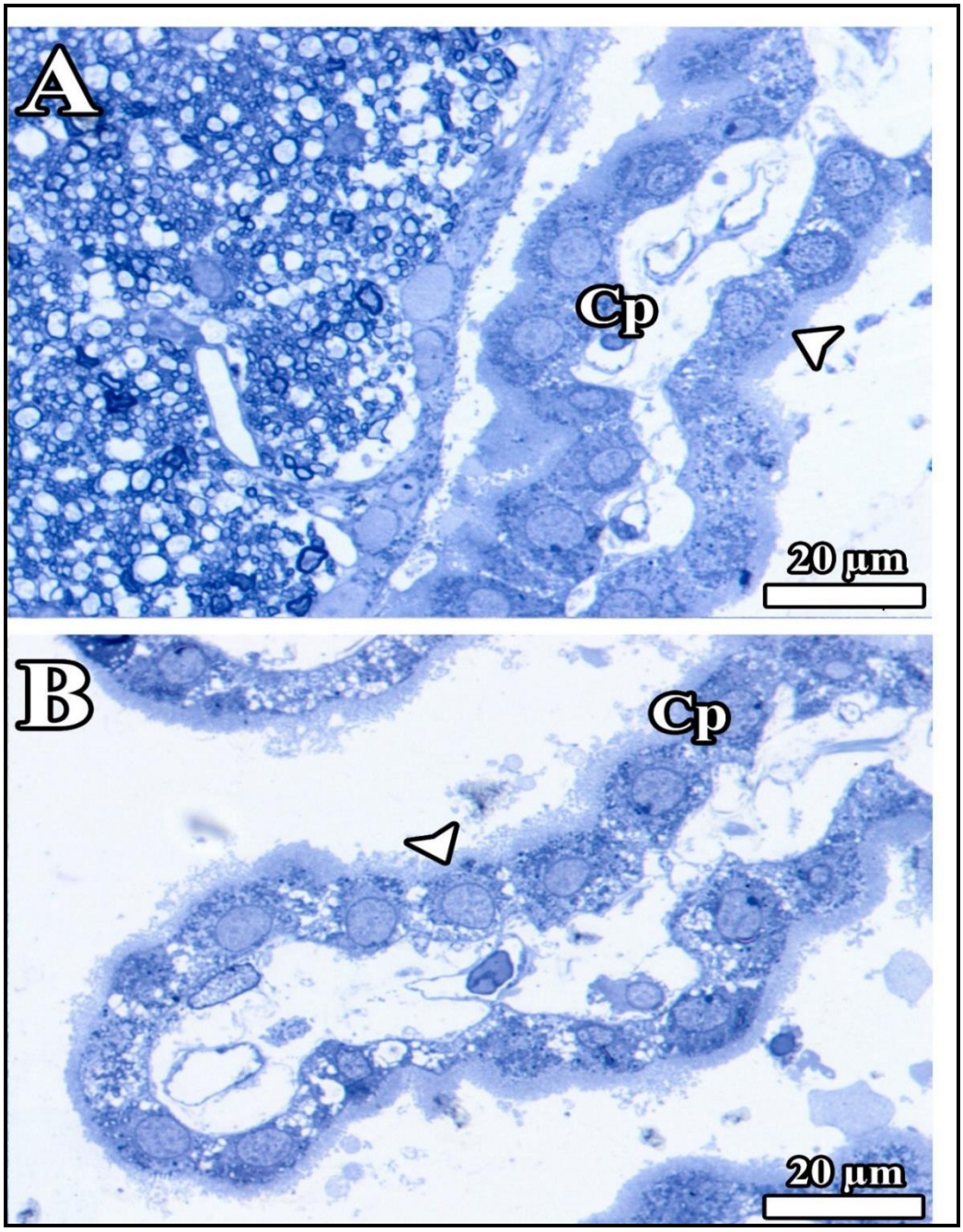

Figure 66. (A, B) Images taken from the third ventricle of brain that belong to the AD group are observed. A well-preserved choroid plexus (Cp) and plexus cells (arrowhead) are seen. Cross sections of axons are found in the white matter of brain. Some capillaries in the loose connective tissue of choroid plexus are observed. Apical poles of plexus cells are lined by microvilli and a blood cell is seen in the lumen of capillary. Toluidine blue stained semi-thin (0.5 µm) resin section

Regarding the NS group the images taken from hippocampal region showed that, general structure of CA region looks in normal (**Figure 67, 68, 69, 70 and 71**). Although architecture of the pyramidal cells appears normal, there are many densely stained pyramidal cells as well as neuroglia would be seen in this region.

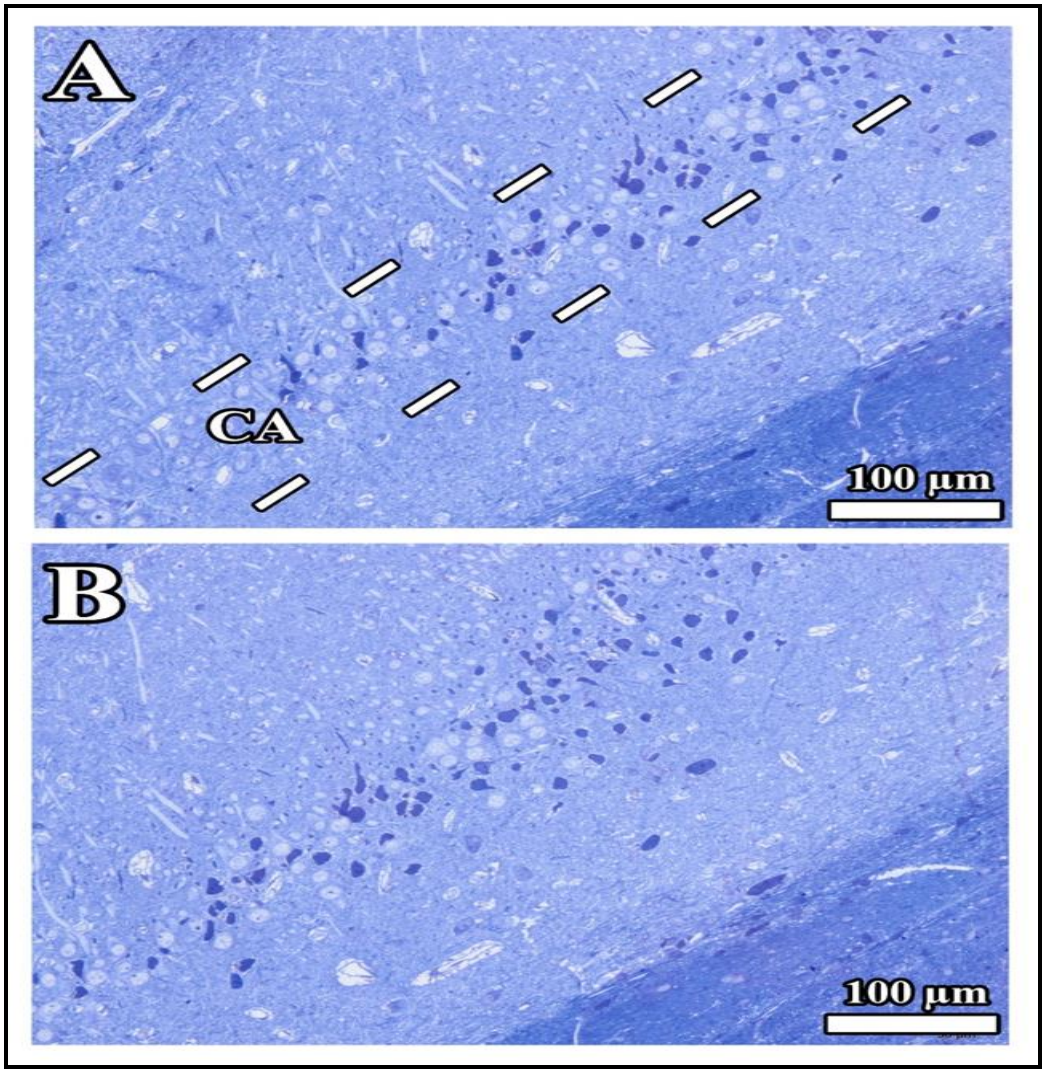

Figure 67. (A, B) Images taken from the hippocampus belong to the NS group are seen. Although general structure of CA looks normal, but there are many densely stained pyramidal cells in this region. These dark cells might be non-functional cells. The reason of an increased dark cells number in the CA region of NS group is unknown, but it may depend on a low quality of perfusion during the fixation or negative side effect of NS exposure on this region. Toluidine blue stained semi-thin (0.5 µm) resin section

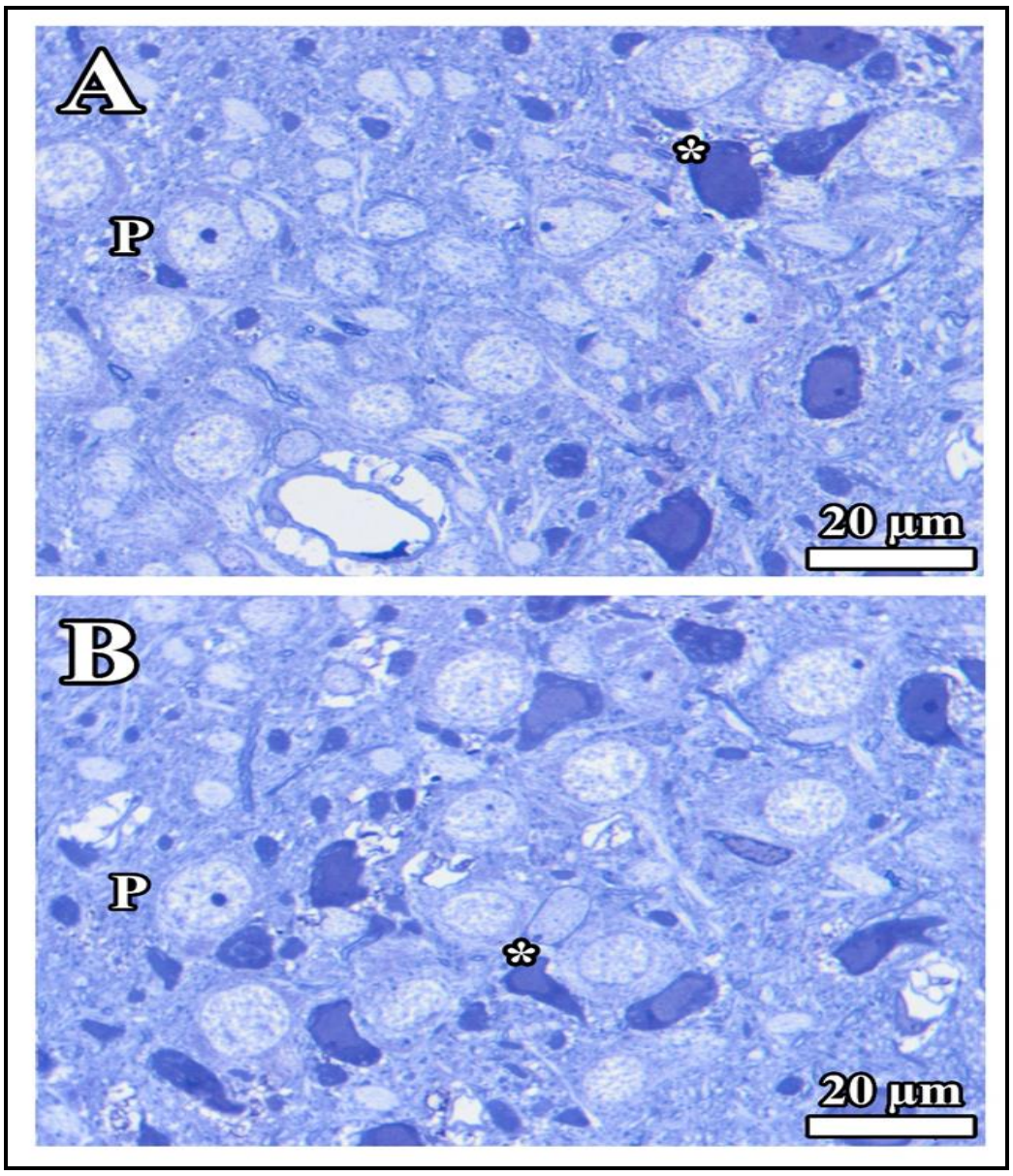

Figure 68. (A, B) High magnifications of the images taken from the hippocampus belong to the NS group are seen. Although pyramidal cells (P) structure of CA looks normal, there are many densely stained pyramidal cells as well as neuroglia in this region. Both types of dark cells (*) might be non-functional cells. The reason of an increased dark cell number in the CA region may depend on the side effect of NS exposure. An increased number of spaces around pyramidal cells is seen, this may be a result of bad fixation. Most of intact neurons have well delineated nucleus and conspicuous nucleolus. Toluidine blue stained semi-thin (0.5 µm) resin section

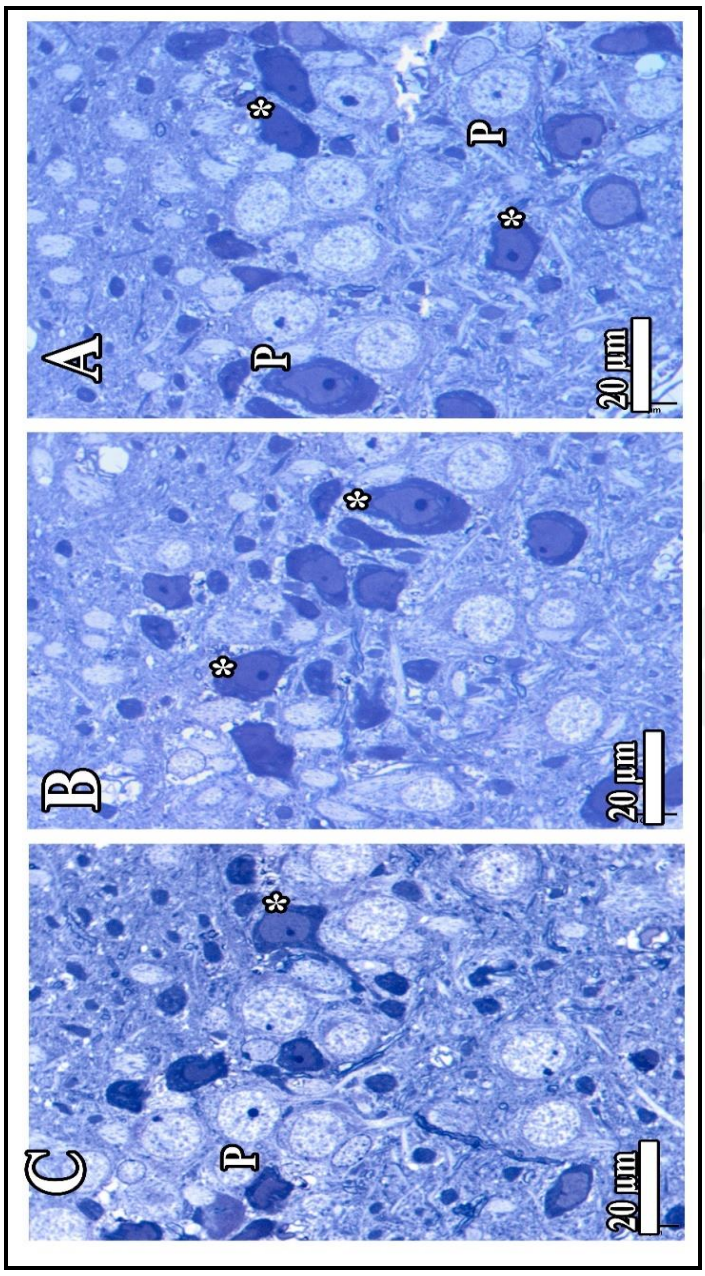

Figure 69. (A, B, C) High magnifications of the images taken from the hippocampus belong to the NS group are seen. Although pyramidal cells (P) structure of CA looks normal, but there are many densely stained pyramidal as well as neuroglia in this region are observed. It is interesting that densely stained cells (*) have angular shape and branches, and a conspicuous nucleolus in the nucleus. Darkly stained neuroglia has granular shape. There are many circular shape spaces around dark cells. Toluidine blue stained semi-thin (0.5 µm) resin section

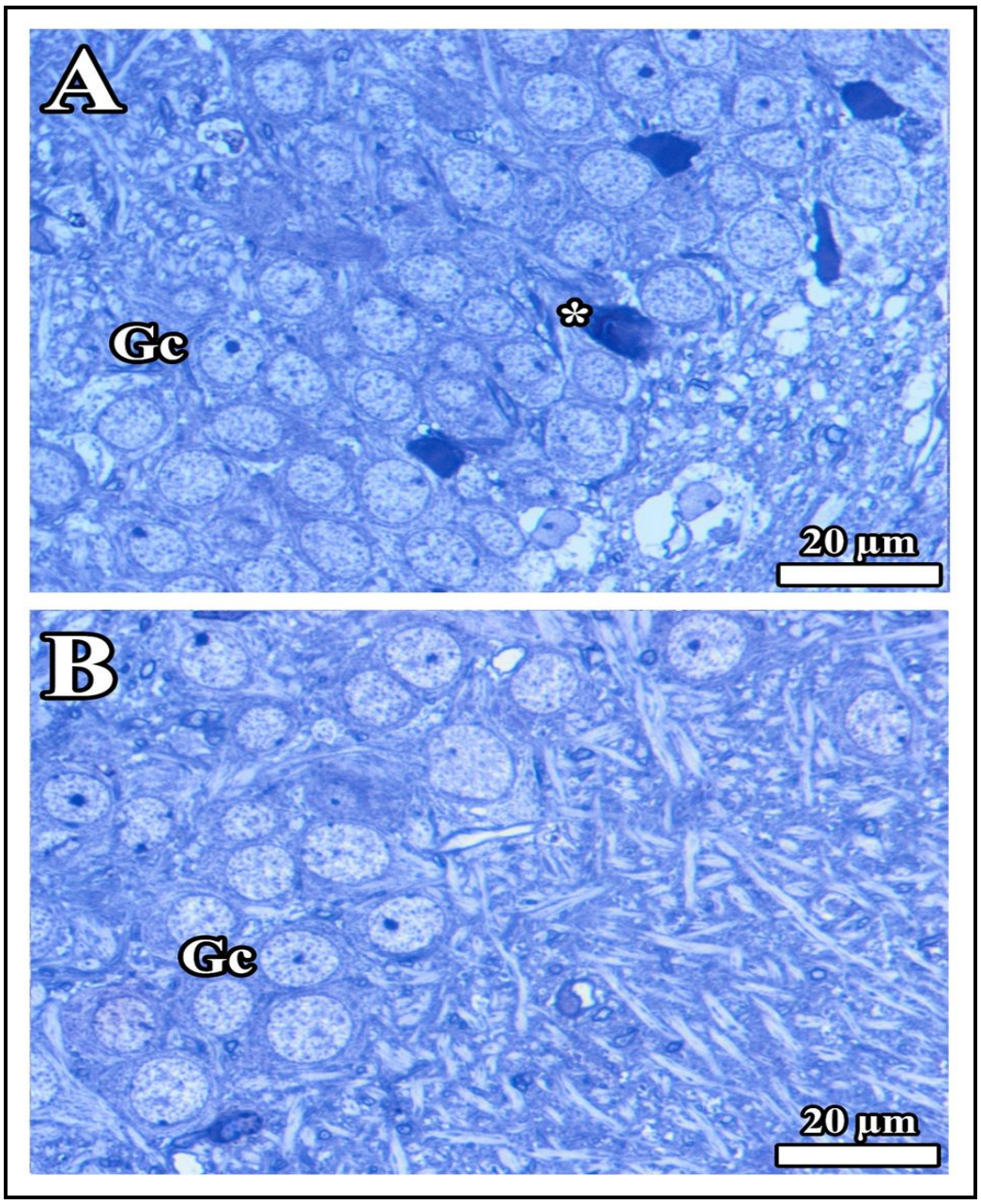

Figure 70. (A, B) High magnifications of the images taken from the DG of hippocampus belong to the NS group are seen. Although the structure of most of the granular (Gc) in the DG looks normal, there are some densely stained granular cells in this region. The borders of granular cells are clear and their nucleoli are in spherical shape. A very pronounced neuropil accumulation is found around this cell layer. Darkly stained cells (*) generally have a rectangular shape. Toluidine blue stained semi-thin (0.5 µm) resin section

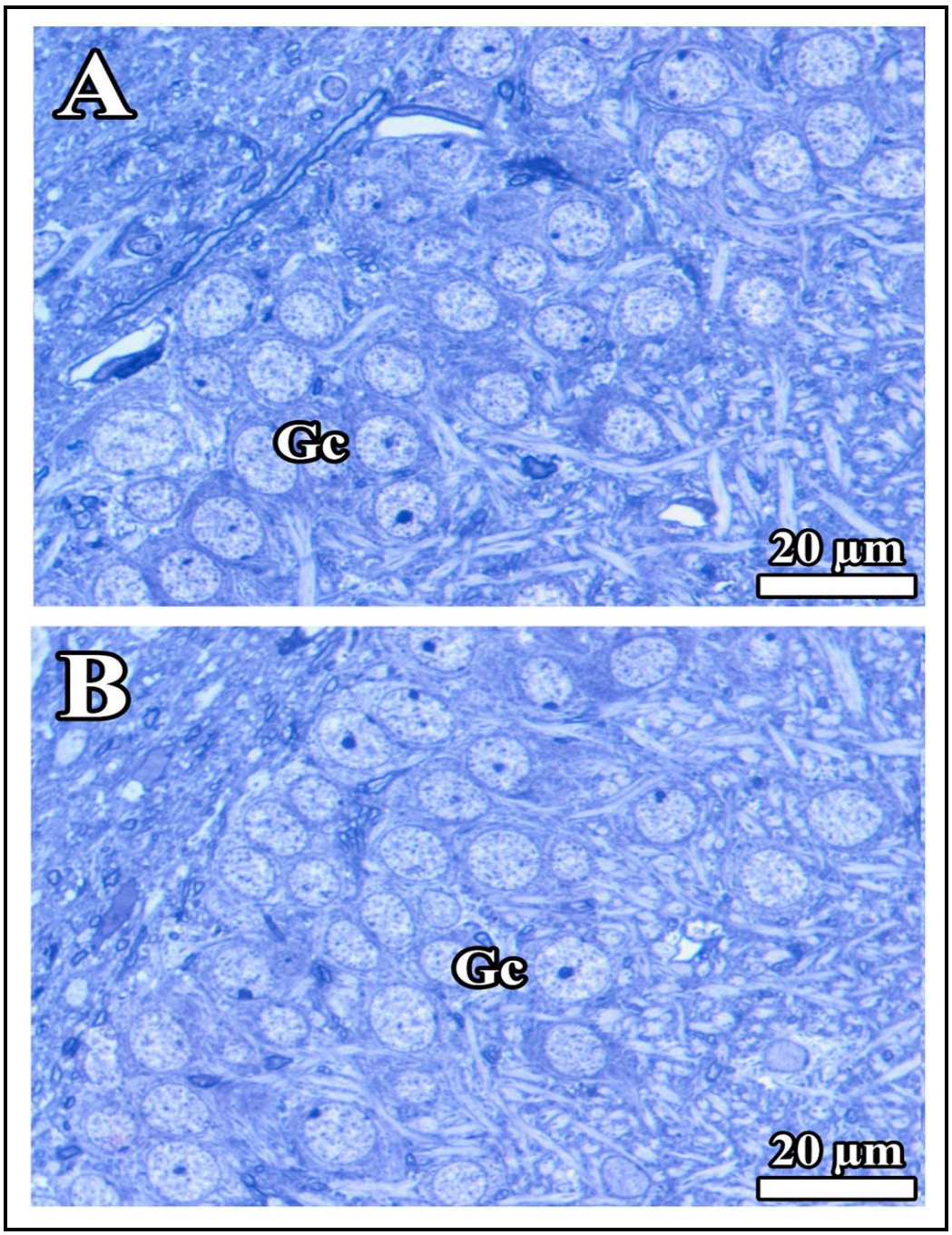

Figure 71. (A, B) High magnifications of the images taken from the GD of hippocampus belong to the NS group are seen. Granular cells (Gc) structure in the GD looks in normal. The borders of granular cells and their nucleus, spherical shape, are observed clearly. A very pronounced neuropil accumulation is found around this cell layer. Toluidine blue stained semi-thin (0.5 µm) resin section

In the EMF group, the images showed that, general structure of CA region looks in abnormal (**Figure 72, 73, 74, 75, 76 and 77**) since the pyramidal and granular cells have indistinct boundaries and heavily darkly stained pyramidal neurons in CA as well as neuroglia are observed.

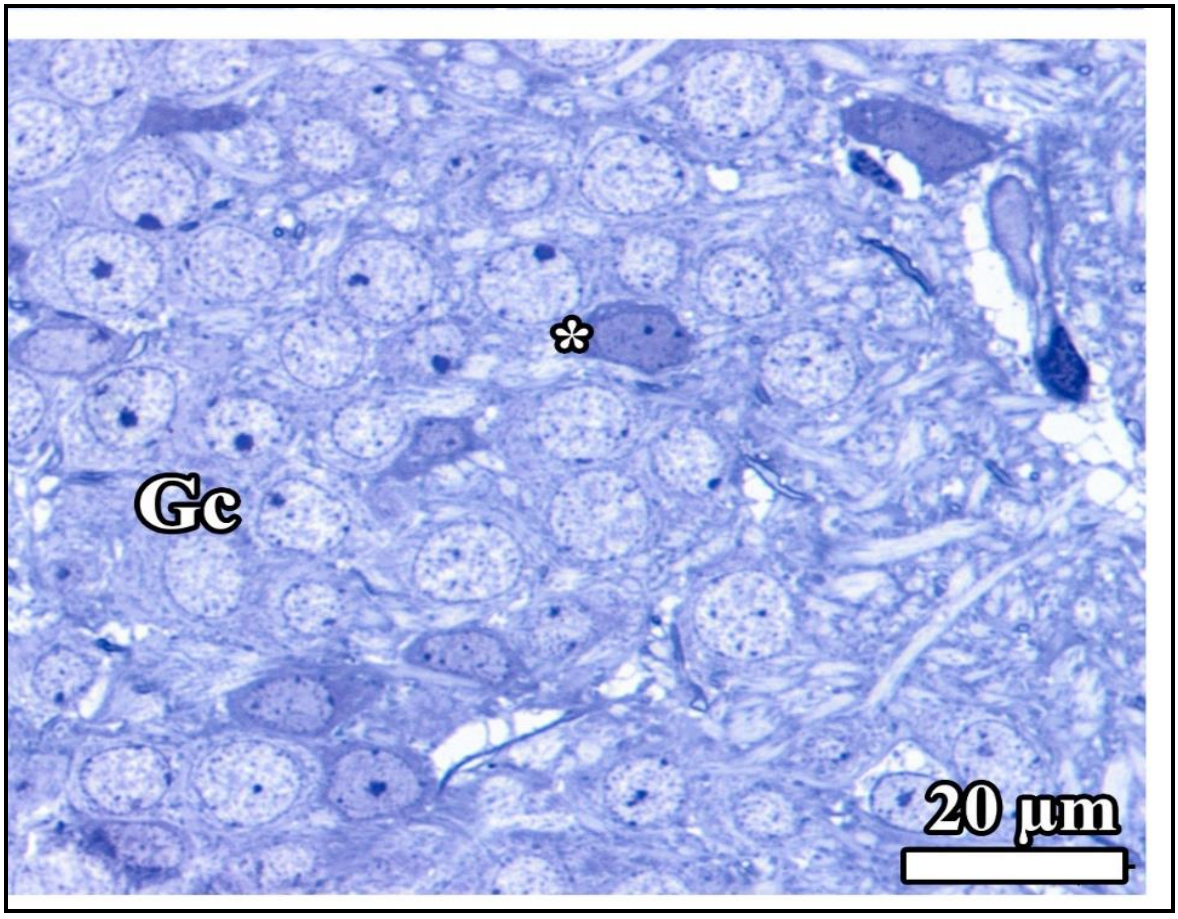

Figure 72. The image taken from the GD region of hippocampus belong to the EMF group are seen. General structures of most granular cells (Gc) in this region are observed in abnormal, since the sizes of cells and their nucleus substantially were decreased. The border of these cells cannot be clearly observed. Heavily darkly stained granular cells (*) are commonly seen. These cells may be lost their function and going to death. Toluidine blue stained semi-thin (0.5 µm) resin section

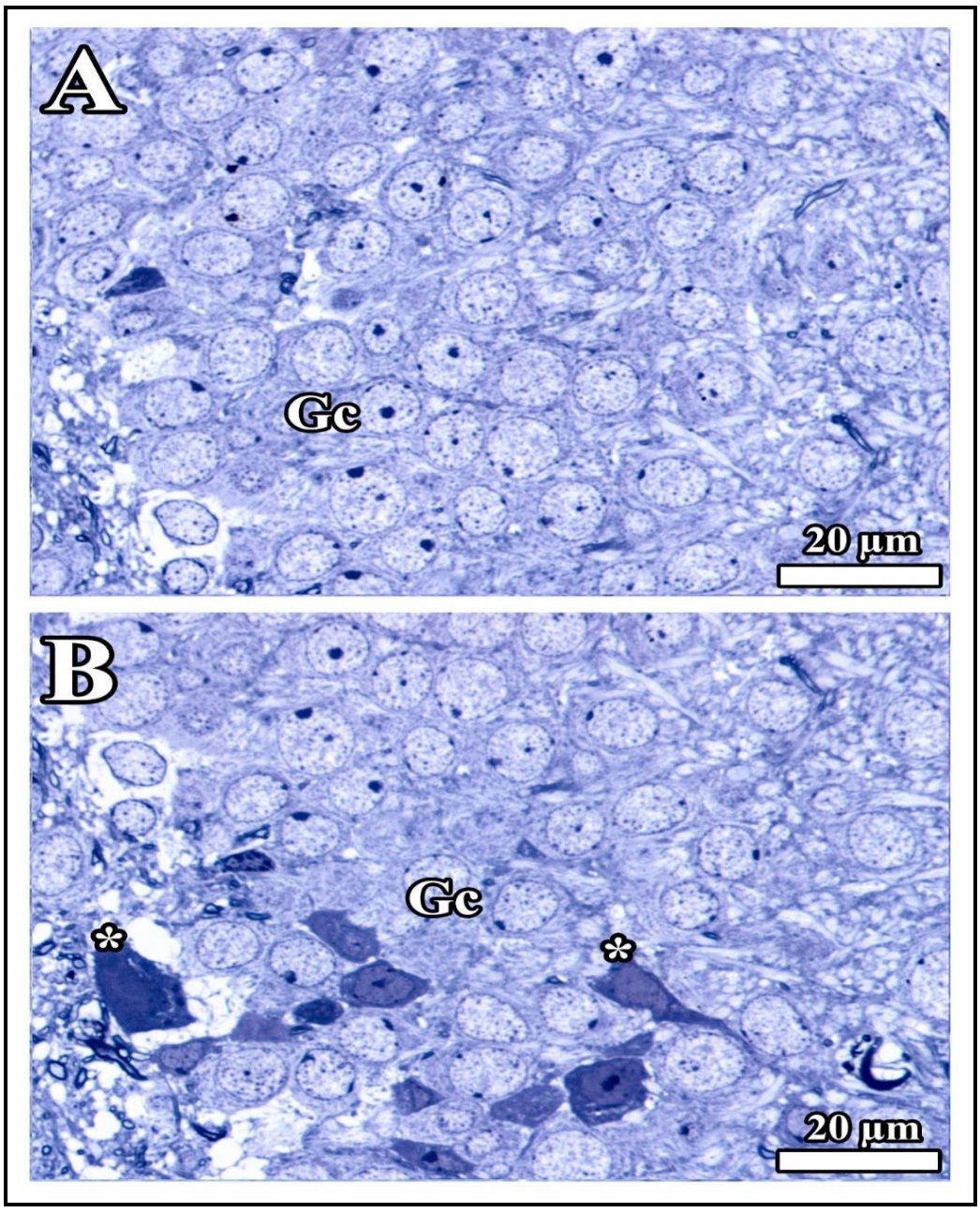

Figure 73. (A, B) The images taken from the GD region of hippocampus belong to the EMF group are seen. General structures of most granular cells (Gc) in this region are observed in abnormal. Since the sizes of cells and their nucleus substantially were decreased. Heavily darkly stained granular cells (*) are found and these cells look as non-functional and may be going to death. Toluidine blue stained semi-thin (0.5 µm) resin section

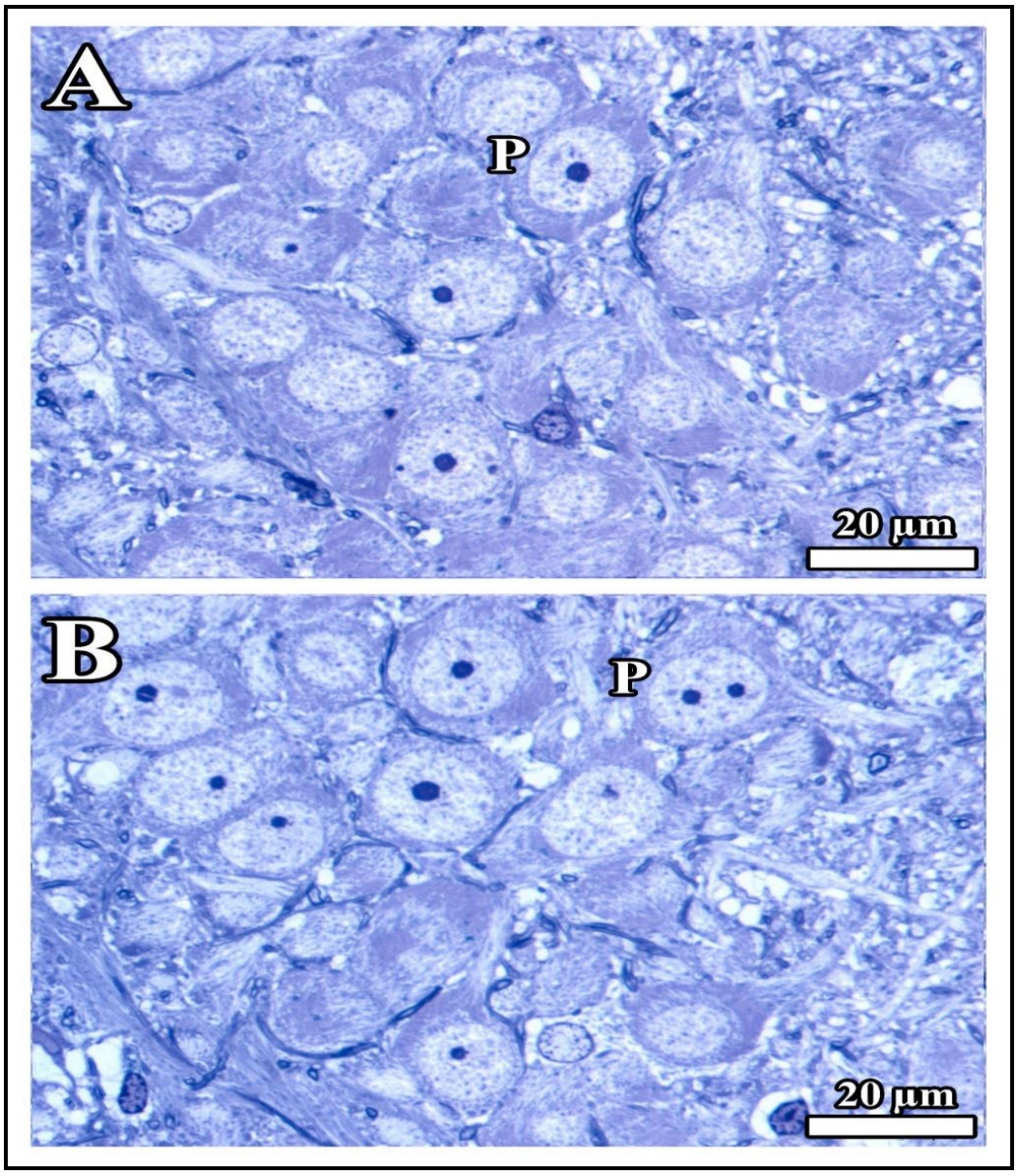

Figure 74. (A, B) Images taken from the CA region of hippocampus belong to the EMF group are seen. General structures of most pyramidal cells in this region showed normal feature. The cytoplasm of some pyramidal cells is lightly dark stained. The size of perikaryon and its nucleus of pyramidal cells (P) are relatively decreased. The dimension decreasing of neuroglia can also be observed. Some of the borders of the pyramidal cells cannot be easily seen. (A) A neuroglia is stained very darkly. Toluidine blue stained semi-thin (0.5 µm) resin section

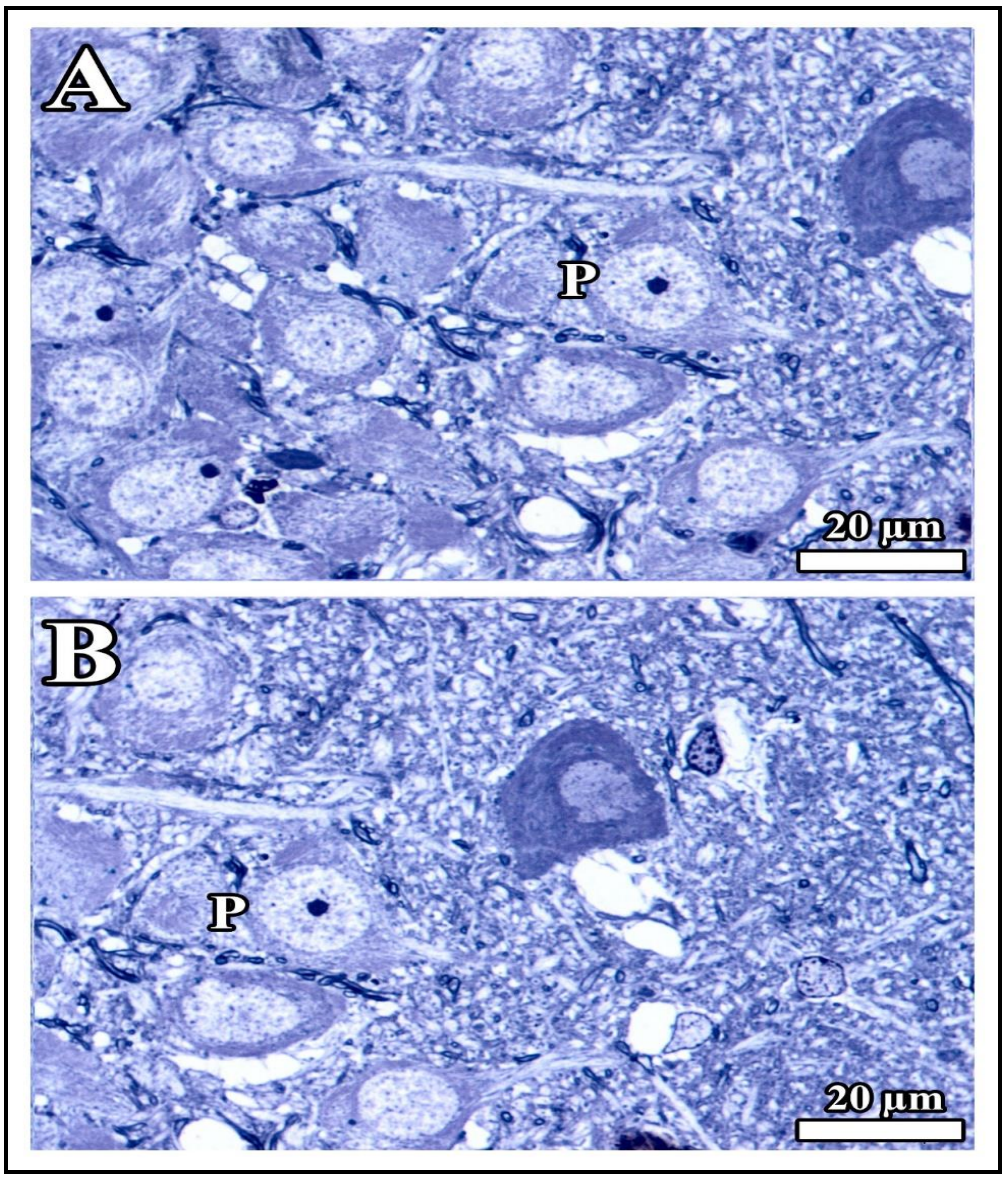

Figure 75. (A, B) Images taken from the CA region of hippocampus belong to the EMF group are seen. General structures of most pyramidal cells in this region are observed in abnormal since the cytoplasm of some pyramidal cells (P) were heavily dark stained and the border of nucleus of them is also were not so clear. Not only the size of perikaryon and its nucleus of these cells in this region are substantially decreased but also the size of neuroglia is also diminished. Cross- and longitudinal sections of axons are seen circular and longitudinal. (B) A neuroglia is stained very darkly. Many of large spaces around pyramidal cells as well as neuroglia and capillary are seen. Toluidine blue stained semi-thin (0.5 µm) resin section

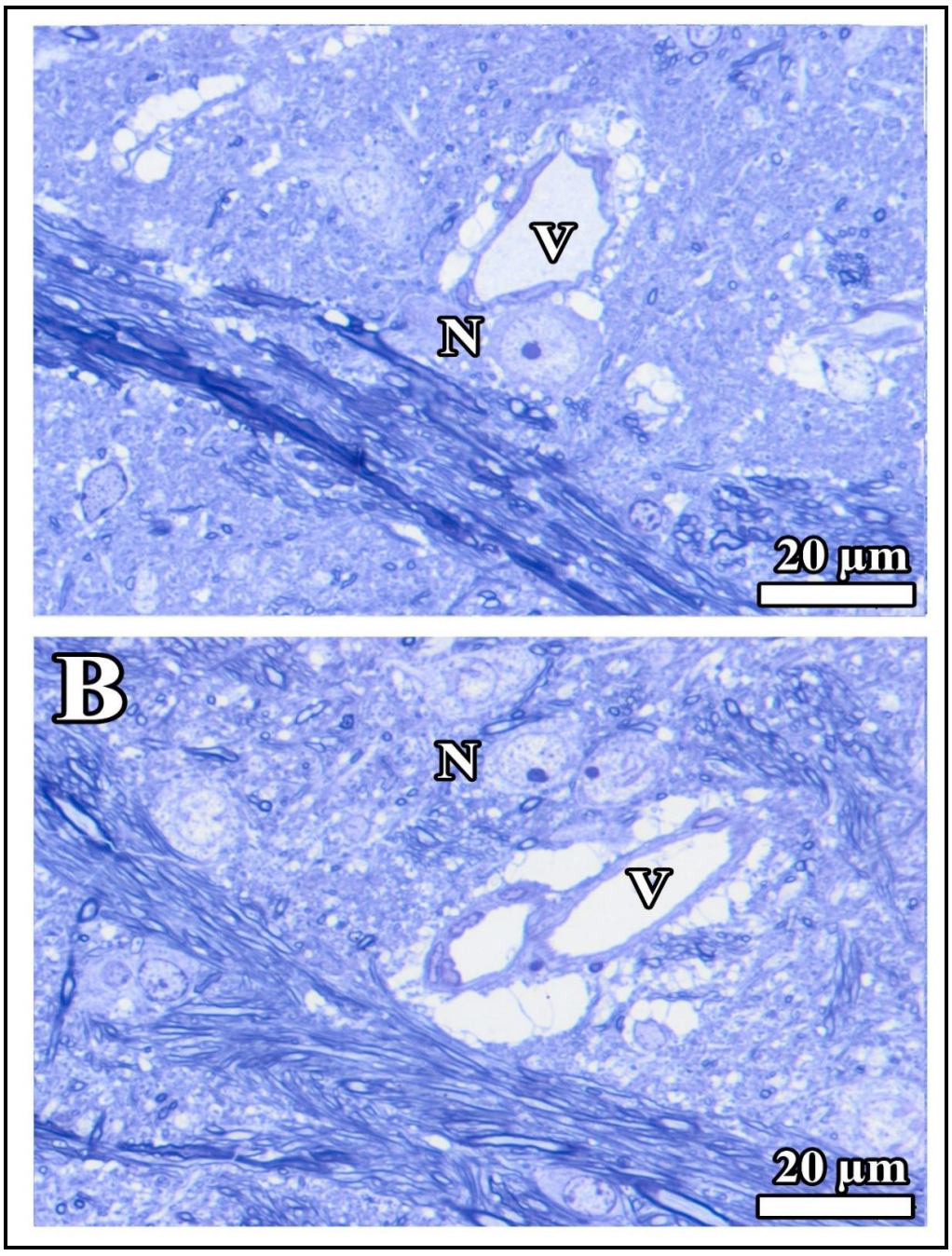

Figure 76. (A, B) Images taken from the brain of the EMF exposed group are seen. Most of vessels (V) in the brain of this group were separated from their surrounding tissues and create different sized spaces around them. These create many spaces around vessels as well as neurons (N) and neuroglia. Longitudinal and cross sections of axons, and small size spaces are seen. Toluidine blue stained semi-thin (0.5 µm) resin section

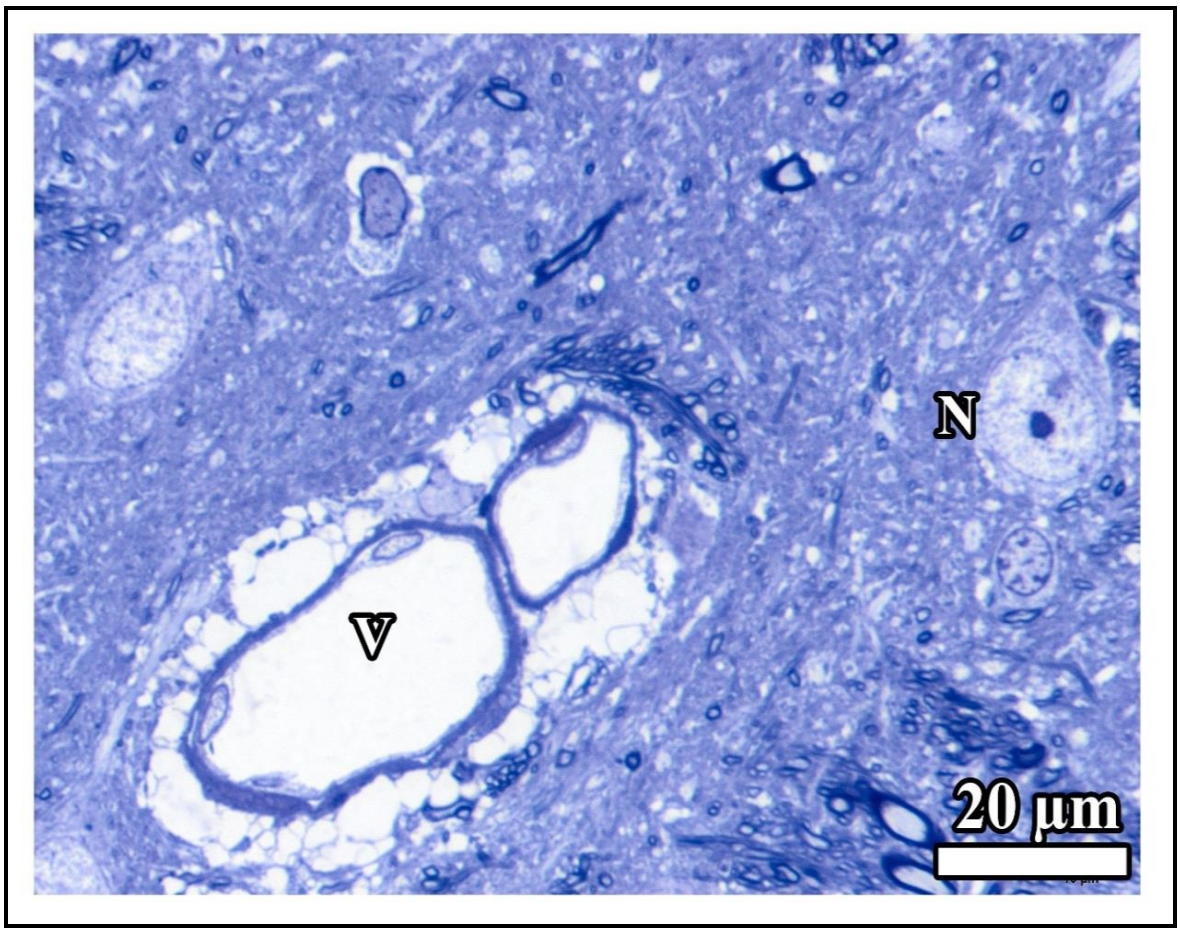

Figure 77. The image taken from the brain of the EMF group is seen. Vessels (V) in the brain of this group were separated from their surrounding tissues and these create many spaces around vessels. Longitudinal and cross sections of axons, and small size spaces around them are seen, neuron (N). Toluidine blue stained semi-thin (0.5 µm) resin section

Regarding the EMF + AD group, the images showed that, general structure of CA region looks in normal and healthy (**Figure 78, 79, 80, 81, 82, 83 and 84**). Pyramidal cells have oval shape distinguished boundaries. A rich capillaries network and many axons of pyramidal neurons are observed.

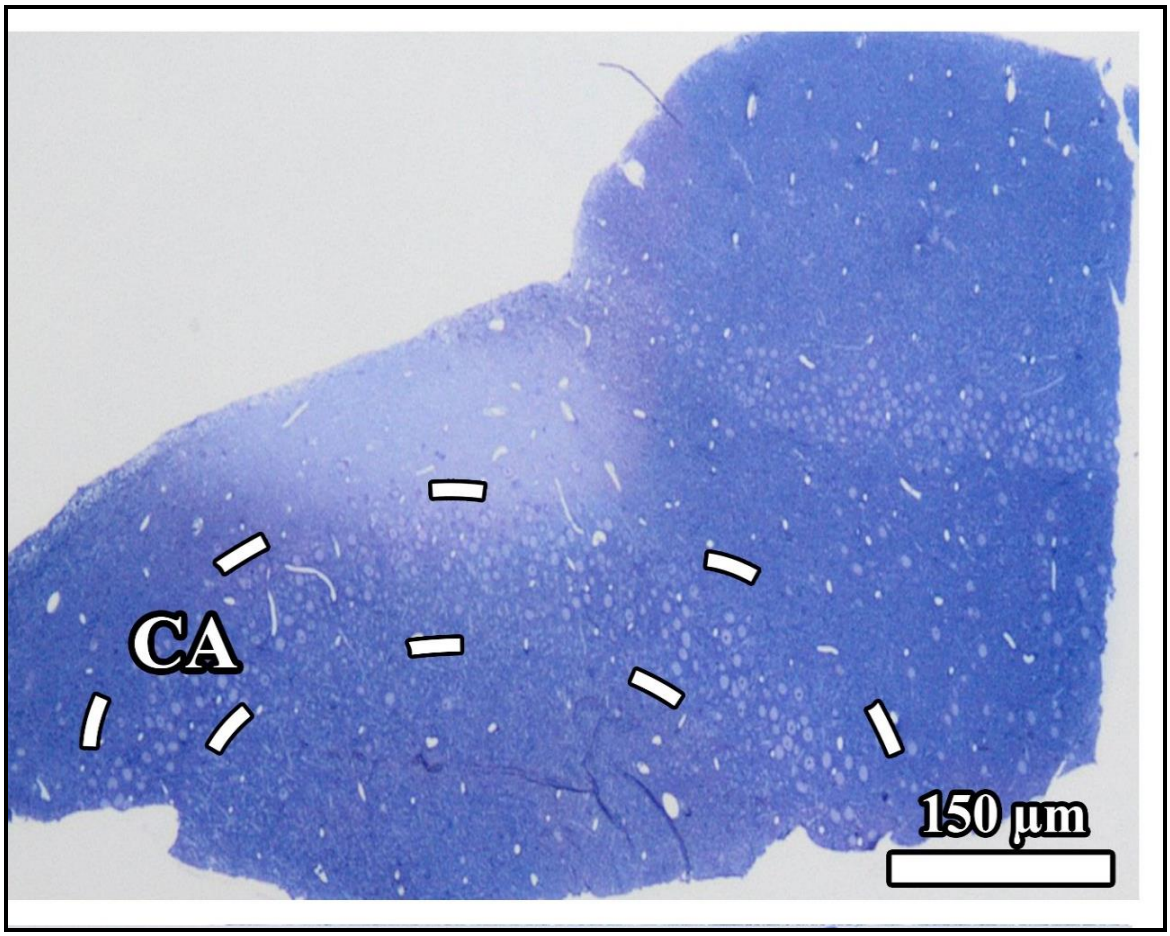

Figure 78. The image taken from the CA region of hippocampus belongs to the EMF + AD group is seen. General structure of CA region looks in normal appearance. Toluidine blue stained semi-thin (0.5 µm) resin section

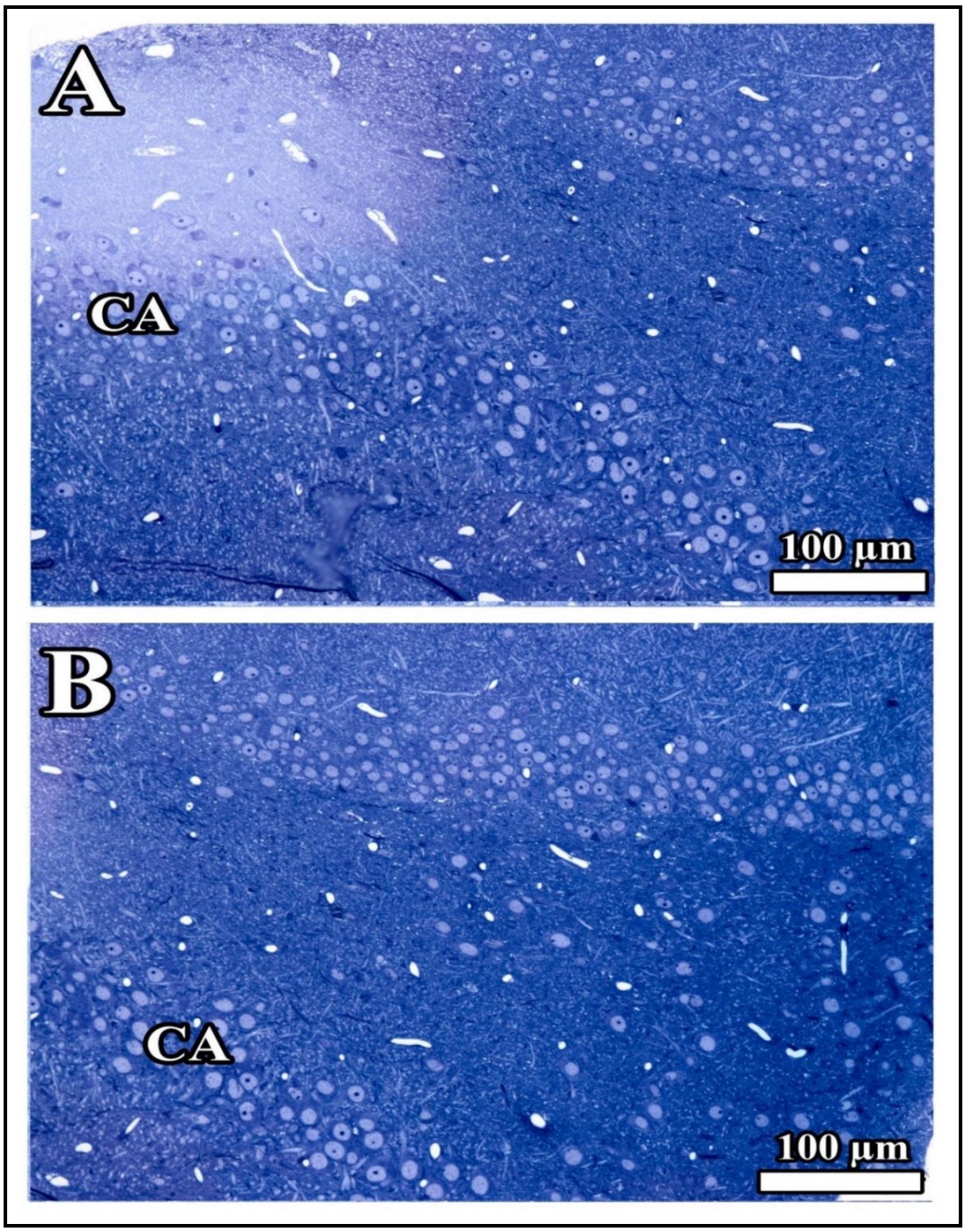

Figure 79. (A, B) Images taken from the CA region of hippocampus belong to the EMF + AD group is seen. General structure of CA shows normal appearance. Pyramidal cells in the CA region have oval shape nucleus and conspicuous nucleolus. The distance between pyramidal cells is normal and the border of this cell layer in the hippocampus is clearly observed. Toluidine blue stained semi-thin (0.5 µm) resin section

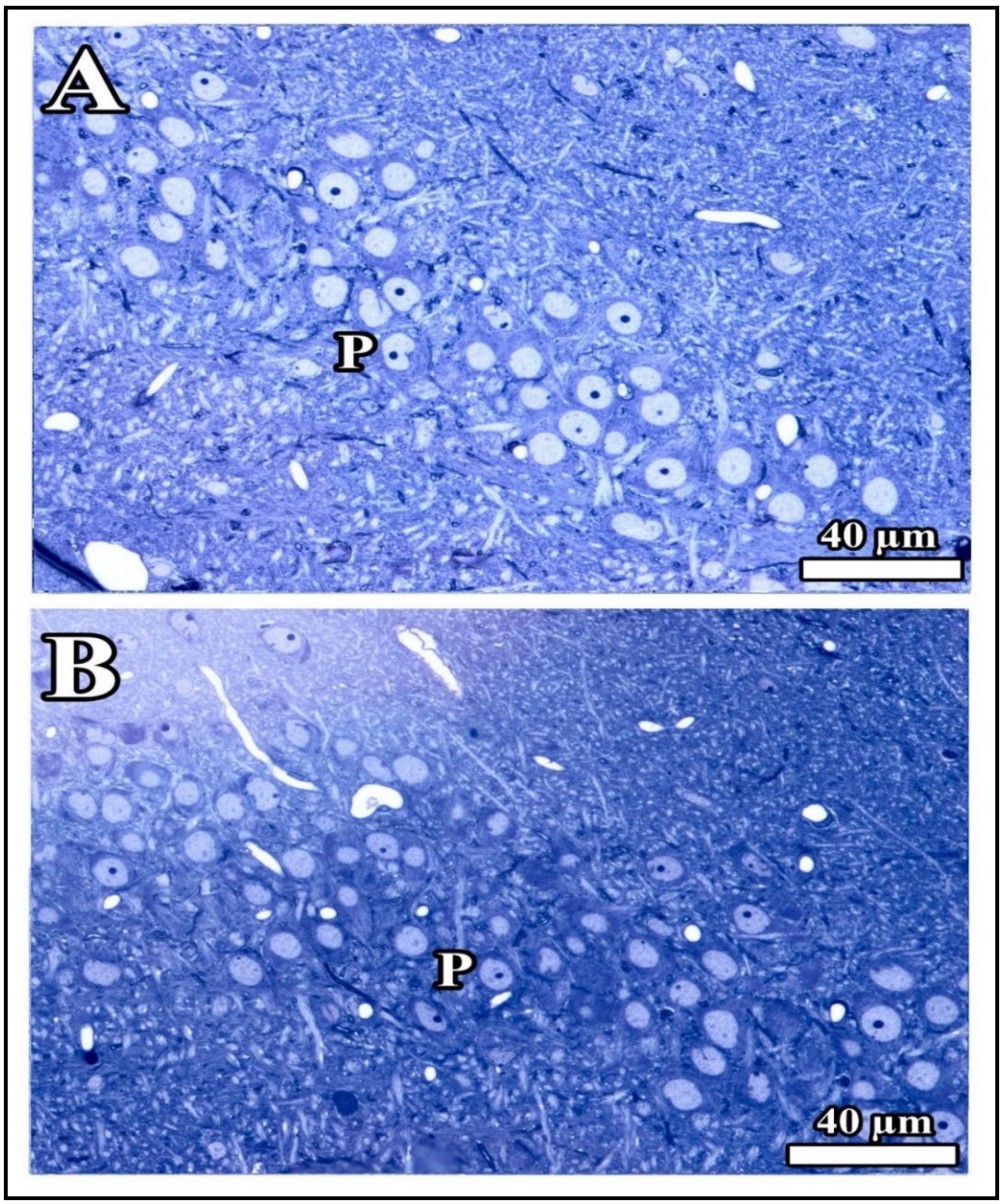

Figure 80. Images taken from the CA region of hippocampus belong to the EMF + AD group is seen. Both general structures of CA region and its pyramidal cells (P) show normal appearance. The nuclei of pyramidal cell have oval shape. Most of cells in this region have very clear borders and the distance between pyramidal cells is normal. A huge number of vessels in this region look normal since their wall and lumen intact. An accumulation of cross-sectioned axons, can be seen in this region as a small sized white colour dots. Toluidine blue stained semi-thin (0.5 µm) resin section

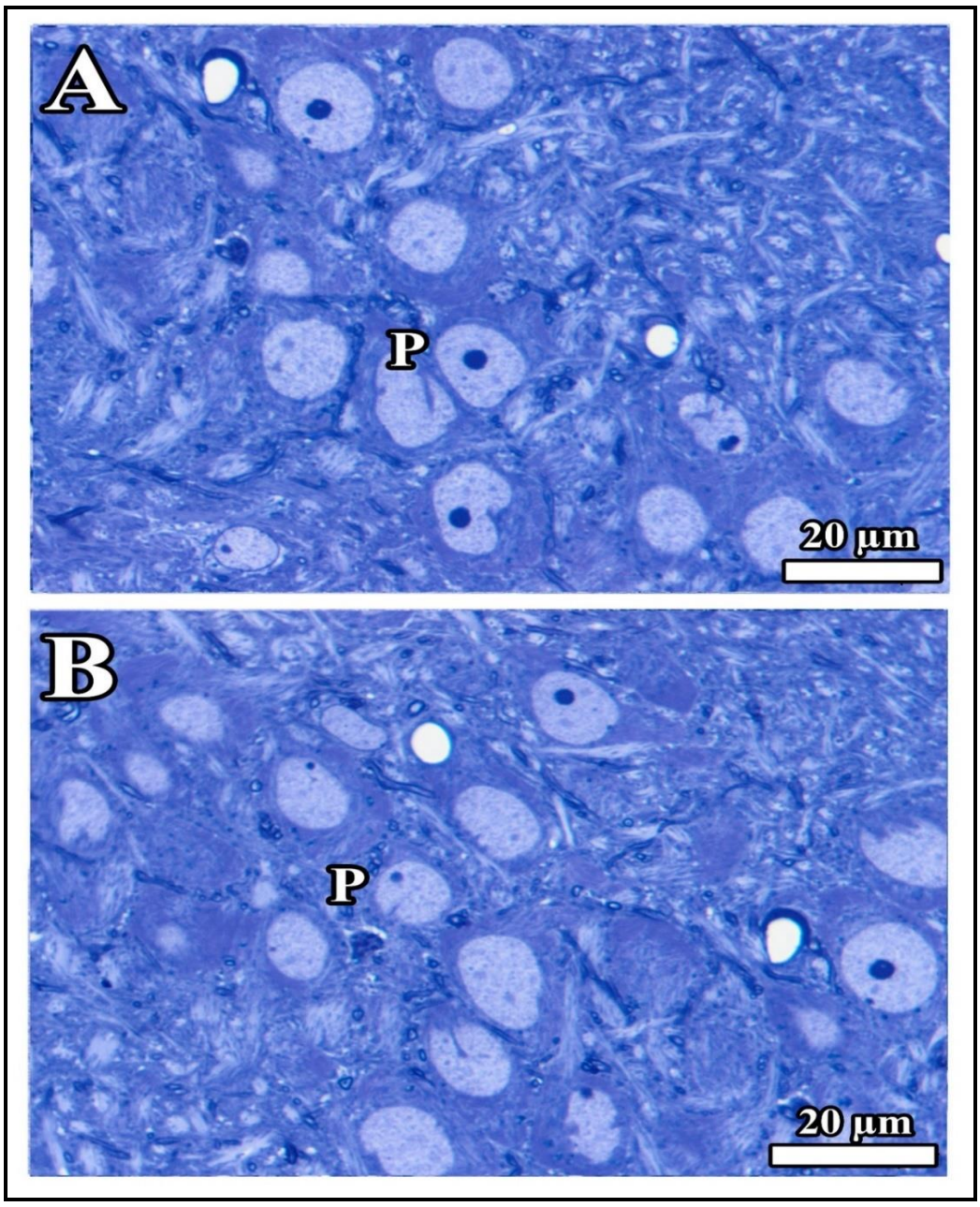

Figure 81. (A, B) Images taken from the CA region of hippocampus belong to the EMF + AD group is seen. The distance between pyramidal cells (P) is normal and the border of nuclei as well as perikaryon of cells can be seen clearly. Cross-and longitudinal sections of axons are seen circular and longitudinal. Most of neuron perikaryon borders are delineated by cross sections of myelinated axons. A rich capillary network is a common structure of this region; some of cross section of small sized capillaries is seen. Toluidine blue stained semi-thin (0.5 µm) resin section

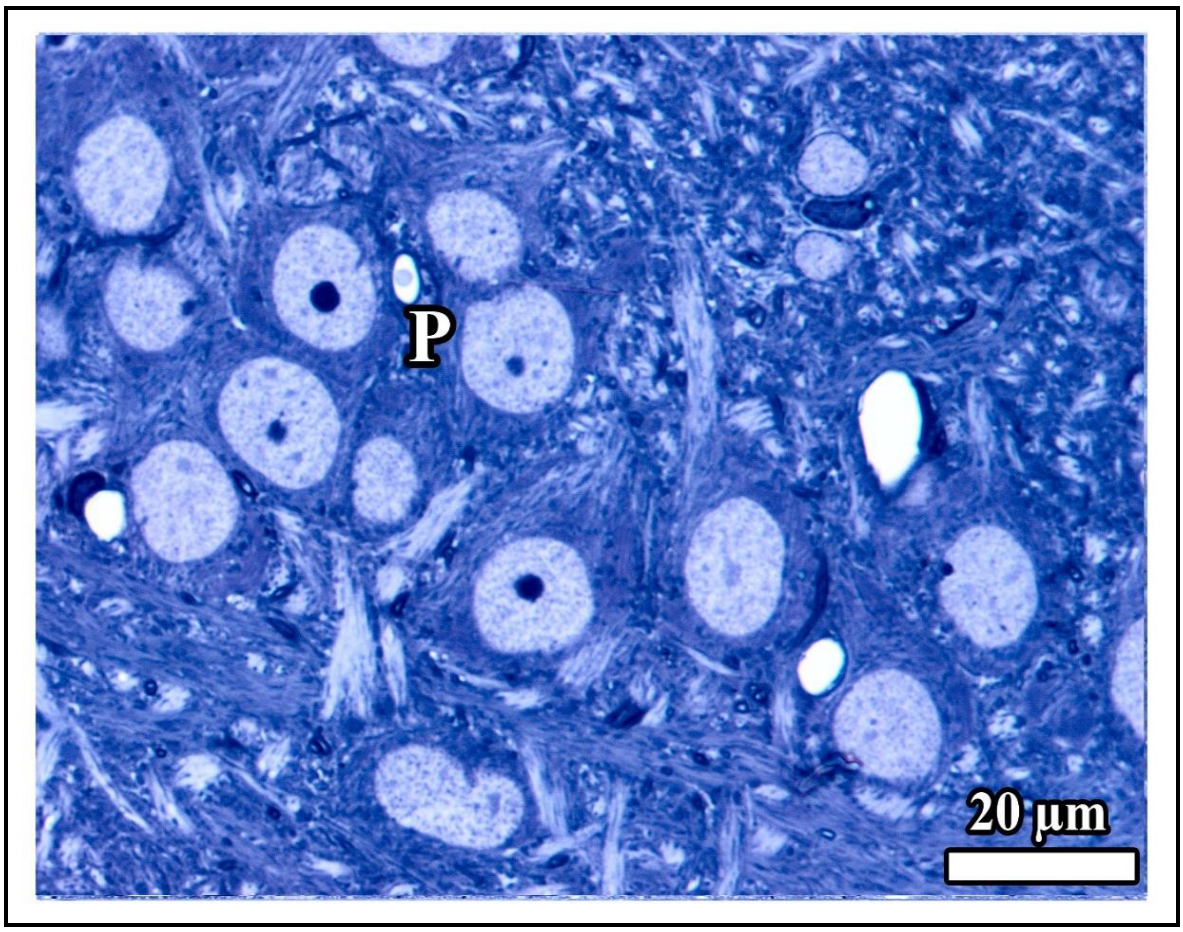

Figure 82. The image taken from the CA region of the hippocampus belongs to the EMF + AD group is seen. All of pyramidal cells (P) in the CA region look healthy. The nuclei of pyramidal cells have oval shape and the border of its clear. Most of cells have a very dark and large nucleolus. The distance between cells looks normal, axons of pyramidal neurons, transverse and longitudinal sectioned, are observed as a small sized white colour dots. Vessels in this region look in normal structure. Toluidine blue stained semi-thin (0.5 µm) resin section

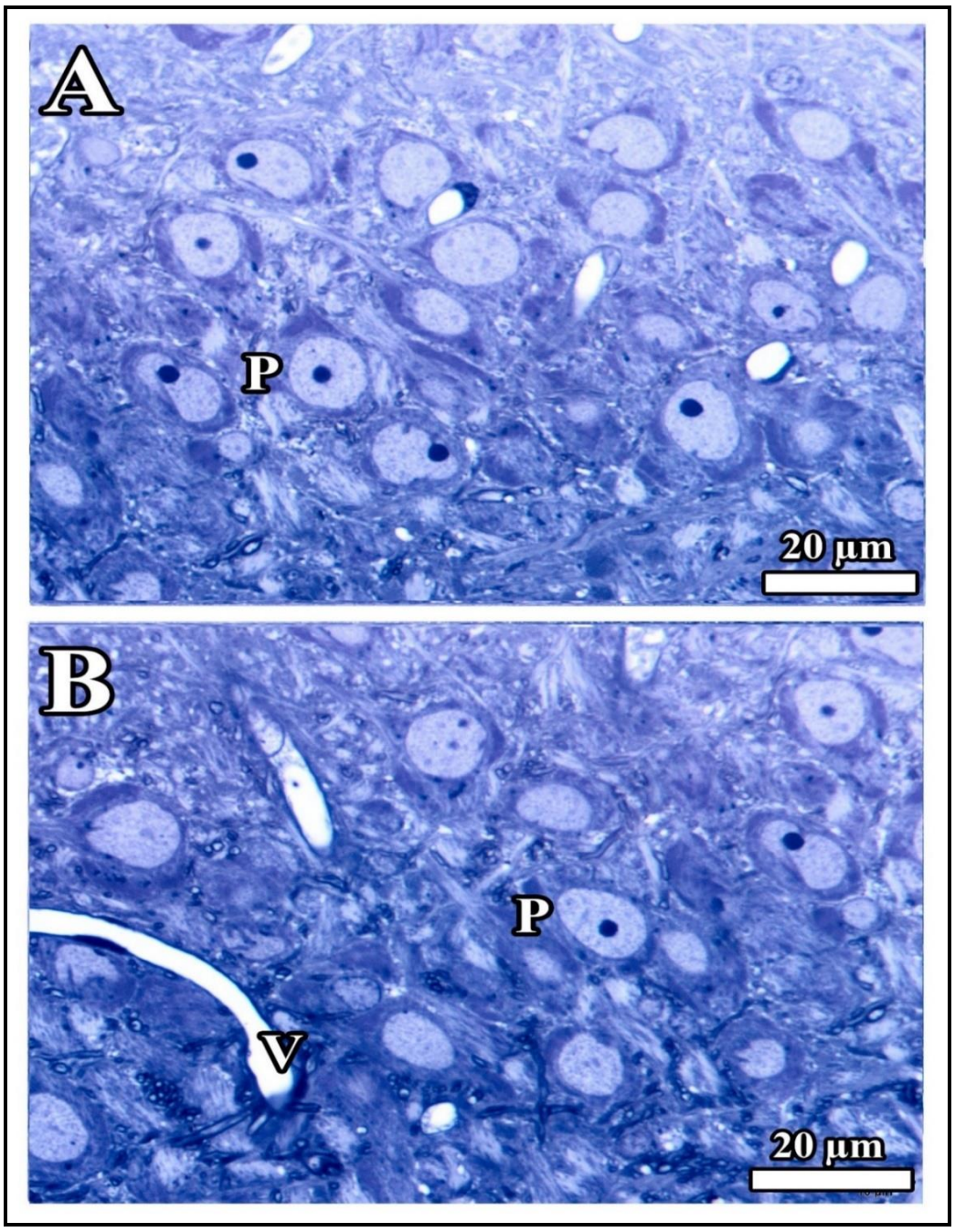

Figure 83. Images taken from a different area of the CA region belong to the EMF + AD group are seen. The pyramidal cells (P) in this region have oval shape nucleus and conspicuous nucleolus. The distance between neurons looks fine, many axons of pyramidal neurons are observed. Cross and longitudinal sections of axons are seen circular and longitudinal. Vessels (V) in this region look normal and there is no space between the wall and surrounding tissue. Toluidine blue stained semi-thin (0.5 µm) resin section

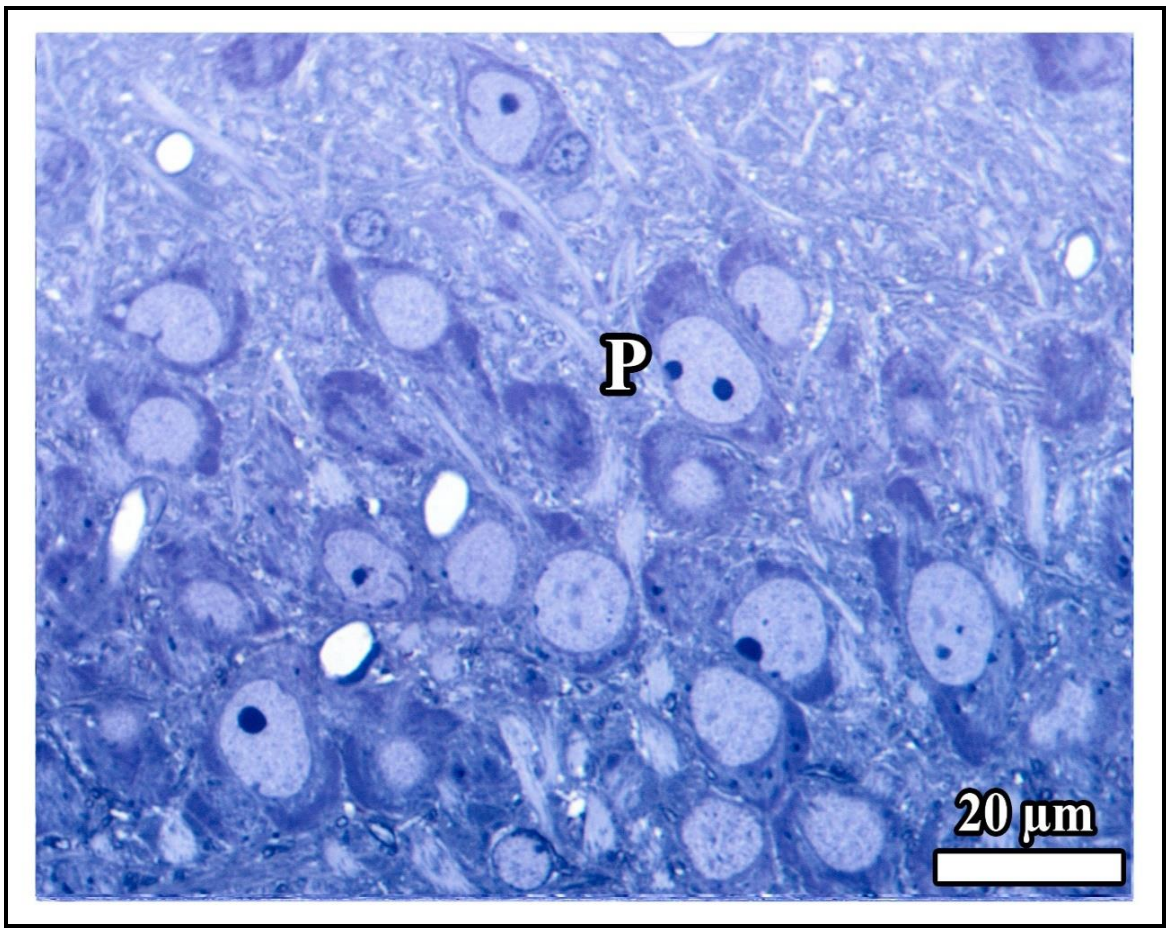

Figure 84. Image taken from the CA region of hippocampus belong to the EMF + AD group is seen. The border of pyramidal neurons (P) and their nuclei in the CA region are clearly observed. Each pyramidal cell has an oval shaped nucleus. Some of axons belong to neurons are also seen. Images of cross and the longitudinal section of axons are seen circular and longitudinal. Vessels in this region are intact and there is no gap between them and the surrounding tissue, they are seen as circular empty areas. Toluidine blue stained semi-thin (0.5 µm) resin section

Regarding the EMF + NS group the images showed that, general architecture of CA region shows normal appearance (**Figure 85, 86, 87, 88, 89, 90 and 91**). Although the border of nucleus is clearly seen but neurons perikaryon borders is not clear. There are many of axons accumulation can be observed between pyramidal cells. Some of darkly stained cells are observed.

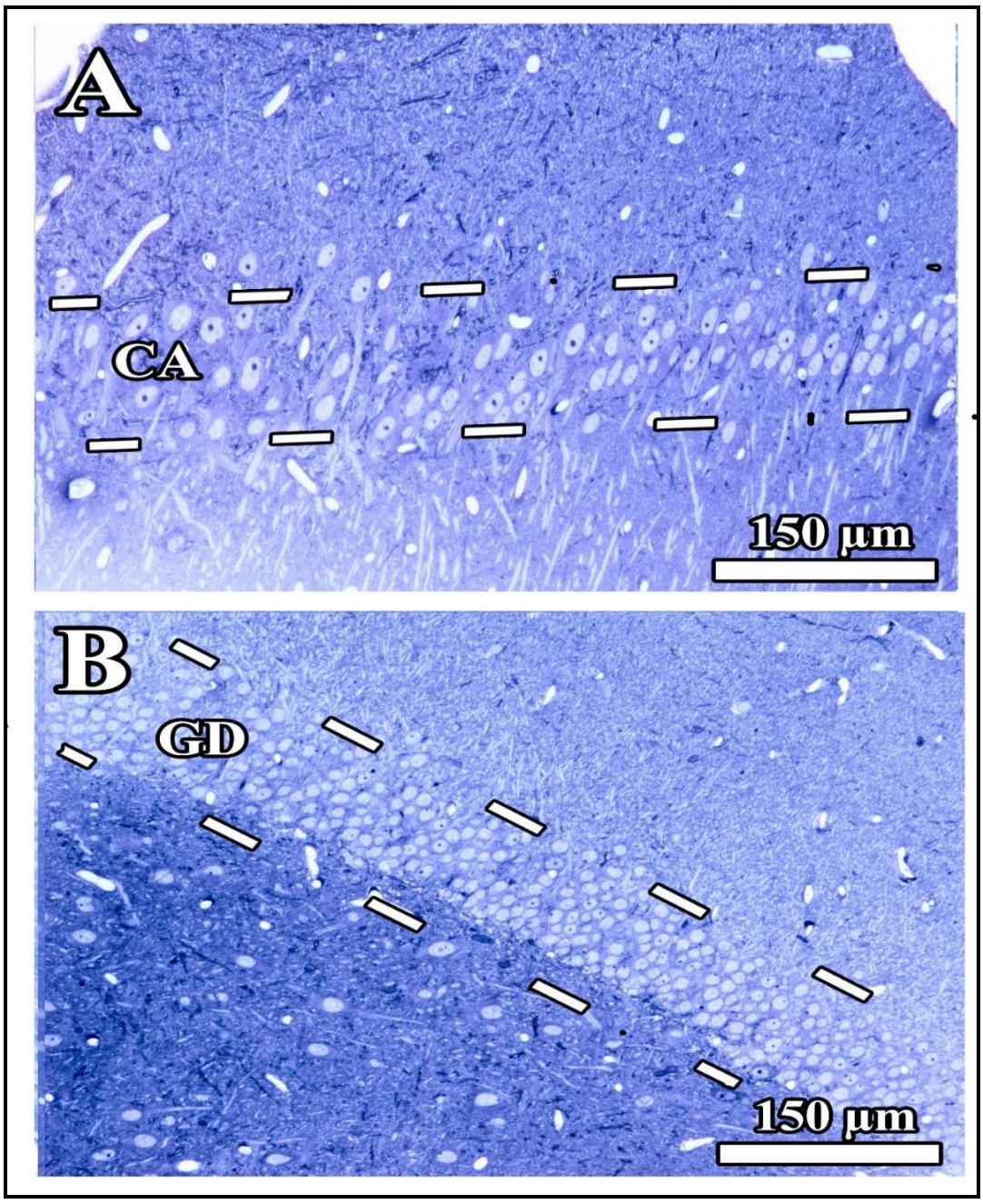

Figure 85. (A, B) Images taken from the hippocampus belong to the EMF + NS group are seen. General structure of CA and GD shows normal appearance. Pyramidal cells in the CA region have oval shaped nucleus and conspicuous nucleolus. Granular cells in the GD regions are fine and they have spherical nucleus. Toluidine blue stained semi-thin (0.5 µm) resin section

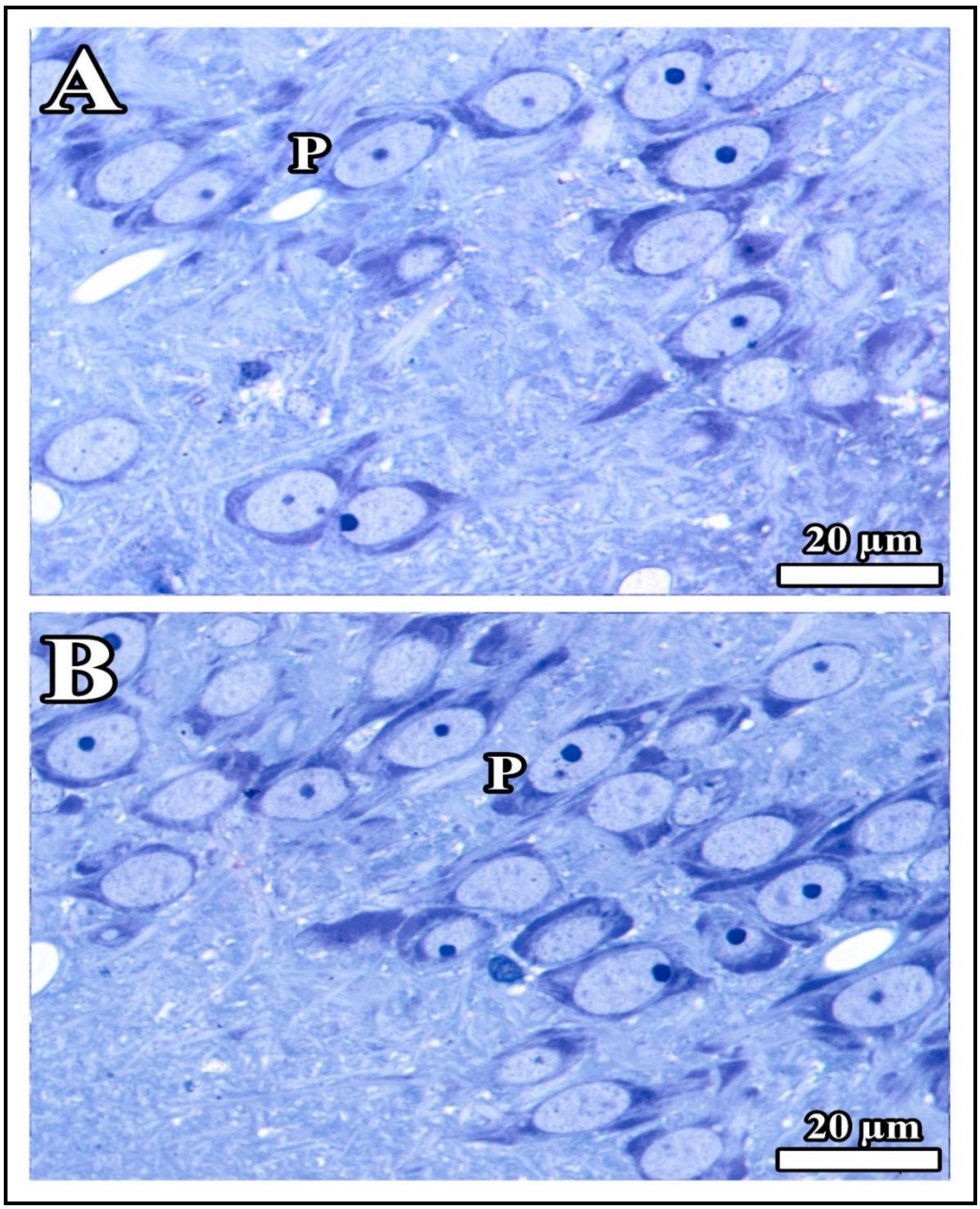

Figure 86. (A, B) Images taken from the hippocampus belong to the EMF + NS group are seen. Pyramidal cells (P) in the CA region have oval shape nucleus and conspicuous nucleolus. Most of cells in this region they have very clear cell borders. Vessels in this region (circular or oval shape) look normal and there is no space between the wall and surrounding tissues. Toluidine blue stained semi-thin (0.5 µm) resin section

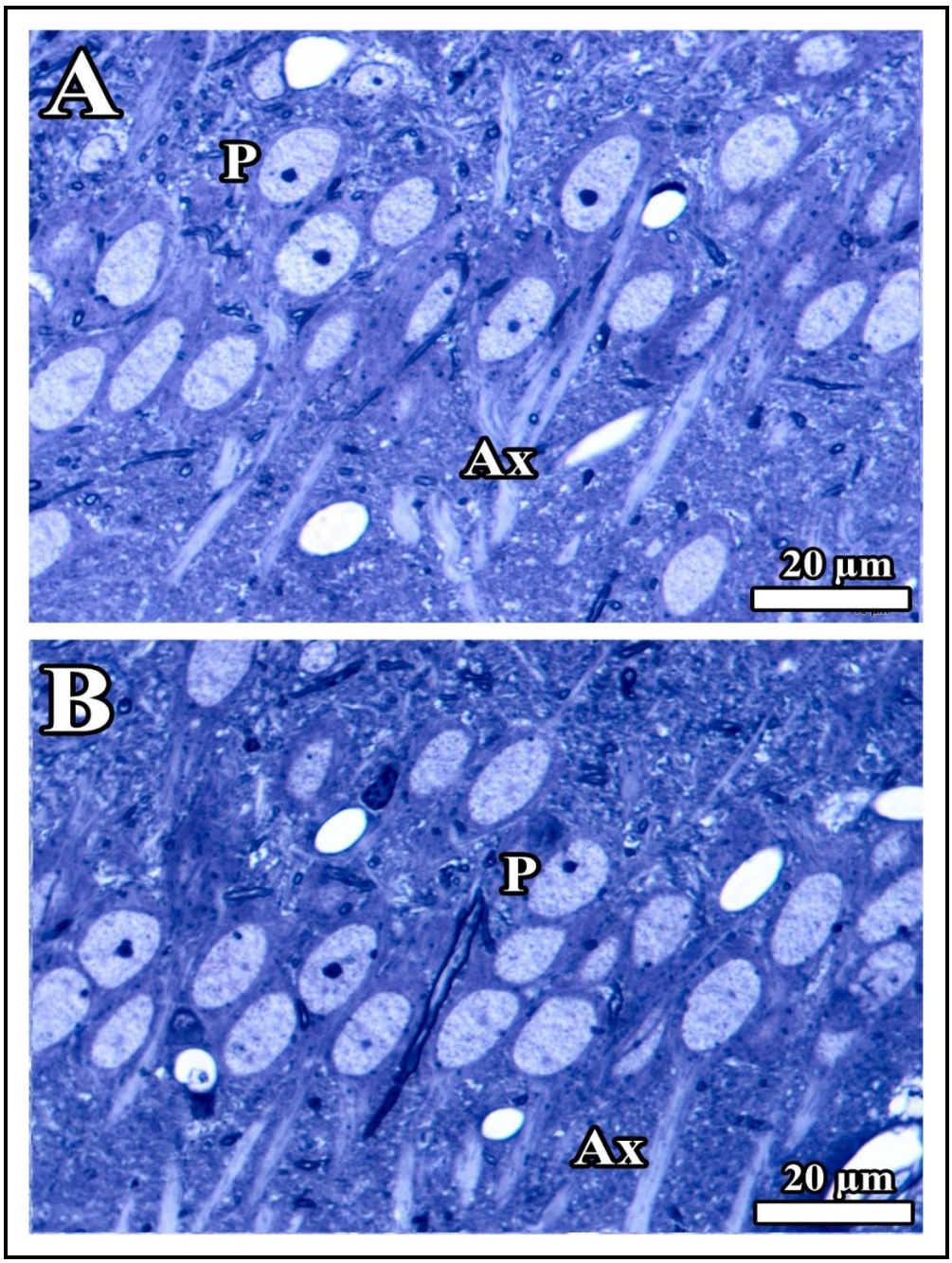

Figure 87. (A, B) Images taken from the CA region of the hippocampus belong to the EMF + NS group are seen. Pyramidal cells (P) in the CA region have oval shape nucleus and conspicuous nucleolus. The distance between them looks fine, axons (Ax) of pyramidal cells are observed. Although the border of nucleus is clearly seen but perikaryon borders not clear. Vessels in this region look normal and there is no space between its wall and surrounding tissues. Toluidine blue stained semi-thin (0.5 µm) resin section

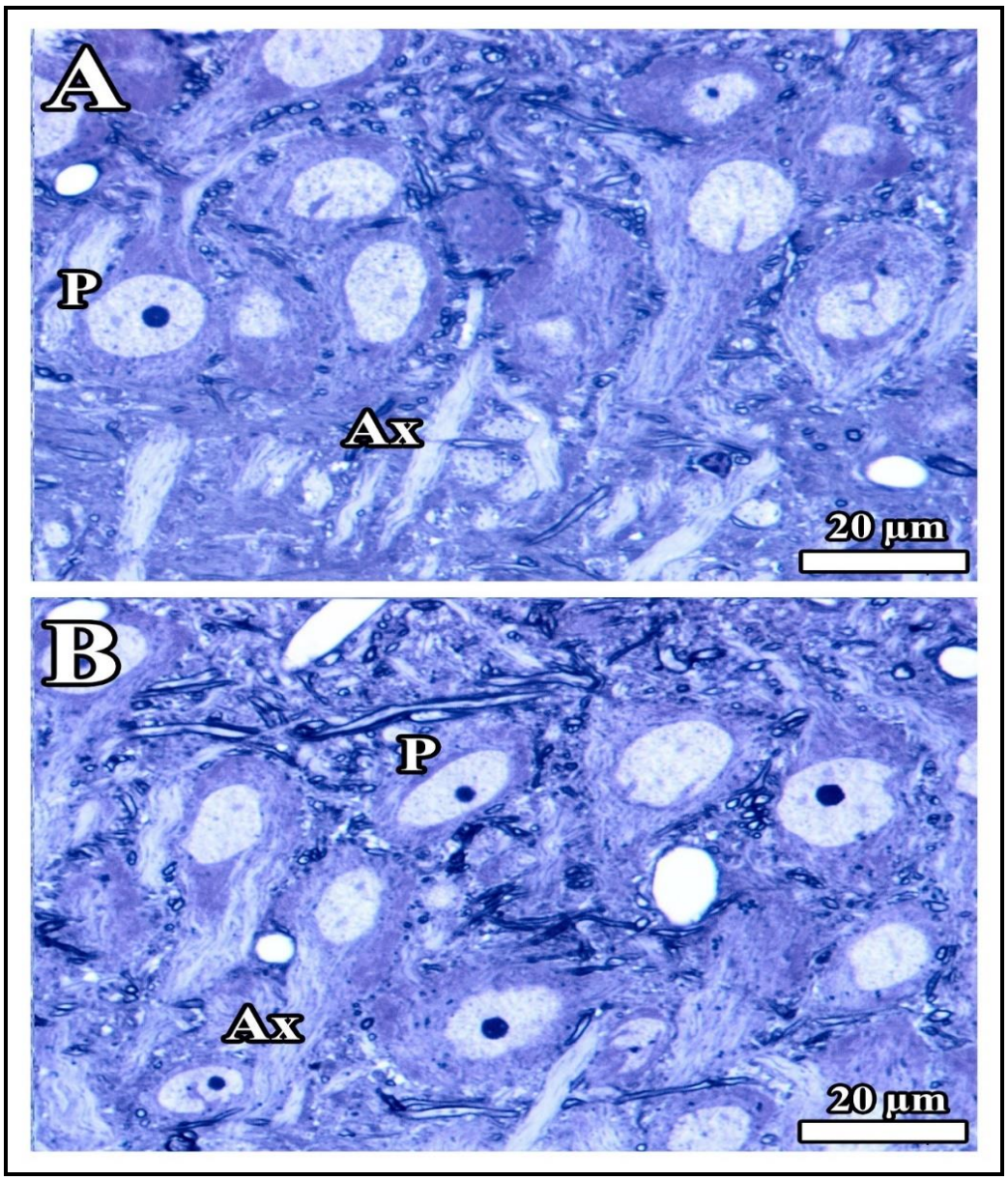

Figure 88. (A, B) Images taken from a different area of the CA region belong to the EMF + NS group are seen. The size of pyramidal cells (P) in this region is larger than the pyramidal cells of the previous group; between these cells many of axons (Ax) accumulation can be observed. The pyramidal cells in this region have oval shape nucleus and conspicuous nucleolus. The distance between neurons looks fine, axons of pyramidal cells are observed. Not only the border of nucleus is clearly seen but also perikaryon borders are clearly observed, since their borders are delineated by cross-sectioned axons. Vessels in this region look in normal appearance and there is no space between the wall and surrounding tissue. Toluidine blue stained semi-thin (0.5 µm) resin section

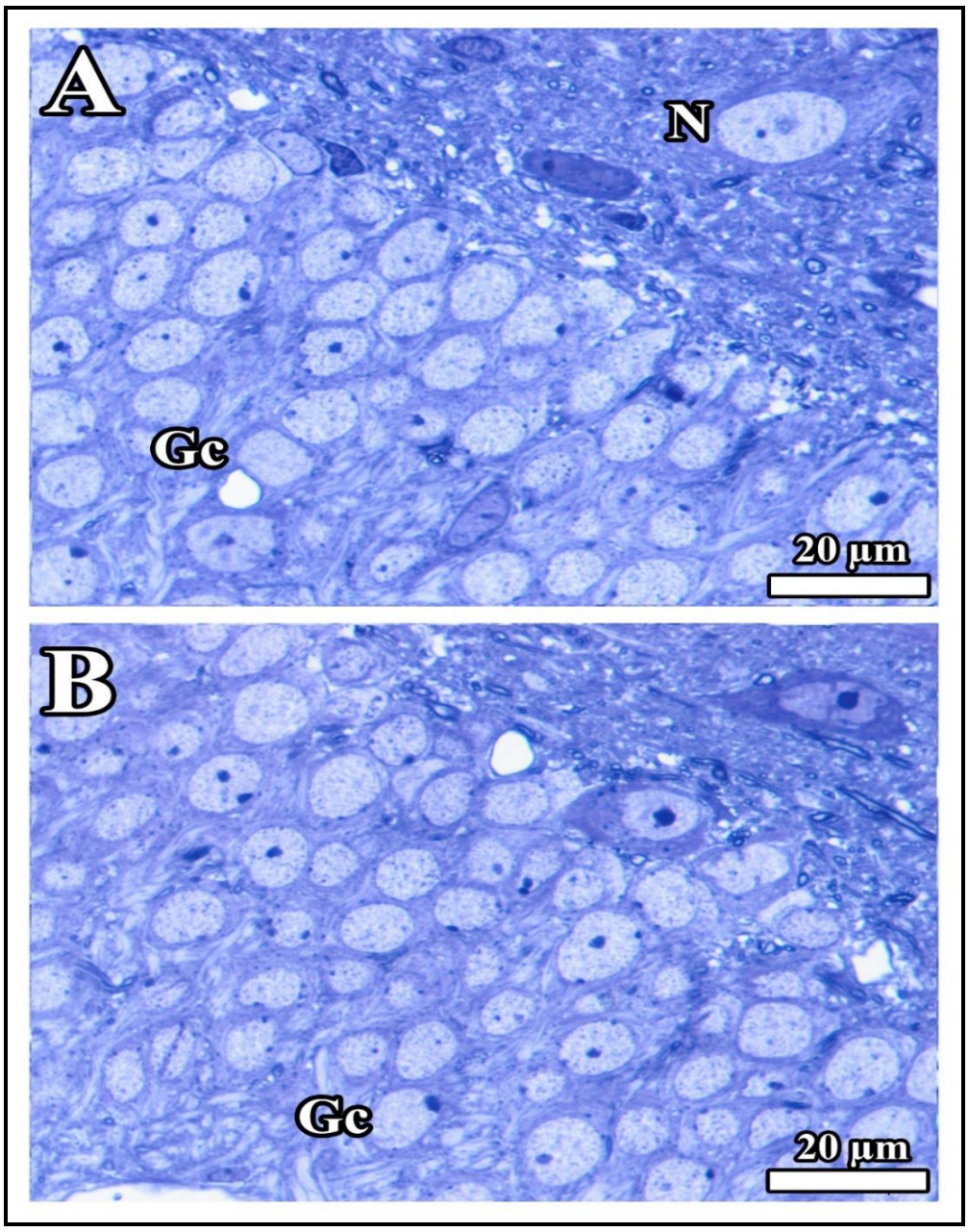

Figure 89. (A, B) Images taken from the GD region belong to the EMF + NS group are seen. The size of granular cells (Gc) in this region looks fine. The cells in this region have spherical shape nucleus and conspicuous nucleolus. The distance between neurons looks fine. Although the border of nucleus is clearly seen, perikaryon borders cannot. Two big size neurons (N) are located near the GD are found. Vessels in this region look normal and there is no space between the wall and surrounding tissues. Toluidine blue stained semi-thin (0.5 µm) resin section

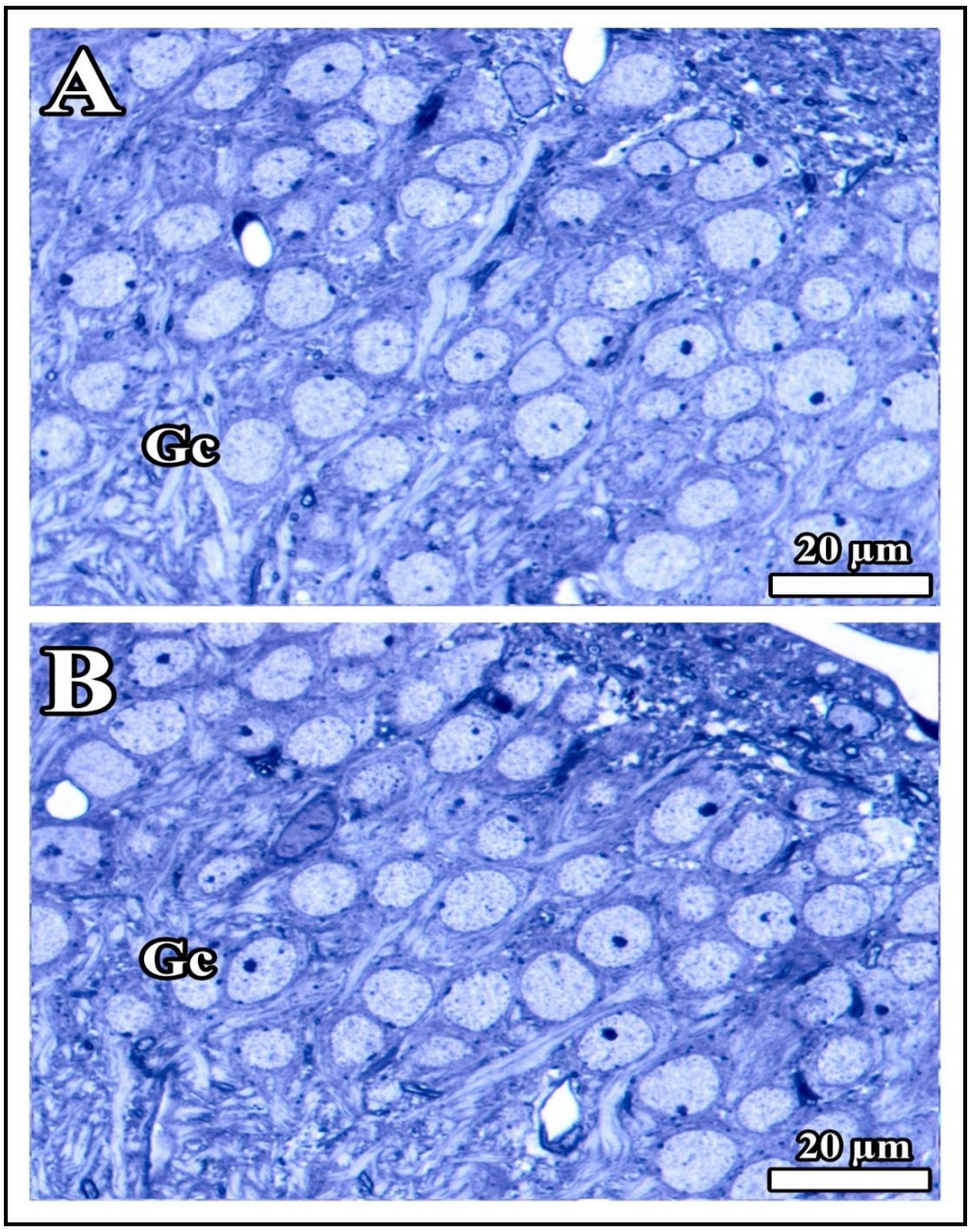

Figure 90. (A, B) Images taken from the GD region belong to the EMF + NS group are seen. The size of granular cells (Gc) in this region looks fine. The cells in this region have spherical shapenucleus and conspicuous nucleolus. The distance between Gc looks fine. Although the border of nucleus is clearly seen, perikaryon borders cannot be observed. There are many longitudinally sectioned axons and some of darkly stained cells are found in this region. Vessels in this region look normal and there is no space between the wall and their surrounding tissues. Toluidine blue stained semi-thin (0.5 µm) resin section

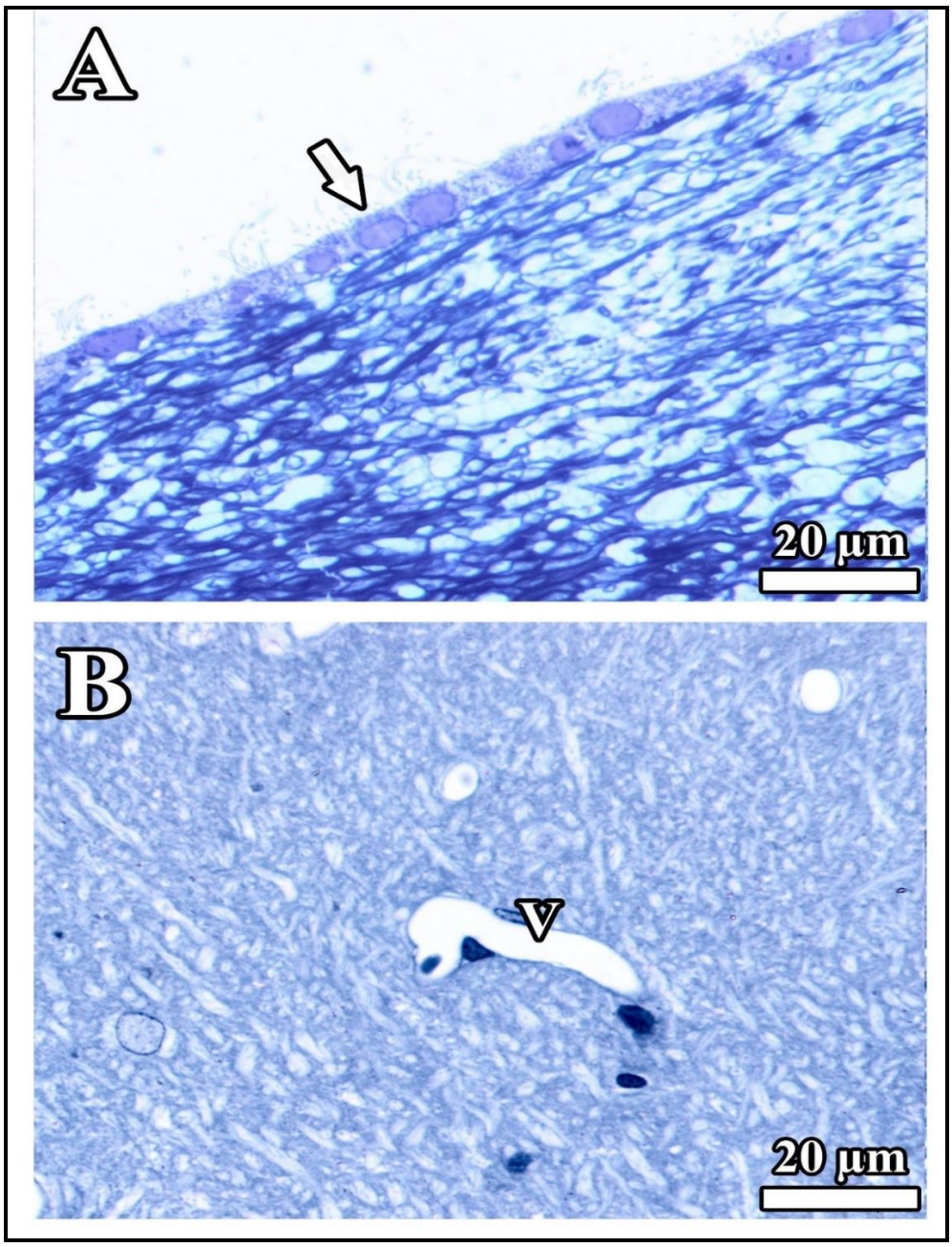

Figure 91. (A) The image taken from the ventricle belongs to the EMF + NS group is seen. A layer of ependymal cells is lined the ventricle. These cells have a cuboidal shape and many of cilia at the apical pole of cells (arrow). Ependymal cells have spherical nucleus that is slightly darkly stained, below this layer a white mater is seen. (B) The white matter of brain this group is observed, a well-protected vessel that has an intact wall is seen. Toluidine blue stained semi-thin (0.5 µm) resin section

Regarding the EMF + AD + NS group the images showed that, general structure of CA region shows normal appearance (**Figure 92, 93, 94 and 95**). A few numbers of dark cells have a deformed shape and darkly stained.

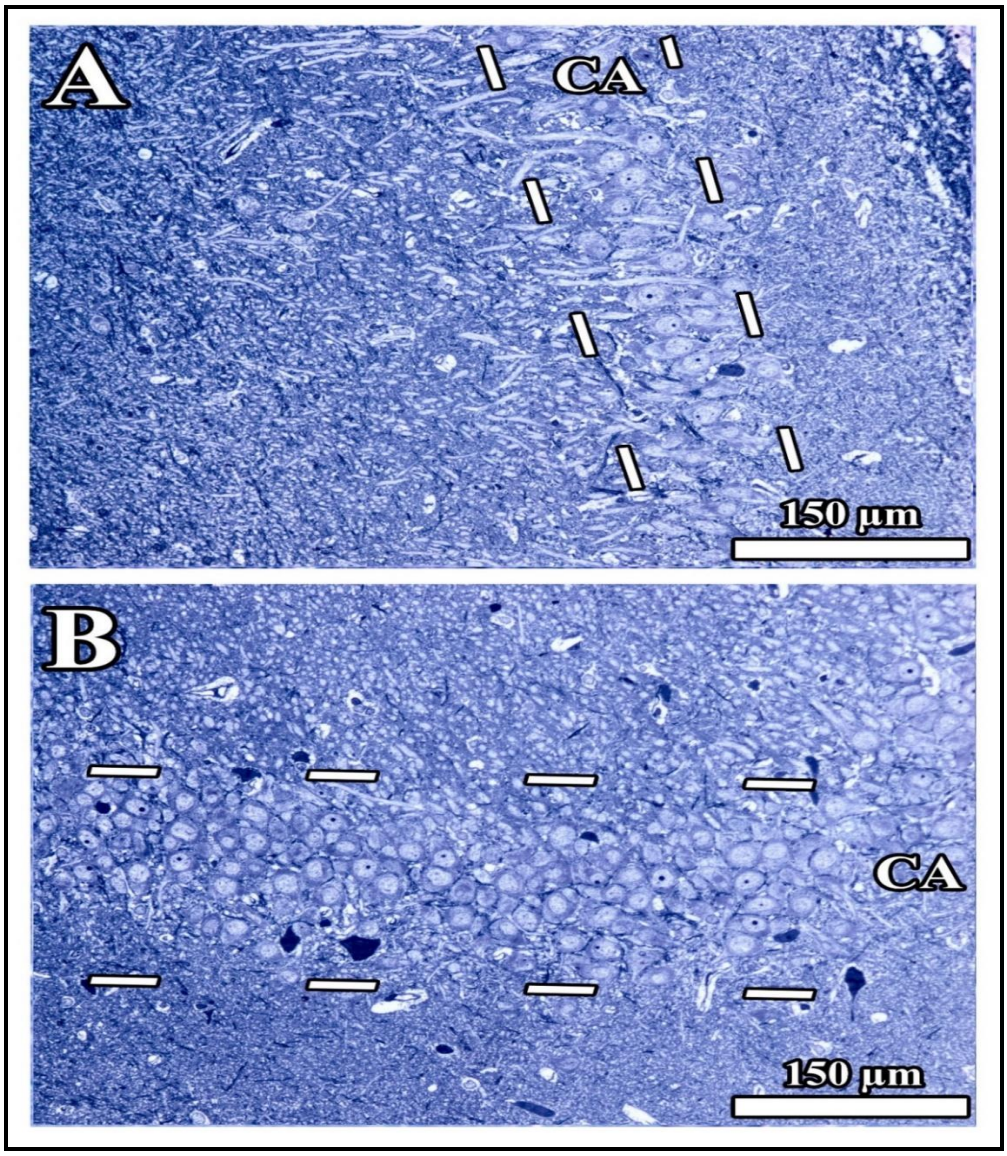

Figure 92. (A, B) Images taken from the CA region of hippocampus belong to the EMF + AD + NS group are seen. General structure of CA region looks in normal, their axons and nucleus can be clearly observed but a few numbers of dark cells are also found. Some of the vessels are collapsed, this might be resulted a low-quality fixation or other unknown factors. Toluidine blue stained semi-thin (0.5 µm) resin section

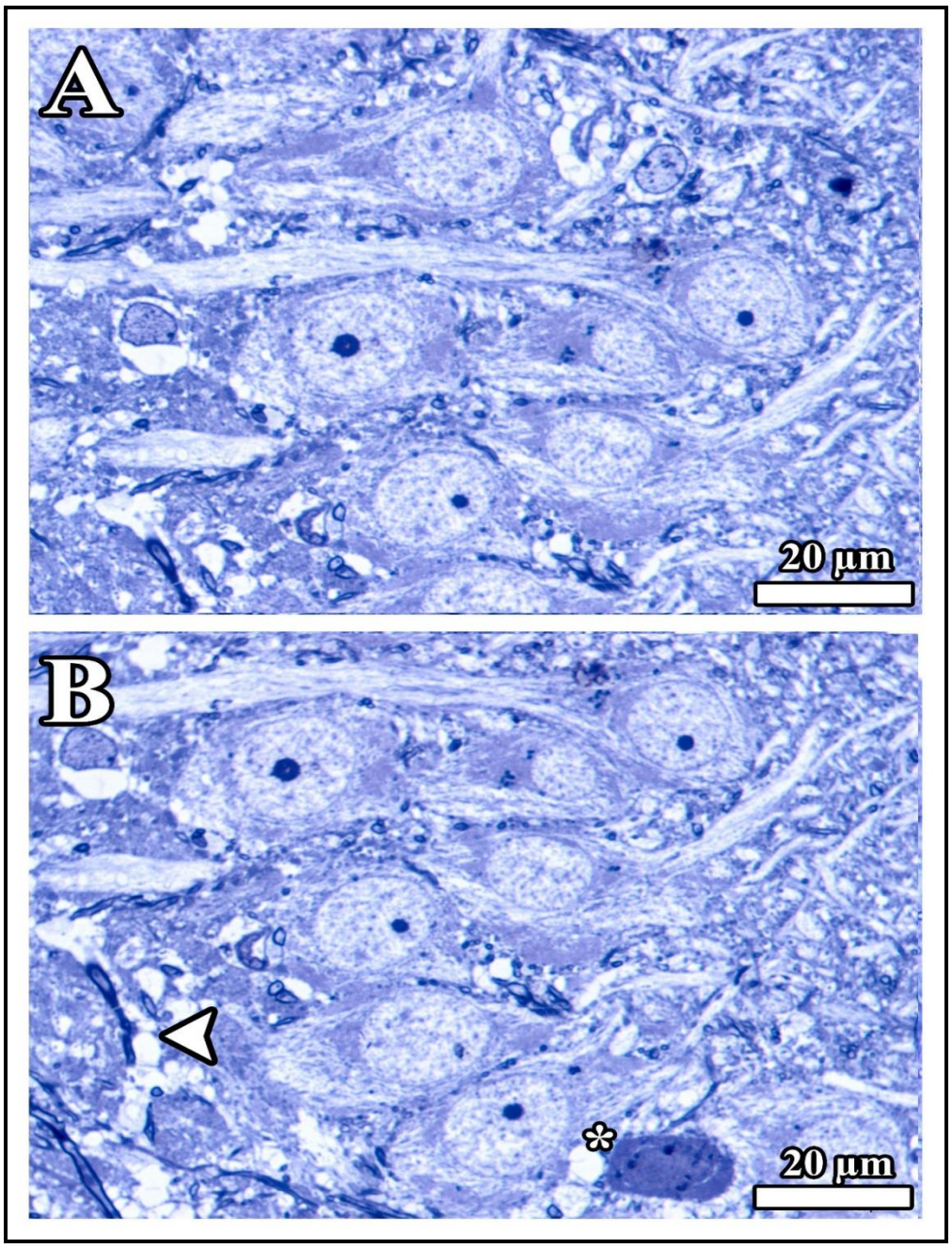

Figure 93. (A, B) Images taken from the CA region of hippocampus belong to the EMF + AD + NS group are seen. General structure of CA region looks in normal, their axons and nucleus can be clearly observed but a few numbers of dark cells are also seen. The border of pyramidal shaped neurons is delineated by cross-sectioned of axons (arrowhead). Some of the axons are sectioned in longitudinal, darkly stained neuroglia are seen between pyramidal neurons. Toluidine blue stained semi-thin (0.5 µm) resin section

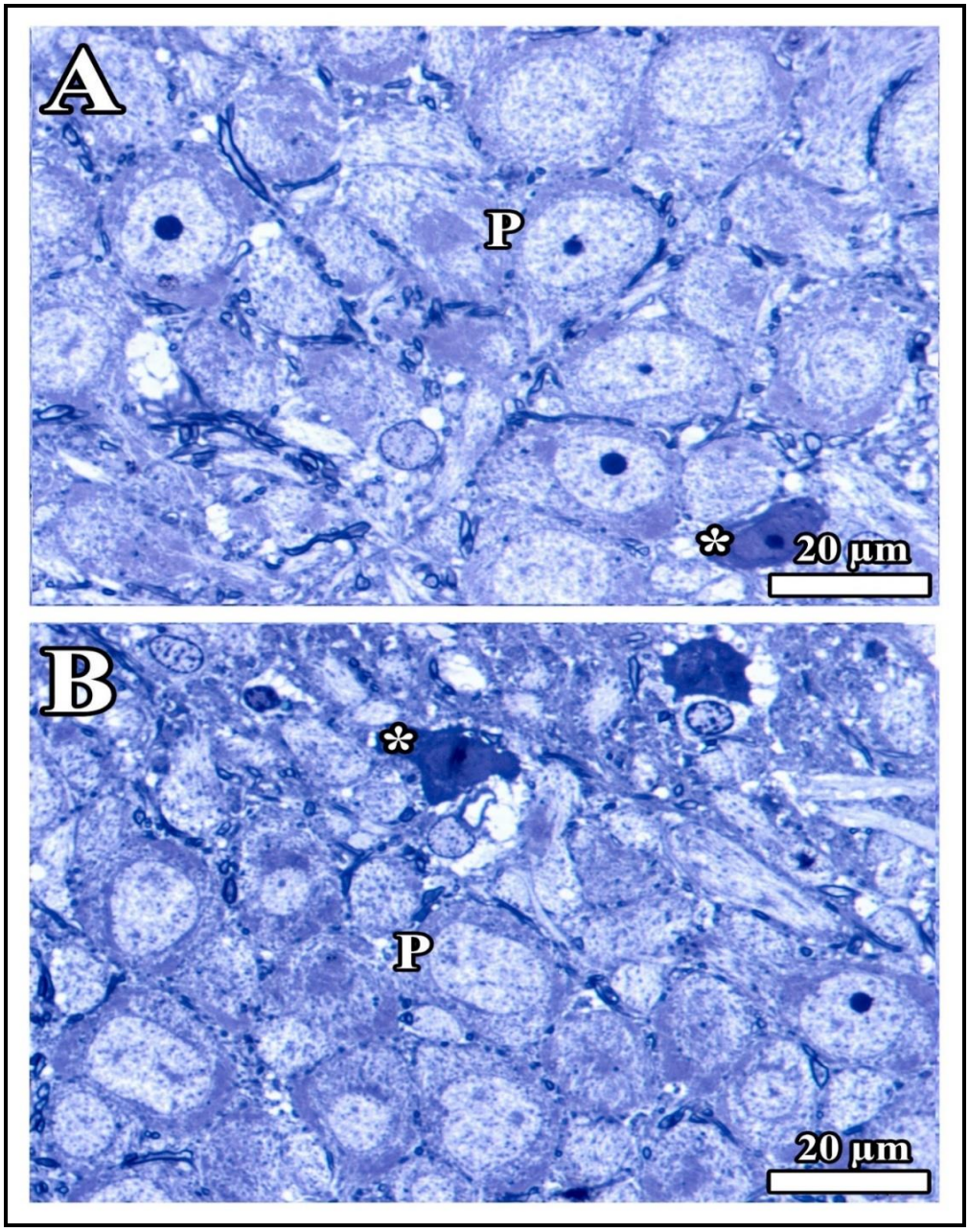

Figure 94. (A, B) Images taken from the CA region of hippocampus belong to the EMF + AD + NS group are seen. General structure of CA region and pyramidal neurons (P) look in normal morphology, their axons and nucleus can be clearly observed but a few numbers of dark cells (*) are also found. In some areas, the border of pyramidal shaped neurons is delineated by cross-sectioned of axons. Some of the axons are sectioned in longitudinal. Dark cells have a deformed shape, the distance between pyramidal cells is normal, and relationship between nucleus and cytoplasm looks fine. Toluidine blue stained semi-thin (0.5 µm) resin section

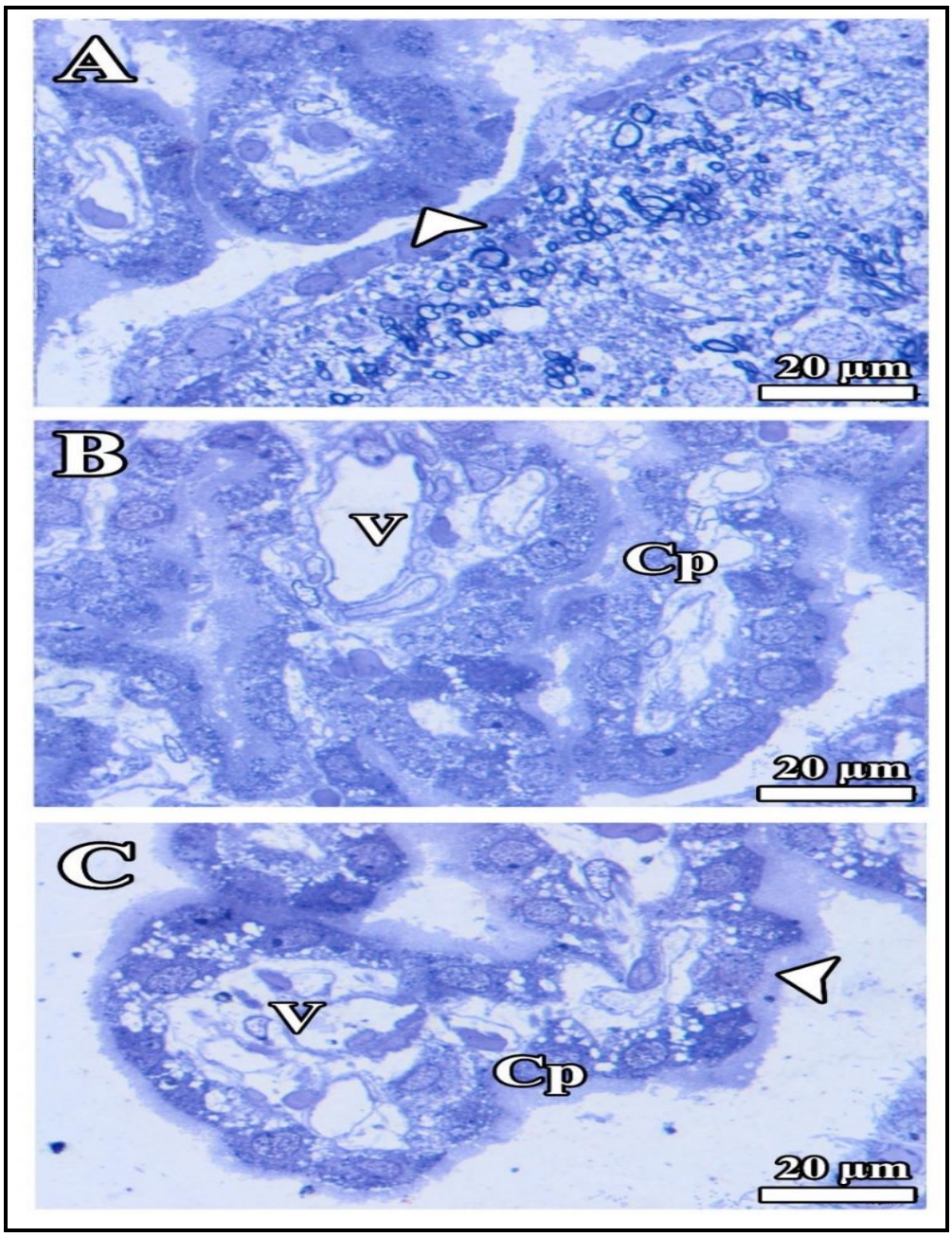

Figure 95. (A, B, C) Images taken from the ventricle of brain that belongs to the EMF + AD + NS group are observed. A well-preserved choroid plexus (Cp) and ependymal cells (arrowhead) are seen. Cross sections of axons are found in the white matter of brain. Many of capillaries (V) in the loose connective tissue of choroid plexus are also observed. Apical pole of plexus cells is lined by microvilli. Toluidine blue stained semi-thin (0.5 µm) resin section

4.3. Electron Microscopic Findings

Concerning the Cont group, the images taken by electron microscope (EM) showed that, the pyramidal cells have oval shaped, they have condensed cytoplasm. The cytoplasmic density of pyramidal cell is darkly stained (**Figure 96, 97, 98, 99,100,101,102,103,104 and 105**).

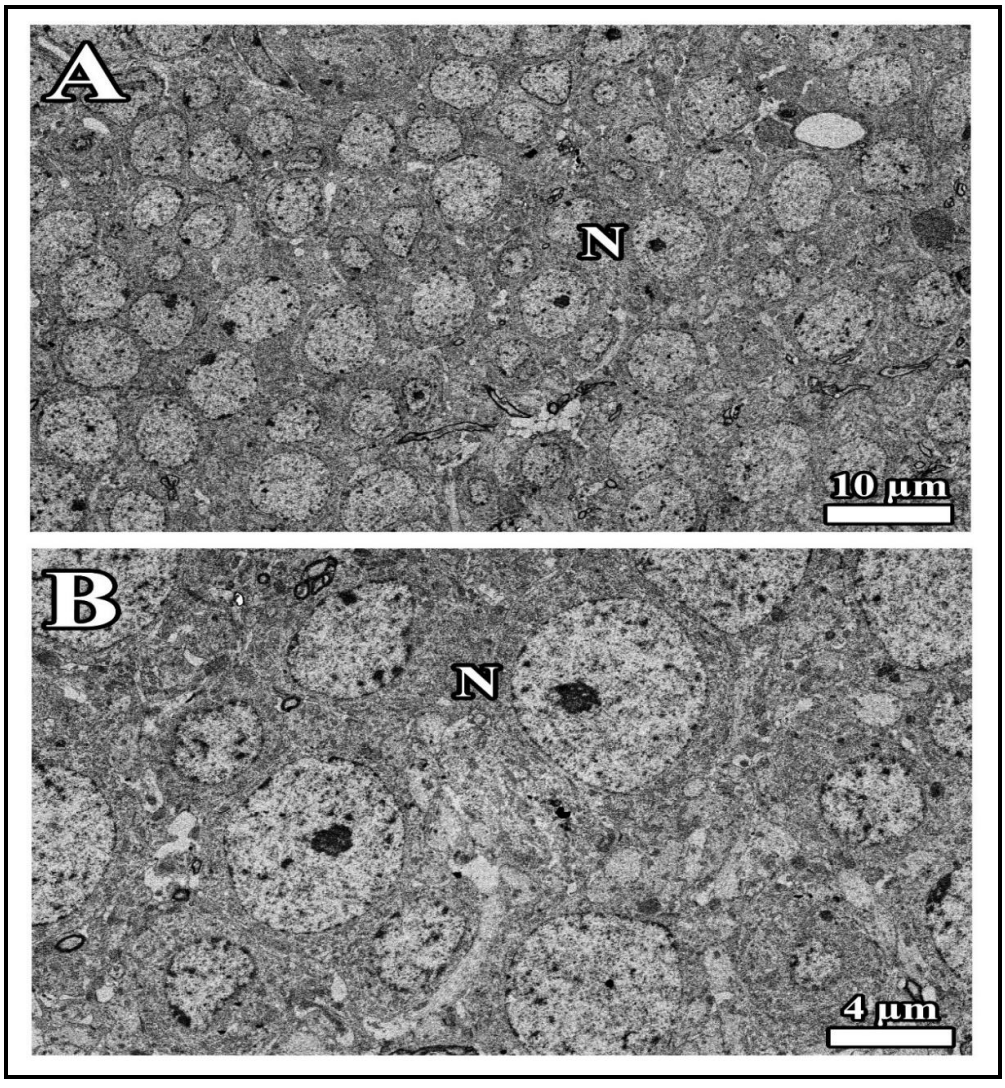

Figure 96. (A, B) Images taken from the GD region of hippocampus belong to the Cont group are seen. (A) Although the border of granular cell nucleus (N) is clearly seen but its perikaryon border cannot be seen clearly. Some cross sections of myelinated axons are observed, and granular cells look healthy and distance between them

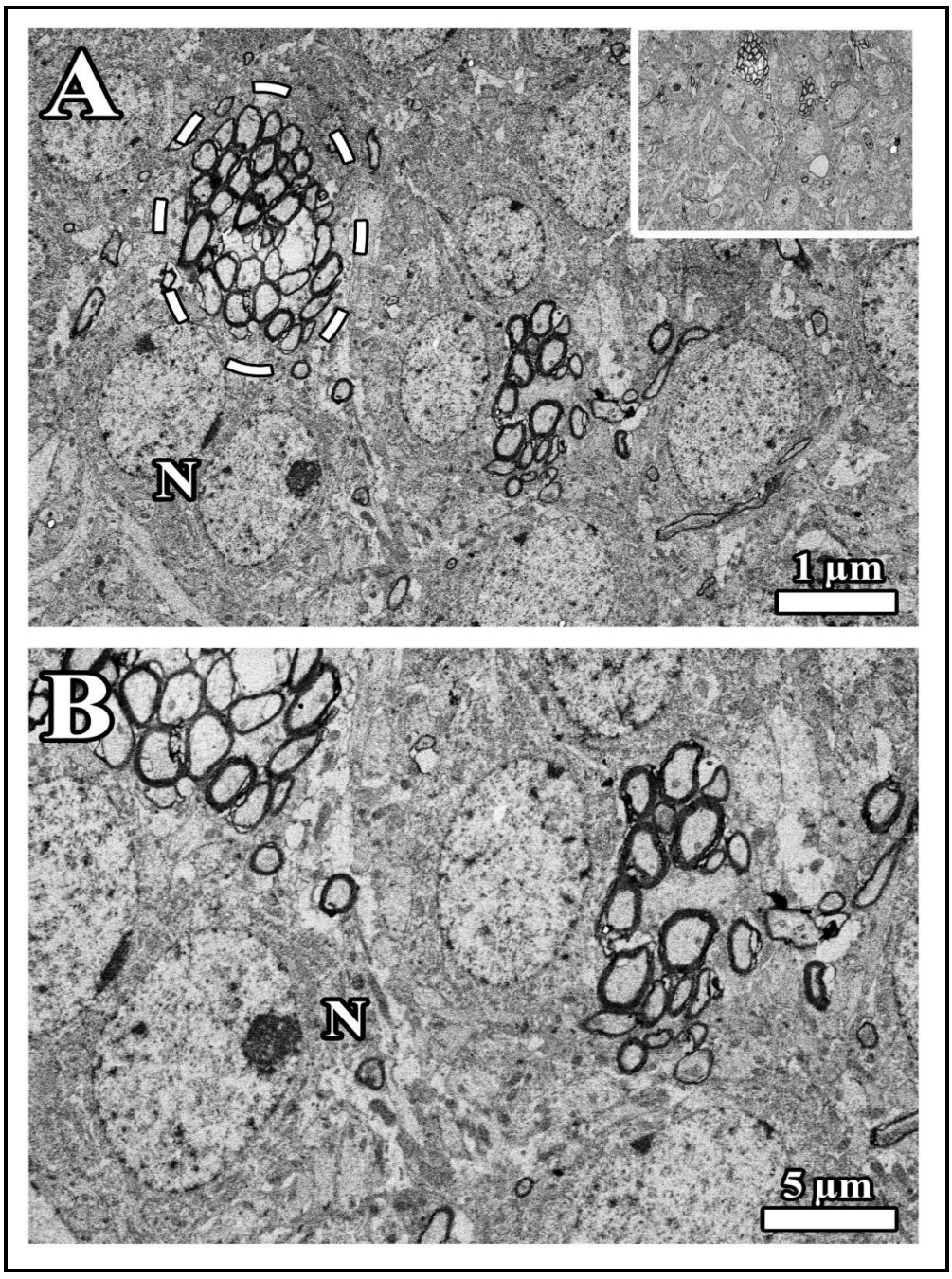

Figure 97. (A, B) Images taken from the CA region of hippocampus belong to the Cont group are seen. An accumulation of myelinated axons (delineated by white colour circle) is observed between pyramidal cells. Both nerve fibres and pyramidal cells (N) have a well-protected structure

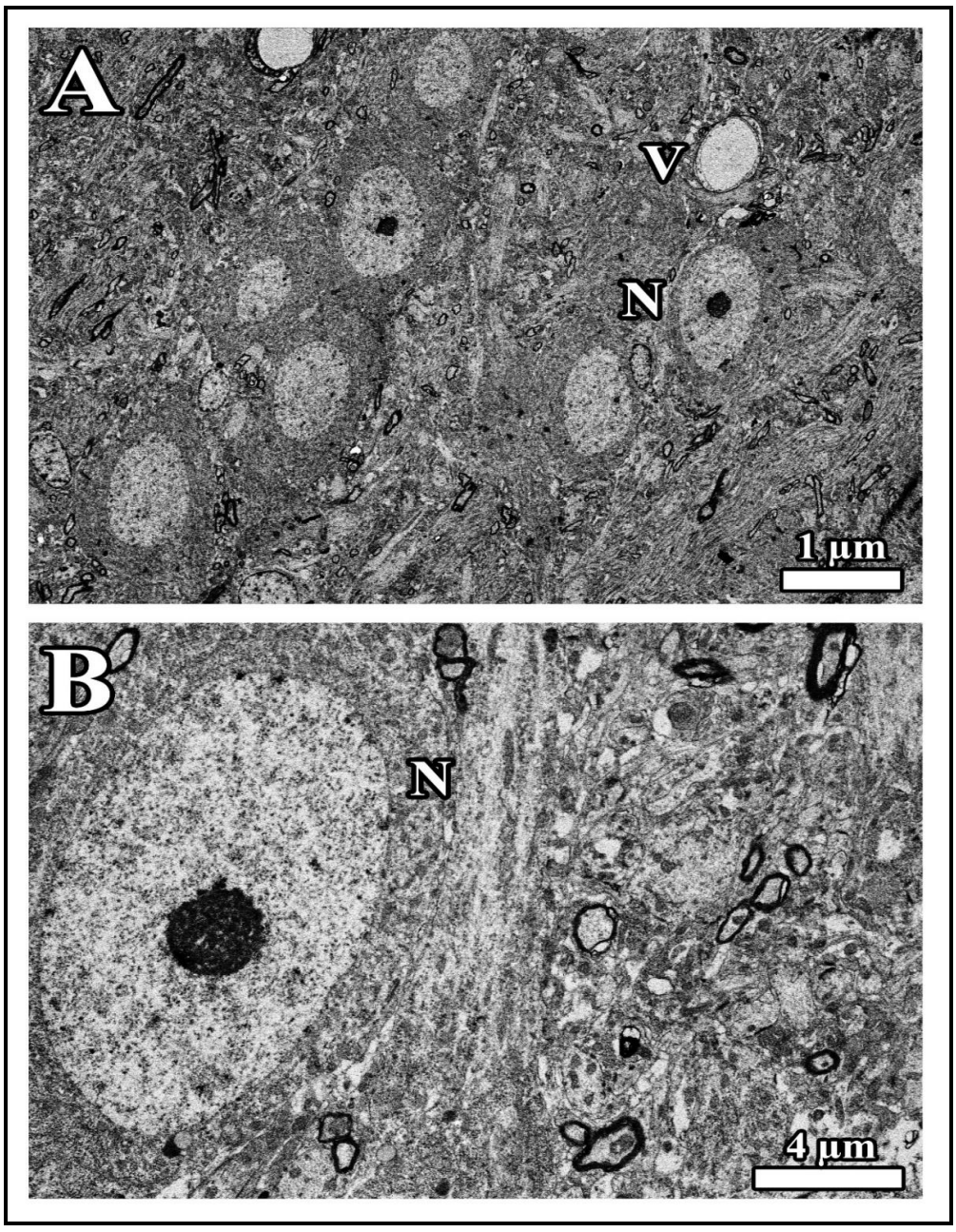

Figure 98. (A, B) Images taken from the CA region of hippocampus belong to the Cont group are seen. The distance between pyramidal neurons (N) is fine and the outline of cell body and nucleus can be clearly observed. The shape of cells and its nucleus is typically pyramidal shaped and they have very condensed cytoplasm as well as euchromatic nucleus and very large nucleolus. Capillaries (V) in this region and other structures have a well-protected structure

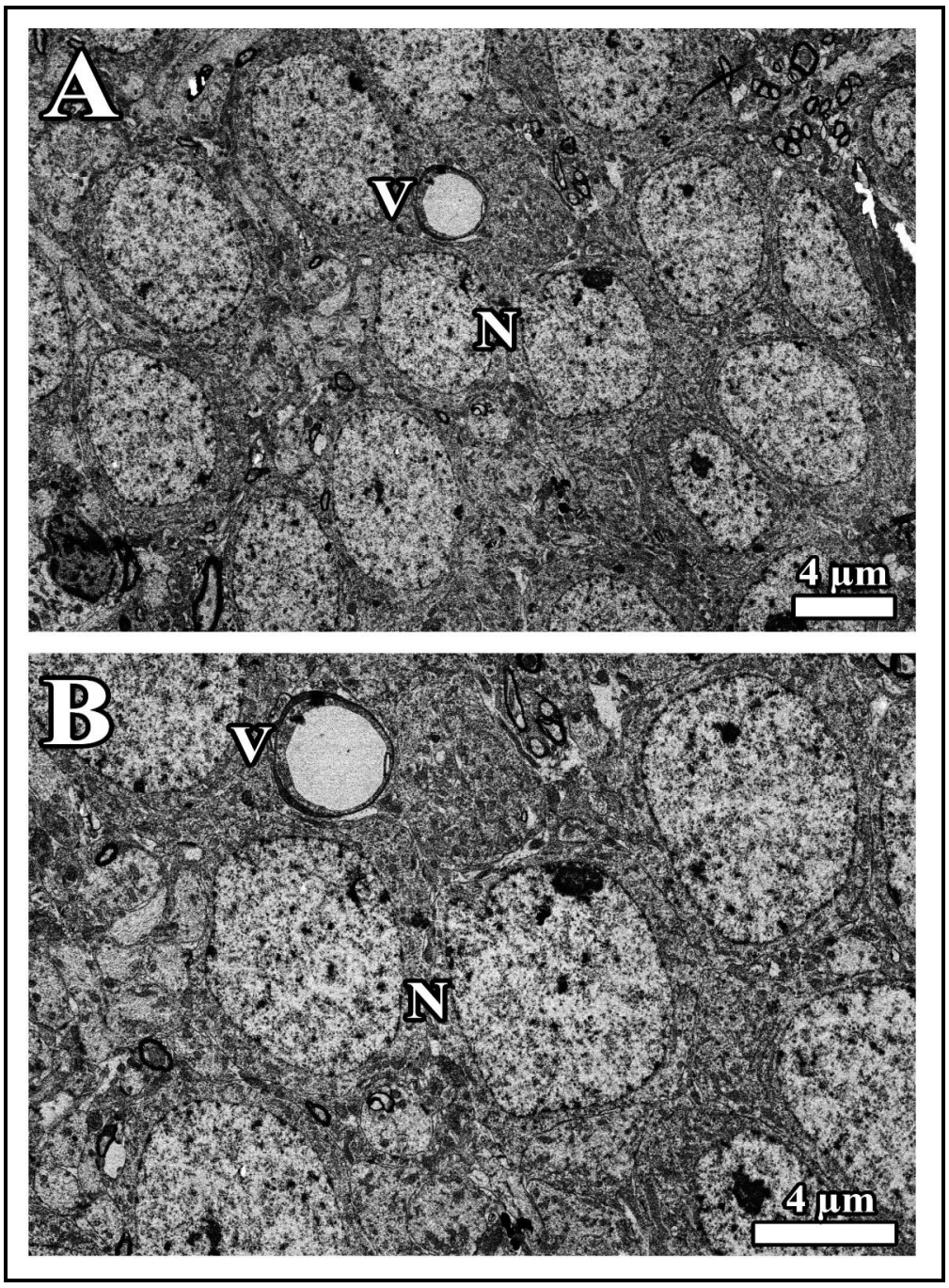

Figure 99. (A, B) Images taken from the CA region of hippocampus belong to the Cont group are seen. The distance between pyramidal cells (N) is fine and the outline of cell body and nucleus can be clearly observed. The shape of cells and nucleus look pyramidal shaped and they have condensed cytoplasm. The capillaries (V) in this region look well protected

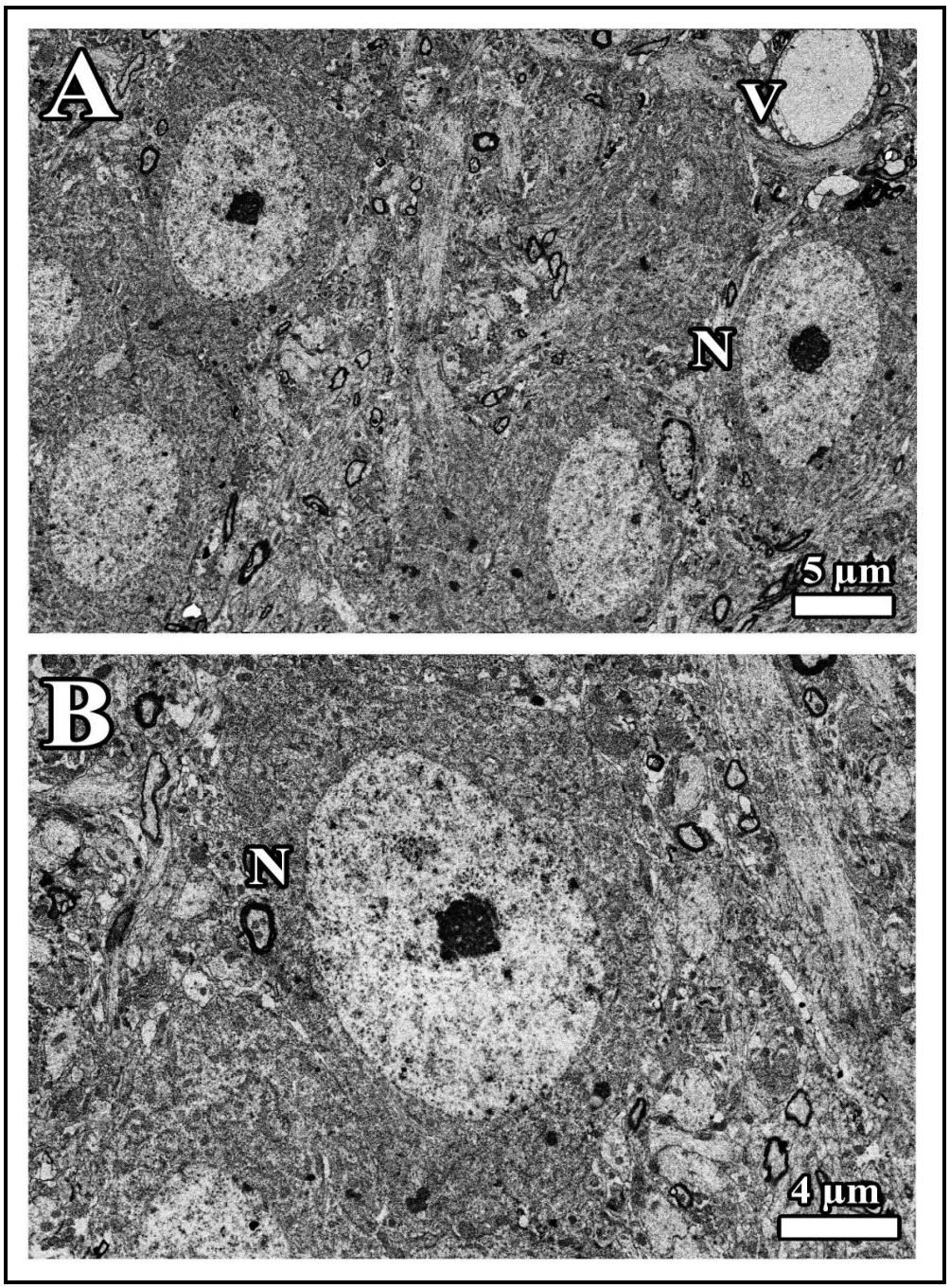

Figure 100. (A, B) Images taken from the CA region of hippocampus belong to the Cont group are seen. A well-preserved nucleus and cytoplasm of pyramidal cells (N) are observed. Between these cells cross sections of myelinated axon are commonly seen. Double unit membranes of nucleus are observed in normal structure. The capillary (V) in this region looks well protected

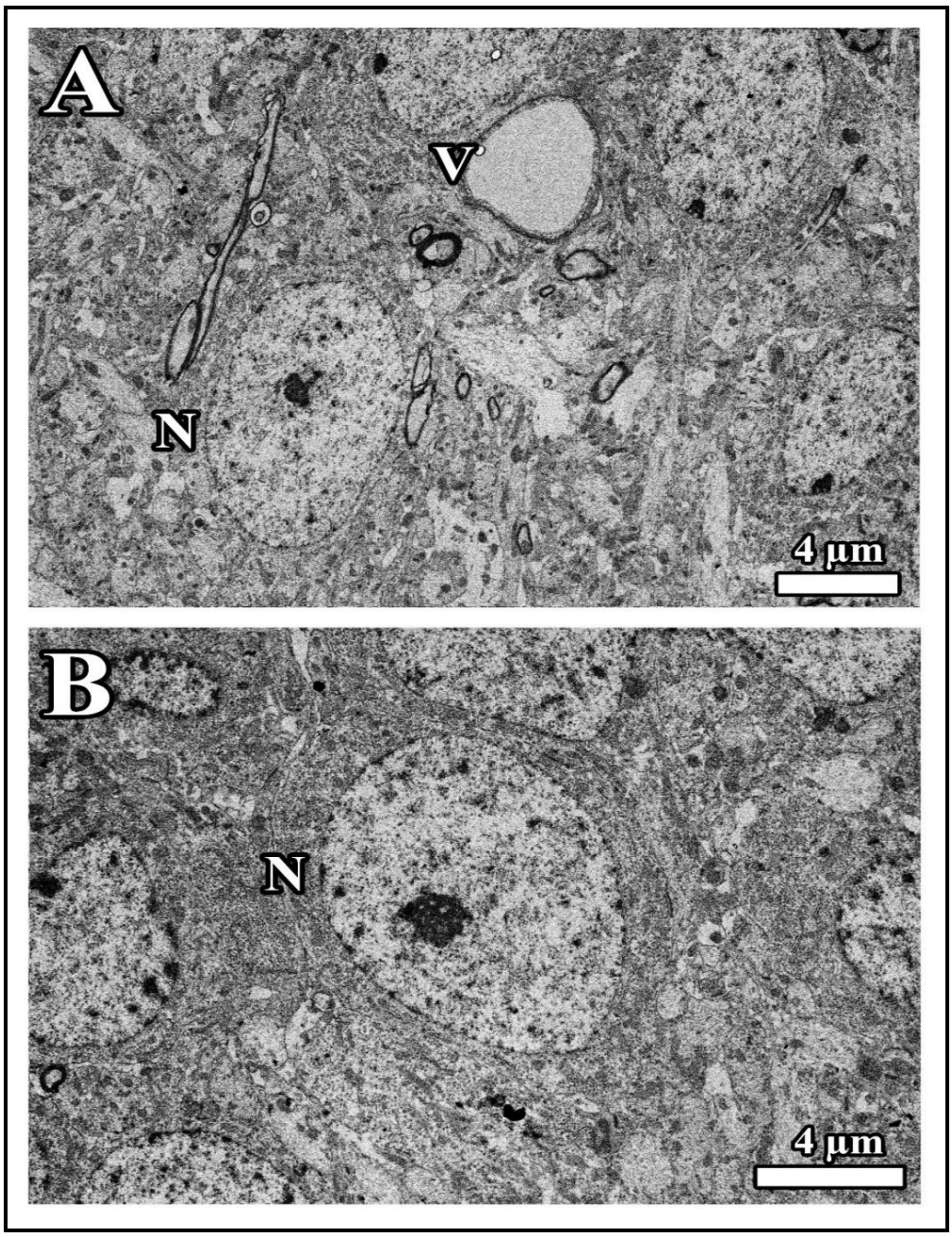

Figure 101. (A, B) Images taken from the CA region of hippocampus belong to the Cont group are seen. (A) A well-preserved nucleus and cytoplasm of pyramidal cells (N) are observed. In this area, the cytoplasm density of pyramidal cells is lightly stained. The capillaries (V) in this region look well protected. Between these neurons, some longitudinal and cross sections of myelinated axon are commonly observed and (B) also double unit membranes around nucleus are found in normal structure. Their nucleoli are in a large sized

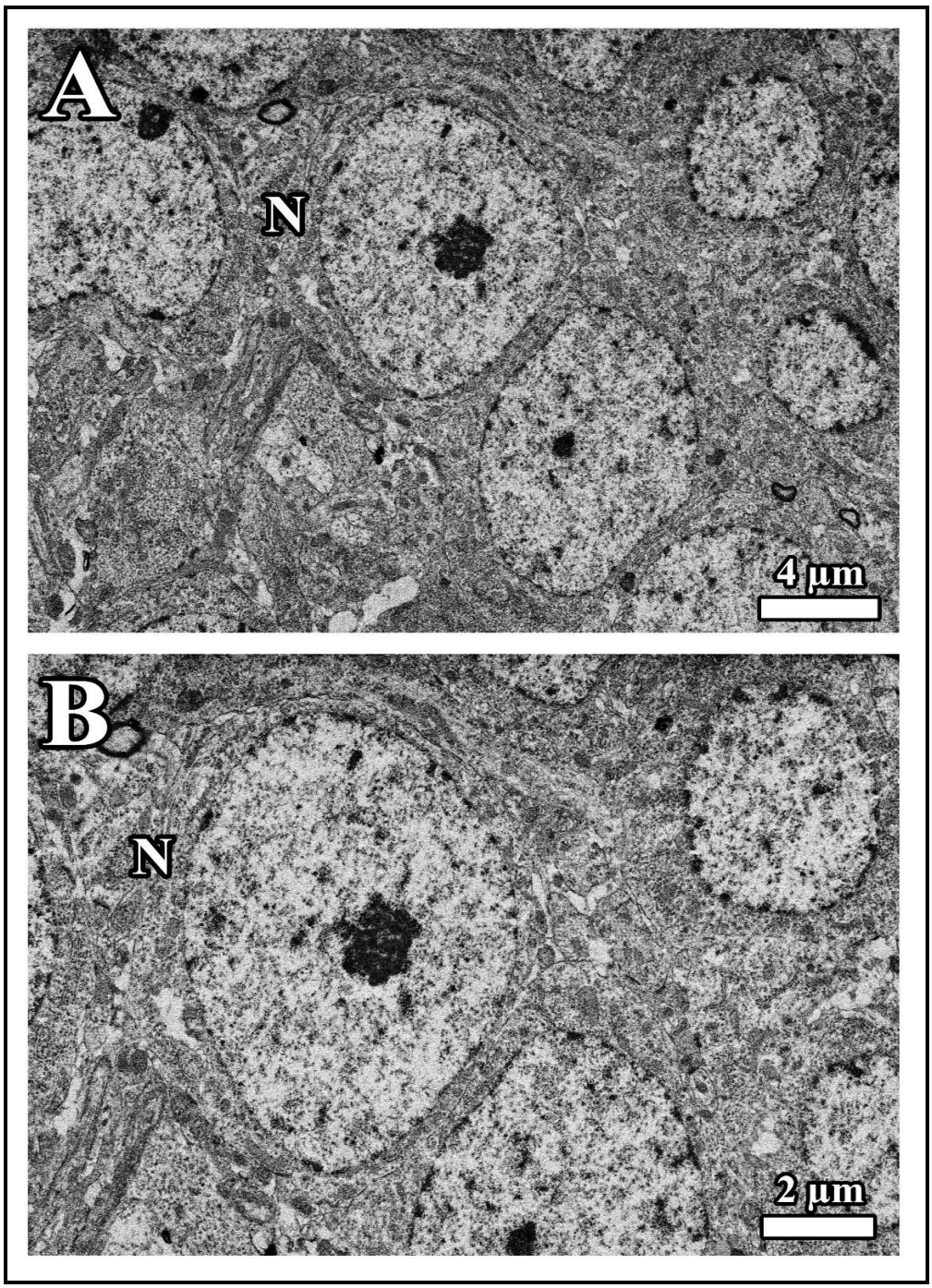

Figure 102. (A, B) Images taken from the CA region of hippocampus belong to the Cont group are seen. A well-preserved nucleus and cytoplasm of pyramidal cells (N) are observed. In this area, the cytoplasm density of pyramidal cells is lightly stained. Double unit membranes around nucleus of neuron are found in normal structure. Their nucleoli are in very large sized

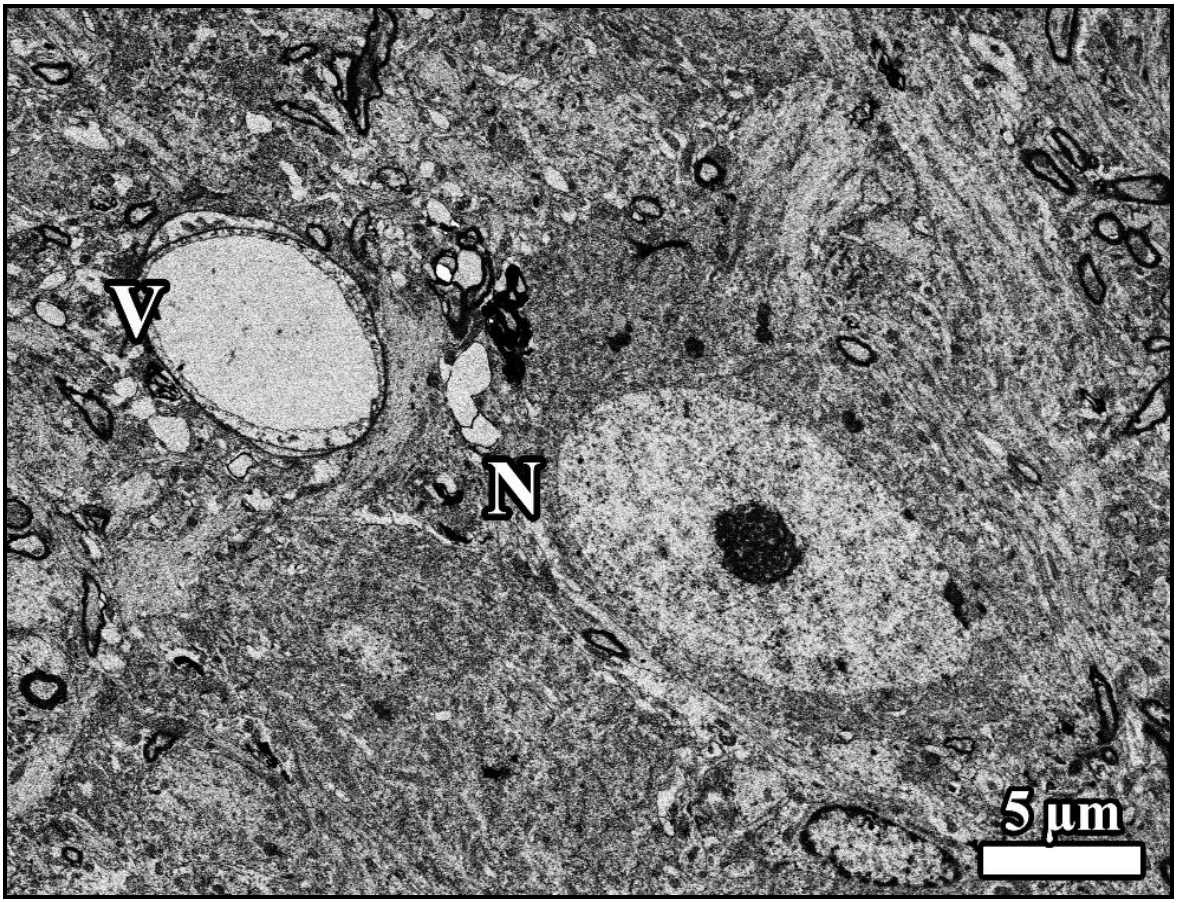

Figure 103. An image taken from the CA region of hippocampus belong to the Cont group are seen. A well-preserved nucleus and cytoplasm of a pyramidal cell (N) are observed. The cytoplasmic density of pyramidal cell is slightly darkly stained. Around this neuron, some longitudinal and cross sections of myelinated axon are seen and also double unit membranes around nucleus are found in normal structure. Their nucleolus is large sized and a cross sectioned capillary (V) has protected wall and microglia is seen near to pyramidal neuron

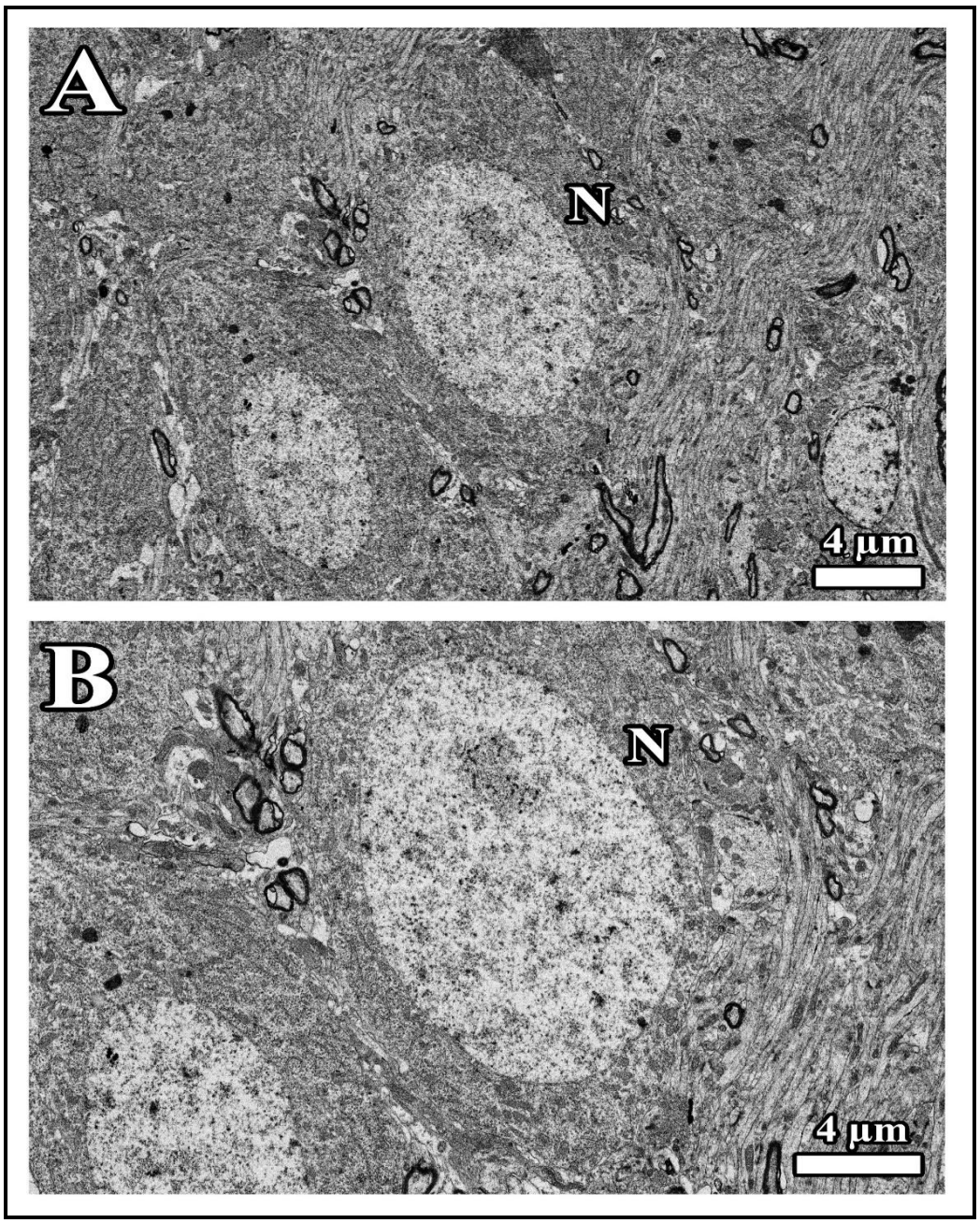

Figure 104. Images taken from the CA region of hippocampus belong to the Cont group are seen. A well-preserved nucleus and cytoplasm of a pyramidal cell are observed. The cytoplasmic density of pyramidal cell (N) is darkly stained. Around this neuron, some longitudinal and cross sections of myelinated axon are seen and also double unit membranes around nucleus are found in normal structure. Their nucleolus is in large sized

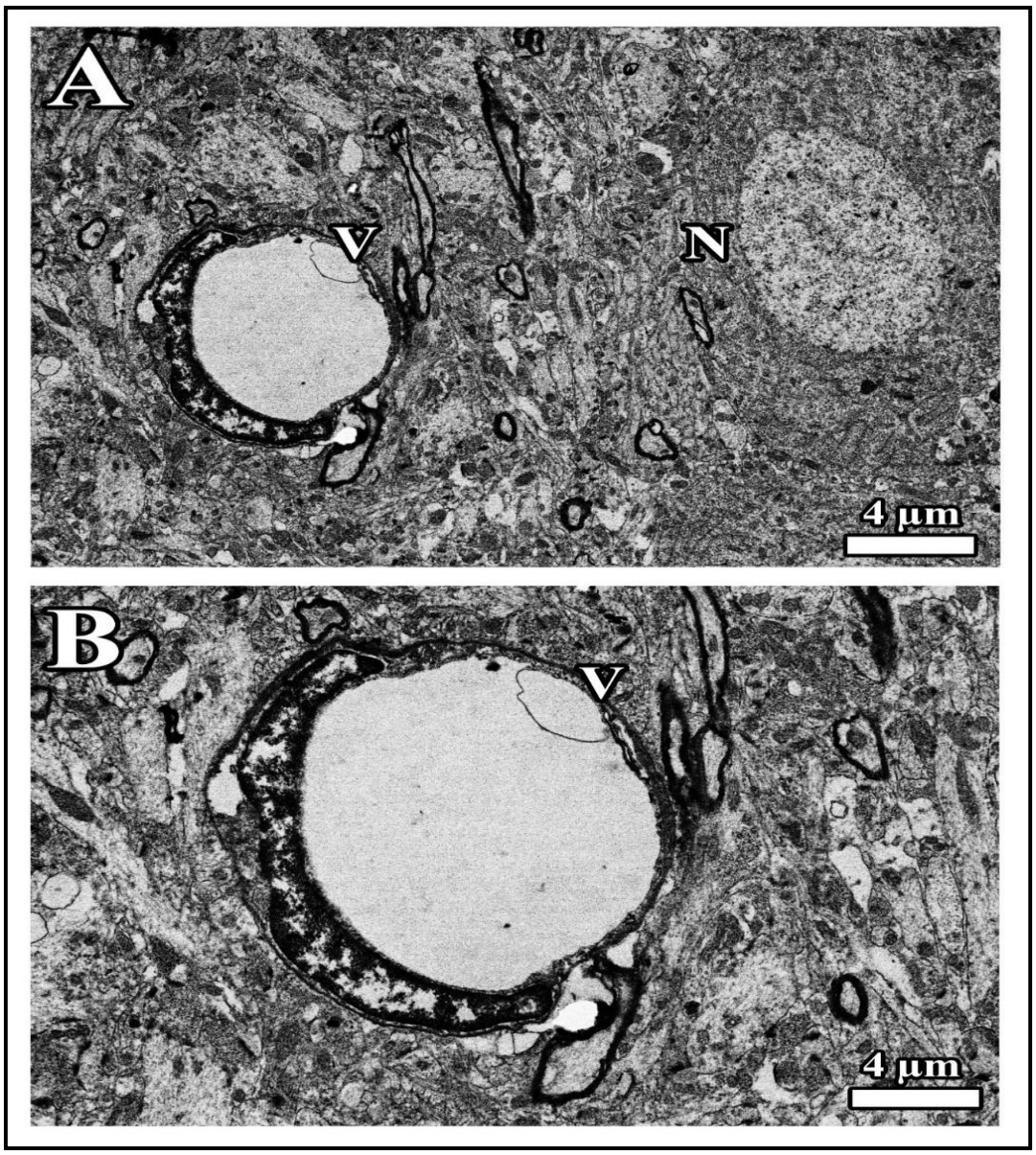

Figure 105. (A, B) Images taken from the CA region of hippocampus belong to the Cont group are seen. A well-preserved nucleus and cytoplasm of a pyramidal cell (N) are observed. The cytoplasmic density of pyramidal cell is darkly stained. Around this neuron, some longitudinal and cross sections of myelinated axon are seen and also double unit membranes around nucleus are found in healthy structure. Their nucleolus is large sized, but the border of neuron cannot be clearly delineated. (B) A large sized capillary (V) is seen, the wall of it is intact, and an endothelial cell lines its lumen. There is no space between its wall and around tissue

Regarding the Sham group the images taken by EM showed that, the pyramidal cells have oval shaped and healthy, they have a condensed cytoplasm (**Figure 106, 107, 108, 109,110 and 111**).The cytoplasmic density of pyramidal cell is darkly stained since they are very active cells.

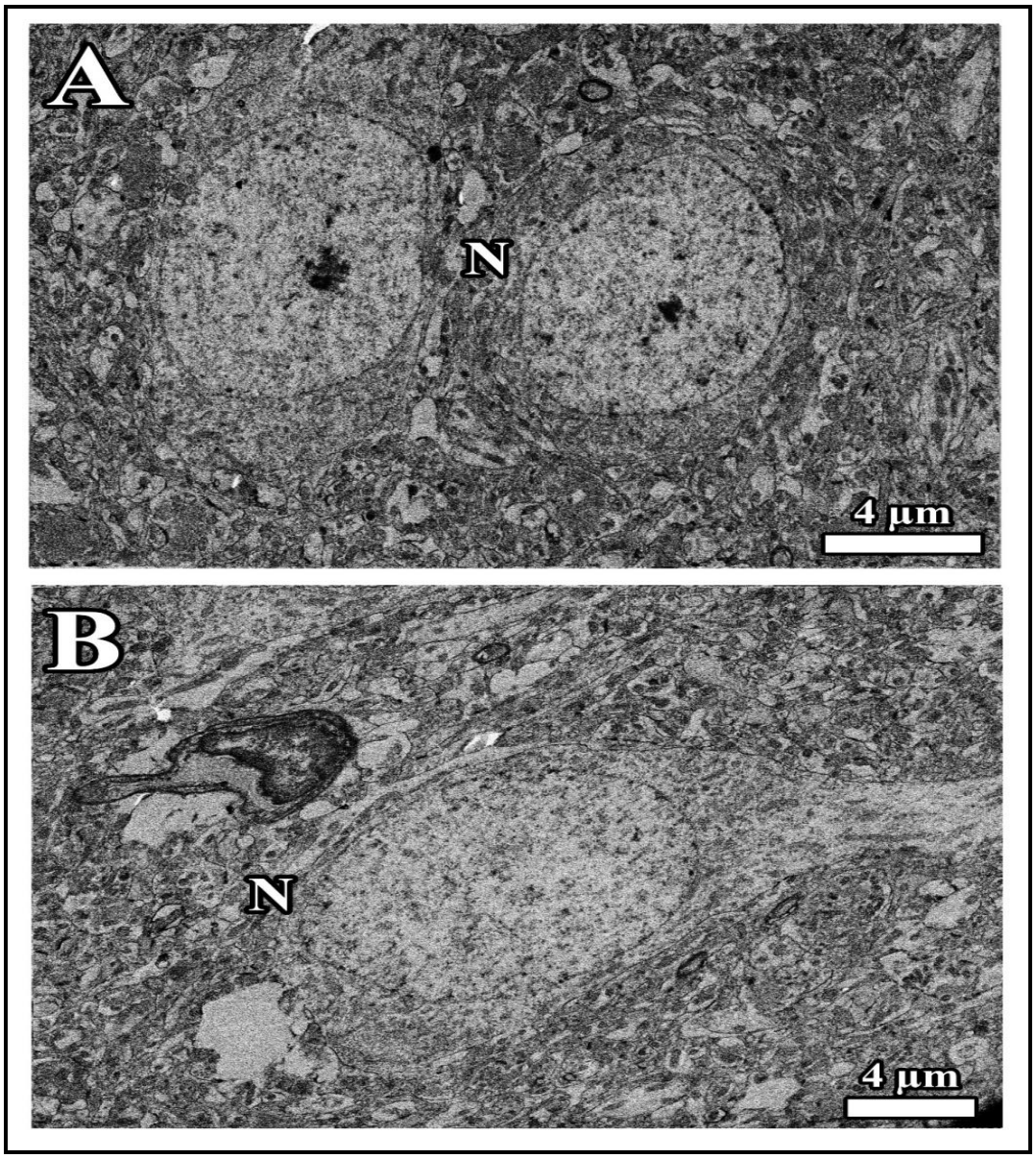

Figure 106. (A, B) Images taken from the CA region of hippocampus belong to the Sham group are seen. The cells (N) have pyramidal shaped and the border of pyramidal cell and nucleus is clearly seen

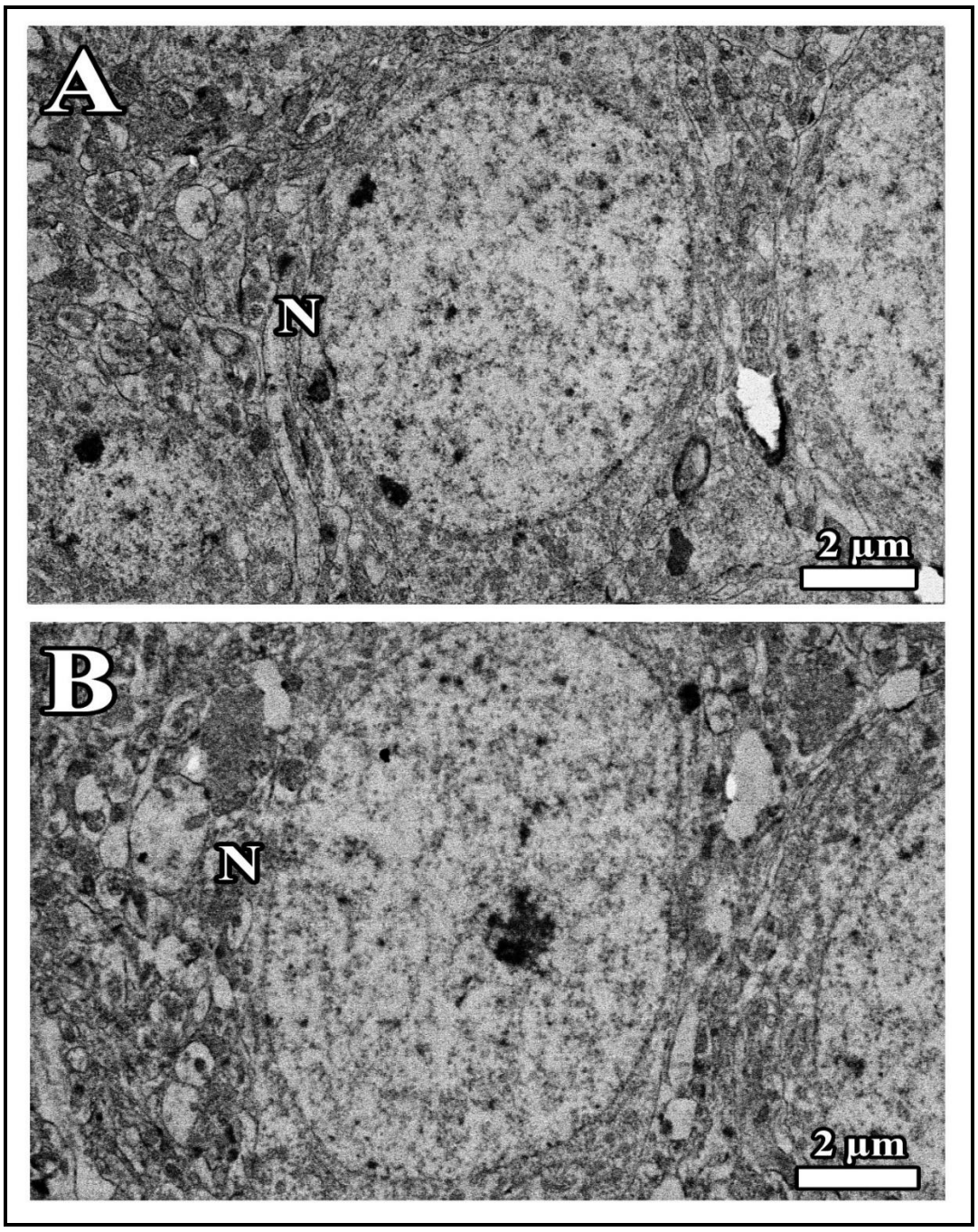

Figure 107. (A, B) Images taken from the CA region of hippocampus belong to the Sham group are seen. A well-preserved nucleus and cytoplasm of a pyramidal cell (N) are observed. (B) Nucleolus of pyramidal cell is a large sized and darkly stained and tissues around the cells look intact

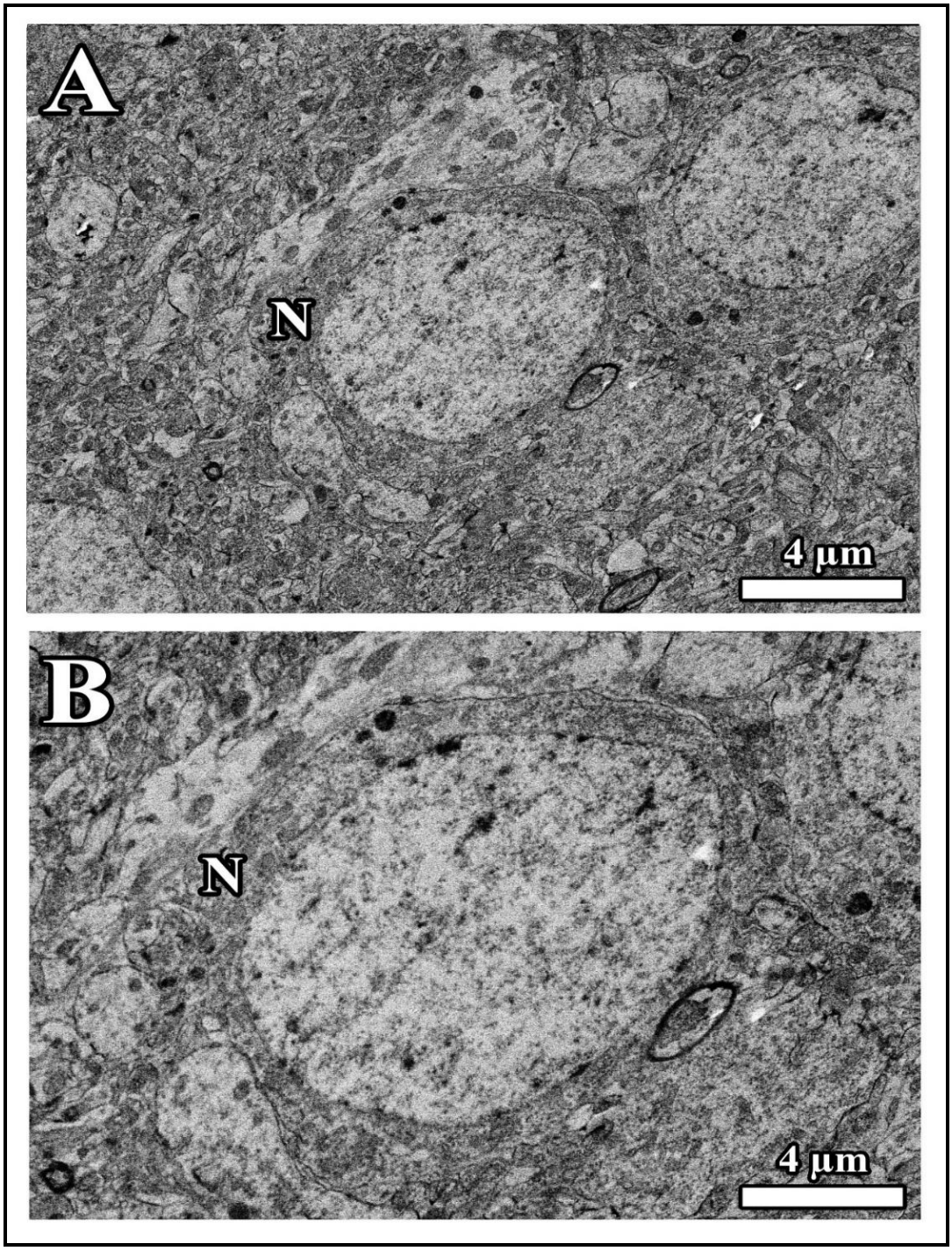

Figure 108. (A, B) Images taken from the CA region of hippocampus belong to the Sham group are seen. A well-preserved nucleus and cytoplasm of pyramidal cells (N) are observed. The border of cells is clearly seen. The distance between cells is normal and cells have a healthy appearance

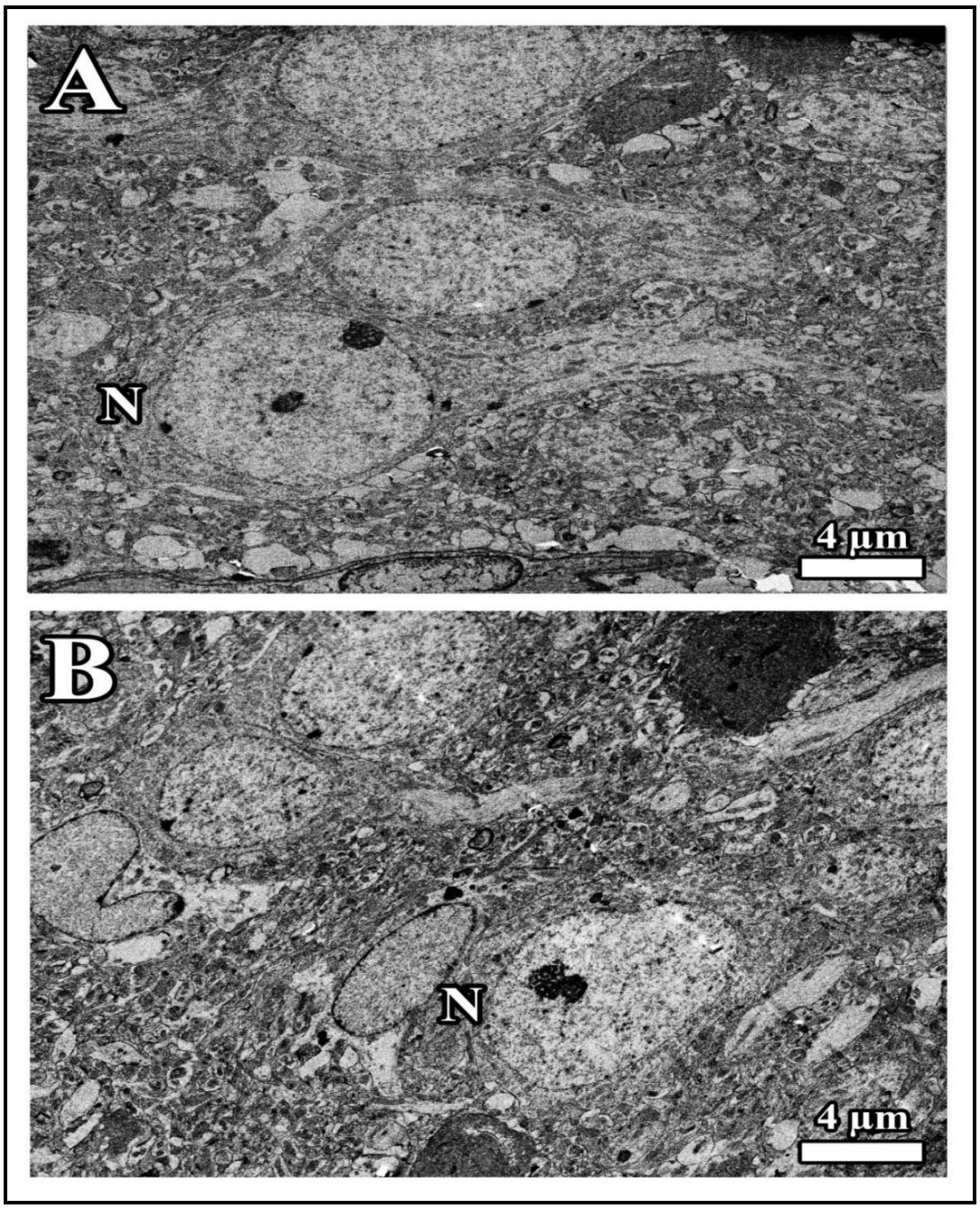

Figure 109. (A, B) Images taken from the CA region of hippocampus belong to the Sham group are seen. Pyramidal cells (N) have oval shape nucleus and conspicuous nucleolus. Axons of pyramidal cells are observed and some of the axons are sectioned in longitudinal. The borders of cells are seen and cells have a healthy appearance. Densely stained cells are also observed these cells might be going to death

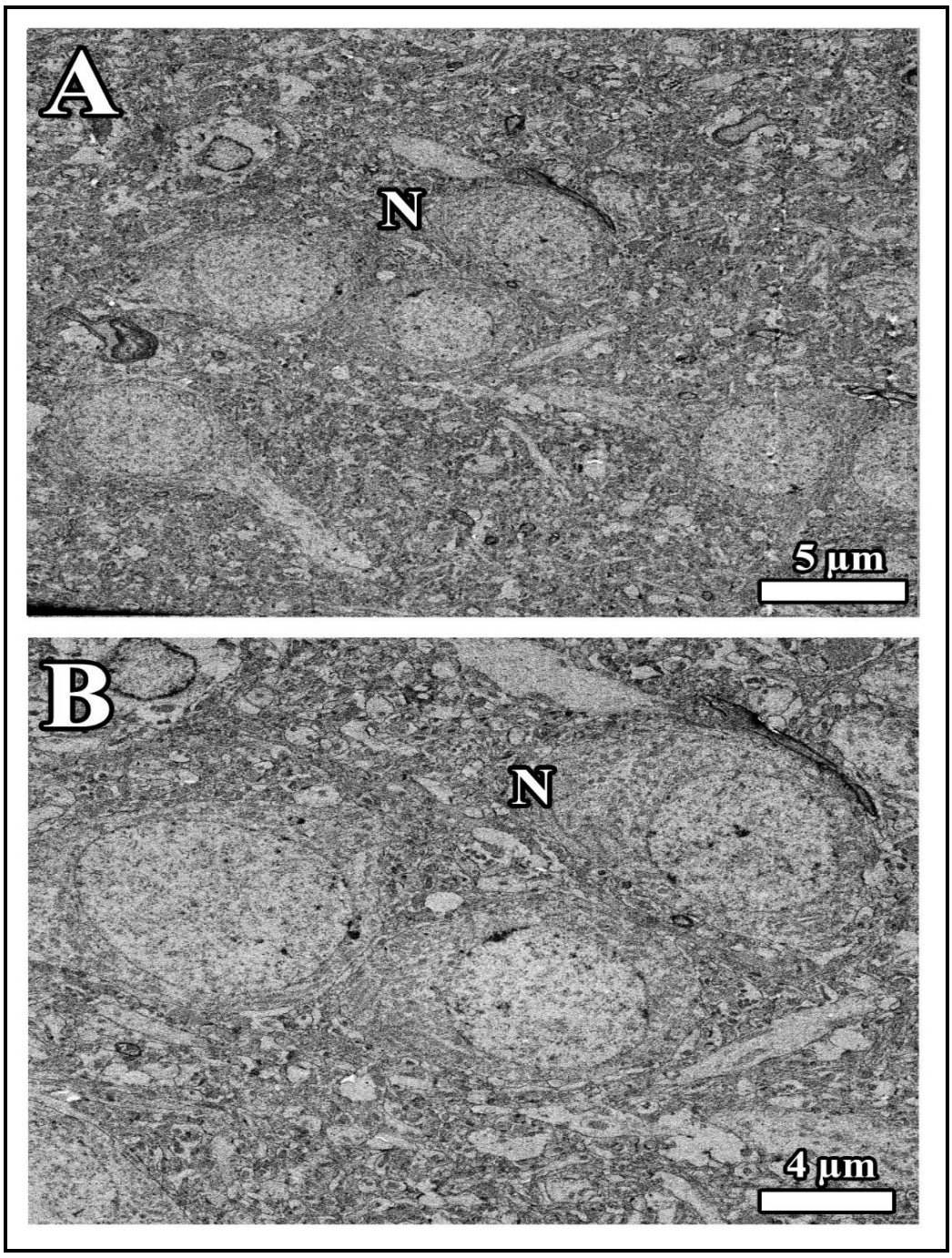

Figure 110. (A, B) Images taken from the CA region of hippocampus belong to the Sham group are seen. Pyramidal cells (N) look healthy and distance between them is normal. Their axons and nucleus can be clearly observed. At the border of pyramidal cells, some of the cross-sectioned of axons are seen

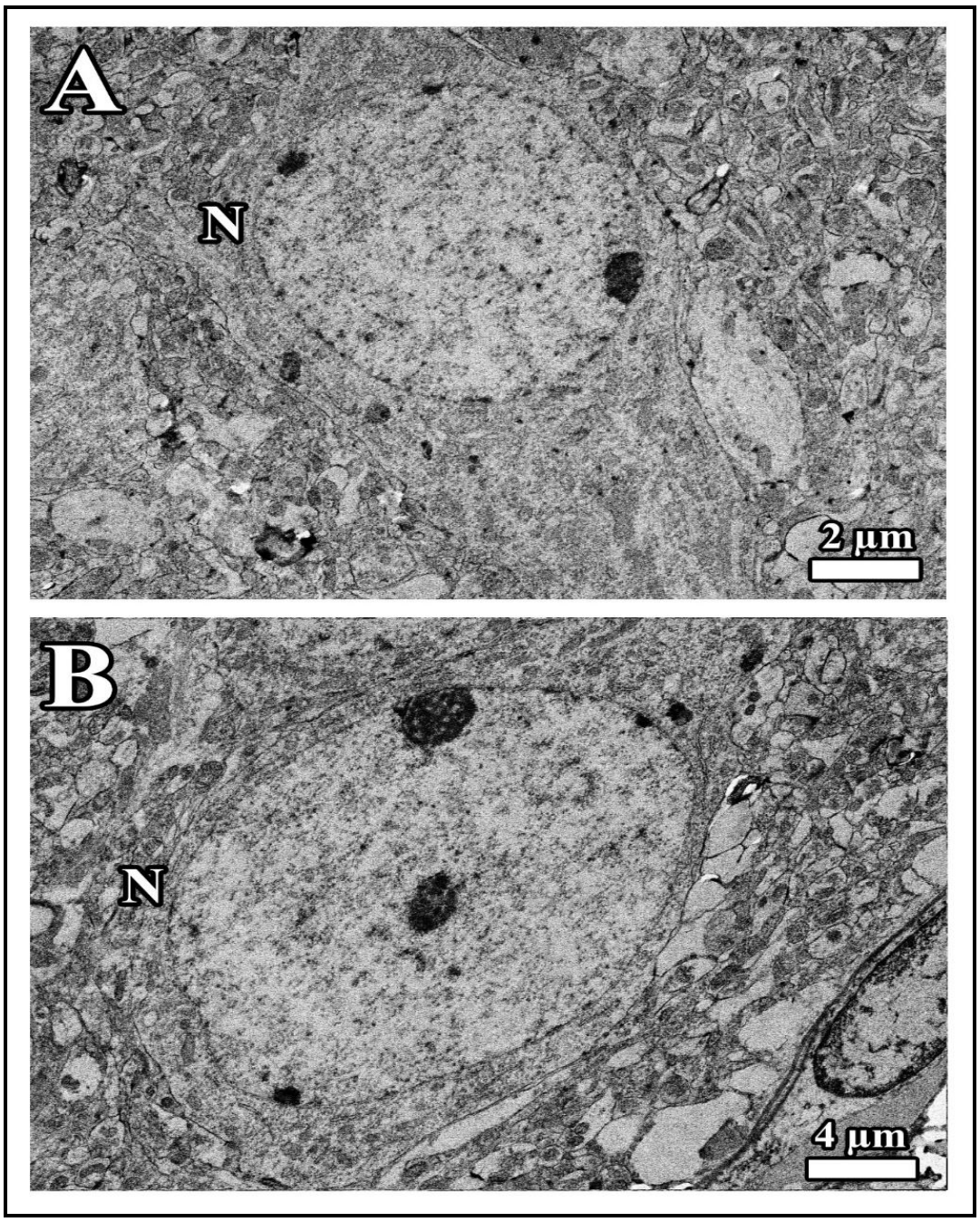

Figure 111. Images taken from the CA region of hippocampus belong to the Sham group are seen. A well-preserved nucleus and cytoplasm of a pyramidal neuron (N) are observed. The density of pyramidal cell cytoplasm is slightly darkly stained and most of organelles look healthy

Regarding the AD group the images taken by EM showed that, the pyramidal cells are oval shaped and healthy, they have slightly dark cytoplasm (**Figure 112, 113, 114, 115 and 116**). Some of neuroglia and myelinated axons are also found.

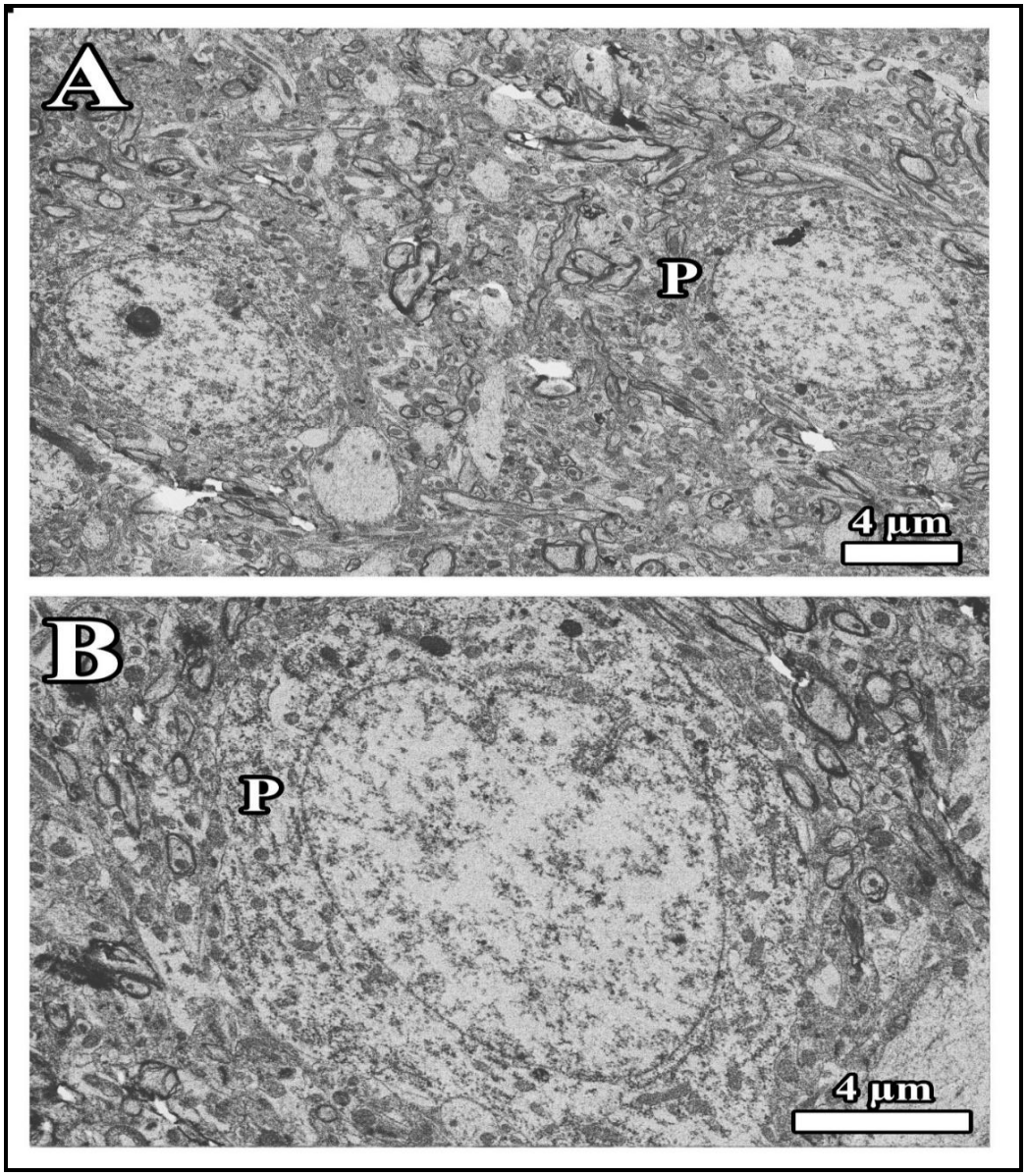

Figure 112. (A, B) Images taken from the CA region of hippocampus belong to the AD group are seen. The cells (P) have pyramidal shape and the border of it and its nucleus is clearly seen. The cytoplasm of neurons is slightly dark and the neurons look healthy and distance between them is also normal. Some cross and longitudinal sections of myelinated axons are also observed

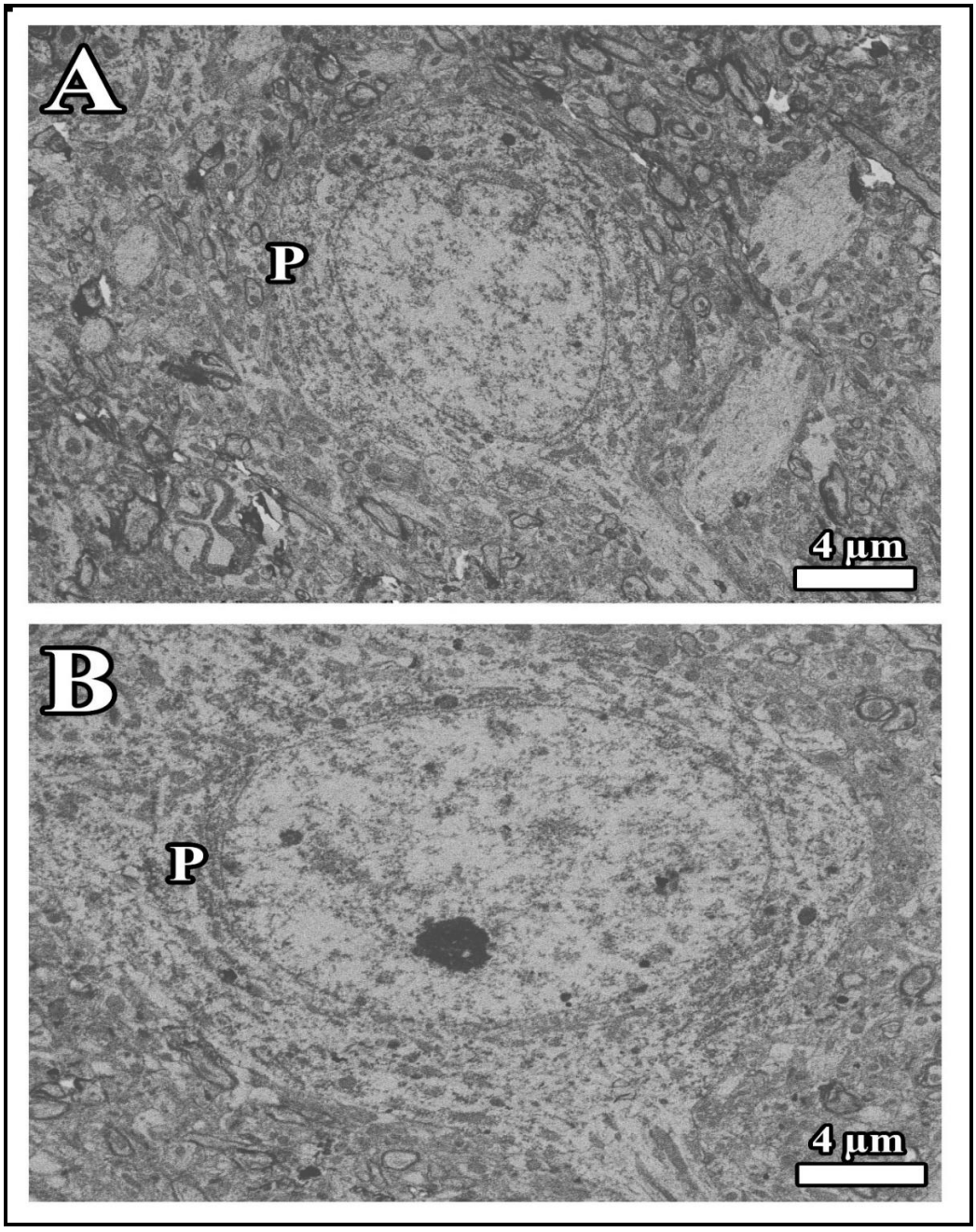

Figure 113. (A, B) Images taken from the CA region of hippocampus belong to the AD group are seen. The cells (P) have pyramidal shape and the border of it and its nucleus is clearly seen, the cytoplasm of neurons is slightly dark and pyramidal neurons look healthy and distance between them is normal. Neurons have a euchromatic nucleus and darkly stained nucleolus. Some cross and longitudinal sections of myelinated axons are also observed

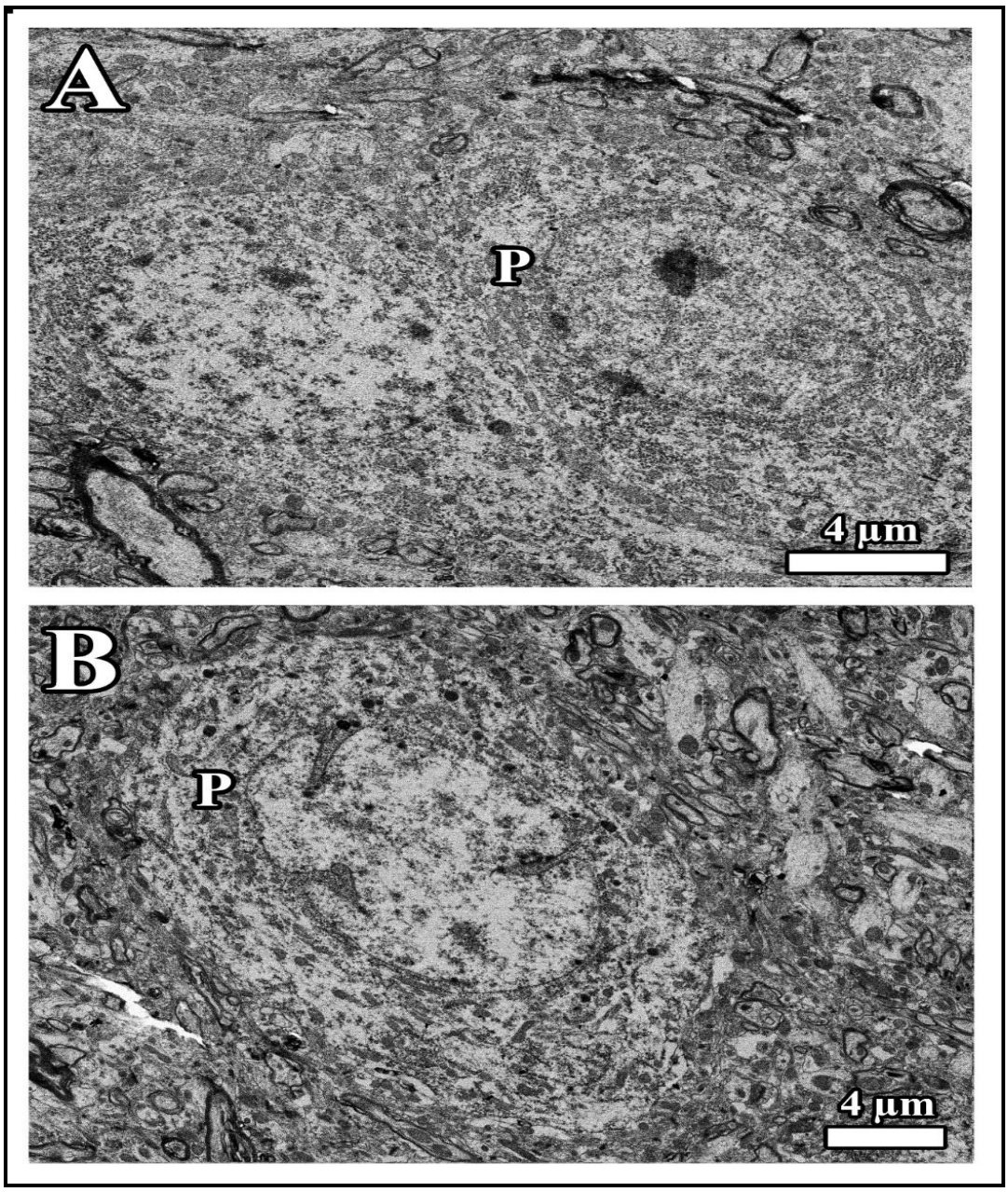

Figure 114. (A, B) Images taken from the CA region of hippocampus belong to the AD group are observed. The neurons (P) have pyramidal shape and the border of them and their nucleus are clearly seen. The cytoplasm of them is slightly darkly stained and these neurons look healthy and distance between them is normal. Some cross and longitudinal sections of myelinated axons are also observed. The diameter of axons are different, some of them have small size but other very large size

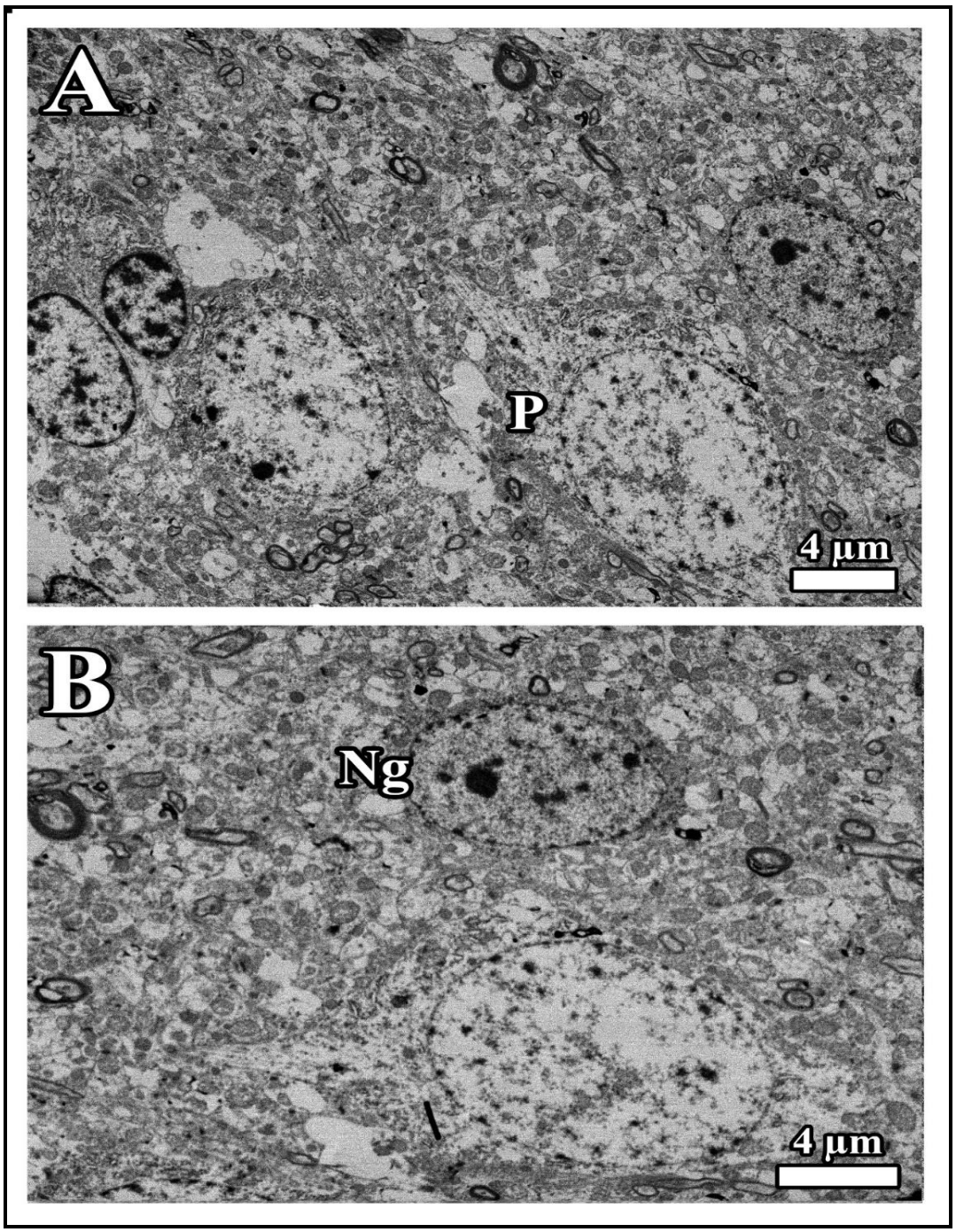

Figure 115. (A, B) Images taken from the brain belong to the AD group are seen. Neuroglia (Ng) has a very well protected nucleus and oval shaped. Nucleolus can be observed in some nucleus. Some cross sections of myelinated axons are also observed. Neurons (P) have oval shaped

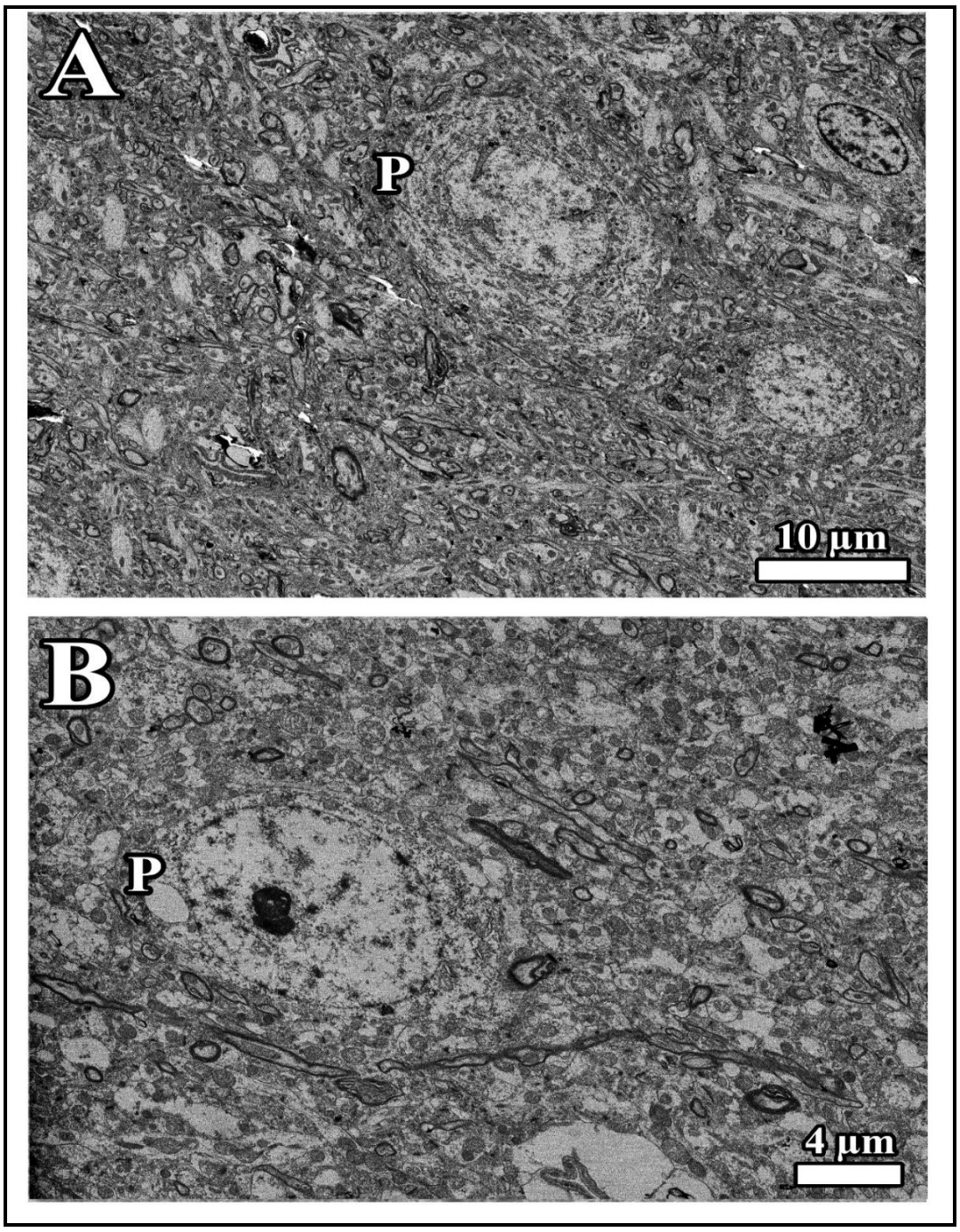

Figure 116. (A, B) Images taken from the brain belong to the AD group are observed. The neurons (P) have a healthy structure and the border of it and its nucleus are clearly seen. Some of neuroglia is also found. Some cross and longitudinal sections of myelinated axons are also observed

Regarding the NS group the images taken by transmission electron microscope (TEM) showed that the healthy pyramidal cells have oval shaped and euchromatic nucleus, but many dark cells are also found in this group (**Figure 117, 118, 119 and 120**). Dark cells have a deformed shape and their nuclei are observed darkly stained, it looks they are non-functional cells.

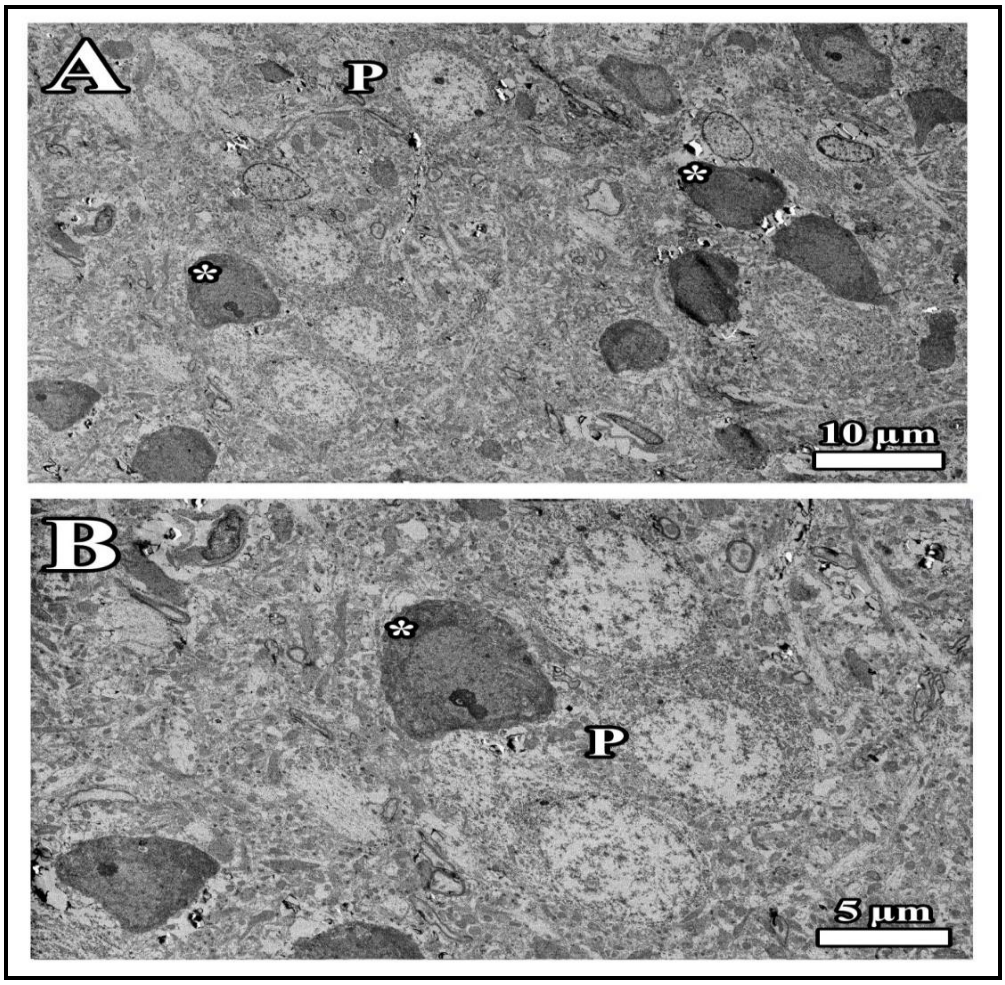

Figure 117. (A, B) Images taken from the pyramidal cell layer of CA region of hippocampus belong to the NS group are seen. Although many of neurons (P), neuroglia and others have a healthy structure and border it can be observed many dark cells (*), neurons and glia. Healthy neurons have oval shape and euchromatic nucleus. Dark cells have a deformed shape and their nucleus and nucleolus are seen even darkly stained. Some cross sections of myelinated axons are also observed

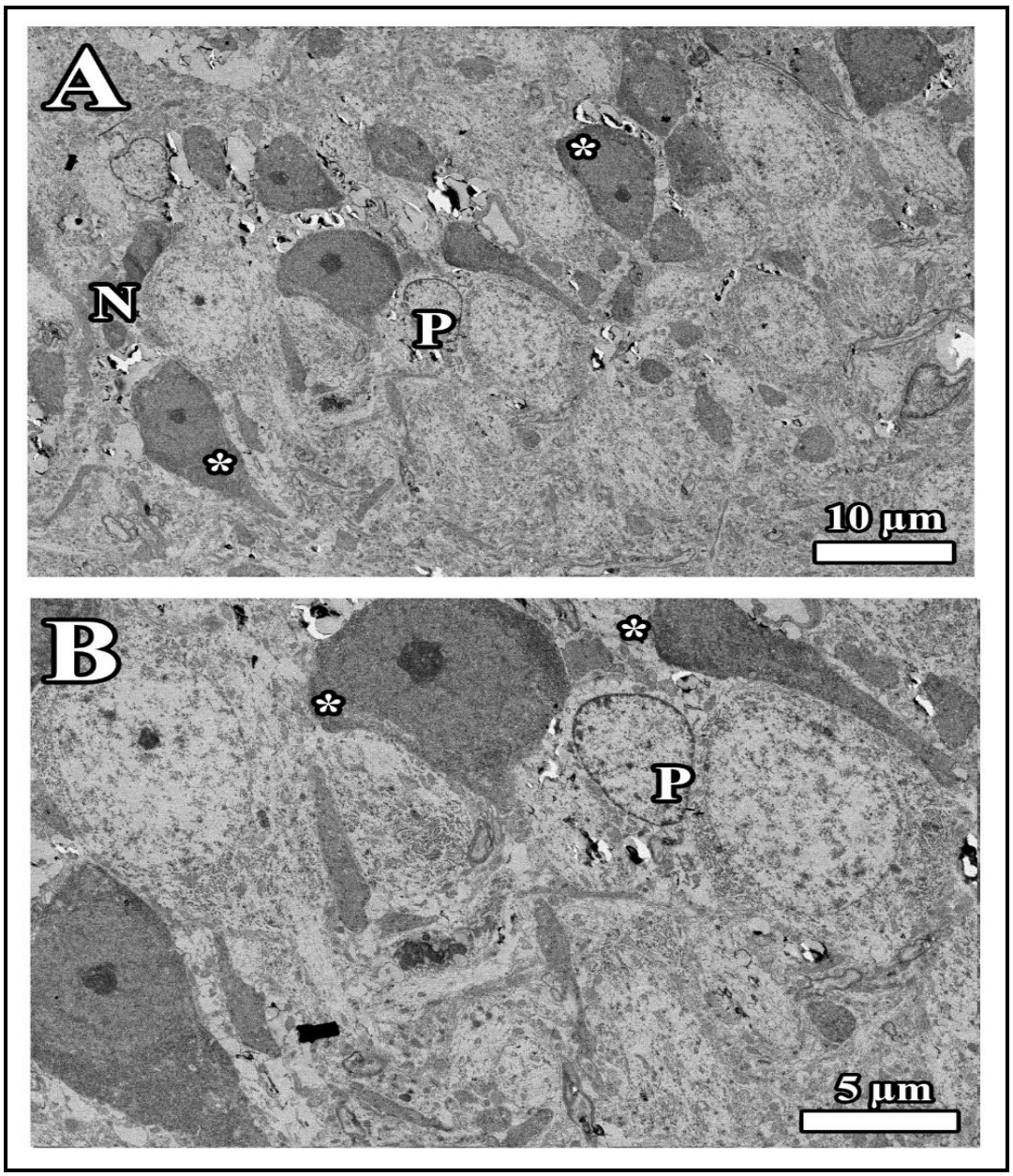

Figure 118. (A, B) Images taken from the pyramidal cell layer of CA region of hippocampus belong to the NS group are seen. A cluster of pyramidal cells (P) in the CA region is observed, although many of neurons and other cells have a healthy structure and border of them seen clearly, but many dark cells (*) are also found in this region. Healthy neurons have oval shape and euchromatic nucleus. Dark cells have a deformed shape and their nucleus and nucleolus are seen even darkly stained

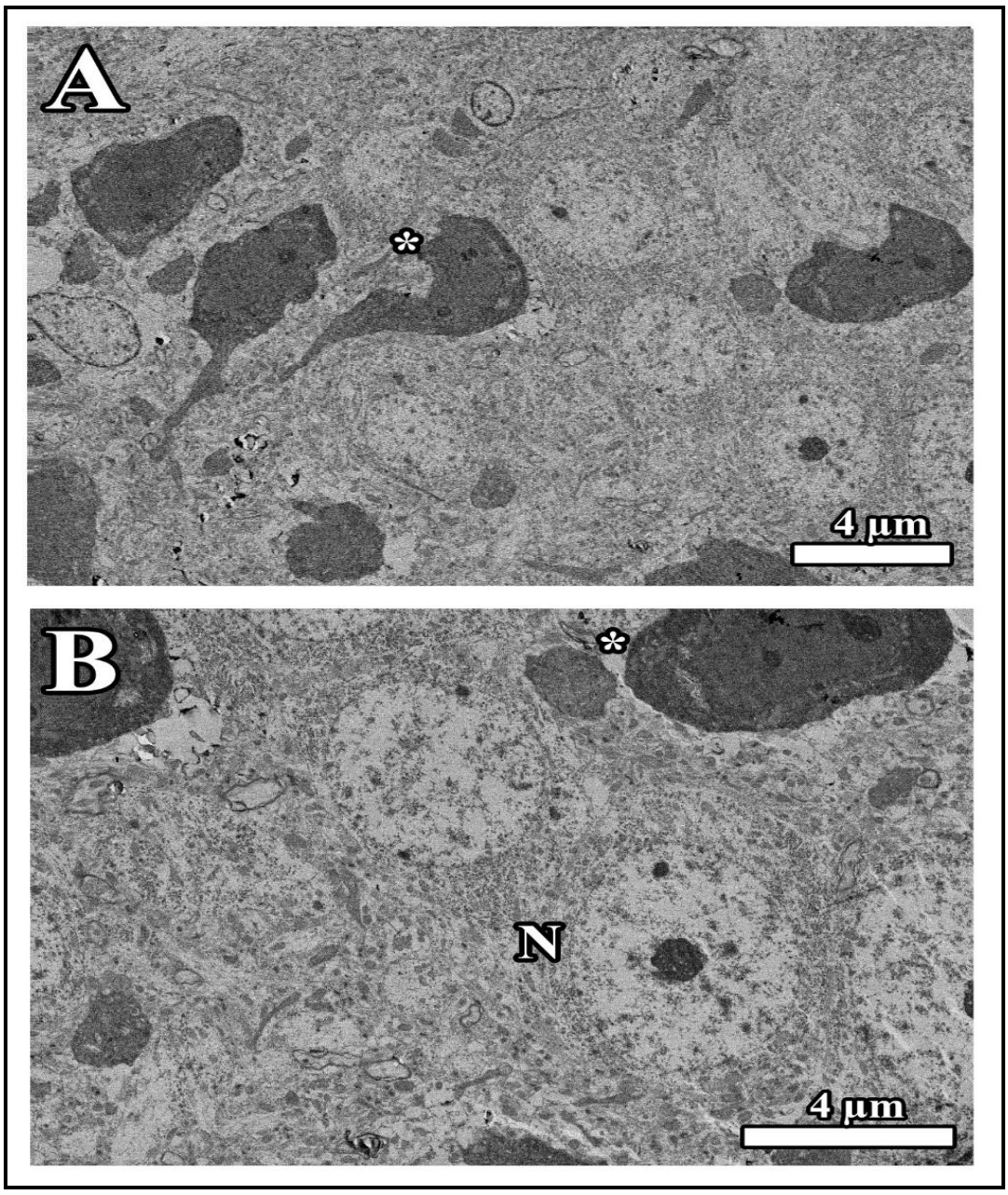

Figure 119. (A, B) Images taken from the pyramidal cell layer of CA region of hippocampus belong to the NS group are seen. A cluster of pyramidal cells (N) in the CA region is observed, although many of neurons and other have a healthy structure and border of them seen clearly, but many dark cells (*) are also found in this region. Healthy neurons have oval shape and euchromatic nucleus. Dark cells have a deformed shape and their nucleus and nucleolus are seen even darkly stained. They looks no-functional cells in this region, it seems to their going to death

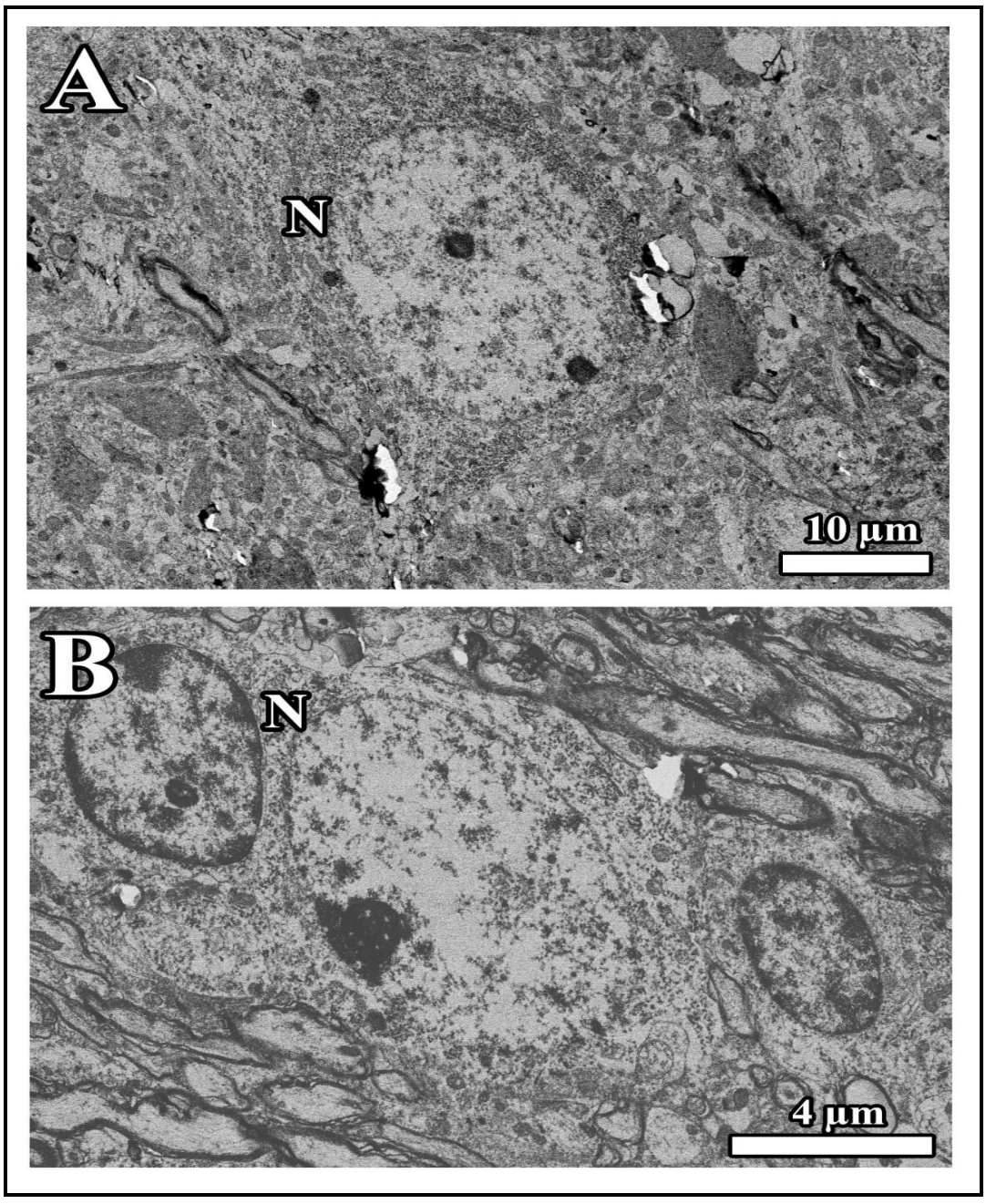

Figure 120. (A, B) Images taken from the pyramidal cell layer of CA region of hippocampus belong to NS group are seen. Pyramidal cells (N) in the CA region are observed; they have a healthy structure and border of them seen clearly. (B) Neurons have oval shape and euchromatic nucleus. Two neuroglias are found around neuron. Some cross and longitudinal sections of myelinated axons are also observed

Regarding the EMF group the images taken by EM showed that many of pyramidal cells in the hippocampus have deformed shaped and most of them is stained darkly (**Figure 121, 122, 123, 124 and 125**). Many degenerated pyramidal neurons with shrinkage perikaryon can be observed, this means they are non functional and going to death.

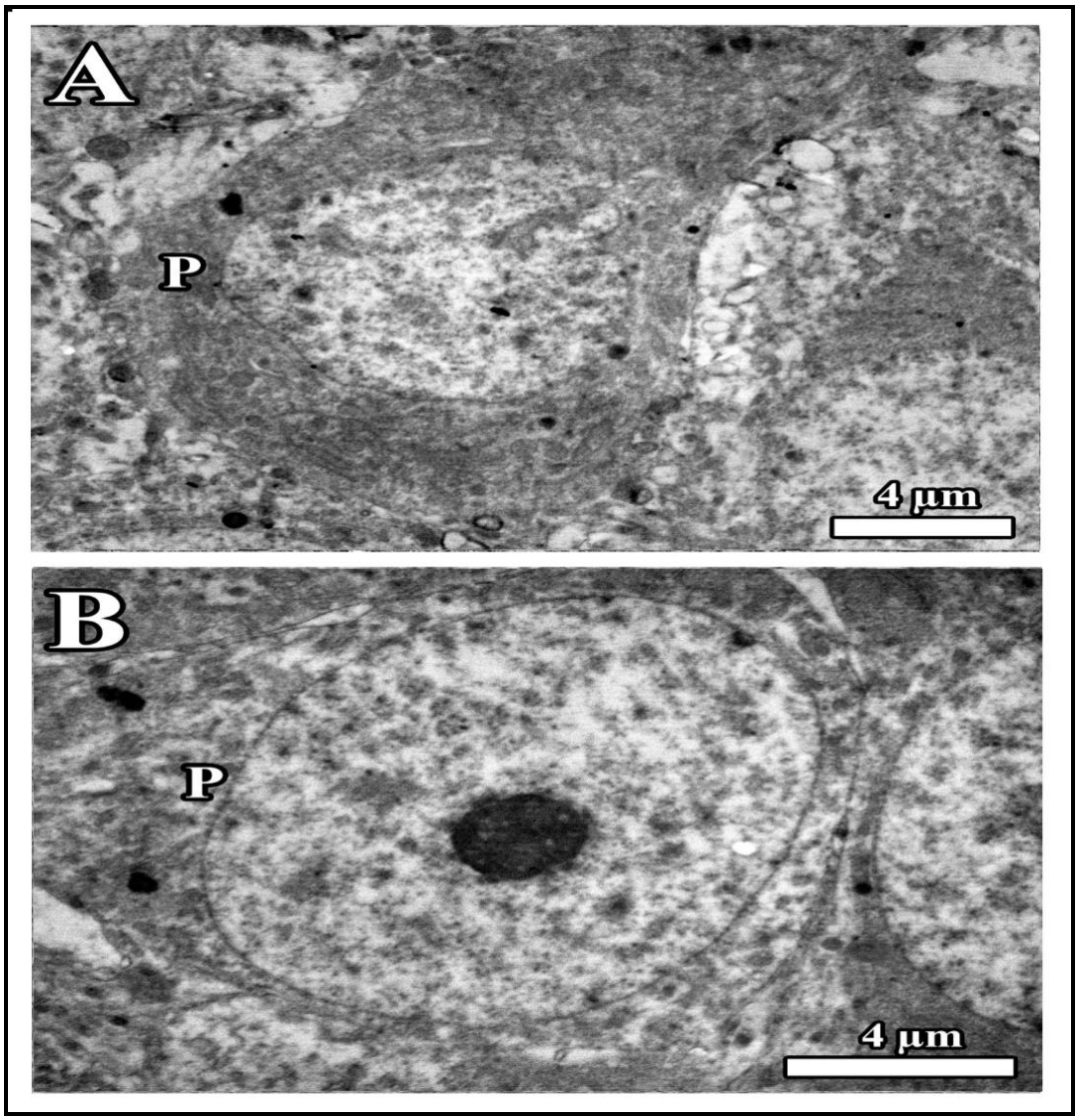

Figure 121. (A, B) Images taken from the CA region of hippocampus belong to the EMF group are seen. The shapes of perikaryon and nucleus are deformed from the pyramidal shaped and the cytoplasm of cells is stained darkly. Distance between neurons (P) is shortening since the size of perikaryon and its nucleus of pyramidal cells are decreased

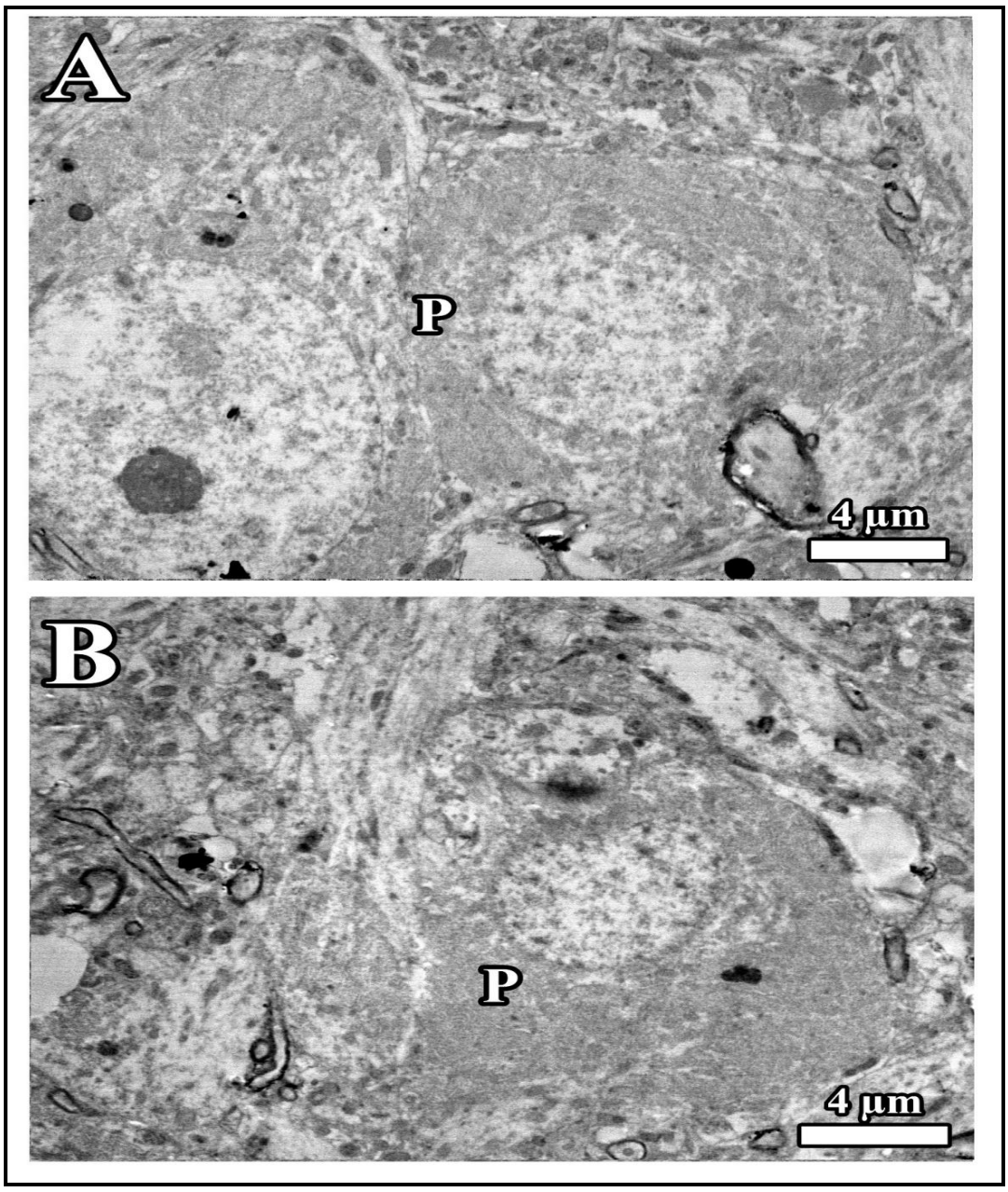

Figure 122. (A, B) Images taken from the CA region of hippocampus belong to the EMF group are seen. General structures of pyramidal cells in this region are observed in abnormal. And cytoplasm of some pyramidal cells (P) was heavily darkly stained and the border of cells and nucleus is also not clear. The sizes of pyramidal cells and their nucleus are decreased. There are many empty spaces around neurons are also seen

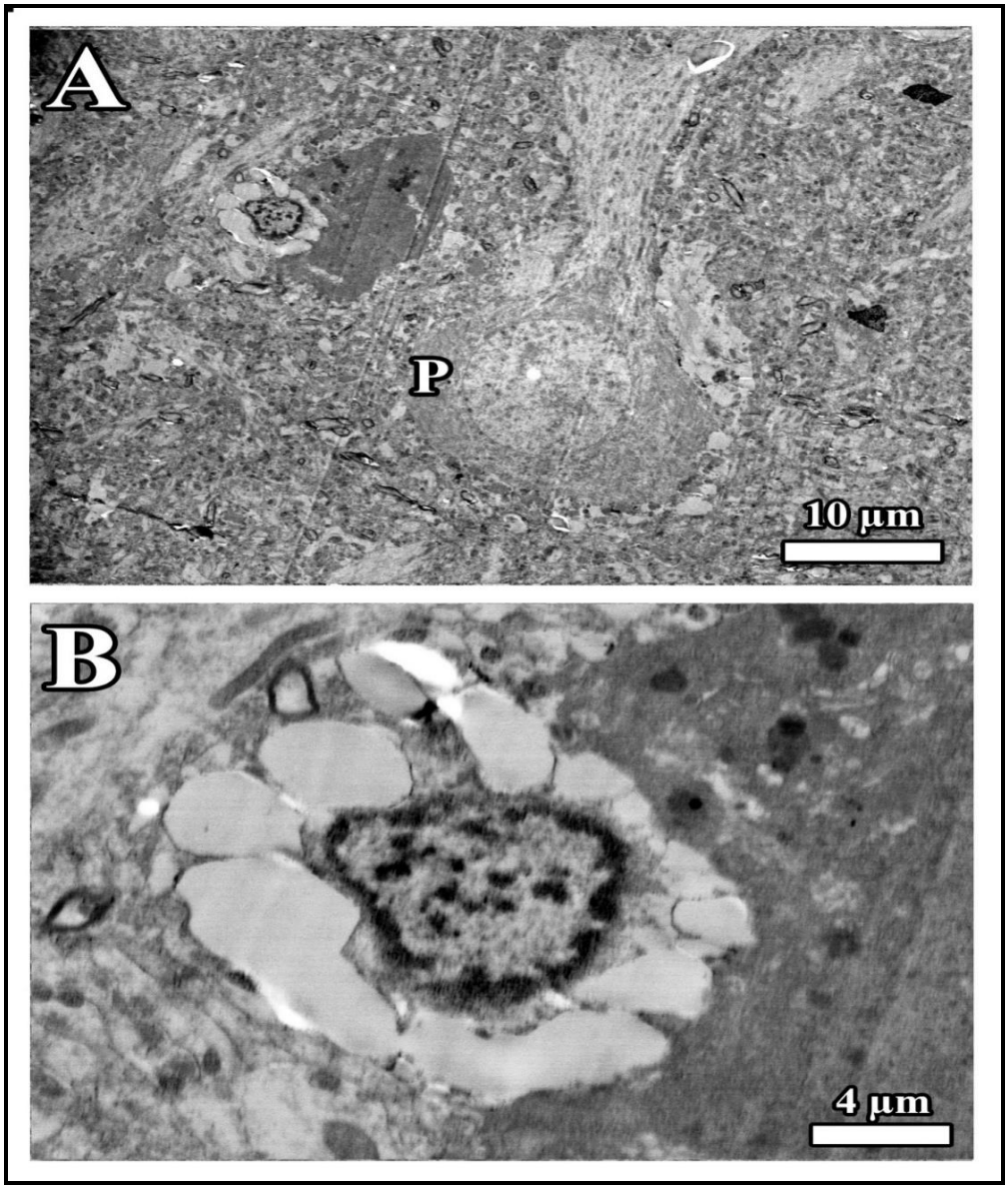

Figure 123. (A, B) Images taken from the CA region of hippocampus belong to the EMF group are seen. Cytoplasm of pyramidal cell was heavily darkly stained and the border of nucleus of them is also not clear. (B) A darkly stained structure and a neuroglia, it might be microglia, are observed. There are many vacuoles in the cytoplasm of microglia; this might be a result of phagocytic function of the cell. (A) Not only the size of perikaryon and its nucleus of pyramidal cell (P) in this region are substantially decreased

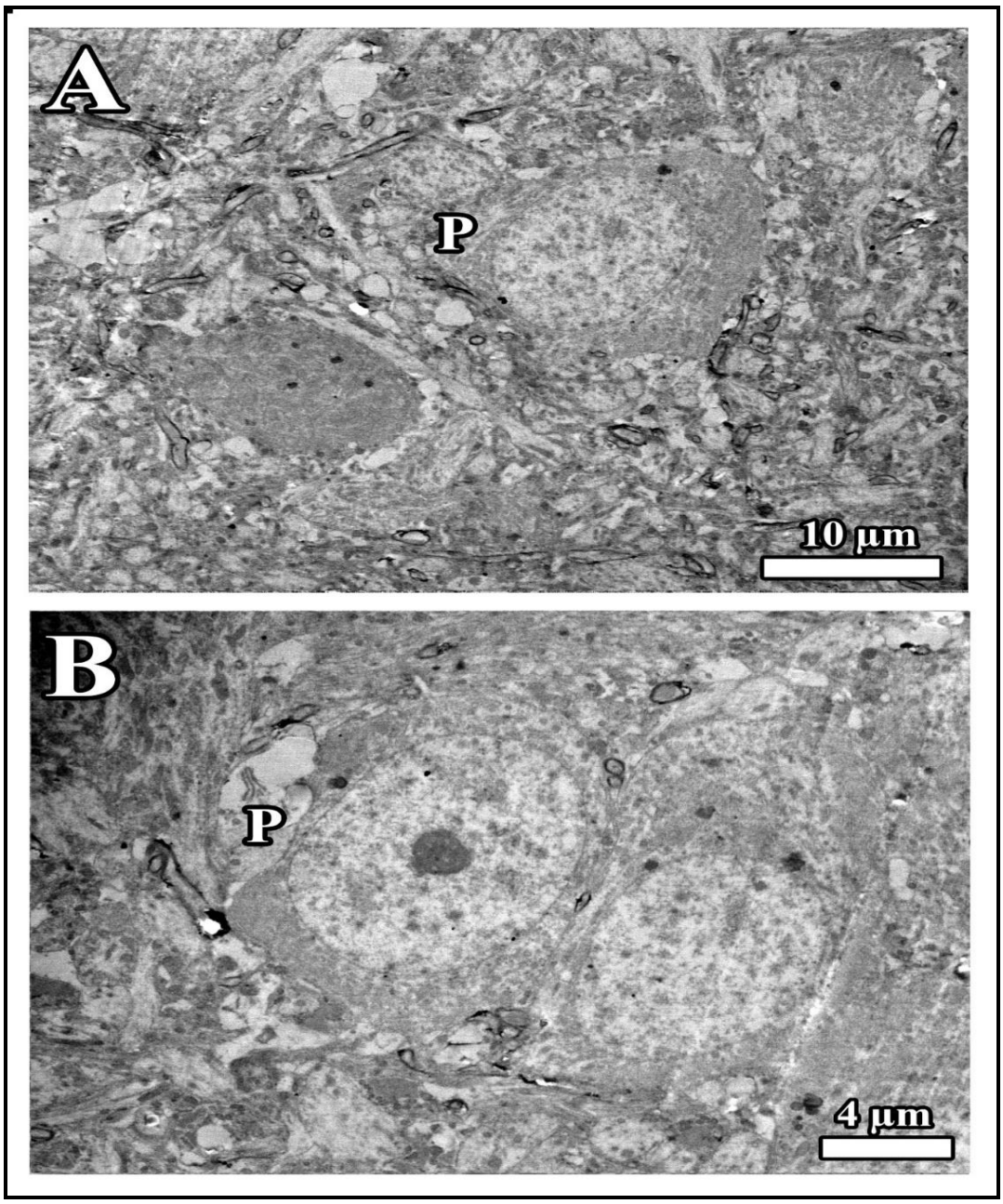

Figure 124. (A, B) Images taken from the CA region of hippocampus belong to the EMF group are seen. The most of pyramidal cells (P) borders is deformed and their cytoplasm is densely stained, it looks that they may lose most of their function, i.e. they are going to death. As seen, the size of cells substantially is decreased

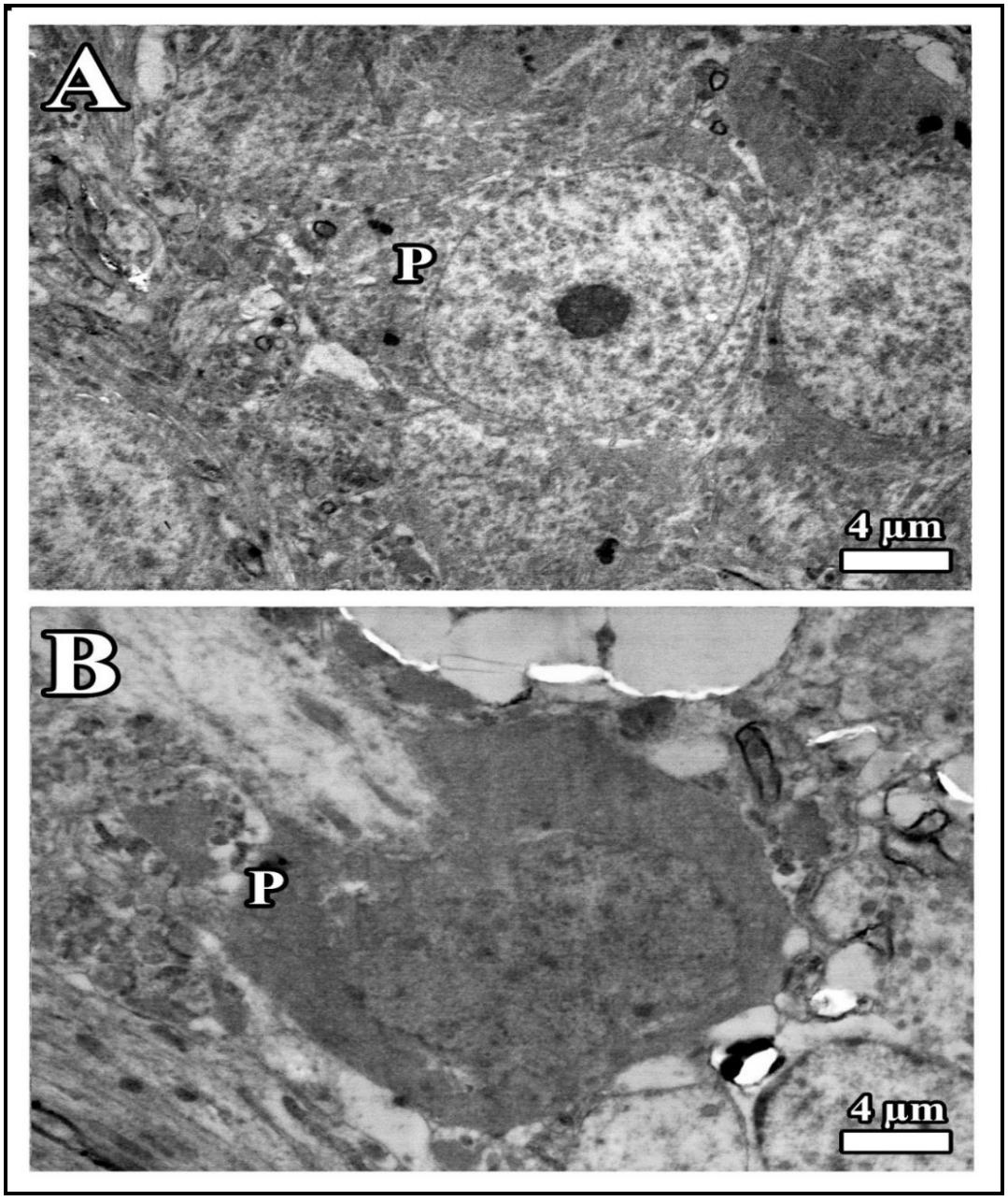

Figure 125. (A, B) Images taken from the CA region of hippocampus belong to the EMF group are seen. General structures of pyramidal cells in this region are observed in abnormal. (A) Two pyramidal neurons are seen, distance between them is very narrow and size of them is decreased. The border of cells cannot be clearly observed; the density of cytoplasm was highly increased. (B) A degenerated pyramidal neuron is seen, it has a shrinkage perikaryon, nucleus of it is also deformed, and axon hillock can be observed. This cell is darkly stained; it looks that this cell may be going to death

Regarding the EMF + AD group the images taken by EM showed that, healthy pyramidal cells have oval shaped nucleus and cytoplasm is slightly darkly stained (**Figure 126, 127, 128, 129, 130, 131, 132 and 133**). Myelinated axons and neuroglia are also observed.

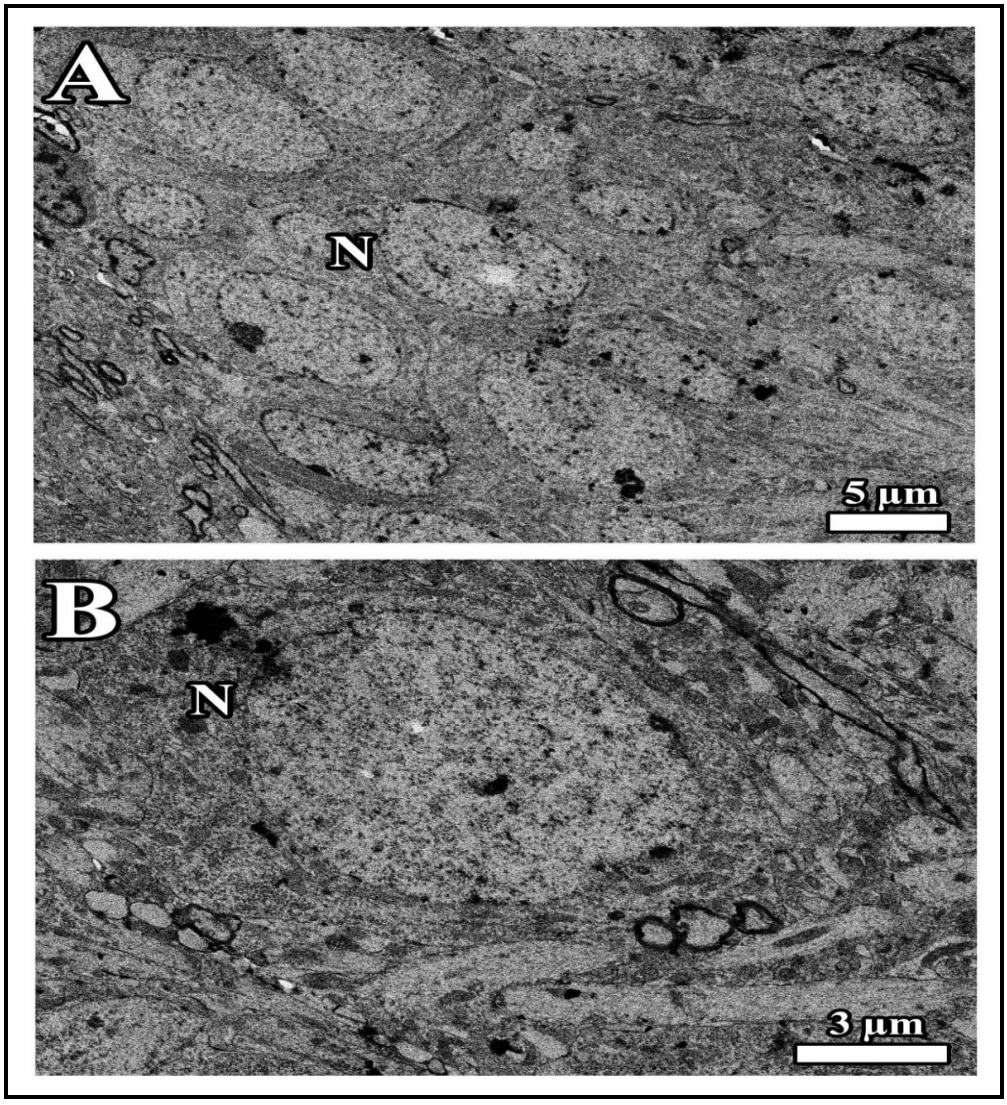

Figure 126. (A, B) Images taken from the CA region of hippocampus belong to EMF + AD group are seen. The cells (N) have pyramidal shape and the border of it and its nucleus is clearly seen, the cytoplasm of neurons is slightly dark and these neurons look healthy and distance between them is normal. Some cross sections of myelinated axons are also observed

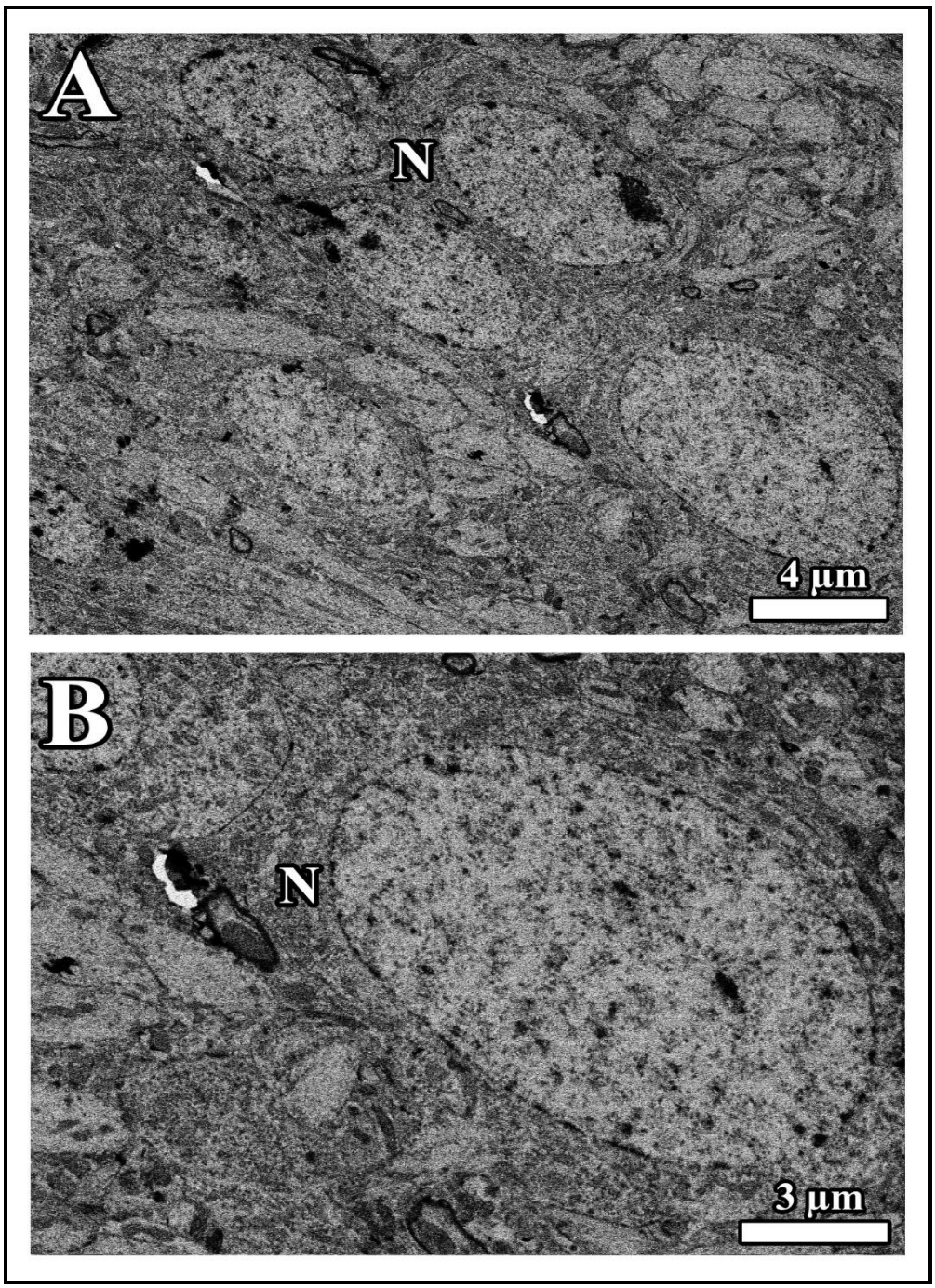

Figure 127. (A, B) Images taken from the CA region of hippocampus belong to the EMF + AD group are seen. The distance between cells is fine. The cells (N) have pyramidal shape and the border of these cells and its nucleus is clearly observed, cross sections of axons around neurons are also seen

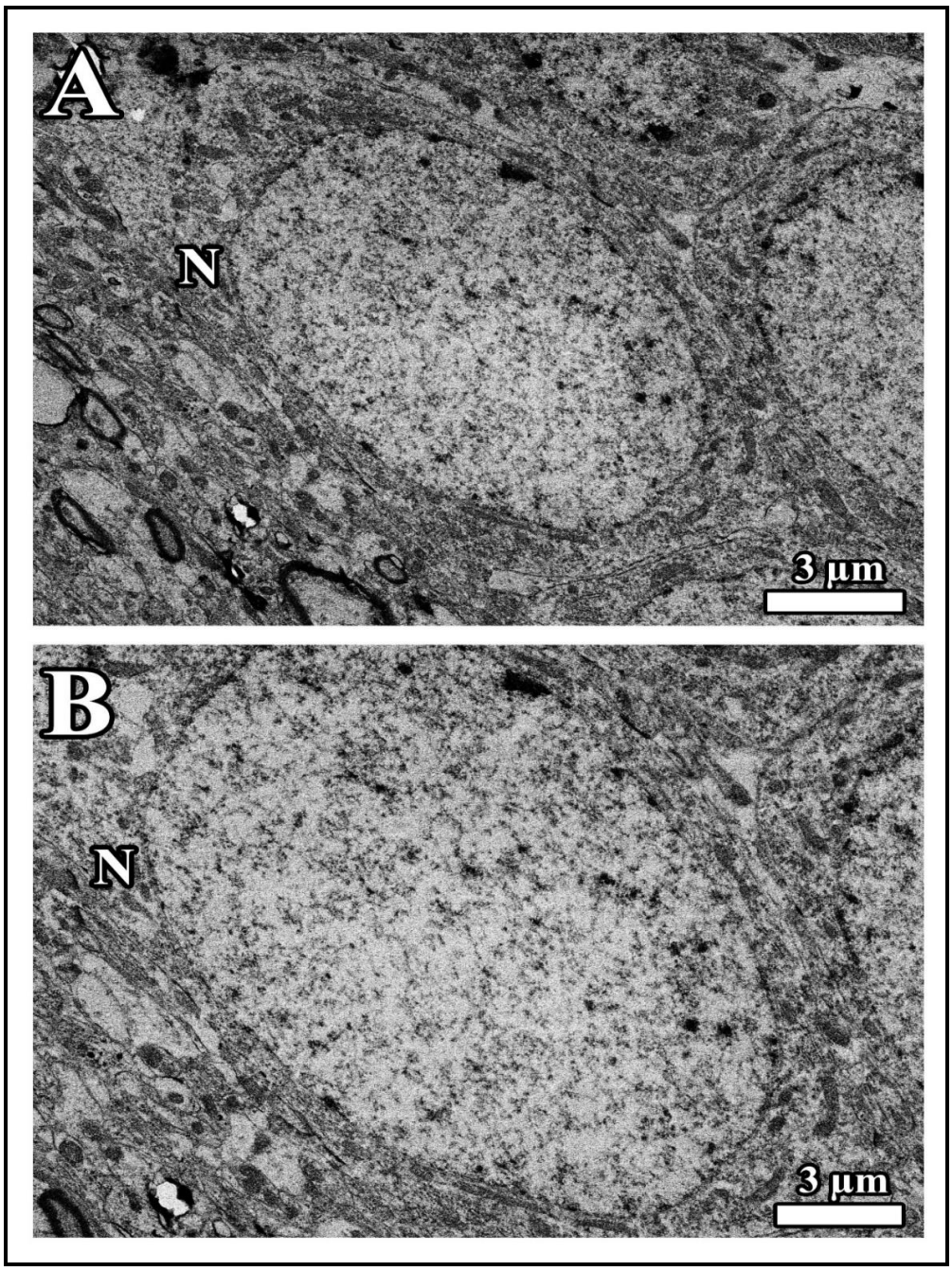

Figure 128. (A, B) Images taken from the CA region of hippocampus belong to the EMF + AD group are seen. The cells (N) have pyramidal shape and the border of cells and their nuclei are clearly observed. The neurons in this region look healthy, and double unit membranes around the nucleus are seen. Around this neuron, some cross sections of myelinated axon are also found

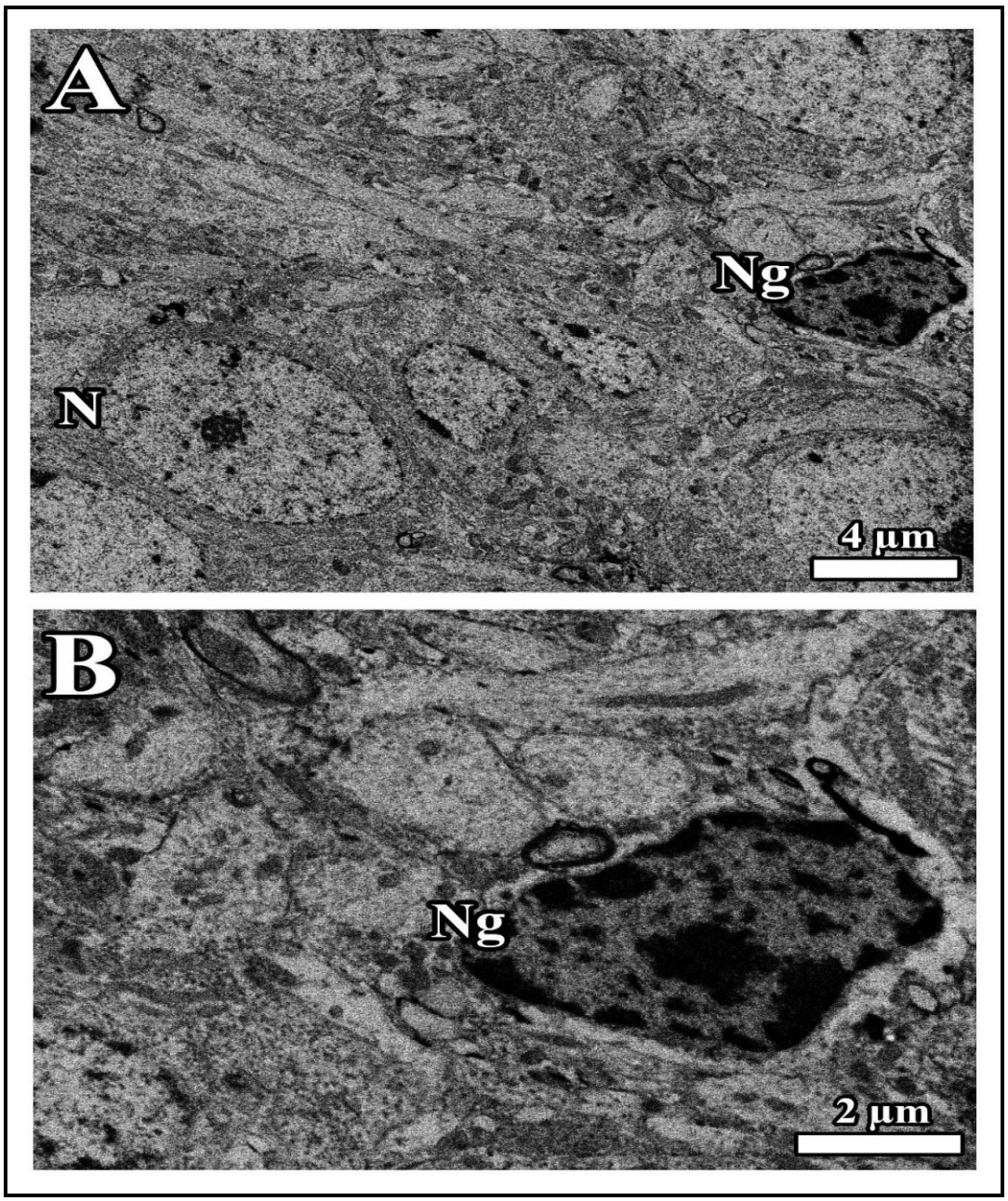

Figure 129. (A, B) Images taken from the CA region of hippocampus belong to the EMF + AD group are seen. The distance between cells is fine. A well-preserved nucleus and cytoplasm of a pyramidal cell (N) are observed. A darkly stained structure and a neuroglia (Ng), it might be microglia, is observed. There are many of spaces are seen around this cell

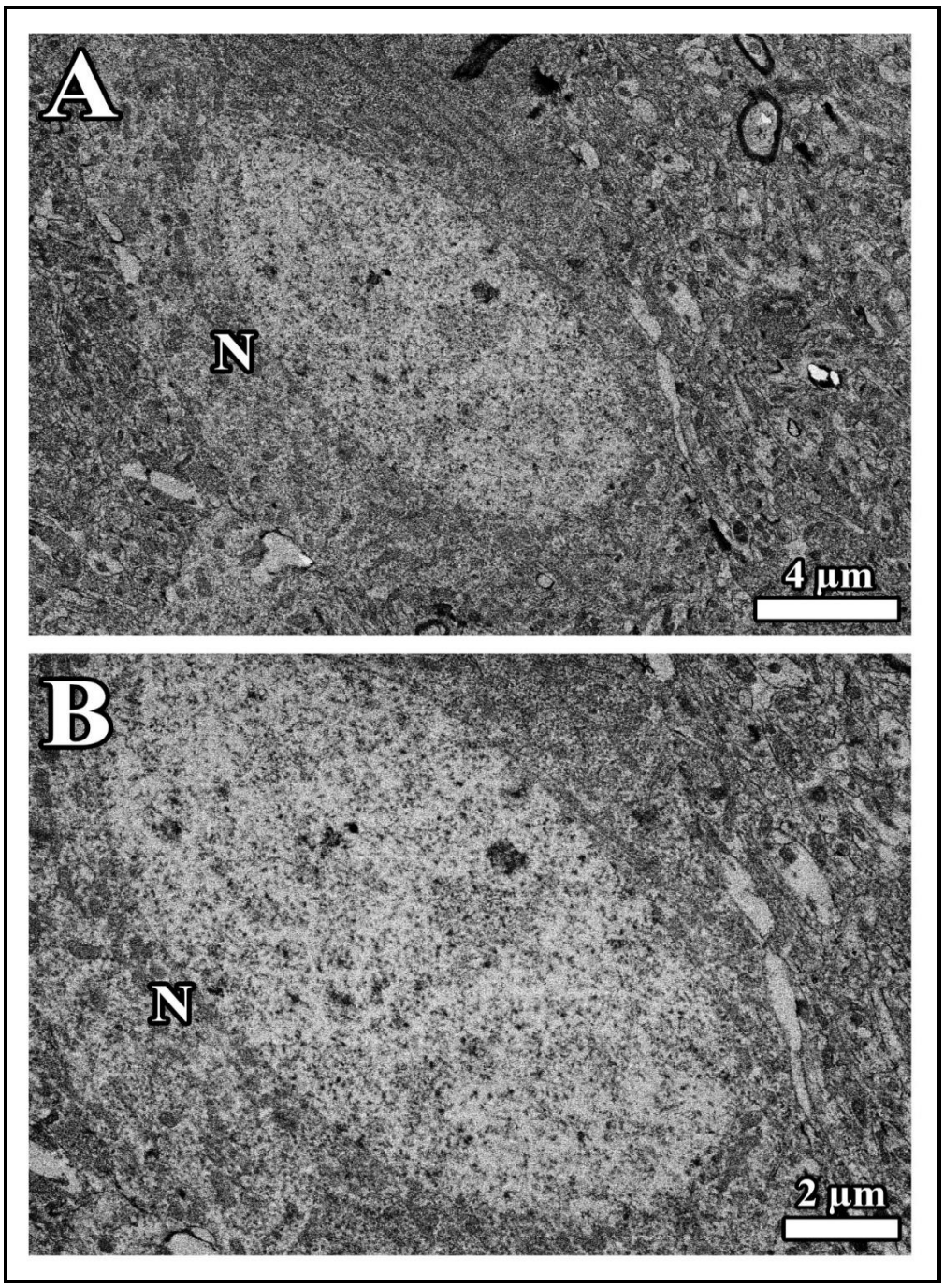

Figure 130. (A, B) Images taken from the CA region of hippocampus belong to the EMF + AD group are seen. A well-preserved nucleus and cytoplasm of a pyramidal cell (N) are observed. Circular and cross sections of myelinated axon are seen

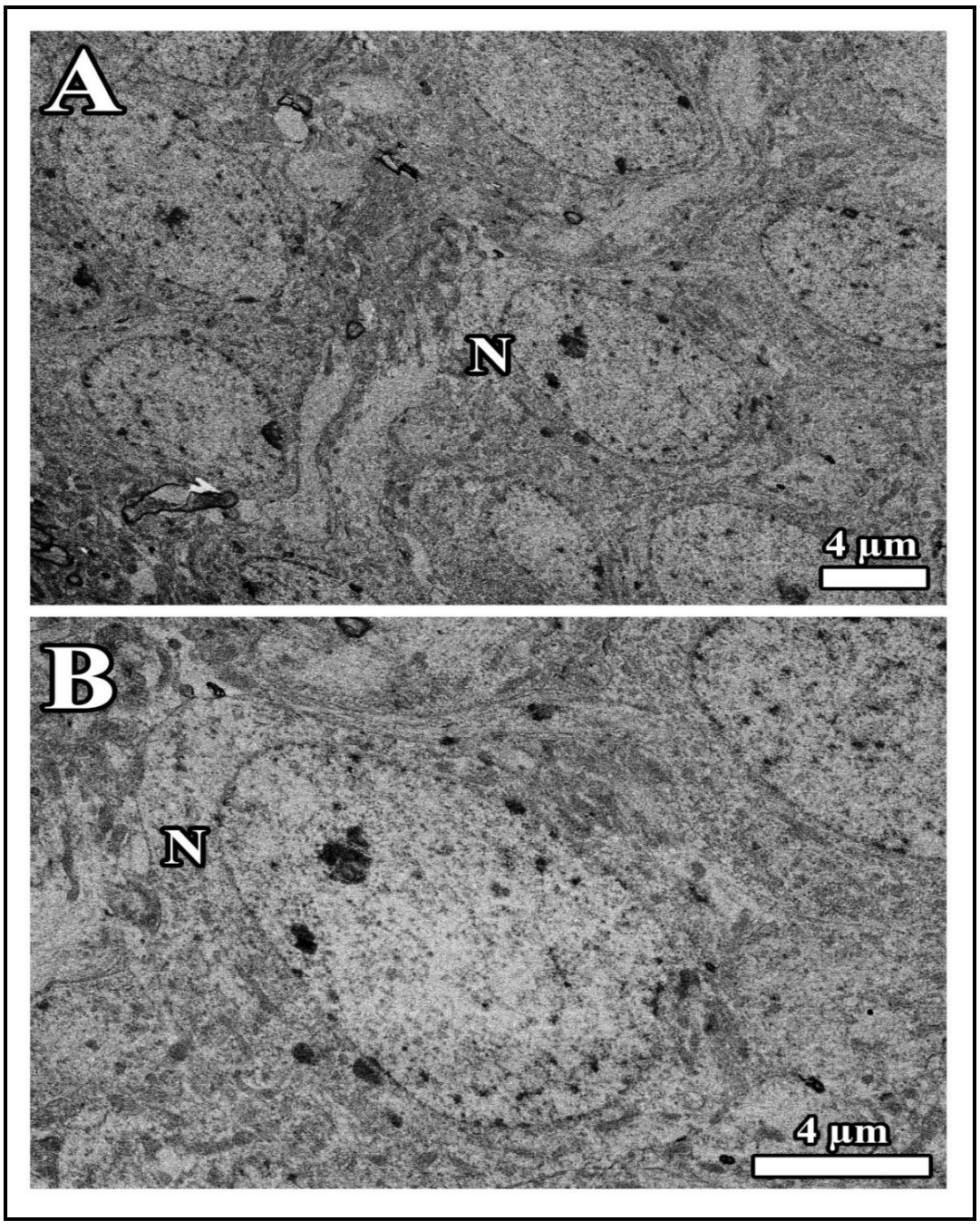

Figure 131. (A, B) Images taken from the CA region of hippocampus belong to the EMF + AD group are seen. The cells (N) have pyramidal shape and the border of these cells and their nuclei are clearly observed, the cytoplasm of neurons is slightly darkly stained and pyramidal neurons look healthy and distance between them is also normal. Some cross sections of myelinated axons are also seen

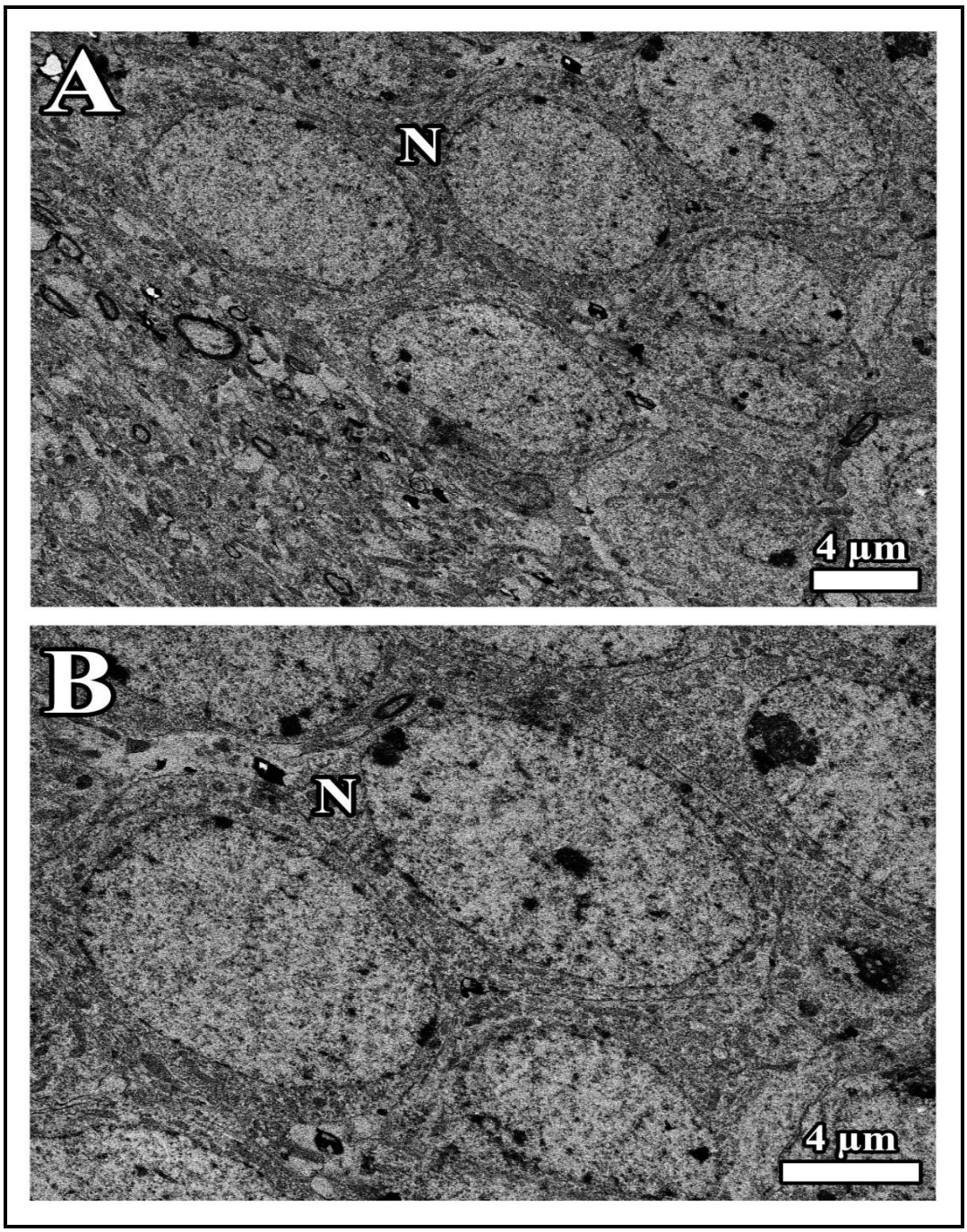

Figure 132. (A, B) Images taken from the CA region of hippocampus belong to the EMF + AD group are seen. The cells (N) have pyramidal shape and the border of these cells and their nuclei are clearly seen, the cytoplasm of neurons is slightly dark and these neurons look healthy and distance between them is normal. (A) Some cross sections of myelinated axons are also observed

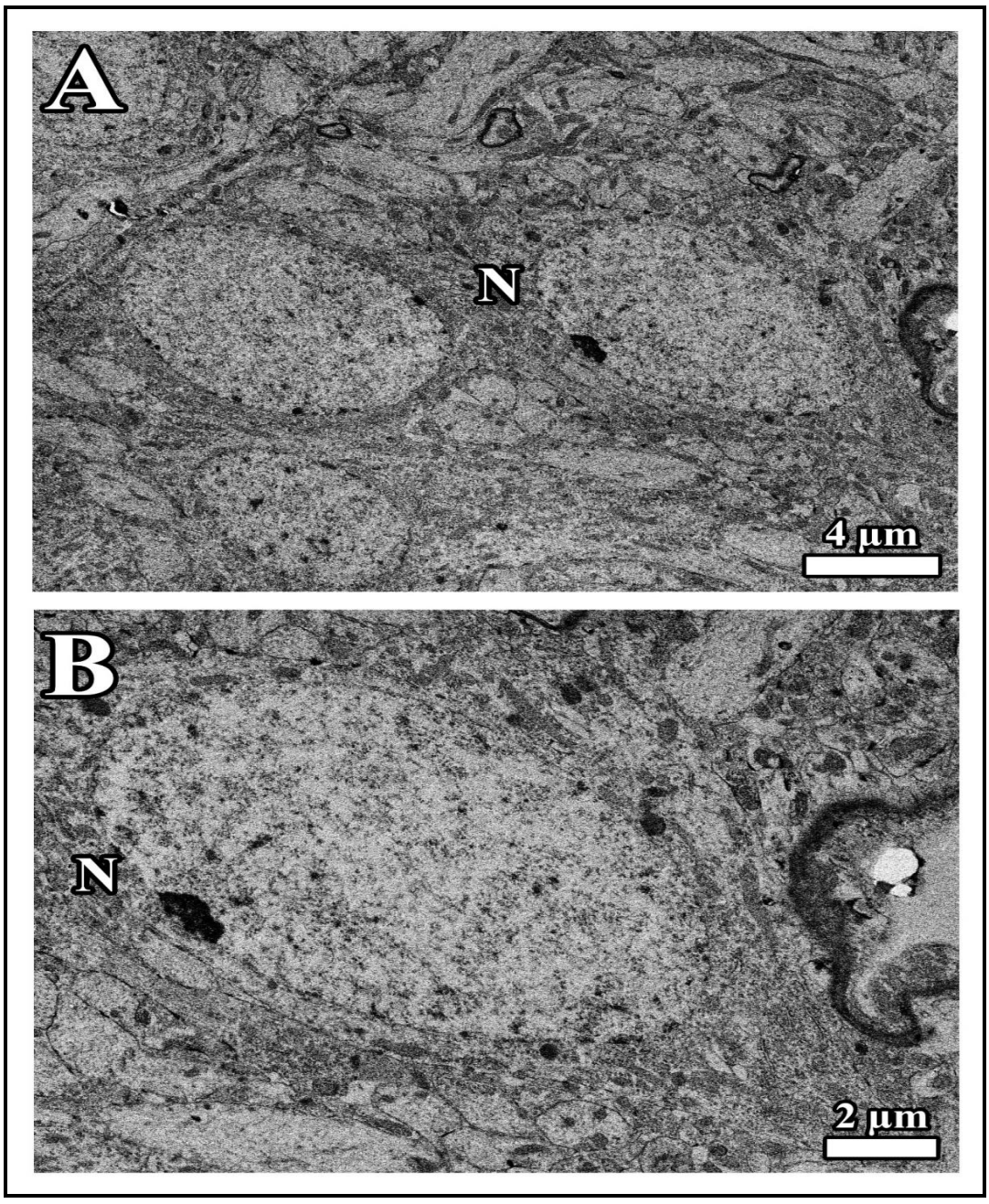

Figure 133. (A, B) Images taken from the CA region of hippocampus belong to the EMF + AD group is seen. The cells (N) have pyramidal shape and the border of these cells and their nuclei are clearly observed, the cytoplasm of neurons is slightly dark and these neurons look healthy and distance between them looks normal. Some cross sections of myelinated axons are also observed

Concerning the EMF+NS group, the images taken by EM showed that, healthy pyramidal cells have oval shaped and the cytoplasm is slightly dense (**Figure 134, 135, 136 and 137**). Myelinated axons and neuroglia are also observed healthy. Vessels are seen in normal.

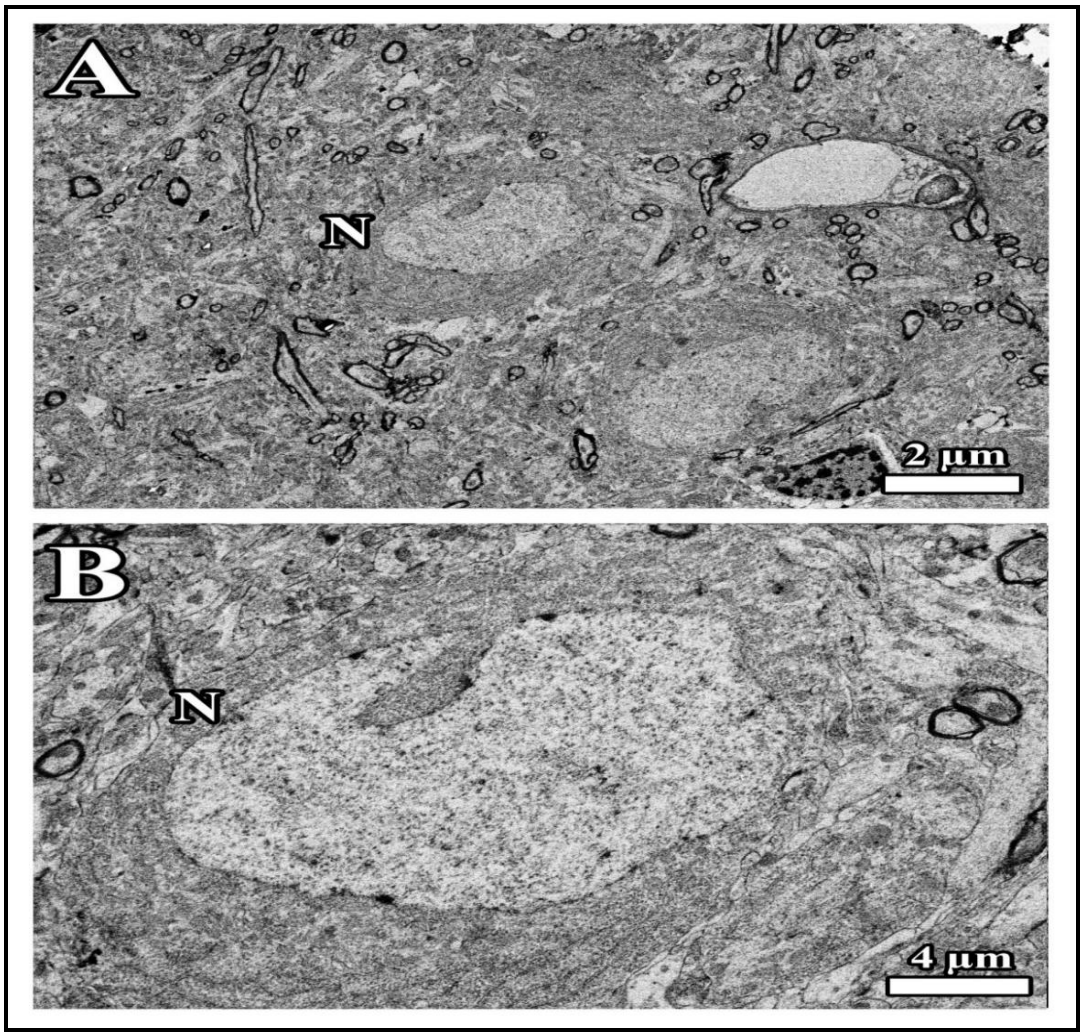

Figure 134. (A, B) Images taken from the CA region of hippocampus belong to the EMF + NS group are seen. Border of pyramidal cells (N) and nucleus can be seen clearly. These neurons look healthy since all of the organelles are intact. Some cross and longitudinal sections of myelinated axons are observed around neurons. (A) A cross section of microglia is seen, there are many vacuoles observed around it. Vessel in this region looks normal and there is no space betweenits wall and surrounding tissues

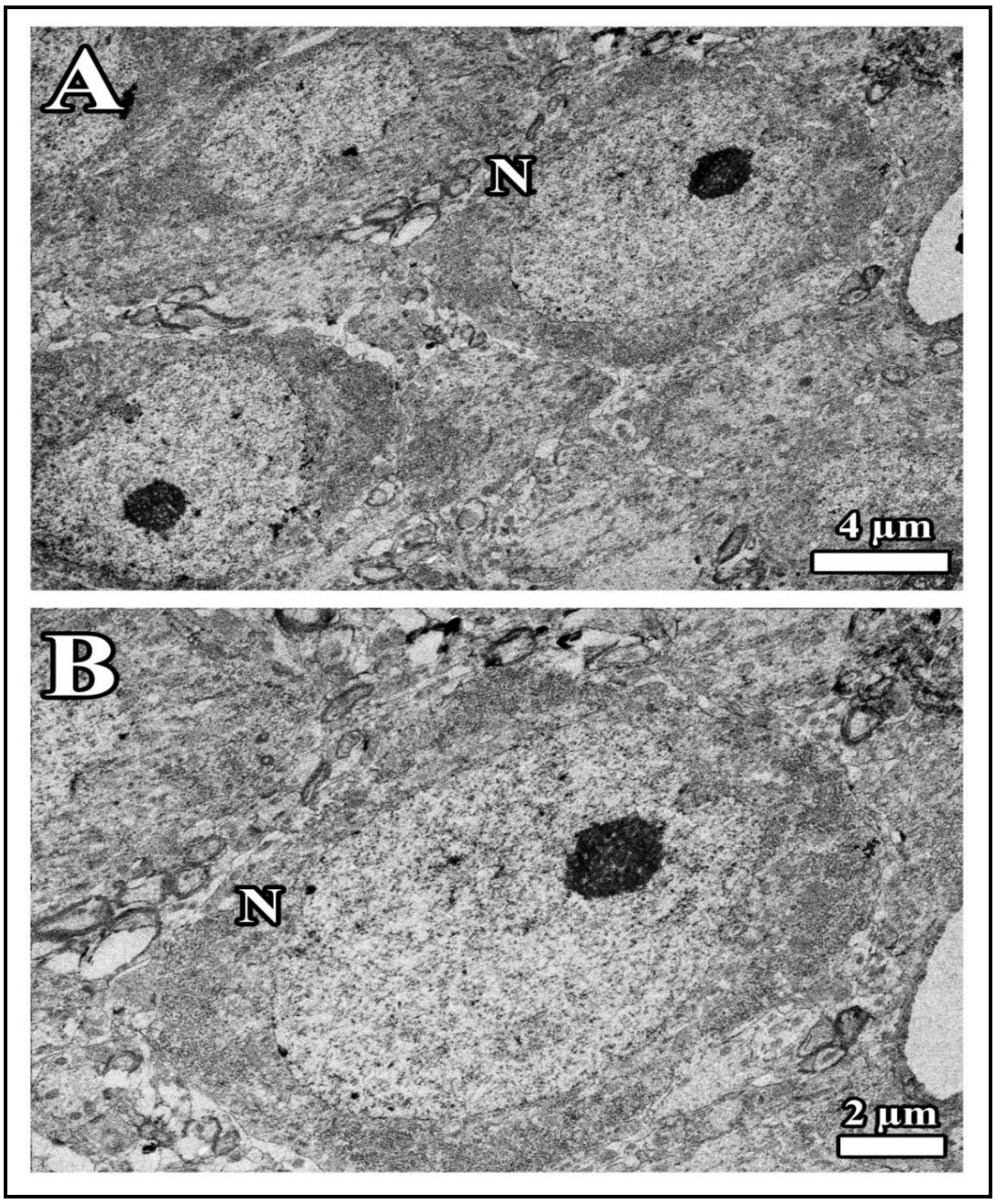

Figure 135. (A, B) Images taken from the CA region of hippocampus belong to the EMF + NS group are seen. A well-preserved nucleus and cytoplasm of a pyramidal cell (N) are observed. The cytoplasm density of pyramidal cell is slightly darkly stained. Around these neurons, some circular and longitudinal sections of myelinated axon are seen. The distance between neurons is fine and many of cross-sectioned axons are delineated the border of perikaryon. A small part of vessel is seen.

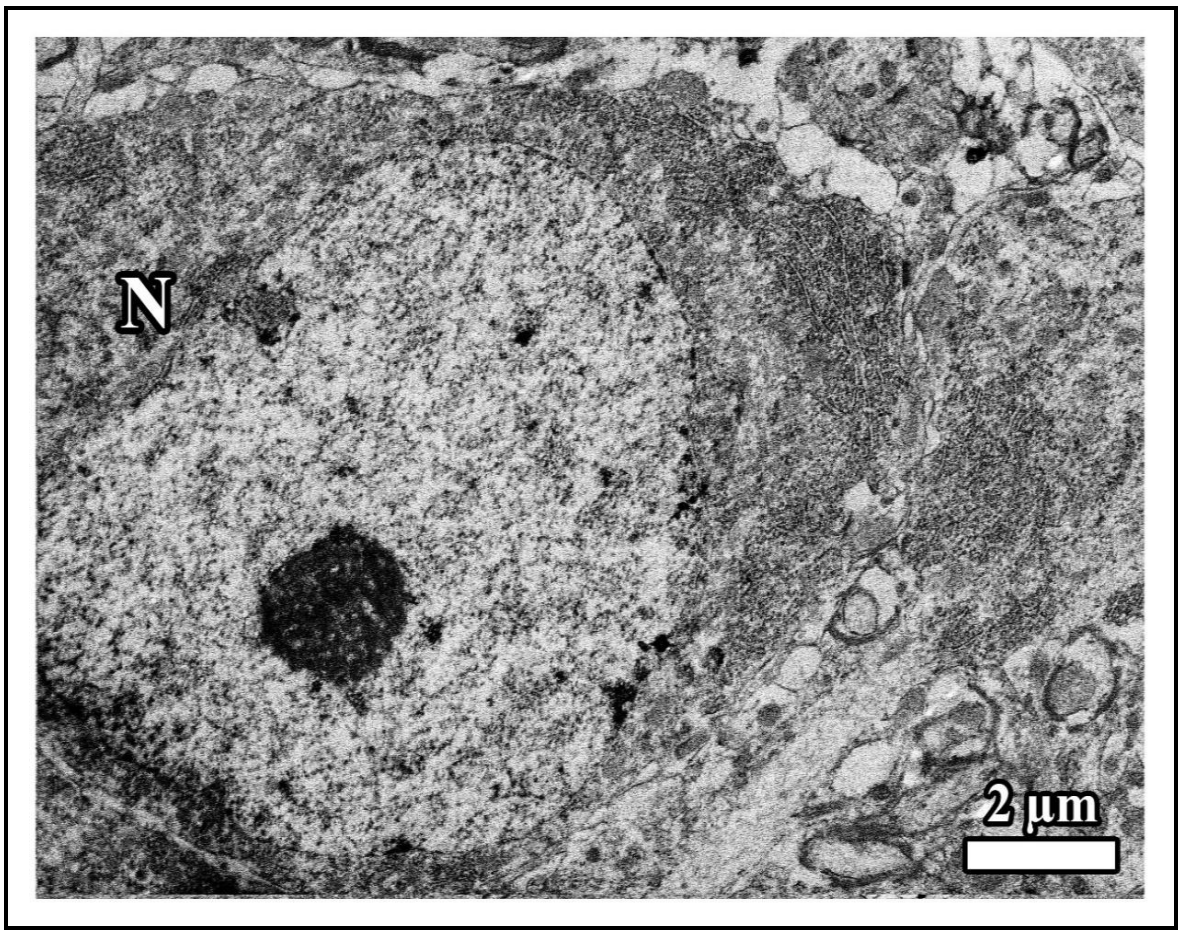

Figure 136. Image taken from the CA region of hippocampus belong to the EMF + NS group is seen. A pyramidal cell (N) in this region has oval shape nucleus. Its nucleolus is large size and darkly stained, and also cytoplasm of this cell is slightly dense. Some cross sections of myelinated axons are observed

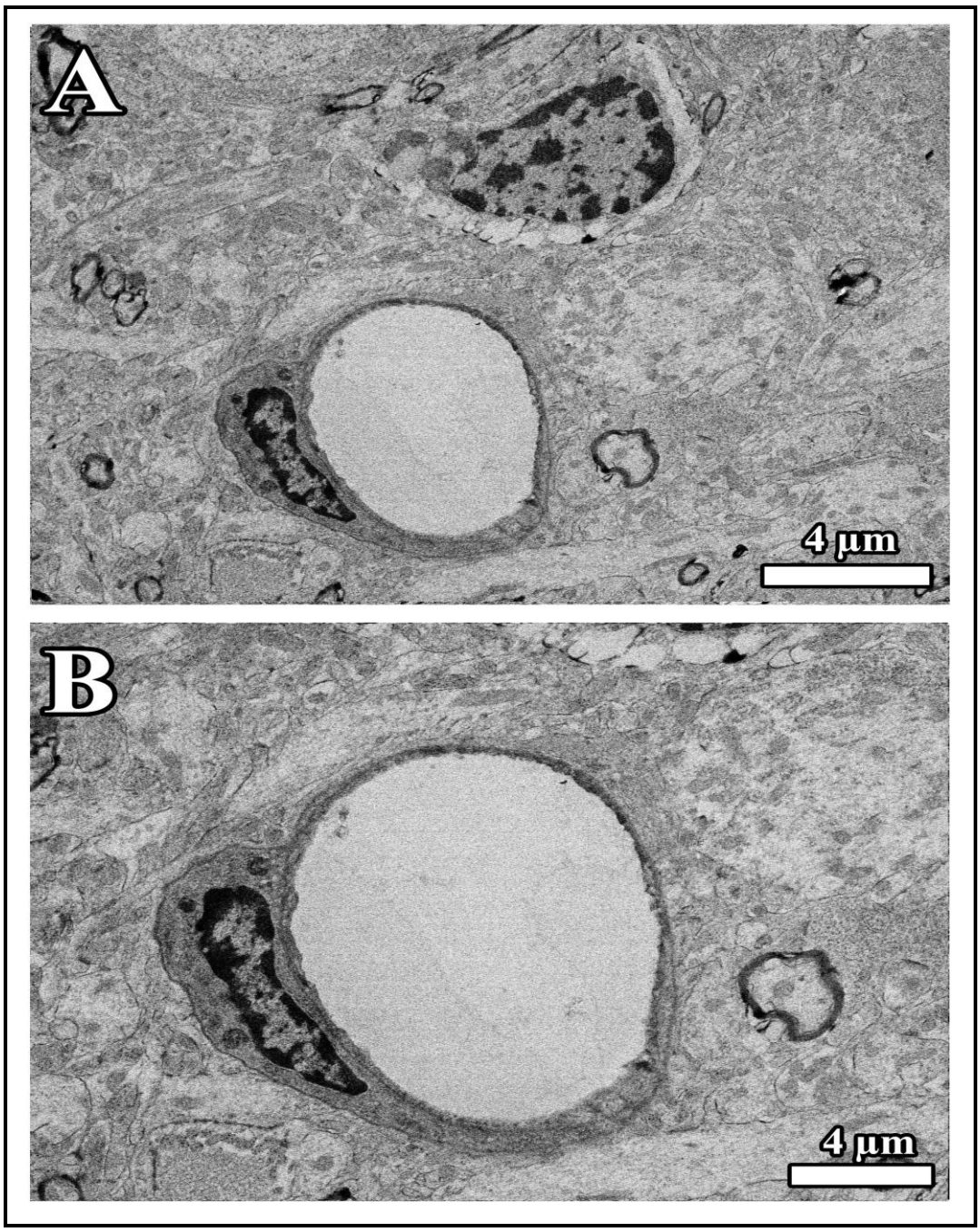

Figure 137. (A, B) Images taken from the brain belong to the EMF + NS group are seen. A large sized capillary is observed and the wall of it is intact, an endothelial cell lines its lumen, a pericyte (N) around capillary wall is also seen. Microglia is also found (in the upper part of A); around it many of vacuoles can be seen. Cross sections of axons are also observed

Concerning the EMF+AD+NS group the images taken by EM showed that, healthy pyramidal cells have oval shaped nucleus, their borders are seen clearly. Each pyramidal cell has a euchromatic nucleus and an obvious nucleolus (**Figure 138, 139, 140, 141 and 142**). Some accumulation of myelinated axons and neuroglia are observed around them.

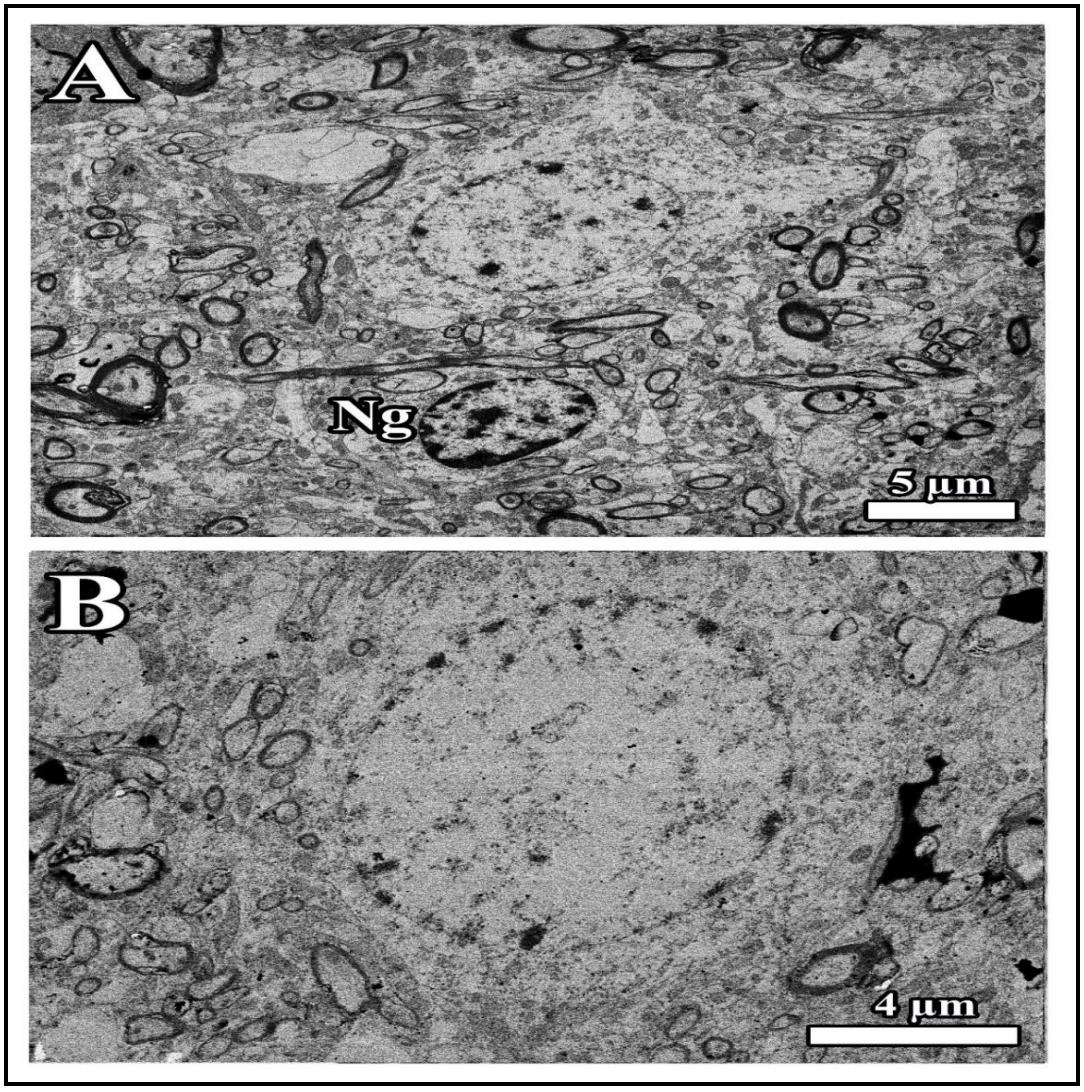

Figure 138. (A, B) Images taken from the brain belong to the EMF + AD + NS group are seen. Neuroglia (Ng) and other have a healthy structure; border of them can be seen clearly. Some cross and longitudinal sections of myelinated axons are also observed

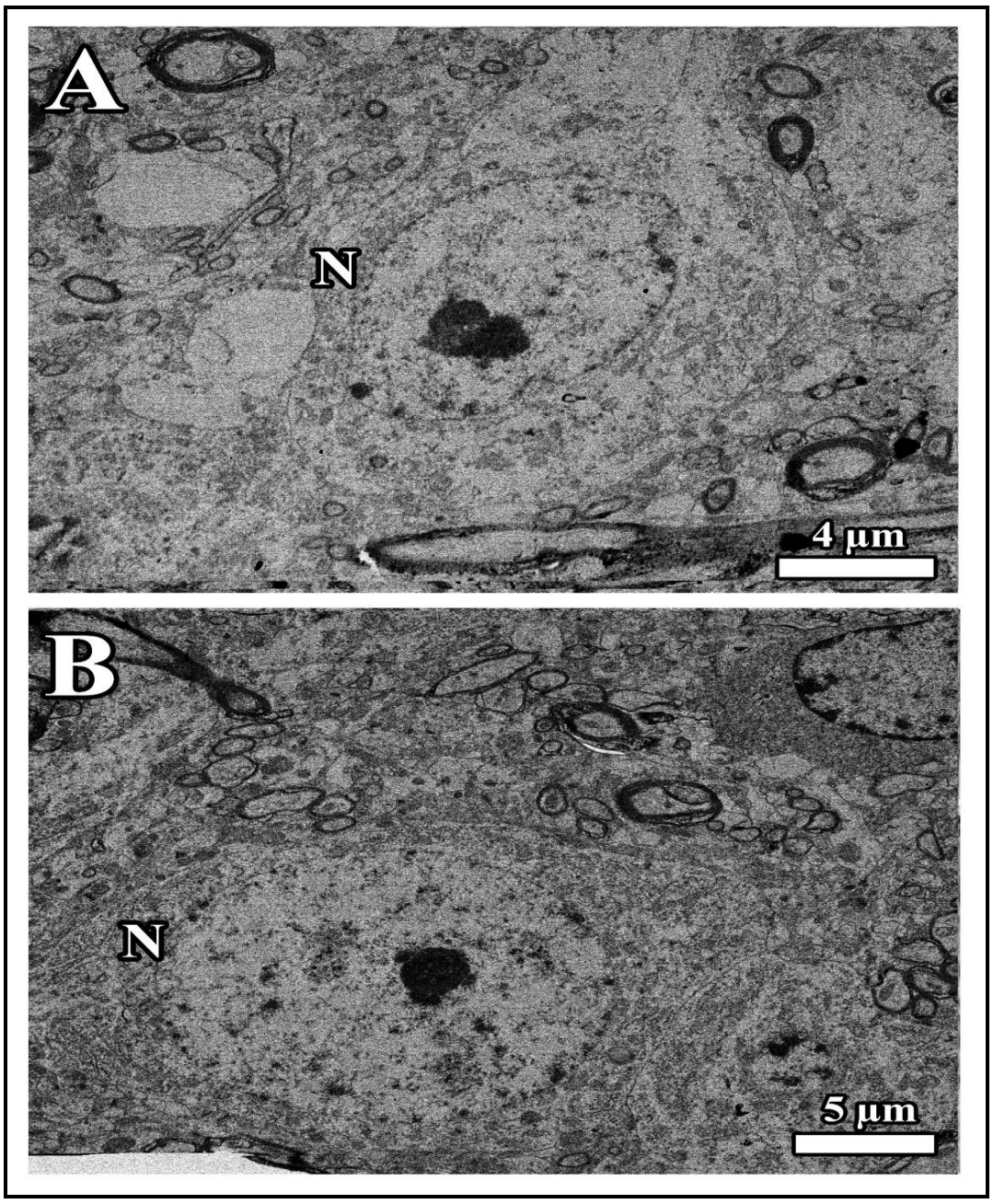

Figure 139. (A, B) Images taken from the brain belong to EMF + AD + NS group are seen. Neurons, neuroglia and other have a healthy structure; border of them can be seen clearly. Some of spaces around neurons are found, the meaning of these spaces is not clear. Each neuron (N) has a euchromatic nucleus and a conspicuous nucleolus. Some cross and longitudinal sections of myelinated axons are also observed

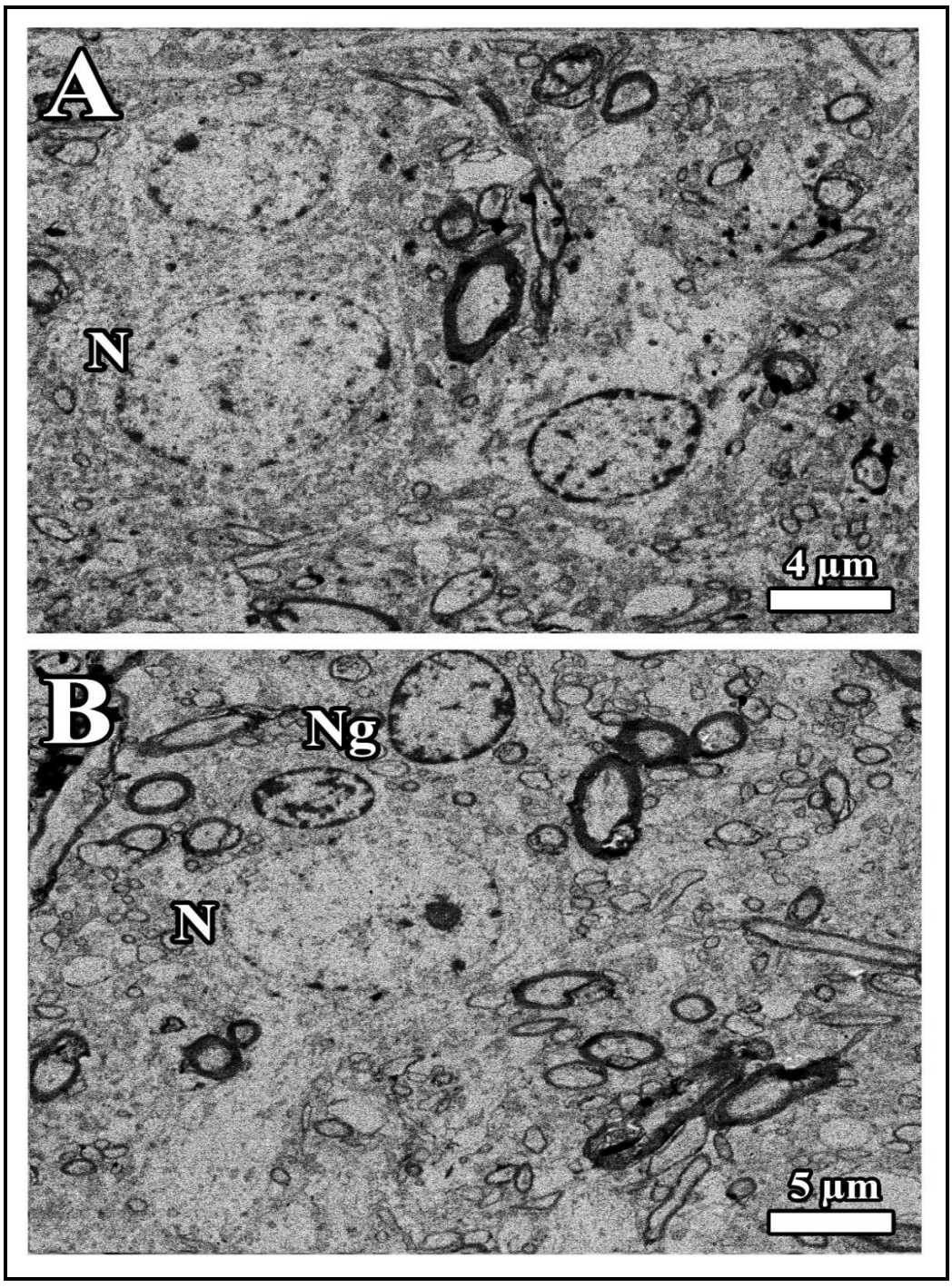

Figure 140. (A, B) Images taken from the brain belong to the EMF + AD + NS group are seen. Neuroglia (Ng) and neurons (N) have a healthy structure; the border of them is seen clearly. Cross and longitudinal sections of myelinated axons are also observed

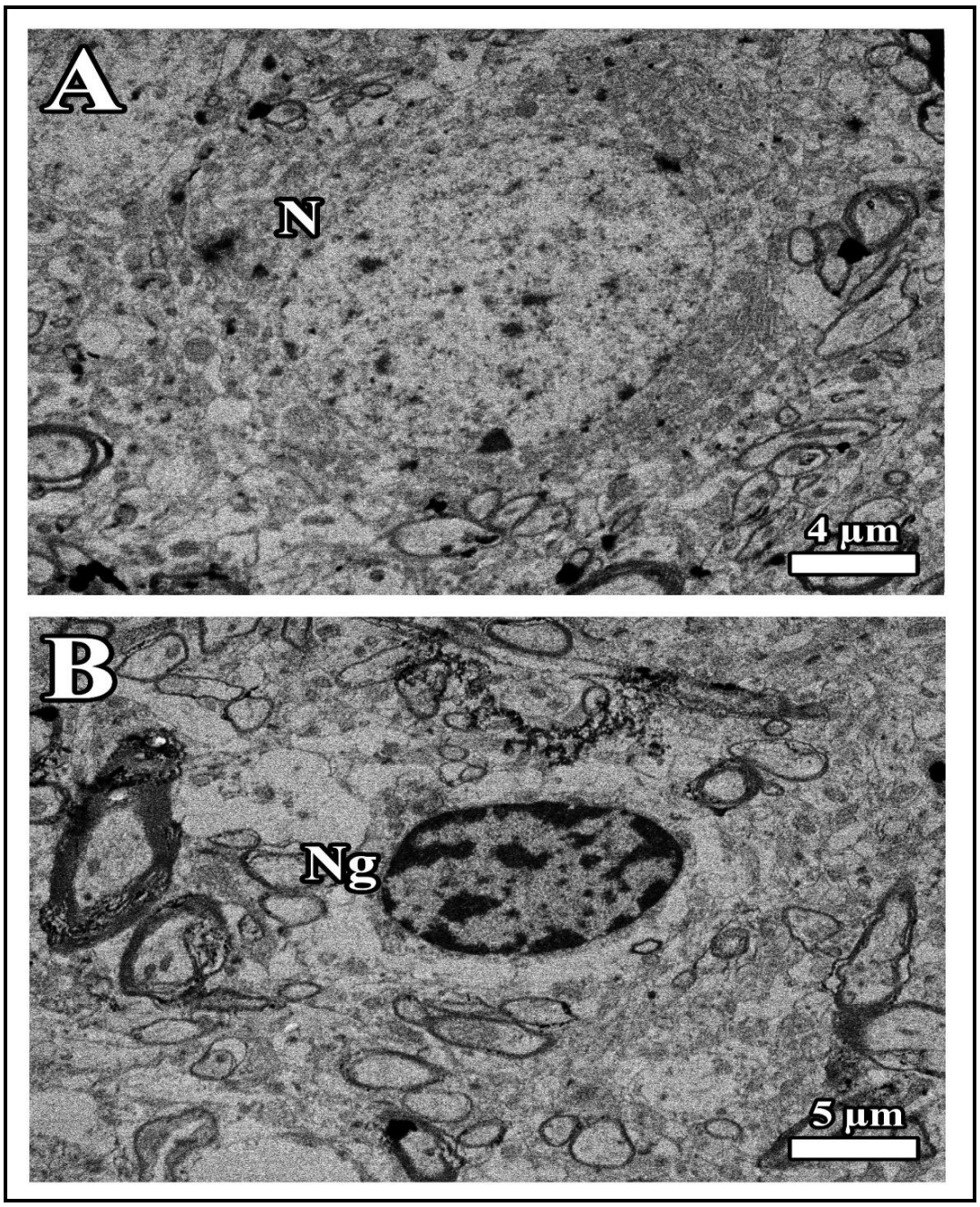

Figure 141. (A, B) Images taken from the brain belong the EMF + AD + NS group are seen. Neurons (N), neuroglia (Ng) and others have a healthy structure, border of them are seen clearly. Some of spaces around structures are found, the meaning of them is not clear. Some accumulation of the cross and longitudinal sections of myelinated axons are also observed

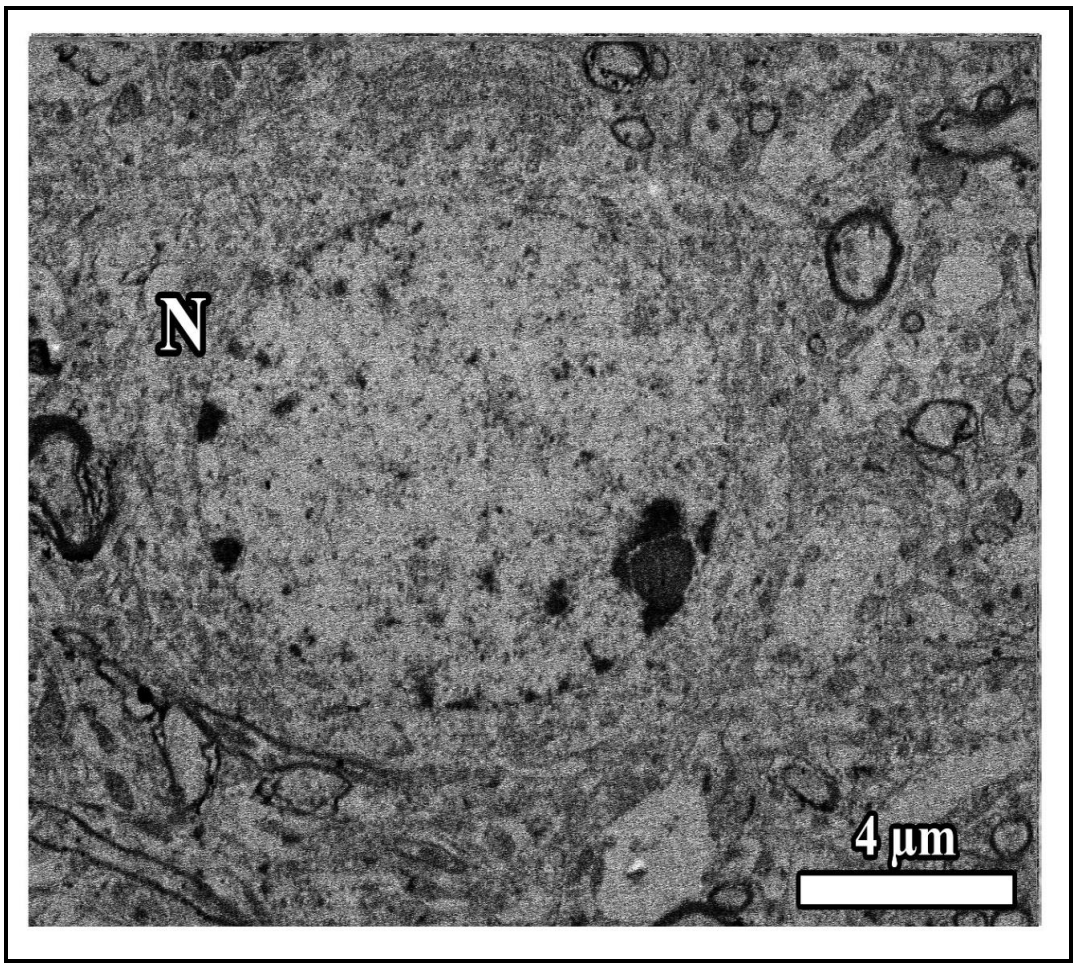

Figure 142. The image taken from the brain belonging to the EMF + AD+ NS group is seen. Neuron (N) and other structure have a healthy appearance; the border of neuron is seen clearly. It has a euchromatic nucleus and conspicuous nucleolus. Some of spaces around structures are found, the meaning of them is not clear. Some cross and longitudinal sections of myelinated axons are also observed

4.4. Biochemical Findings

4.4.1. Mean CAT Enzyme Activity for the Groups

CAT enzyme activity was measured in the blood serum samples which taken from the rats of all groups. The results are presented in the following table and figure (**Table 10**; **Figure 143**).

Table 10. CAT enzyme activity (nmol/min/ml (540 nm) (mean ± SD) values for all groups

Groups	**CAT enzyme activity**
Cont	2.295±0.202
Sham	2.198±0.299
EMF	2.287±0.136
EMF+AD	2.285±0.284
EMF+ NS	2.491±0.316
EMF+AD+NS	2.097±0.341
AD	2.406±0.274
NS	2.328±0.311

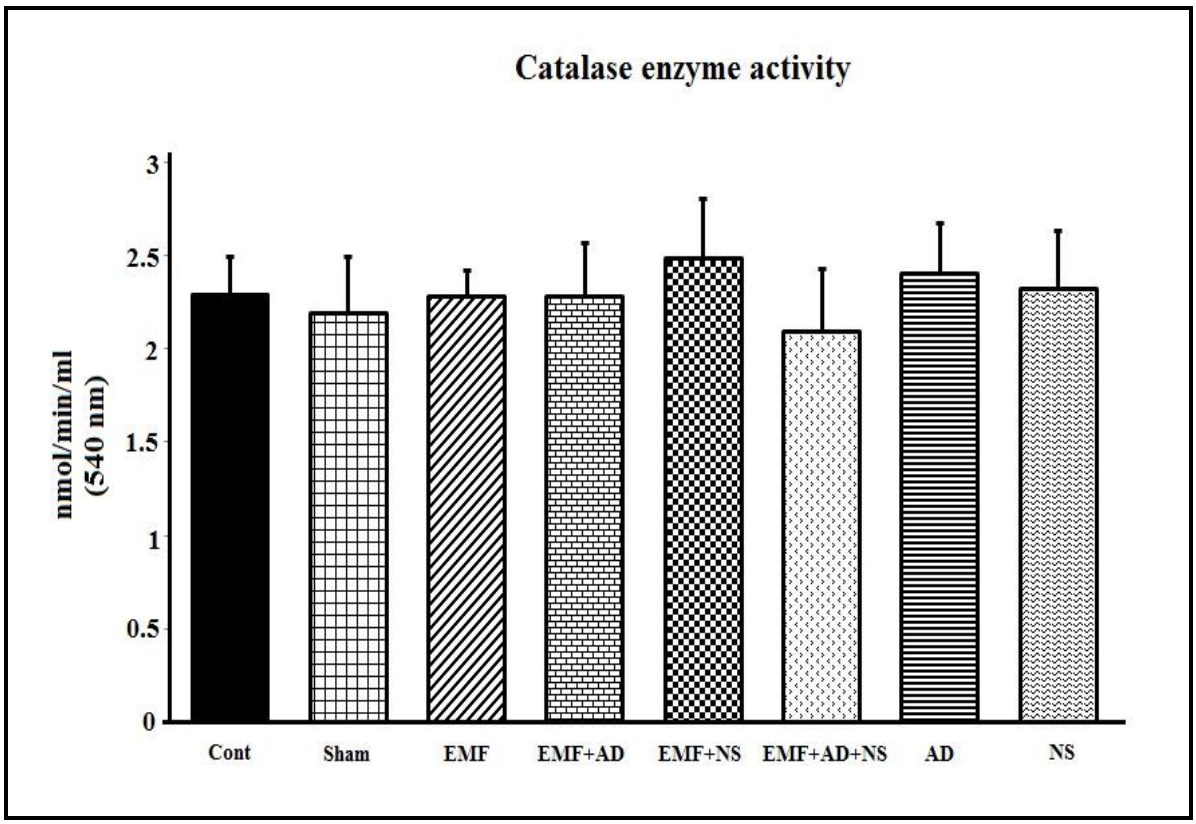

Figure 143. It shows the mean CAT enzyme activity values for all groups. Statistically no significant differences were observed

The CAT enzyme activity level of all the groups were analysed, it was found that the data of EMF exposed group showed that there is no significant difference among the groups ($p>0.05$).

4.4.2. Mean SOD Enzyme Activity for the Groups

SOD enzyme activity was measured in the blood serum samples taken from the rats of all groups. The findings are presented in the following table and figures (**Table 11**; **Figure 144**).

Table 11. SOD enzyme activity (U/ml (450 nm) (mean ± SD) values of all groups

Groups	SOD enzyme activity
Cont	0.009±0.007
Sham	0.009±0.004
EMF	0.010±0.004
EMF+AD	0.002±0.001
EMF+ NS	0.012±0.015
EMF+AD+NS	0.014±0.015
AD	0.017±0.009
NS	0.008±0.002

A significant difference of this enzyme activity was observed in the EMF+AD group compared to the NS group ($p<0.05$). On the other hand, no significant difference was observed in the SOD activity level between the EMF and EMF+AD, EMF+NS, EMF+AD+NS groups ($p>0.05$). Also, there was no significant difference between the Cont and Sham, EMF groups in terms of SOD activity level ($p>0.05$). Generally, the amount of enzyme activity was detected at low level in the Cont and Sham groups compared to the EMF group, but these differences were not significant.

4.5. Findings of Total Phenolic Content and Antioxidant Power

In the present study, the total phenolic content, antioxidant capacity, and free radical scavenging effect of various solvent extracts from AD and NS were evaluated. The results are shown in (**Table 12**).

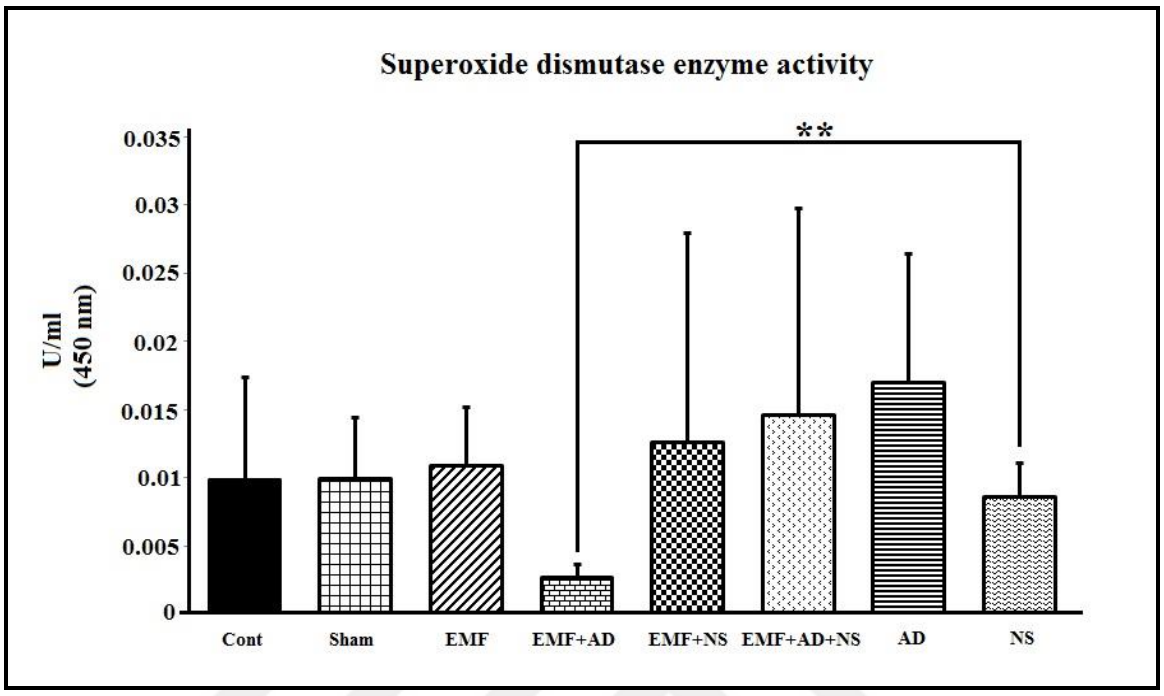

Figure 144. It shows the mean SOD enzyme activity values for all groups. Statistically significant differences at $p<0.05$ were indicated by (**).

Table 12. The total phenolic content, antioxidant capacity and free radical scavenging effect of AD and NS.

Antioxidant	Total phenolic content, mg / kg, gallic acid equivalent (GAE)	FRAP, mmol/g Trolox equivalent	DPPH free radical removal of mmol / g, Trolox equivalent
AD	14812.5	558.66	102.56
NS	4906.25	54.03	25.02

The highest total phenolic content was determined in AD 14812.5 mg/kg, gallic acid equivalent (GAE), while the lowest total phenolic content was determined in NS 4906.25 mg/kg, gallic acid equivalent (GAE). The highest FRAP antioxidant capacity was detected in AD 558.66 mmol/g Trolox equivalent, while the lowest antioxidant activity was showed in NS 54.03 mmol/g Trolox equivalent. The highest DPPH free radicals scavenging effect was seen in AD 102.56 mmol/g, Trolox equivalent, while the lowest free radicals scavenging effect was seen in NS 25.02 mmol/g, Trolox equivalent.

5. DISCUSSION

Stereological methods have efficient and unbiased results because of getting a high quality results in short time and these results would not show a systematic deviation from the true value. In the present study we used these techniques for getting numerical data on cell number in the hippocampal region of rats.

In the African countries, many of herbals have been used routinely for a better life, since it is well known that many of them have a very strong antioxidant capacity. In the current study we examined the influence of some herbals that are named AD and NS for protecting pyramidal cells in the hippocampus that vulnerable to EMF radiation.

In the present study, in well-known hippocampal regions the CA1, CA2 and CA3, we did not find a considerable reduction in the mean total number of the pyramidal neurons in the EMF group compared to the mean total of the Cont group. Furthermore, it was found that the mean number of the pyramidal neurons in the sham group was not statistically different from the mean total number of the Cont group. On the other hand, it is a strange and unexpected results we found that the mean total of the hippocampal pyramidal neurons in the CA regions of the AD and NS groups were more numerous in comparison to the Cont group. This means that those herbals with a high degree of antioxidants may stimulate neurogenesis in this region, but such comment should be supported by means of immunohistochemical analysis, and new generated neurons in this region must be shown by these techniques.

Beside of these numerical data, optical evaluation carried out by electron and light microscope on the sections from the groups showed opposite results from the cell number estimation in the hippocampus. Since substantial morphological changes as results of EMF exposure in EMF groups in comparison of the Cont and herbal treated groups have been observed in the granule and pyramidal cells of the hippocampus. Therefore, the changes in the morphology of pyramidal neurons at the hippocampal regions are important indicators to observe the side effects of EMF exposure. Histopathological findings obtained from the presented study groups consistent with some previous studies (Erdem Koç et al., 2016; Kerimoğlu et al., 2016; Altun et al., 2017) but inconsistent with our stereological analysing results i.e. numerical data.

EMFs 900 MHz exposure to the hippocampal regions would destroy the pyramidal neurons by inducing the neuronal apoptosis mechanism in rat (Kesari et al., 2011). The radiation emitted from the EMF exposure promotes the production of substances harmful to the neurons, such as free radicals, that can destroy the structure of the neurons, especially the nucleus and the cell membrane. Accordingly, EMF exposure increases the amount of oxidative stress (Yokus et al., 2005; Ongel et al., 2009; Duan et al., 2015).

In the current study, we would like to show decreasing side effects of the EMF exposure in the hippocampal pyramidal cell number in all CA regions, we have used herbal-based substances for this purpose such as AD and NS which support the endogenous antioxidant defence system of the experimental animals. The possible serious action of EMF exposure and the protective effects of these common herbs substance on the neurons were also evaluated through biochemical use of CAT and SOD enzyme activities. The results of the biochemical tests showed that when comparing the exposed EMF group with the Cont and Sham groups, no significant difference was found in the level of the enzyme activities in the cell number comparison.

5.1. Electromagnetic Field and Hippocampus

Modern means of communication such as mobile phones use radiation power and radio frequencies for communication. Every day in our lives we are exposed to electromagnetic waves through the use of a mobile phone, an invention that has contributed significantly to the development of communication around the world. Modern mobile phones and electromagnetic fields play a major role in the pollution and damage to cells. Several studies have been conducted to demonstrate the damage caused by exposure to electromagnetic fields on the pyramidal cells of the hippocampal CA regions (Kivrak et al., 2017; Belyaev, 2018). It was observed that using a mobile phone for 4 weeks continuously for 60 minutes a day may damage the pyramidal cells in the hippocampus. This confirms that using the phone near the brain may damage various brain cells, because it works at a frequency of 900 MHz. As we noticed recently, mobile phone usage has increased, therefore, the health damage may also increase (Kim et al., 2016).

Studies are ongoing and a number of reports of electromagnetic radiation (EMR) damage have been published. However until now, the mechanism of the biological effect of emitted radiation is unclear (Ibrahim and Gharib, 2010). Many studies on electromagnetic fields have been carried out recently and have been shown to increase the incidence of cancer in the brain. It also reduces the number of pyramidal cells in the hippocampus, which affects the intellectual performance, especially in children (Merzenich et al., 2008; Söderqvist et al., 2011).

The hippocampus is an essential entity in the limbic system that integrates with other brain regions to control mental action, emotional behaviour and memory (Toyoda et al., 2011). Its function may be influenced by microwave radiation exposure. It is well known that a low level of cholinergic activity in these important areas, such as the hippocampus and cortex in animals would affect many brain and related functions. Then, exposure to mobile phone radiation may increase the degree of behavioural changes (Veena et al., 2015).

Furthermore, frequent use of a phone for a long time may cause headaches and dizziness at times. As well, some of epidemiological studies have indicated that excessive use of cell phones may be one of the causes of worsening migraine (Arns et al., 2007; Kaplan et al., 2016). Most studies claim that EMF at a frequency of 900 MHz increases the oxidative stress in the tissue, which affects the structure of fats, carbohydrates and proteins due to increasing free radicals (Johansen et al., 2005). Impairment of DNA might trigger the uncontrolled cell division, which is known as cancer (Ongel et al., 2009). Instructions must be followed to minimize the risk of exposure to RF EMR from a cell phone and other devices that use electromagnetic energy (Narayanan et al., 2014).

In some recently published studies that they have showed by means of the stereological analyses, 900 MHz EMF-exposed groups have less the pyramidal neurons in hippocampus compared to groups non-exposed (Altunkaynak et al., 2016; Erdem Koç et al., 2016). In this study, the number of pyramidal neurons in the entire hippocampus and in different hippocampal regions CA1, CA2 and CA3 was estimated using an unbiased stereological method, the fractionator. The actual method for counting pyramid neurons was carried out with this precise technique in the entire hippocampus as well as in the

regions CA1, CA2 and CA3. One of pioneers in the EMF subject who is Odaci et al. (2008) have suggested that 900 MHz EMF exposures negatively affects the number of granule cell in the DG as well as its morphology during its developmental period. A comparable finding was reported by Bas et al. (2009) who found that 900 MHz EMF exposure destroyed the pyramidal neurons in the CA regions of the hippocampus. Şahin et al .(2015) reported that the 900 MHz EMF was exposed to male rats at the age of 8 weeks, and found that, there was a marked reduction in the number of pyramidal neurons in the CA in the EMF exposed group in comparison to the sham and Cont groups. Also, structural changes were seen in the components of neurons. The number of the pyramidal neurons in the hippocampus was estimated by Kerimoglu et al. (2016) in the EMF, Sham, and Cont groups, and the results showed that a low number of neurons were found in the EMF group compared to the Sham and Cont groups. While, no significant difference was found between the Sham and Cont groups. Referring to these findings, it is clear that exposure to the electromagnetic fields cause damage to memory function and mental activities (Hao et al., 2012; Ragy, 2015). The destruction of neurons was more obvious in the EMF group than in the Cont group. This result was reported by Altun et al. (2017) when 900 MHz EMF was exposed to the hippocampal granule and pyramidal neurons and the cerebellar Purkinje cells. A vastly significant difference was also observed in the hippocampal regions CA1, CA2 and CA3 when the EMF exposed group was compared with the Sham group.

On the other hand, no significant difference was observed when comparing the Sham group with the Cont group (Erdem Koç et al., 2016). Based on these finding, it would be expressed that the stress (putting animals in the EMF exposure system without EMF radiation) during the prenatal period, appears to have no adverse effect on the number of pyramidal cells in the hippocampus, although some of the previous studies have showed side effects of stress on cell number of developing brain as well as hippocampal region (Odaci et al., 2008; Aygün et al., 2012; Kaplan et al., 2013; Türkmen et al., 2016).

In this context, since the hippocampus is one of the regions in which new neurons are produced over a lifetime, it is possible that stress on the hippocampal neurons can impair the function of the hippocampus in terms of learning and memory. Besides, other

functions of the hippocampus are also likely to be affected (Zhao et al., 2008; Samuels and Hen, 2011).

As expressed in the above, some of stereological results in this study are inconsistent with results of previous studies (Şahin et al., 2015; Erdem Koç et al., 2016).

In this regard, current results are compatible with findings of Ragbetli et al. (2009) but, not compatible to findings of Erdem Koç et al. (2016) because when they comparing these groups Cont, Sham and EMF a significant difference was observed in terms of number of pyramidal neurons. Ragbetli et al. (2009) stated that no statistically significant decrease was observed in the group exposed to EMF compared to the Cont group in relation to the number of pyramidal neurons in the rat hippocampus. By referring to recent stereological results, no side effects of EMF radiation in terms of total neuron number but our histopathological evaluation did not confirm those for sake of clearance this discrepancy should be investigated.

In terms of histopathological examination, Şahin et al. (2015) reported that EMF exposure changes the structure of hippocampus. These observed results have showed many abnormal darkly stained cells and shrinkage perikaryon in the EMF group compared to the Cont group in the hippocampus. Keleş et al. (2018) also showed a pronounced impairment in the pyramidal cells in CA1, CA2, and CA3 and damaged in the granule cells in the DG region, this means, darkly stained cells were commonly observed in the EMF group of the present study under the light microscope. Salford et al. (2003) reported that the invisible cell structure of neurons with dark-colored neurons are mostly destroyed neurons as a result of EMF exposure, this was observed in the exposed neurons in the hippocampus and cerebral cortex.

Light and electron microscopic findings in aforementioned studies largely correspond to our histopathological findings. We have seen pronounced structural changes in the pyramid neurons of the EMF subjected group compared to the Sham and Cont groups. These results showed that the black or dark colored neurons are most likely destroyed neurons that are more common in the EMF exposed group than in the Sham and Cont groups. Microscopic findings of this study show that, a large number of dark-colored

neurons in the EMF exposed groups, it would be the result of excessive heterochromatin accumulation in destroyed neurons.

According to electron microscopic findings, Srivastava and Taufiq (2018) revealed single shrunken cells with dark cytoplasm and nucleus, disordered mitochondrial cristae and vacuolated mitochondria in the different regions of the brains belonging to the EMF exposed rats. Also, Faridi and Khan (2013) observed that there is shrinkage in the size of pyramidal cells due to the damaging effects of EMF, which finally may lead to the programmed cell death. These morphologic changes may be due to decreased nuclear activity. The histopathological findings of the electron microscopic sections obtained from above studies are consistent with the results of our study, we observed numerous degenerated pyramidal neurons with shrunken and darkly stained perikaryon and many vacuoles in the cytoplasm of microglia.

A biochemical analysis of rat blood serum samples was accomplished in this study. There was no significant difference in the CAT and SOD activity levels in EMF groups compared to those in Sham and Cont groups. Based on this result, the production of free radicals in the serum was not significantly accumulated.

The results of our study contradict the results of Altun et al. (2017) who examined the efficacy of CAT and SOD and reported that a higher level of enzyme activity was observed in the EMF group compared to the Sham and Cont groups.

CAT and SOD enzyme activity was tested by Bahreyni Toossi et al. (2018) in the prenatally exposed EMF group for 120 minutes per day in mice brain tissue samples. The results showed that the EMF group showed a low CAT enzyme activity compared to the Cont group. This finding is not compatible with our study results, since no significant difference in the enzyme activity level between EMF and Cont groups was found for SOD. The brain is part of the tissue that uses a large amount of oxygen for metabolism. Therefore, it could be more sensitive to lack of oxygen and oxidative stress (Ozmen et al., 2007). We have claimed that a negative impact of the radiation emitted by the EMF source can catalyze the release of ROS and inhibit intrinsic antioxidants.

In this context, we believe that devices that generate electromagnetic fields can cause tissue damage due to the high oxidative stress. In this study, we found no effect of SOD and CAT activity on free radicals.

5.2. *Adansonia digitata*

Since the AD is polysaccharide, it has been shown to have a radical scavenger activity. It also acts as an essential agent in preventing cancer as it prevents free radicals formation in the human body and removes free radicals (Ibrahim et al., 2014).

The aqueous fluid extracted from AD can improve impaired kidney function. The plant-promoting effect can be caused by the content of micronutrients such as vitamins C and E. In addition, the most striking point about the plant is that the pulp is very rich in vitamins such as vitamin C and the antioxidant capacity of the pulp is is more pronounced than most well-known herbs with antioxidant substance. Numerous studies on AD biological activities are conducted and promising results have been shown (Kamatou et al., 2011). AD has large amount of antioxidants, due to the presence of carotenoids, polyphenols and vitamins such as C and E. which made it more efficient in preventing oxidative-related diseases (Besco et al., 2007), such as inflammation, diseases associated with cardiovascular disease and cancer (Abiona et al., 2015).

One of the properties of AD fruit is that it has pain relievers and are highly antimicrobial. This can be seen in the alcoholic extract from pulp and AD leaves (Giri, 2018). The antioxidant contained in AD made it possible to trap free radicals that result from oxidation reactions. This can be attributed to the fact that AD develops the ability of the liver and kidneys to remove lipid peroxides (Adegoke et al., 2015).

Due to the presence of antioxidants and minerals in the AD, their extracts are advantageous versus oxidative stress (Althwab et al., 2019). Human health and body protection system depend to a large extent on the consumed nutritional value and antioxidant properties (Salih and Yahia, 2015). The substance extracted from AD pulp and seeds has been found to have a potent antioxidant effect, a pain reliever effect, an antipyretic effect, (lower body temperature when a fever is present), cardio-protective effect and anti-cancer impact, also has a therapeutic effect against sickle cell anemia

(Elsaid, 2013; Ghoneim et al., 2016). Furthermore, AD capable of decreasing the glycemic response to the food rich in carbohydrate (Coe et al., 2013).

Adeoye and Bewaji (2015) reported that the AD pulp showed no toxic action, and therefore many societies consume the pulp of the fruit, its seeds and leaves. Upon surveying the literature, it was seen that no studies had been conducted on the potential effects of AD on the brain cells subjected to EMF. Based on the stereological results of our study, we found that mango increases the number of pyramidal neurons in AD group in comparison to the CA regions of the control and sham groups. In addition to this, the results of the stereological analysis showed that AD has a strong protective effect on the number of neurons in the hippocampus regions. This is observed when the pyramidal cells in CA regions are exposed to the EMF. A remarkable increase was observed in EMF + AD compared to the EMF exposed group. Imge et al. (2010) reported that, possession of mango to vitamin C makes it capable to protect the brain from detrimental influence of cell phone. In this study, the AD has proven that it can protect nerve cells from damage, and this can be attributed to the presence of a high percentage of vitamins, especially vitamins C and E. With regard to these results, it is clear that the AD is able to improve the function of neurons and protect them from the destructive effects when exposed to EMF by increasing endogenous antioxidant enzymes and suppressing oxidative stress. In this context, we can say that the AD defends against nerve cell damage and protects hippocampal neurons in CA regions from the free radicals accretion, which can cause dangerous damage to nerve cells . Therefore, we consider our study to be unique because it demonstrated the positive effect of aqueous extract of AD on brain cells in the hippocampus regions after being exposed to 900 MHz electromagnetic field. This was not clearly available in previous studies.

When the histopathological changes in the hippocampal CA regions were examined by light and electron microscopes, it was observed that, the quantity of normal-looking neurons were more abundant in the EMF + AD group than in the EMF group, since clearly seen the cell and nucleus boundaries is a characteristic of the EMF+ AD group. A few darkly stained neurons were also observed in this group. The visibility of dark-colored pyramid neurons in relation to the large number of normal neurons in this group suggests that this AD can protect the morphology of pyramidal neurons, i.e. function, from the

adverse effects of the EMF radiation. Beside of these general positive effects, our electron microscopic examination showed that the AD group showed healthy and oval-shaped pyramidal cells with they have slightly dark cytoplasm and also the neuroglia cells and myelinated axons are seen in normal structure in comparison of EMF exposed group.

It was not seen any significant difference in terms of CAT enzyme activity between AD group and other groups in the present study. On the other hand, there was a significant difference in the SOD enzyme activity of the EMF+AD group was observed when it compared to the NS group. Based on this result, it would be suggested that the antioxidant action of AD is higher than NS. Based on our knowledge, this novel study examined the histological changes and the antioxidant power in the AD versus the deleterious effects of EMF exposure in the hippocampus using electron microscopy.

5.3. *Nigella sativa*

In our study, we calculated the number of pyramidal cells in the hippocampus regions. The analysis showed a marked increase in the total number of pyramidal cells in the EMF+NS group versus the EMF group. The presence of TQ in NS has been shown to be beneficial in many of NS activities. It is available in some seeds, which made it very useful (Gali-Muhtasib et al., 2006). Also, Mohamadin et al. (2010) claimed that when comparing most of the body's organs, especially the liver and lungs, with the brain, it was found that the hippocampal region had relatively low antioxidants. For this reason, brain tissue is more sensitive to oxidative stress than tissue in other organs. As a result, the hippocampus is more sensitive to oxidative damage than the cortex. TQ can therefore remove free radicals and protect cells from damage caused by oxidative stress (Harzallah et al., 2012). It is concluded that NS has a neuroprotective effect by intercepting the oxidative stress generated by the EMF and promoting the antioxidant response to the deleterious effects of EMF exposure. It has also been shown that the protective effects of NS are related to its antioxidant capacity, anti-inflammatory and anti-fibrotic agents. Furthermore, NS can inhibit the generation of free radicals (Erboga et al., 2015).

On the other hand, chronic exposure of the rat hippocampus to toluene showed that the NS and its derivatives, such as TQ, had a positive effect on the damage of the hippocampus caused by toluene (Kanter, 2008).

The therapeutic effect of NS in attacking cancer cells may occur as a result of the antioxidant effect. It has been observed that it is effective in fighting various types of carcinogenic cells by increasing and activating macrophage cells (Randhawa and Alghamdi, 2011; Ermumcu and Şanlıer, 2017). Asiaei et al. (2017) mentioned that the aqueous alcoholic extract of NS hinders the growth of apoptotic cells and the production of dark neurons in the hippocampus. Moreover, modern studies have confirmed that NS and TQ extracts hinder cell death in the hippocampus and also show a neuroprotective action in a rat model with cerebral ischemia (Al-Majed et al., 2006; Hobbenaghi et al., 2014). Previous studies mentioned the effectiveness of black seed antioxidants and their positive impact in maintaining memory function and protecting neurons from destruction in seizures models (Ezz et al., 2011; Vafaee et al., 2015; Seghatoleslam et al., 2016). Also, Hosseinzadeh et al. (2007) reported that NS suppress the increase in lipid peroxidation in the hippocampal regions after EMF exposure.

NS extract can lead to an anti-neuroinflammatory influence on the hippocampal neurons (Babar et al., 2018). A comparable study found that NS is able to improve the destroyed hippocampal neurons (Seghatoleslam et al., 2016). The stereological results of our study are consistent with the results of those studies in which the NS showed an obvious protective effect on the pyramidal neurons in the hippocampus after they were exposed to the serious effects of EMF.

The obtained results confirmed that the NS showed a convincing effect as neuroprotective agent against the dangerous effects of 900 MHz EMF on hippocampal pyramidal neurons. Based on the results mentioned above, we recommend further studies on NS and protection of nerve cells from the deleterious effects of oxidative stress and electromagnetic field. In this study, histopathological examinations of the hippocampal sections stained with cresyl violet were carried out. The results of the examined tissue showed that the histopathological assessment largely corresponds to the stereological analysis. The presence of an antioxidant in NS reduces the amount of destructive cells in

the EMF+NS group, resulted from EMF exposure. For this reason, in the EMF+NS group compared to the EMF group, many normally structured neurons could be seen, in addition to the less frequently dark-colored damaged neurons in the EMF+NS group compared EMF group. Neuron boundaries and nuclei were more visible in the EMF+NS group than in the EMF-destroyed group. Based on microscopic observation, we can assume that NS improves the function of neurons in CA regions by promoting the endogenous antioxidant system.

In the present study, histopathological examination of the light microscopic results in resin sections showed that the structure of the pyramidal cells was in normal appearance, whereas it is also observed many densely stained pyramidal as well as neuroglia. An increased number of darkly stained cells in the NS group may be due to the side effect of *Nigella sativa*. Our result compatible with Ong et al. (2016) study which reported that TQ caused the toxicity of some cells to the liver but not to extent of altering organ function .On the other hand, the healthy neurons in EMF+NS group were observed abundantly in comparison to the EMF group. Bensiameur-Touati et al. (2017) proved that, the aqueous extract of NS protects its safety at low doses but it can show hepatotoxicity when administered at a very high dose (21 g/kg), leading to a high death rate at 60 g/kg. At this point, it would be concluded that NS is not toxic because it performed protective activity against EMF radiation.

Regarding our EM histopathological result in the NS group showed that the healthy pyramidal neurons have an oval shape and euchromatic nucleus. Dark cells have deformed shape and their nucleus and nucleolus are seen darkly stained. In the EMF+ NS group, the observed results displayed that the healthy pyramidal cells have oval shape and the cytoplasm is slightly dense. Myelinated axons and neuroglia are observed in normal structure.

In the literature, there is no previous study focusing on the biochemical assessments on NS with regard to the harmful effects of 900 MHz in the hippocampal cells. Sheikh and Mohamadin (2012) studied the impact of TQ on the brain in which they examined propoxur (PPr) oxidative stress model in rats using biochemical analysis. This study found that the

CAT and SOD activity levels were elevated when the TQ group was compared to the PPr-induced oxidative stress group.

Based on the stereological and histopathological findings, we suggested that herb plants that contain a strong antioxidant such as NS can be used to minimize the serious effects of cell phone radiation that cause neurological problems. A combined herbal remedy was used in this study and demonstrated acceptable results in terms of reducing side effects of electromagnetic fields. It should be stated that there is obvious that we need further studies concerning the biological effects of NS on the cells of the brain.

6. CONCLUSION AND RECOMMENDATIONS

6.1. Conclusion

1. The exposure to radiation 900 MHz EMF did not decrease the pyramidal neuron numbers in the hippocampus in comparison of the EMF group and the Cont group using stereological techniques. But a side impact of EMF radiation on structure of pyramidal neurons in the CA region of hippocampus was observed since numerical density of darkly stained neurons was very high in comparison of the Cont group. This observation was confirmed by both light and electron microscopes.

2. The plants with high antioxidant properties, such as in the AD and NS, reduce the destructive influence of the EMF on the pyramidal neurons of the hippocampus by inhibiting the generation of ROS and increasing the activities of the endogenous antioxidant enzymes if they were used together i.e. the EMF+AD+NS group.

3. AD and NS herbals do not have a toxic effect on the pyramidal cells in hippocampal region against EMF radiation. They may stimulate neurogenesis in this region since the mean total number of pyramidal neurons was higher in the pure AD and NS groups in comparison of the Cont and Sham groups.

4. Histopathological results from the light microscope and EM evaluations have showed that EMF exposure was found to raise the level of oxidative stress by increasing the production of free radicals that cause destruction of pyramidal neurons in the hippocampus. Substantial cell damage in the EMF exposed group was a common feature of this group.

5. Histopathological findings have showed that NS group appear side of effect of toxicity in healthy group of pyramidal neurons when evaluate in the light microscope and EM.

6. It was found a high level of phenolic content and antioxidant power in the AD and NS herbals.

6.2. Recommendations

1. We recommend that using natural antioxidants in appropriate amounts together as foodstuffs, it would inhibit or reduce the harmful effects of EMF radiation on the brain neurons.

2. We recommend placing the mobile phone away from the head by using headphones since it decreases the influence of mobile phone radiation.

3. Electronic devices must be developed and processed to reduce their biological effects on human health and the environment.

4. We recommend that our communities, especially children should be protected from radiation exposure emitted from cell phones and electronic devices.

5. Further studies, focusing on the mechanism of antioxidants especially AD and NS that may be novel protective substances against side effects of EMF radiation hippocampus are needed.

REFERENCES:

Abiona D, Adedapo Z, Suleiman M. Proximate analysis, phytochemical screening and antimicrobial activity of baobab (*Adansonia digitata*) leaves. J Appl Chem 2015;8(5):60-65.

Adegoke AM, Gbadegesin MA, Otitoju AP, Odunola OA. Hepatotoxicity and genotoxicity of sodium arsenite and cyclophosphamide in rats: Protective effects of aqueous extract of *Adansonia digitata* L. fruit pulp. J Adv Med Med Res 2015;8(11):963-974.

Adeoye AO, Bewaji CO. Therapeutic potentials of *Adansonia digitata* (Bombacaceae) stem bark in Plasmodium berghei-infected mice. J Biol Sci 2015;15(2):78-84.

Adler DH, Wisse LEM, Ittyerah R, Pluta JB, Ding SL, Xie L, Wang J, Kadivar S, Robinson JL, Schuck T, Trojanowski JQ, Grossman M, Detre JA, Elliott MA, Toledo JB, Liu W, Pickup S, Miller MI, Das SR, Wolk DA, Yushkevich PA. Characterizing the human hippocampus in aging and alzheimer's disease using a computational atlas derived from ex vivo mri and histology. Proc Natl Acad Sci 2018;115(16):4252-4257.

Aerts S, Calderon C, Valič B, Maslanyj M, Addison D, Mee T, Goiceanu C, Verloock L, Van Den Bossche M, Gajšek P, Vermeulen R, Röösli M, Cardis E, Martens L, Joseph W. Measurements of intermediate-frequency electric and magnetic fields in households. Environ Res 2017;154:160-170.

Ali B, Blunden G. Pharmacological and toxicological properties of *Nigella sativa*. Phytother Res 2003;17(4):299-305.

Al-Majed AA, Al-Omar FA, Nagi MN. Neuroprotective effects of thymoquinone against transient forebrain ischemia in the rat hippocampus. Eur J Pharmacol 2006;543:40-47.

Al-Rouby NM, Gawish SM. Histological study on the possible protective effect of *Nigella sativa* oil on experimentally induced hepatotoxicity in albino rats treated with sodium valproate. Glob Adv Res J Med Sci 2013;2(4):090-099.

Althwab SA, Alsattame SM, Al-Mundarij TI, Hamad EM, Mousa HM. Protective Effect of baobab fruit pulp (*Adansonia digitata* L.) from oxidative stress induced in rats by high-fat diet. Life Sci J 2019;16(1):63-71.

Altun G, Kaplan S, Deniz OG, Kocacan SE, Canan S, Davis D, Marangoz C. Protective effects of melatonin and omega-3 on the hippocampus and the cerebellum of adult wistar albino rats exposed to electromagnetic fields. J Microsc Ultrastruct 2017;5(4):230-241.

Altunkaynak BZ, Altun G, Yahyazadeh A, Kaplan AA, Deniz OG, Türkmen AP, Önger ME, Kaplan S. Different methods for evaluating the effects of microwave radiation exposure on the nervous system. J Chem Neuroanat 2016;75:62-69.

Altunkaynak BZ, Onger ME, Altunkaynak ME, Ayrancı E, Canan S. A brief introduction to stereology and sampling strategies: basic concepts of stereology. NeuroQuantology 2012;10(1): 31-43.

Aly AA, Crum R. Research review for possible relation between mobile phone radiation and brain tumor. Int J Inf Technol Convergence Serv 2016;6:1-16.

Andersen P, Morris R, Amaral D, Bliss T, O'Keefe J . The hippocampus book , New York, Oxford University Press. 2007; 868.

Arns M, Van Luijtelaar G, Sumich A, Hamilton R, Gordon E. Electroencephalographic, personality, and executive function measures associated with frequent mobile phone use. Int J Neurosci 2007;117(9):1341-1360.

Asiaei F, Fazel A, Rajabzadeh AA, Hosseini M, Beheshti F, Seghatoleslam M. Neuroprotective effects of *Nigella sativa* extract upon the hippocampus in PTU-induced hypothyroidism juvenile rats: A stereological study. Metab Brain Dis 2017;32(5):1755-1765.

Assady M, Farahnak A, Golestani A, Esharghian M. Superoxide dismutase (SOD) enzyme activity assay in fasciola spp. parasites and liver tissue extract. Iran J Parasitol 2011;6(4):17-22.

Assogbadjo AE, Chadare FJ, Kakaï RG, Fandohan B, Baidu-Forson JJ. Variation in biochemical composition of baobab (*Adansonia digitata*) pulp, leaves and seeds in relation to soil types and tree provenances. Agric Ecosyst Environ 2012;157:94-99.

Aygün D, Kaplan S, Odaci E, Onger ME, Altunkaynak ME. Toxicity of non-steroidal anti-inflammatory drugs: A review of melatonin and diclofenac sodium association. Histol Histopathol 2012;27(4):417-436.

Babar ZU, Azad AK, Sulaiman WMaW, Uddin J, Labu ZK. Neuroprotective properties of *Nigella sativa* (L.) seeds extract in Sprague Dawley rats models. Dhaka Univ J Pharm Sci 2018;17(1):113-121.

Bagheri Hosseinabadi M, Khanjani N, Ebrahimi MH, Haji B, Abdolahfard M. The effect of chronic exposure to extremely low-frequency electromagnetic fields on sleep quality, stress, depression and anxiety. Electromagn Biol Med 2019;38(1):96-101.

Bahreyni Toossi MH, Sadeghnia HR, Mohammad Mahdizadeh Feyzabadi M, Hosseini M, Hedayati M, Mosallanejad R, Beheshti F, Alizadeh Rahvar Z. Exposure to Mobile Phone (900–1800MHz) During Pregnancy: Tissue Oxidative Stress after Childbirth. J Matern Fetal Neonatal Med 2018;31(10):1298-1303.

Baptista P, Andrade JPA. Adult hippocampal neurogenesis: regulation and possible functional and clinical correlates. Front Neuroanat 2018;12:44.

Bas O, Odaci E, Kaplan S, Acer N, Ucok K, Colakoglu S. 900 MHz electromagnetic field exposure affects qualitative and quantitative features of hippocampal pyramidal cells in the adult female rat. Brain Res 2009;1265:178-185.

Belyaev I. Health effects of chronic exposure to radiation from mobile communication. In: Markov M, editor. Mobile communications and public health,Boca Raton, CRC Press. 2018;65-99.

Belyaev I, Dean A, Eger H, Hubmann G, Jandrisovits R, Johansson O, Kern M, Kundi M, Lercher P, Mosgöller W. Europaem EMF Guideline 2015 for the prevention, diagnosis and treatment of EMF-related health problems and illnesses. Rev Environ Health 2015;30:337-371.

Benassi B, Filomeni G, Montagna C, Merla C, Lopresto V, Pinto R, Marino C, Consales C. Extremely low frequency magnetic field (ELF-MF) exposure sensitizes SH-SY5Y cells to the pro-Parkinson's disease toxin MPP+. Mol Neurobiol 2016;53(6):4247-4260.

Bensiameur-Touati K, Kacimi G, Haffaf E-M, Berdja S, Aouichat-Bouguerra S. In vivo subacute toxicity and antidiabetic effect of aqueous extract of *Nigella sativa*. Evid Based Complement Alternat Med 2017;2017:1-13.

Besco E, Braccioli E, Vertuani S, Ziosi P, Brazzo F, Bruni R, Sacchetti G, Manfredini S. The use of photochemiluminescence for the measurement of the integral antioxidant capacity of baobab products. Food Chem 2007;102(4):1352-1356.

Bilgici B, Akar A, Avci B, Tuncel OK. Effect of 900 MHz radiofrequency radiation on oxidative stress in rat brain and serum. Electromagn Biol Med 2013;32(1):20-29.

Boccara CN, Kjonigsen LJ, Hammer IM, Bjaalie JG, Leergaard TB, Witter MP. A three-plane architectonic atlas of the rat hippocampal region. Hippocampus 2015;25(7):838-857.

Bolla SR. Effect of mobile phone radio frequency on hippocampal CA3 neurons. Int J Anat Res 2015;3(3):1216-1224.

Bortkiewicz A. Health effects of radiofrequency electromagnetic fields (RF EMF). Ind Health 2019;57(4):403-405.

Brix J, Wettemann H, Scheel O, Feiner F, Matthes R. Measurement of the individual exposure to 50 and 16 2/3 Hz magnetic fields within the bavarian population. Bioelectromagnetics 2001;22(5):323-332.

Brown DL. Bias in image analysis and its solution: unbiased stereology. J Toxicol Pathol 2017;30(3):183-191.

Brown MW, Aggleton JP. Recognition memory: what are the roles of the perirhinal cortex and hippocampus? Nat Rev Neurosci 2001;2(1):51-61.

Brzozek C, Benke K, Zeleke B, Abramson M, Benke G. Radiofrequency electromagnetic radiation and memory performance: sources of uncertainty in epidemiological cohort studies. Int J Environ Res Public Health 2018;15(4):592-611.

Buchmann C, Prehsler S, Hartl A, Vogl CR. The importance of baobab (*Adansonia digitata* L.) in rural West African subsistence - suggestion of a cautionary approach to international market export of baobab fruits. Ecol Food Nutr 2010;49(3):145-172.

Bürgi A, Theis G, Siegenthaler A, Röösli M. Exposure modeling of high-frequency electromagnetic fields. J Expo Sci Environ Epidemiol 2008;18(2):183-191.

Burits M, Bucar F. Antioxidant activity of *Nigella sativa* essential oil. Phytother Res 2000;14(5):323-328.

Burwell RD. The parahippocampal region: corticocortical connectivity. Ann N Y Acad Sci 2000;911:25-42.

Burwell RD, Agster KL. 3.03 - Anatomy of the hippocampus and the declarative memory system. In: Byrne, J.H., editor. Learning and memory: A comprehensive reference,Oxford, Academic Press,2008;47-66.

Butt MS, Sultan MT. *Nigella sativa*: reduces the risk of various maladies. Crit Rev Food Sci Nutr 2010;50(7):654-665.

Cappaert NLM, Van Strien NM, Witter MP. Chapter 20 - Hippocampal formation. In: Paxinos, G., editor. The rat nervous system. 4th Ed.,San Diego, Academic Press, 2015;511-573.

Cardinali DP. Fourth level: The limbic system. In: Cardinali, D.P., editor. Autonomic nervous system: Basic and clinical aspects, Cham, Springer International Publishing, 2018;245-285.

Cascella M, Bimonte S, Barbieri A, Del Vecchio V, Muzio MR, Vitale A, Benincasa G, Ferriello AB, Azzariti A, Arra C, Cuomo A. Dissecting the potential roles of *Nigella sativa* and its constituent thymoquinone on the prevention and on the progression of alzheimer's disease. Front Aging Neurosci 2018;10:1-10.

Chauhan P, Verma H, Sisodia R, Kesari KK. Microwave radiation (2.45 GHz)-induced oxidative stress: Whole-body exposure effect on histopathology of Wistar rats. Electromagn Biol Med 2017;36(1):20-30.

Chen B, Wang J, Qi H, Zhang J, Chen S, Wang X. The specific absorption rate of tissues in rats exposed to electromagnetic plane waves in the frequency range of 0.05–5 GHz and SARwb in free-moving rats. Australas Phys Eng Sci Med 2017;40(1):21-28.

Coe SA, Clegg M, Armengol M, Ryan L. The polyphenol-rich baobab fruit (*Adansonia digitata* L.) reduces starch digestion and glycemic response in humans. Nutr Res 2013;33(11):888-896.

Cutsuridis V, Cobb S, Graham BP. Encoding and retrieval in a model of the hippocampal CA1 microcircuit. Hippocampus 2010;20(3):423-446.

D'angelo C, Costantini E, Kamal MA, Reale M. Experimental model for ELF-EMF exposure: Concern for human health. Saudi J Biol Sci 2015;22(1):75-84.

Das I, Saha T. Effect of garlic on lipid peroxidation and antioxidation enzymes in DMBA-induced skin carcinoma. Nutrition 2009;25(4):459-471.

Dasuri K, Zhang L, Keller JN. Oxidative stress, neurodegeneration, and the balance of protein degradation and protein synthesis. Free Radic Biol Med 2013;62:170-185.

De Caluwé E, Halamová K, Van Damme P. *Adansonia digitata* L.–A review of traditional uses, phytochemistry and pharmacology. Afrika focus 2010;23(1):11-51.

Demir E, Taysi S, Ulusal H, Kaplan DS, Cinar K, Tarakcioglu M. *Nigella sativa* oil and thymoquinone reduce oxidative stress in the brain tissue of rats exposed to total head irradiation. Int J Radiat Biol 2020;96(2):228-235.

Demirel C, Gozen H, Akan M, Tarakcioglu M. Investigation of the protective effects of *Nigella sativa* oil and thymoquinone in radiation exposed rats. Eur J Ther 2018;24(4):224-228.

Deniz OG, Kaplan S, Selçuk MB, Terzi M, Altun G, Yurt KK, Aslan K, Davis D. Effects of short and long term electromagnetic fields exposure on the human hippocampus. J Microsc Ultrastruct 2017;5(4):191-197.

Duan W, Liu C, Zhang L, He M, Xu S, Chen C, Pi H, Gao P, Zhang Y, Zhong M. Comparison of the genotoxic effects induced by 50 Hz extremely low-frequency electromagnetic fields and 1800 MHz radiofrequency electromagnetic fields in Gc-2 cells. Radiat Res 2015;183(3):305-314.

Duhaini I. The effects of electromagnetic fields on human health. Phys Med 2016;32:213-221.

Duvernoy H, Cattin F, Risold P-Y. Structure, functions, and connections. In: Duvernoy, H.M., Cattin, F. , Risold, P.-Y., editors. The human hippocampus: Functional anatomy, vascularization and serial sections with MRI. Berlin, Springer Berlin Heidelberg, 2013;5-38.

Duvernoy HM. The human hippocampus: functional anatomy, vascularization and serial sections with MRI. 3rd Ed.,New York, Springer Science & Business Media, 2005;25-44.

Ebrahim S, Azab AE, Albasha MO, Albishti N. The biological effects of electromagnetic fields on human and experimental animals. Inter Res J Natur Appl Sci 2016;3(10):106-121.

Eichenbaum H, Amaral DG, Buffalo EA, Buzsáki G, Cohen N, Davachi L, Frank L, Heckers S, Morris RG, Moser EI. Hippocampus at 25. Hippocampus 2016;26(10):1238-1249.

Elsaid FG.The effect of seeds and fruit pulp of *Adansonia digitata* L.(Baobab) on Ehrlich ascites carcinoma. Food Nutr Sci 2013;4(8):38-46.

Engiz BK. Electric field levels and its evaluation from the view of public health: Samsun city center example. Turk J Public Health 2018;16(2):146-156.

Erboga M, Erboga ZF, Donmez YB, Aktas C, Kanter M. *Nigella sativa* attenuates bleomycin-induced pulmonary fibrosis in rats by inhibition of inflammation, fibrosis, and inducible nitric oxide synthase. J Exp Clin Med 2015;32(3):121-125.

Erdem Koc G, Kaplan S, Altun G, Gumus H, Gulsum Deniz O, Aydin I, Emin Onger M, Altunkaynak Z. Neuroprotective effects of melatonin and omega-3 on hippocampal cells prenatally exposed to 900 MHz electromagnetic fields. Int J Radiat Biol 2016;92(10):590-595.

Ermumcu MŞK, Şanlıer N. black cumin (*Nigella sativa*) and its active component of thymoquinone: effects on health. J Food Health Sci 2017;3(4):170-183.

Ernst A, Frisén J. Adult neurogenesis in humans-common and unique traits in mammals. PLoS Biol 2015;13(1):1-12.

Ezz HSA, Khadrawy YA, Noor NA. The neuroprotective effect of Curcumin and *Nigella sativa* oil against oxidative stress in the pilocarpine model of epilepsy: a comparison with valproate. Neurochem Res 2011;36(11):2195-2204.

Fanoudi S, Alavi MS, Hosseini M, Sadeghnia HR. *Nigella sativa* and thymoquinone attenuate oxidative stress and cognitive impairment following cerebral hypoperfusion in rats. Metab Brain Dis 2019;34(4):1001-1010.

Faridi K, Khan AA. Effects of Radiofrequency Electromagnetic radiations (RF-EMR) on sector CA3 of hippocampus in albino rats-a light and electron-microscopic study. Curr Neurobiol 2013;4(1):13-18.

Faruque MRI, Islam MT, Misran N. The study of specific absorption rate (SAR) reduction in mobile phones using materials and metamaterials. Int J Phys Sci 2011;6(31):7212-7221.

Fernandez PR, Ng KH, Kaur S. Risk communication strategies for possible health risks from radio-frequency electromagnetic fields (RF-EMF) emission by telecommunication structures. Health Phys 2019;116(6):835-839.

Funk RH, Monsees T, Özkucur N. Electromagnetic effects–from cell biology to medicine. Prog Histochem Cytochem 2009;43(4):177-264.

Gage FH. Mammalian neural stem cells. Science 2000;287(5457):1433-1438.

Gali-Muhtasib H, El-Najjar N, Schneider-Stock R. The medicinal potential of black seed (*Nigella sativa*) and its components. In: Khan, M. T. H. & Ather, A. , Editors. Advances in Phytomedicine. Elsevier. 2006;2:133-153.

Gallastegi M, Jimenez-Zabala A, Molinuevo A, Aurrekoetxea JJ, Santa-Marina L, Vozmediano L, Ibarluzea J. Exposure and health risks perception of extremely low frequency and radiofrequency electromagnetic fields and the effect of providing information. Environ Res 2019;169:501-509.

Gao X, Björk L, Trajkovski V, Uggla M. Evaluation of antioxidant activities of rosehip ethanol extracts in different test systems. J Sci Food Agric 2000;80(14):2021-2027.

Ge X, Shi Y, Li J, Zhang Z, Lin X, Zhan J, Ge H, Xu J, Yu Q, Leng Y. Development of the human fetal hippocampal formation during early second trimester. Neuroimage 2015;119:33-43.

Gebauer J, El-Siddig K, Ebert G. Baobab (*Adansonia digitata* L.): A review on a Multipurpose tree with promising future in the Sudan. Gartenbauwissenschaft 2002;67:155-160.

Genovese MI, Da Silva Pinto M, De Souza Schmidt Gonçalves A, Lajolo FM. Bioactive compounds and antioxidant capacity of exotic fruits and commercial frozen pulps from Brazil. Food Sci Technol Int 2008;14(3):207-214.

Geuna S, Herrera-Rincon C. Update on stereology for light microscopy. Cell Tissue Res 2015;360(1):5-12.

Ghoneim MA, Hassan AI, Mahmoud MG, Asker MS. Protective effect of *Adansonia digitata* against isoproterenol-induced myocardial injury in rats. Anim Biotechnol 2016;27(2):84-95.

Giri S. Antimicrobial and neuropharmacological evaluation of leaves and fruits (fruit-pulp) of *Adansonia digitata* L. Int J Acad Res Dev 2018;3(2):03-05.

Gobba F, Bravo G, Rossi P, Contessa GM, Scaringi M. Occupational and environmental exposure to extremely low frequency-magnetic fields: A personal monitoring study in a large group of workers in Italy. J Expo Sci Environ Epidemiol 2011;21(6):634-645.

Gonçalves JT, Schafer ST, Gage FH. Adult Neurogenesis in the Hippocampus: From Stem Cells to Behavior. Cell 2016;167(4):897-914.

Gould E. How widespread is adult neurogenesis in mammals? Nat Rev Neurosci 2007;8(6):481-488.

Grellier J, Ravazzani P, Cardis E. Potential health impacts of residential exposures to extremely low frequency magnetic fields in Europe. Environ Int 2014;62:55-63.

Gulsen I, Ak H, Colcimen N, Alp HH, Akyol ME, Demir I, Atalay T, Balahroglu R, Ragbetli MC. Neuroprotective effects of thymoquinone on the hippocampus in a rat model of traumatic brain injury. World Neurosurg 2016;86:243-249.

Gundersen H, Jensen E. The efficiency of systematic sampling in stereology and its prediction. J Microsc 1987;147(3):229-263.

Gustafsson E, Thomée S, Grimby-Ekman A, Hagberg M. Texting on mobile phones and musculoskeletal disorders in young adults: a five-year cohort study. Appl Ergon 2017;58:208-214.

Haminiuk CW, Maciel GM, Plata-Oviedo MS, Peralta RM. Phenolic compounds in fruits–an overview. Int J Food Sci 2012;47(10):2023-2044.

Hao D, Yang L, Chen S, Tian Y, Wu S. 916 MHz electromagnetic field exposure affects rat behavior and hippocampal neuronal discharge. Neural Regen Res 2012;7(19): 1488-1492.

Hardell L. World Health Organization, radiofrequency radiation and health-a hard nut to crack. Int J Oncol 2017;51(2):405-413.

Harzallah HJ, Grayaa R, Kharoubi W, Maaloul A, Hammami M, Mahjoub T. Thymoquinone, the *Nigella sativa* bioactive compound, prevents circulatory oxidative stress caused by 1, 2-dimethylhydrazine in erythrocyte during colon postinitiation carcinogenesis. Oxid Med Cell Longev 2012;2012:1-6.

Hassan W, Noreen H, Rehman S, Gul S, Amjad Kamal M, Paul Kamdem J, Zaman B, Bt Da Rocha J. Oxidative stress and antioxidant potential of one hundred medicinal plants. Curr Top Med Chem 2017;17(12):1336-1370.

Hintzsche H, Stopper H. Micronucleus frequency in buccal mucosa cells of mobile phone users. Toxicol Lett 2010;193(1):124-130.

Hobbenaghi R, Javanbakht J, Sadeghzadeh S, Kheradmand D, Abdi F, Jaberi M, Mohammadiyan M, Khadivar F, Mollaei Y. Neuroprotective effects of *Nigella sativa* extract on cell death in hippocampal neurons following experimental global cerebral ischemia-reperfusion injury in rats. J Neurol Sci 2014;337:74-79.

Hossain MI, Faruque MRI, Islam MT. Analysis on the effect of the distances and inclination angles between human head and mobile phone on SAR. Prog Biophys Mol Biol 2015;119(2):103-110.

Hosseinzadeh H, Parvardeh S, Asl MN, Sadeghnia HR, Ziaee T. Effect of thymoquinone and *Nigella sativa* seeds oil on lipid peroxidation level during global cerebral ischemia-reperfusion injury in rat hippocampus. Phytomedicine 2007;14(9):621-627.

Hussain ZTE, Yagi S, Mahomoodally MF, Mohammed I, Zengin G. A comparative study of different solvents and extraction techniques on the anti-oxidant and enzyme inhibitory activities of *Adansonia digitata* L. (baobab) fruit pulp. S Afr J Bot 2019;126:207-213.

Hussein AA. Histological and morphological analysis of the hippocampal. J Fac Med Baghdad 2009;51(3):323-327.

Hybertson BM, Gao B, Bose SK, Mccord JM. Oxidative stress in health and disease: the therapeutic potential of Nrf2 activation. Mol Aspects Med 2011;32:234-246.

Ibrahim AY, Mahmoud M, Asker MM. Anti-inflammatory and antioxidant activities of polysaccharide from *Adansonia digitata*: An in vitro study. Int J Pharm Sci Rev Res 2014;25(2):174-182.

Ibrahim N, Gharib O. The protective effect of antioxidants on oxidative stress in rats exposed to the 950 MHz electromagnetic field. J Rad Res Appl Sci 2010;3:1143-1155.

İmge EB, Kiliçoğlu B, Devrim E, Çetin R, Durak İ. Effects of mobile phone use on brain tissue from the rat and a possible protective role of vitamin C - a preliminary study. Int J Radiat Biol 2010;86(12):1044-1049.

Insausti R. Postnatal development of the human hippocampal formation. Springer Science & Business Media. 2010;1:27-59.

Islam MH, Ahmad IZ, Salman MT. Neuroprotective effects of *Nigella sativa* extracts during germination on central nervous system. Pharmacogn Mag 2015;11:182-189.

Iyama T, Onishi T, Tarusawa Y, Uebayashi S, Nojima T. Novel specific absorption rate (SAR) measurement method using a flat solid phantom. IEEE Trans Electromagn Compat 2008;50(1):43-51.

Jadia S, Qureshi S, Jain L, Shringirishi M. Adverse effect of mobile phone on hearing in healthy individuals: A clinical study. Indian J Otolaryngol Head Neck Surg 2019;71(2):1169-1173.

Jaswal A, Shukla S. Therapeutic efficacy of *Nigella sativa* Linn. seed extract against CCl 4 induced hepatic injury in Wistar rats. Indian J Exp Biol 2015;53:44-50.

Jin X. The role of neurogenesis during development and in the adult brain. Eur J Neurosci 2016;44(6):2291-2299.

Johansen C. Brain tumour risk in relation to mobile telephone use: results of the Interphone international case-control study. Int J Epidemiol 2010;39(3):675-694.

Johansen JS, Harris AK, Rychly DJ, Ergul A. Oxidative stress and the use of antioxidants in diabetes: linking basic science to clinical practice. Cardiovasc Diabetol 2005;4(1):1-5.

Kabine O, Mamadou B, Fatoumata B, Namagan K, Luopou HN, Mamadou BA. Anti-oxidative activity of fruit extracts of some medicinal plants used against chronic diseases (diabetes, hypertension) in Kankan, Guinea. J Plant Sci 2015;3:1-5.

Kaboré D, Sawadogo-Lingani H, Diawara B, Compaoré CS, Dicko MH, Jakobsen M. A review of Baobab (*Adansonia digitata*) products: Effect of processing techniques, medicinal properties and uses. Afr J Food Sci 2011;5(16):833-844.

Kamatou G, Vermaak I, Viljoen A. An updated review of *Adansonia digitata*: A commercially important African tree. S Afr J Bot 2011;77(4):908-919.

Kanter M. *Nigella sativa* and derived thymoquinone prevents hippocampal neurodegeneration after chronic toluene exposure in rats. Neurochem Res 2008;33(3):579-588.

Kaplan S, Deniz OG, Önger ME, Türkmen AP, Yurt KK, Aydın I, Altunkaynak BZ, Davis D. Electromagnetic field and brain development. J Chem Neuroanat 2016;75:52-61.

Kaplan S, Eşrefoglu M, Aktaş A, Gül M, Önger ME, Altunkaynak ME, Ulkay MB, Ragbetli MÇ. The effect of prenatal exposure of a non-steroidal anti-inflammatory drug on the optic nerve of female rats: A stereological, histological, and electron microscopic study. J Matern Fetal Neonatal Med 2013;26(18):1860-1864.

Keleş Aİ, Yıldırım M, Gedikli Ö, Çolakoğlu S, Kaya H, Baş O, Sönmez OF, Odacı E. The effects of a continuous 1-h a day 900-MHz electromagnetic field applied throughout early and mid-adolescence on hippocampus morphology and learning behavior in late adolescent male rats. J Chem Neuroanat 2018;94:46-53.

Kempermann G, Song H, Gage FH. Neurogenesis in the adult hippocampus. Cold Spring Harb Perspect Biol 2015;7(9):1-14.

Kerimoğlu G, Hancı H, Baş O, Aslan A, Erol HS, Turgut A, Kaya H, Çankaya S, Sönmez OF, Odacı E. Pernicious effects of long-term, continuous 900-MHz electromagnetic field throughout adolescence on hippocampus morphology, biochemistry and pyramidal neuron numbers in 60-day-old Sprague Dawley male rats. J Chem Neuroanat 2016;77:169-175.

Kesari KK, Kumar S, Behari J. 900-MHz microwave radiation promotes oxidation in rat brain. Electromagn Biol Med 2011;30(4):219-234.

Kesner RP. An analysis of the dentate gyrus function. Behav Brain Res 2013;254:1-7.

Khan MA. Thymoquinone, a constituent of prophetic medicine-black seed, is a miracle therapeutic molecule against multiple diseases. Int J Health Sci 2019;13(1):1-2.

Kheifets L, Repacholi M, Saunders R, Van Deventer E. The sensitivity of children to electromagnetic fields. Pediatrics 2005;116(2):303-313.

Kim GH, Kim JE, Rhie SJ, Yoon S. The role of oxidative stress in neurodegenerative diseases. Exp Neurobiol 2015;24:325-340.

Kim K-H, Kabir E, Jahan SA. The use of cell phone and insight into its potential human health impacts. Environ Monit Assess 2016;188(4):221-232.

Kivrak EG, Altunkaynak BZ, Alkan I, Yurt KK, Kocaman A, Onger ME. Effects of 900-MHz radiation on the hippocampus and cerebellum of adult rats and attenuation of such effects by folic acid and Boswellia sacra. J Microsc Ultrastruct 2017;5(4):216-224.

Koehl M, Abrous DN. A new chapter in the field of memory: adult hippocampal neurogenesis. Eur J Neurosci 2011;33(6):1101-1114.

Kooti W, Hasanzadeh-Noohi Z, Sharafi-Ahvazi N, Asadi-Samani M, Ashtary-Larky D. Phytochemistry, pharmacology, and therapeutic uses of black seed (*Nigella sativa*). Chin J Nat Med 2016;14(10):732-745.

Koyu A, Cesur G, Ozguner F, Akdogan M, Mollaoglu H, Ozen S. Effects of 900 MHz electromagnetic field on TSH and thyroid hormones in rats. Toxicol Lett 2005;157(3):257-262.

Lahkola A, Auvinen A, Raitanen J, Schoemaker MJ, Christensen HC, Feychting M, Johansen C, Klæboe L, Lönn S, Swerdlow AJ. Mobile phone use and risk of glioma in 5 North European countries. Int J Cancer 2007;120(8):1769-1775.

Lawson M, Jomova K, Poprac P, Kuča K, Musílek K, Valko M. Free radicals and antioxidants in human disease. In: Al-Gubory, K.H. , Laher, I., editors. Nutritional antioxidant therapies: Treatments and perspectives. 1st Ed., Cham, Springer International Publishing, 2017;283-305.

Lazarov O, Hollands C. Hippocampal neurogenesis: Learning to remember. Prog Neurobiol 2016;138-140:1-18.

Lee A-K, Hong S-E, Kwon J-H, Choi H-D, Cardis E. Mobile phone types and SAR characteristics of the human brain. Phys Med Biol 2017;62(7):2741-2761.

Liguori I, Russo G, Curcio F, Bulli G, Aran L, Della-Morte D, Gargiulo G, Testa G, Cacciatore F, Bonaduce D, Abete P. Oxidative stress, aging, and diseases. Clin Interv Aging 2018;13:757-772.

Liu Z, Zhou T, Ziegler AC, Dimitrion P, Zuo L. Oxidative stress in neurodegenerative diseases: from molecular mechanisms to clinical applications. Oxid Med Cell Longev 2017;2017:1-11.

Makawi A, Mustafa A, Adiamo O, Ahmed IM. Effect of natural fermentation on the physicochemical, nutritional, functional, and microbiological properties of baobab (*Adansonia digitata* L.) fruit pulp flour. Int Food Res J 2019;26(6):1707-1715.

Marín-Burgin A, Mongiat LA, Pardi MB, Schinder AF. Unique processing during a period of high excitation/inhibition balance in adult-born neurons. Science 2012;335:1238-1242.

Merzenich H, Schmiedel S, Bennack S, Brüggemeyer H, Philipp J, Blettner M, Schüz J. Childhood leukemia in relation to radio frequency electromagnetic fields in the vicinity of TV and radio broadcast transmitters. Am J Epidemiol 2008;168(10):1169-1178.

Miah T, Kamat D. Current understanding of the health effects of electromagnetic fields. Pediatr Ann 2017;46(4):172-174.

Migault L, Bowman JD, Kromhout H, Figuerola J, Baldi I, Bouvier G, Turner MC, Cardis E, Vila J. Development of a job-exposure matrix for assessment of occupationalexposure to high-frequency electromagnetic fields (3 KHz–300 GHz). Ann Work Expo Health 2019;63(9):1013-1028.

Miguel-Bilbao SD, Karpowicz J, Febles V, Hernández JA, Suárez S, Ramos V, Leszko W, Gryz K. Electromagnetic exposure hot-spots in a healthcare environment, caused by smart metering to control public utilities 2017 E-Health and Bioengineering Conference (EHB), Sinaia, Romania, IEEE, 2017;603-606.

Ming G-L, Song H. Adult neurogenesis in the mammalian central nervous system. Annu Rev Neurosci 2005;28:223-250.

Mishra SK, Chowdhary R. Does radiations emitted from cell phone effects orofacial structures and dental implants? Int. J. Environ. Health Eng 2018;7(1):1-1.

Mohamadin AM, Sheikh B, El-Aal AaA, Elberry AA, Al-Abbasi FA. Protective effects of *Nigella sativa* oil on propoxur-induced toxicity and oxidative stress in rat brain regions. Pestic Biochem Physiol 2010;98(1):128-134.

Mohamed AF, Hanafy SM, Mahmoud A. The possible protective effect of black seed (*Nigella sativa*) oil on the testes of adult male albino rat exposed to noise. J Histol Histopathol 2015;2(1):1-9.

Molnar E. Long-term potentiation in cultured hippocampal neurons. Semin Cell Dev Biol 2011;22(5):506-513.

Morgado-Bernal I. Learning and memory consolidation: linking molecular and behavioral data. Neuroscience 2011;176:12-19.

Narayanan S, Kumar R, Kedage V, Nalini K, Nayak S, Bhat P. Evaluation of oxidant stress and antioxidant defense in discrete brain regions of rats exposed to 900 MHz radiation. Bratisl Med J 2014;115(5):260-266.

Narayanan SN, Kumar RS, Potu BK, Nayak S, Bhat PG, Mailankot M. Effect of radio-frequency electromagnetic radiations (Rf-emr) on passive avoidance behaviour and hippocampal morphology in wistar rats. Ups J Med Sci 2010;115(2):91-96.

Nasreen S, Safeer S, Dar KK, Andleeb S, Ejaz M, Khan MA, Ali S. Etiology of hepatocellular carcinoma and treatment through medicinal plants: a comprehensive review. Orient Pharm Exp Med 2018;18(3):187-197.

Nittby H, Grafstrom G, Eberhardt JL, Malmgren L, Brun A, Persson BR, Salford LG. Radiofrequency and extremely low-frequency electromagnetic field effects on the blood-brain barrier. Electromagn Biol Med 2008;27(2):103-126.

O'neill J, Boccara CN, Stella F, Schönenberger P, Csicsvari J. Superficial layers of the medial entorhinal cortex replay independently of the hippocampus. Science. 2017;355:184-188.

Odaci E, Bas O, Kaplan S. Effects of prenatal exposure to a 900 Mhz electromagnetic field on the dentate gyrus of rats: A stereological and histopathological study. Brain Res 2008;1238:224-229.

Ogawa K, Suzuki Y, Akimoto T, Shiobara K, Hara M, Morita A, Kamei S, Soma M. Relationship between cytotoxicity in the hippocampus and an abnormal high intensity area on the diffusion-weighted images of three patients with transient global amnesia. Intern Med 2018;57(18):2631-2639.

Ong YS, Saiful Yazan L, Ng WK, Noordin MM, Sapuan S, Foo JB, Tor YS. Acute and subacute toxicity profiles of thymoquinone-loaded nanostructured lipid carrier in balb/c mice. Int J Nanomedicine 2016;11:5905-5915.

Ongel K, Gumral N, Ozguner F. The potential effects of electromagnetic field: A review. Cell Mem Free Rad Res 2009;1(3):85-89.

Organization WH. WHO research agenda for radiofrequency fields [Online]. Geneva: WHO 2010 Available: https://apps.who.int/iris/handle/10665/44396. Access date: 17.12.2010

Ozmen I, Naziroglu M, Alici HA, Sahin F, Cengiz M, Eren I. Spinal morphine administration reduces the fatty acid contents in spinal cord and brain by increasing oxidative stress. Neurochem Res 2007;32(1):19-25.

Pall ML. Microwave frequency electromagnetic fields (EMFs) produce widespread neuropsychiatric effects including depression. J Chem Neuroanat 2016;75:43-51.

Panagopoulos DJ, Chavdoula ED, Nezis IP, Margaritis LH. Cell death induced by GSM 900-MHz and DCS 1800-MHz mobile telephony radiation. Mutat Res Genet Toxicol Environ Mutagen 2007;626(1):69-78.

Pang CC, Kiecker C, O'brien JT, Noble W, Chang RC-C. Ammon's Horn 2 (CA2) of the hippocampus: a long-known region with a new potential role in neurodegeneration. Neuroscientist 2019; 25(2):167-180.

Parasuraman S, Sam AT, Yee SWK, Chuon BLC, Ren LY. Smartphone usage and increased risk of mobile phone addiction: A concurrent study. Int J Pharm Investig 2017;7(3):125-131.

Pena-Bautista C, Baquero M, Vento M, Chafer-Pericas C. Free radicals in alzheimer's disease: Lipid peroxidation biomarkers. Clin Chim Acta 2019;491:85-90.

Perez FP, Morisaki JJ, Bandeira JP. Repeated electromagnetic field stimulation in aging and health. In: Rattan SIS , Kyriazis M, editors. The science of hormesis in health and longevity. 1st Ed. Academic Press. 2019;189-197.

Perveen R. Therapeutic effects of black cumin (*Nigella sativa*). A systematic review. Prog Nutr 2019;21:40-49.

Pham-Huy LA, He H, Pham-Huy C. Free radicals, antioxidants in disease and health. Int J Biomed Sci 2008;4(2):89-96.

Piatti VC, Ewell LA, Leutgeb JK. Neurogenesis in the dentate gyrus: carrying the message or dictating the tone. Front Neurosci 2013;7:1-11.

Pizzino G, Irrera N, Cucinotta M, Pallio G, Mannino F, Arcoraci V, Squadrito F, Altavilla D, Bitto A. Oxidative stress: harms and benefits for human health. Oxid Med Cell Longev 2017; 2017:1-13.

Poprac P, Jomova K, Simunkova M, Kollar V, Rhodes CJ, Valko M. Targeting free radicals in oxidative stress-related human diseases. Trends Pharmacol Sci 2017;38(7):592-607.

Rağbetli MÇ, Aydinlioğlu A, Koyun N, Rağbetli C, Karayel M. Effect of prenatal exposure to mobile phone on pyramidal cell numbers in the mouse hippocampus: A stereological study. Int J Neurosci 2009;119(7):1031-1041.

Ragy MM. Effect of exposure and withdrawal of 900-MHz-electromagnetic waves on brain, kidney and liver oxidative stress and some biochemical parameters in male rats. Electromagn Biol Med 2015;34(4):279-284.

Rahul J, Jain MK, Singh SP, Kamal RK, Naz A, Gupta AK, Mrityunjay SK. *Adansonia digitata* L.(baobab): A review of traditional information and taxonomic description.Asian Pac J Trop Biomed 2015;5(1):79-84.

Randhawa MA, Alghamdi MS. Anticancer activity of *Nigella sativa* (black seed) a review. Am J Chin Med 2011;39(6):1075-1091.

Ranganath C, Heller A, Cohen MX, Brozinsky CJ, Rissman J. Functional connectivity with the hippocampus during successful memory formation. Hippocampus 2005;15(8):997-1005.

Röösli M, Frei P, Mohler E, Hug K. Systematic review on the health effects of exposure to radiofrequency electromagnetic fields from mobile phone base stations. Bull World Health Organ 2010;88:887-896.

Russell CL. 5G wireless telecommunications expansion: Public health and environmental implications. Environ Res 2018;165:484-495.

Sadler TW. Langman's medical embryology 13th Ed., Philadelphia, Wolters Kluwer Health, 2015; 322-326.

Sage C, Burgio E. Electromagnetic fields, pulsed radiofrequency radiation, and epigenetics: How wireless technologies may affect childhood development. Child Dev 2018;89(1):129-136.

Sahak MKA, Kabir N, Abbas G, Draman S, Hashim NH, Adli H, Sharifah D. The role of *Nigella sativa* and its active constituents in learning and memory. Evid Based Complement Alternat Med 2016;2016:1-6.

Şahin A, Aslan A, Baş O, İkinci A, Özyılmaz C, Sönmez OF, Çolakoğlu S, Odacı E. Deleterious impacts of a 900-mhz electromagnetic field on hippocampal pyramidal neurons of 8-week-old sprague dawley male rats. Brain Res 2015;1624:232-238.

Saikhedkar N, Bhatnagar M, Jain A, Sukhwal P, Sharma C, Jaiswal N. Effects of mobile phone radiation (900 mhz radiofrequency) on structure and functions of rat brain. Neurol Res 2014;36(12):1072-1079.

Salford LG, Brun AE, Eberhardt JL, Malmgren L, Persson BR. Nerve cell damage in mammalian brain after exposure to microwaves from GSM mobile phones. Environ Health Perspect 2003;111(7):881-883.

Salih NKM, Yahia E. Nutritional value and antioxidant properties of four wild fruits commonly consumed in Sudan. Int Food Res J 2015;22(6):2389-2395.

Salim S. Oxidative stress and the central nervous system. J Pharmacol Exp Ther 2017;360(1):201-205.

Samuels BA, Hen R. Neurogenesis and affective disorders. Eur J Neurosci 2011;33(6):1152-1159.

Sandhu K, Rana A. Aeview of plant *Nigella sativa*: A brief consideration of its pharmacognostic characters, chemical constituents and therapeutic benefits. Int J Pharm Sci 2013;4:323-343.

Santo A, Zhu H, Li YR. Free radicals: from health to disease. ROS 2016;2(4):245-263.

Satti NME. Sudanese baobab (*Adansonia digitata*). JNBAS 2018;3(2):131-147.

Sauter C, Dorn H, Bahr A, Hansen ML, Peter A, Bajbouj M, Danker-Hopfe H. Effects of exposure to electromagnetic fields emitted by GSM 900 and WCDMA mobile phones on cognitive function in young male subjects. Bioelectromagnetics 2011;32(3):179-190.

Scheidegger M, Henning A, Walter M, Lehmann M, Kraehenmann R, Boeker H, Seifritz E, Grimm S. Ketamine administration reduces amygdalo-hippocampal reactivity to emotional stimulation. Hum Brain Mapp 2016;37(5):1941-1952.

Schmitz C, Eastwood BS, Tappan SJ, Glaser JR, Peterson DA, Hof PR. Current automated 3D cell detection methods are not a suitable replacement for manual stereologic cell counting. Front Neuroanat 2014;8:27-39.

Schmitz C, Hof P. Design-based stereology in neuroscience. Neuroscience 2005;130(4):813-831.

Sedaghat R, Roghani M, Khalili M. Neuroprotective effect of thymoquinone, the *Nigella sativa* bioactive compound, in 6-hydroxydopamine-induced hemi-parkinsonian rat model.Iran J Pharm Res 2014;13(1):227-234.

Seghatoleslam M, Alipour F, Shafieian R, Hassanzadeh Z, Edalatmanesh MA, Sadeghnia HR, Hosseini M. The effects of *Nigella sativa* on neural damage after pentylenetetrazole induced seizures in rats. J Tradit Complement Med 2016;6(3):262-268.

Seress L, Abraham H, Tornoczky T, Kosztolanyi G. Cell formation in the human hippocampal formation from mid-gestation to the late postnatal period. Neuroscience 2001;105(4):831-843.

Sharma N, Ahirwar D, Jhade D, Gupta S. Medicinal and phamacological potential of *Nigella sativa*: a review. Ethno Leaf 2009;13:946-955.

Sheikh BY, Mohamadin AM. Thymoquinone a potential therapy for cerebral oxidative stress. Asian J Nat Appl Sci 2012;1:76-92.

Silva DFD, Barros WR, Almeida MDCCD, Rêgo MaV. Exposure to non-ionizing electromagnetic radiation from mobile telephony and the association with psychiatric symptoms. Cad Saude Publica 2015;31(10):2110-2126.

Slomianka L, Amrein I, Knuesel I, Sørensen JC, Wolfer DP. Hippocampal pyramidal cells: the reemergence of cortical lamination. Brain Struct Funct 2011;216(4):301-317.

Snell RS. Clinical neuroanatomy. 7th Ed., Philadelphia, Lippincott Williams & Wilkins, 2010; 509-511.

Söderqvist F, Carlberg M, Mild KH, Hardell L. Childhood brain tumour risk and its association with wireless phones: A commentary. Environ Health 2011;10:106-111.

Sokeng AJT, Sobolev AP, Di Lorenzo A, Xiao J, Mannina L, Capitani D, Daglia M. Metabolite characterization of powdered fruits and leaves from *Adansonia digitata* L.(Baobab): A multi-methodological approach. Food Chem 2019;272:93-108.

Sonmez OF, Odaci E, Bas O, Kaplan S. Purkinje cell number decreases in the adult female rat cerebellum following exposure to 900 MHz electromagnetic field. Brain Res 2010;1356:95-101.

Spalding KL, Bergmann O, Alkass K, Bernard S, Salehpour M, Huttner HB, Boström E, Westerlund I, Vial C, Buchholz BA. Dynamics of hippocampal neurogenesis in adult humans. Cell 2013;153(6):1219-1227.

Srivastava DM, Taufiq DF. Effects of radio-frequency electromagnetic radiations (RF-EMR) on cerebral cortex of albino rats-a light and electron microscopic study. Int J Med Sci Clin Invent 2018;5(3):3662-3668.

Stefi AL, Margaritis LH, Skouroliakou AS, Vassilacopoulou D. Mobile phone electromagnetic radiation affects amyloid precursor protein and alpha-synuclein metabolism in SH-SY5Y cells. Pathophysiology 2019;26(3):203-212.

Stella F, Cerasti E, Si B, Jezek K, Treves A. Self-organization of multiple spatial and context memories in the hippocampus. Neurosci Biobehav Rev 2012;36(7):1609-1625.

Sterio D. The unbiased estimation of number and sizes of arbitrary particles using the disector. J Microsc 1984;134(2):127-136.

Storz P. Reactive oxygen species–mediated mitochondria-to-nucleus signaling: A key to aging and radical-caused diseases. Sci STKE 2006;232:1-7.

Su L, Hayes L, Soteriades S, Williams G, Brain SA, Firbank MJ, Longoni G, Arnold RJ, Rowe JB, O'brien JT. Hippocampal stratum radiatum, lacunosum, and moleculare sparing in mild cognitive impairment. J Alzheimers Dis 2018;61:415-424.

Surai PF, Kochish, Ii, Fisinin VI, Kidd MT. Antioxidant defence systems and oxidative stress in poultry biology: An update. Antioxidants 2019;8(7):235.

Talari S, Gundu C, Koila T, Nanna RS. In vitro free radical scavenging activity of different extracts of *Adansonia digitata* L. Int J environ Agric Biotech 2017;2(3):1169-1172.

Tavakkoli A, Ahmadi A, Razavi BM, Hosseinzadeh H. Black seed (*Nigella sativa*) and its constituent thymoquinone as an antidote or a protective agent against natural or chemical toxicities. Iran J Pharm Res 2017;16:2-23.

Tembo DT, Holmes MJ, Marshall LJ. Effect of thermal treatment and storage on bioactive compounds, organic acids and antioxidant activity of baobab fruit (*Adansonia digitata*) pulp from Malawi. J Food Compost Anal 2017;58:40-51.

Terzi M, Ozberk B, Deniz OG, Kaplan S. The role of electromagnetic fields in neurological disorders. J Chem Neuroanat 2016;75:77-84.

Toda T, Parylak SL, Linker SB, Gage FH. The role of adult hippocampal neurogenesis in brain health and disease. Mol Psychiatry 2019;24(1): 67-87.

Toyoda H, Li XY, Wu LJ, Zhao MG, Descalzi G, Chen T, Koga K, Zhuo M. Interplay of amygdala and cingulate plasticity in emotional fear. Neural Plast 2011;2011:1-9.

Türkmen AP, Kaplan S, Aksoy A, Altunkaynak B, Yurt K, Elibol E, Çokluk C, Onger M. Effects of diclofenac sodium on the hippocampus of rats with acute subdural hematoma: histological, stereological, and molecular approach. Folia Neuropathol 2016;54(2):167-179.

Union IT. ICT facts and figures. Switzerland, Geneva, 2013.

Vafaee F, Hosseini M, Hassanzadeh Z, Edalatmanesh MA, Sadeghnia HR, Seghatoleslam M, Mousavi SM, Amani A, Shafei MN. The effects of *Nigella sativa* hydro-alcoholic extract on memory and brain tissues oxidative damage after repeated seizures in rats. Iran J Pharm Res 2015;14(2):547-557.

Valko M, Leibfritz D, Moncol J, Cronin MT, Mazur M, Telser J. Free radicals and antioxidants in normal physiological functions and human disease. Int J Biochem Cell Biol 2007;39(1):44-84.

Vaz NP, De Oliveira DR, Abouelella GA, Khater H. The black seed, *Nigella sativa* (Ranunculaceae), for prevention and treatment of hypertension. Vol 48: Hypertension of the series "Recent progress in medicinal plants". Studium Press, 2018;48:222-244.

Veena V, Janarthan M, Saka V, Siddappa RD, Jilani S, Basha SR, Kumar GK. Evaluation of behavioral and neuroprotective activity of Curcuma amada against cell phone radiation induced brain damage in rats. Indian J Res Pharm Biotechnol 2015;3(6):452-457.

Vermaak I, Kamatou GPP, Komane-Mofokeng B, Viljoen A, Beckett K. African seed oils of commercial importance Cosmetic applications. S Afr J Bot 2011;77(4):920-933.

Vertuani S, Braccioli E, Buzzoni V, Manfredini S. Antioxidant capacity of *Adansonia digitata* fruit pulp and leaves. Acta Phytother 2002;2(5):2-7.

Von Bohlen Und Halbach O, Draguhn A, Storm-Mathisen J. Recent advances in hippocampal structure and function. Cell Tissue Res 2018;373(3):521-523.

Wall S, Wang ZM, Kendig T, Dobraca D, Lipsett M. Real-world cell phone radiofrequency electromagnetic field exposures. Environ Res 2019;171:581-592.

Wang X, Michaelis EK. Selective neuronal vulnerability to oxidative stress in the brain. Front Aging Neurosci 2010;2:1-13.

Waxman SG. Clinical neuroanatomy. 26th Ed., New York, McGraw Hill, 2010.

Wessapan T, Rattanadecho P. Temperature induced in human organs due to near-field and far-field electromagnetic exposure effects. Int J Heat Mass Transf 2018;119:65-76.

West M, Slomianka L, Gundersen HJG. Unbiased stereological estimation of the total number of neurons in the subdivisions of the rat hippocampus using the optical fractionator. Anat Rec 1991;231(4):482-497.

Wible C. Hippocampal physiology, structure and function and the neuroscience of schizophrenia: a unified account of declarative memory deficits, working memory deficits and schizophrenic symptoms. Behav Sci 2013;3(2):298-315.

Wiehle M, Prinz K, Kehlenbeck K, Goenster S, Mohamed SA, Finkeldey R, Buerkert A, Gebauer J. The African baobab (*Adansonia digitata*, *Malvaceae*): Genetic resources in neglected populations of the Nuba Mountains, Sudan. Am J Bot 2014;101(9):1498-1507.

Wyszkowska J, Jankowska M, Gas P. Electromagnetic fields and neurodegenerative diseases. Przegląd Elektrotechniczny 2019;1(95):129-133.

Yaman I, Balikci E. Protective effects of *Nigella sativa* against gentamicin-induced nephrotoxicity in rats. Exp Toxicol Pathol 2010;62(2):183-190.

Yildirim ME, Kaynar M, Badem H, Cavis M, Karatas OF, Cimentepe E. What is harmful for male fertility: Cell phone or the wireless internet? Kaohsiung J Med Sci 2015;31(9):480-484.

Yokus B, Cakir DU, Akdag MZ, Sert C, Mete N. Oxidative DNA damage in rats exposed to extremely low frequency electro magnetic fields. Free Radic Res 2005;39(3):317-323.

Yurt KK, Kaplan S, Kıvrak EG. The neuroprotective effect of melatonin on the hippocampus exposed to diclofenac sodium during the prenatal period. J Chem Neuroanat 2018;87:37-48.

Zhao C, Deng W, Gage FH. Mechanisms and functional implications of adult neurogenesis. Cell 2008;132(4):645-660.

APPENDICES

Ethical Committee Approval Certificate

T.C.
ONDOKUZ MAYIS ÜNİVERSİTESİ
Hayvan Deneyleri Yerel Etik Kurulu

Sayı : 68489742-604-E.7974 03/04/2018
Konu : Hadyek İzin Onayı Hk.

PROF.DR. SÜLEYMAN KAPLAN
PROJE YÜRÜTÜCÜSÜ

Laboratuvar Hayvanlar üzerinde Araştırma amaçlı çalışma yapmak üzere başvuran Prof.Dr. Süleyman KAPLAN 'ın 2018/17 Kabul nolu" **900 MHz elektromanyetik alana maruz kalmış sıçan hipokampusu üzerine Baobab ve çörek otu'nun muhtemel etkilerinin araştırılması** başlıklı projesi 30.03.2018 tarihli Kurul toplantısında OMU- HADYEK 'in yönergesi kapsamında değerlendirilmiş ve Hayvan Hakları ve Deney Etik İlkelerine Uygun bulunmuştur. Karar onayı ekte sunulmuştur.

Gereğini bilgilerinize rica ederim

e-imzalıdır
Prof. Dr. Ferşat KOLBAKIR
HADYEK

CURRICULUM VITAE

Full Name: Hamza Mohamed Sharif Alamin MOHAMED

Place of Birth: Shandi- SUDAN

Date of Birth: 01/11/1981

Marital Status: Married

Nationality: Sudanese

Educational Status (Institution and Year):

B.Sc.: Human Anatomy-Omdurman Islamic University-Faculty of Basic Medical Sciences 2000-2004 Khartoum, Sudan.

M.Sc.: Human Anatomy-University of Gezira- College of Medicine- Deanship of Graduate Studies and Scientific Research 2009-2011, Wad Medani, Sudan

Ph.D.: Department of Histology and Embryology, Faculty of Medicine, Ondokuz Mayis University (2013-2020), Samsun, Turkey

E-mail: Hamza-mk@hotmail.com